

2013

# Development of Hybrid Polymeric/ Inorganic Ion Exchanger: Preparation, Characterization, and Environmental Applications

Surapol Padungthon  
*Lehigh University*

Follow this and additional works at: <http://preserve.lehigh.edu/etd>

 Part of the [Environmental Engineering Commons](#)

---

## Recommended Citation

Padungthon, Surapol, "Development of Hybrid Polymeric/ Inorganic Ion Exchanger: Preparation, Characterization, and Environmental Applications" (2013). *Theses and Dissertations*. Paper 1582.

This Dissertation is brought to you for free and open access by Lehigh Preserve. It has been accepted for inclusion in Theses and Dissertations by an authorized administrator of Lehigh Preserve. For more information, please contact [preserve@lehigh.edu](mailto:preserve@lehigh.edu).

**DEVELOPMENT OF HYBRID POLYMERIC/ INORGANIC ION  
EXCHANGERS: PREPARATION, CHARACTERIZATION, AND  
ENVIRONMENTAL APPLICATIONS**

by

Surapol Padungthon

A Dissertation

Presented to the Graduate and Research Committee

of Lehigh University

in Candidacy for the Degree of

Doctor of Philosophy

in

Environmental Engineering

Lehigh University

May 2013

# DISSERTATION SIGNATURE SHEET

Approved and recommended for acceptance as a dissertation in partial fulfillment of the requirements for the degree of Doctor of Philosophy.

\_\_\_\_\_  
Date

\_\_\_\_\_  
Dr. Arup K. SenGupta  
Dissertation Advisor

\_\_\_\_\_  
Accepted Date

Committee Members:

\_\_\_\_\_  
Dr. Derick G. Brown  
Committee Chair

\_\_\_\_\_  
Dr. Kristen Jellison  
Committee Member

\_\_\_\_\_  
Dr. James E. Roberts  
Committee Member, External

\_\_\_\_\_  
Dr. John E. Greenleaf  
Committee Member, External

## **Acknowledgement**

I would like to express my sincere appreciation to my advisor Dr. Arup SenGupta for his long-term support, patience, encouragement, and continuous guidance for both teaching and research over many years at Lehigh University. I would like to extend my thanks to my dissertation committee members: Dr. Derick Brown, Dr. Kristen Jellison, Dr. James Roberts, Dr. John Greenleaf. I want to express my gratitude to all of my teachers who taught me in the past. I also would like to thank all other staff members for their help: Prisca Vidanage, Christine Moyer, Dawn McClay, Dan Zeroka, Channy Tokura, and Beth Yen.

I would like to thank my colleagues and friends: Dr. Prasun Chatterjee, Dr. Sudipta Sarkar, Dr. Pijit Jiemvarangkul, Dr. Medhat Mohamed El-moselhy, Jin-Chen Lin, Ryan Smith, Mike German, Nelly Cheruiyot, Li Wang. Thank you all for your assistance in experiments and for your friendship. In addition, I would like to give my special thanks to my friend, Pornsawai Praipipat for her companionship and support.

I gratefully acknowledge the financial support provided by the Royal Thai Government and funding from Dr. SenGupta. I would like to thank Khon Kaen University for the support throughout the study at Lehigh University. Finally I wish to thank my parents and my family, who always support and encourage me throughout my studies. I would like to share this honor with my father Kanok, my mother Tong-arb, my brother Adisak and my sister Nittaya Padungthon.

# DEVELOPMENT OF HYBRID POLYMERIC/ INORGANIC ION EXCHANGERS: PREPARATION, CHARACTERIZATION, AND ENVIRONMENTAL APPLICATIONS

## Table of Contents

Description	Page no.
Certificate of Approval	ii
Acknowledgement	iii
Table of Contents	iv
List of Figures	xi
List of Tables	xx
<b>ABSTRACT</b>	1
<b>CHAPTER 1: INTRODUCTION</b>	5
1.1 Polymeric Ion Exchanger	5
1.1.1 Inability to Selectively Remove Trace Ionic Species	9
1.1.2 High Concentration of Waste Generated from the Regeneration of Ion Exchange Processes	13
1.2 Hybrid Polymeric Ion Exchanger Supported Zr(IV) Oxide Nanoparticle for Selective Removal of Trace Anionic Ligands and Heavy Metal	16
1.2.1 Trace Environmental Contaminants: Ligands and Heavy Metals	16
1.2.2 Arsenic and Fluoride Problems	17
1.2.3 Adsorption by Metal Oxide Particles and Their Limitation	21

1.2.4	Mechanism of Ligands and Heavy Metal Sorption onto the Surface of Metal Oxide Particles	24
1.2.5	Concept of Hybrid Polymeric/Inorganic Ion Exchanger	27
1.2.6	Role of Donnan Membrane Effect	29
1.2.7	Disadvantages of Hydrated Fe(III) Oxide (HFO) Nanoparticles	30
1.2.8	Use of Chemically Stable Hydrated Zirconium Oxide (HZO) Nanoparticles	31
1.3	Water Softening Process: Problems, Challenges, and New Opportunities	33
1.3.1	Current Technologies: Problems and Challenges	34
	1.3.1.1 Lime–Soda Softening	34
	1.3.1.2 Ion Exchange Processes	36
1.3.2	Need for Salt/Acid Free Water Softening Processes	37
1.3.3	Previous Development of Salt-Free Water Softening Process Using IX-Fibers and CO <sub>2</sub> Regeneration	38
1.3.4	Development of Salt Free Water Softening Process	39
	1.3.4.1 Use of Shallow Shell Technology (SST) Resin and Solid CO <sub>2</sub> Regeneration	39
	1.3.4.2 Use of Weak Acid Cation (WAC) Exchange Resin and Biodegradable Organic Acid Regeneration	42
	1.3.4.3 Simultaneous Hardness and Ligands Removal using Strong Acid Cation Exchange Resin in Polyvalent (Al <sup>3+</sup> ) Form	43
1.4	Premise of the Studies	44
1.4.1	Development of HIX-Zr for Selective Removal of Arsenic,	

Fluoride, and Zinc	44
1.4.2 Development of Salt-Free Water Softening Process	45
<b>CHAPTER 2: MATERIALS AND EXPERIMENTAL PROCEDURES</b>	47
2.1 Materials and Chemicals	47
2.1.1 Ion Exchange Resins and Fibers	47
2.1.2 Zirconium Compounds and Other Chemicals	48
2.2 Analytical Methods	51
2.2.1 Dissolve Metals and Metalloids	51
2.2.2 Anionic Species	52
2.2.3 Fluoride and Aluminum Analysis	52
2.2.4 Zirconium and Silica Analysis	53
2.2.5 X-Ray Diffraction (XRD)	53
2.2.6 Scanning Electron Microscopy with Energy Dispersive X-ray (SEM/EDX)	53
2.3 Experimental Procedures	55
2.3.1 Batch Equilibrium Test and Sorption Isotherm	55
2.3.2 Fixed-bed Column Runs	56
2.3.3 Kinetic Tests	59
<b>CHAPTER 3: HAIX-Zr SYNTHESIS AND CHARACTERIZATION</b>	61
3.1 Previous Development of Hybrid Ion Exchanger (HIX)	62
3.1.1 Hybrid Cation Exchangers Supported Fe(III) Oxide Nanoparticles: HCIX-Fe	63

3.1.2 Hybrid Anion Exchanger Supported Fe(III) Oxide Nanoparticle: HAIX-Fe	65
3.2 Synthesis of Hybrid Polymeric Ion Exchanger Supported Hydrated Zr(IV) Oxide (HZO) Nanoparticles	67
3.2.1 Batch Preparation Method	69
3.2.2 Column Preparation Method	70
3.3 Arsenic and Fluoride Removal using HAIX-Zr Prepared from Reagent Grade $ZrOCl_2 \cdot 8H_2O$ by Batch Method#1	72
3.4 Arsenic Removal using HAIX-Ti Prepared from Titanium Tetra-Chloride ( $TiCl_4$ ) by Batch Method#1	75
3.5 HAIX-Zr from Inexpensive Industrial Grade Zirconium Oxide ( $ZrO_2$ ) by Batch Method	78
3.6 HAIX-Zr Prepared from Zirconium Oxide by Column Method	80
3.7 Determination of Zirconium Contents from the HAIX-Zr	82
3.8 Characterization of HAIX-Zr	84
 <b>CHAPTER 4: RESULTS AND DISCUSSION: ARSENIC REMOVAL BY HAIX-Zr</b>	 95
4.1 Materials Characterization and Evidences of HZO Nanoparticles	96
4.2 Fixed-Bed Column Runs using HAIX-Zr	100
4.2.1 Sorption of Trace As(V) under High Concentration of Competing ions	101
4.2.2 Sorption of As(III)	103



4.2.3 Arsenic Sorption Behaviors with Hydrated Zirconium Oxide in the HAIX-Zr	104
4.2.4 As(V) Removal Between HAIX-Zr and HCIX-Zr	109
4.2.5 Donnan Membrane Effect	110
4.2.6 Regeneration and Reuse of HAIX-Zr	112
4.3 Equilibrium Batch Test with HAIX-Zr	116
4.3.1 Sorption Isotherm of As(V) using HAIX-Zr	116
4.3.2 Effect of pH for the Sorption of As(V) using HAIX-Zr	118
4.3.3 Influence of Competing Ions	119
4.3.3.1 Effect of Silica	119
4.3.3.2 Effect of Phosphate	121
4.3.3.3 Effect of Sulfate	123
4.4 Sorption Kinetics	124
4.4.1 Mathematical model	125
<b>CHAPTER 5: RESULTS AND DISCUSSION: FLUORIDE REMOVAL BY HAIX-Zr</b>	128
5.1 Fixed-bed Column Runs Using HAIX-Zr	129
5.1.1 Comparison of Fluoride Removal Using Different Metal Oxides Sorbents	129
5.1.2 Effect of Donnan Membrane Effect	130
5.1.3 Multiple Sorption-Desorption of Fluoride with HAIX-Zr and AA	131
5.1.4 Mechanism of Fluoride Sorption onto the HZO Nanoparticles	134
5.1.5 Regeneration and Reuse	135

5.2 Equilibrium Isothermal Test	137
5.3 Effect of the Feed pH and Stability of Hybrid Adsorbents	139
5.4 Fluoride Sorption Kinetics	141
<b>CHAPTER 6: RESULTS AND DISCUSSION: ZINC REMOVAL BY HCIXF-Zr AND CO<sub>2</sub> REGENERATION</b>	145
6.1 Synthesis of Hybrid Cation Exchange Fibers impregnated with HZO Nanoparticles or HCIXF-Zr	148
6. 2 Metals (Zinc) Removal during Fixed-bed Column Runs	149
6.3 Regeneration using Solid CO <sub>2</sub> (Dry Ice) Sparged 1% Ca <sup>2+</sup> Solution	153
6.4 Fiber Morphology and Regeneration	154
6.5 The Use and Sequestration of Carbon Dioxide	156
<b>CHAPTER 7: SALT FREE WATER SOFTENING PROCESSES</b>	157
7.1 Underlying Principal of the Proposed Processes	158
7.1.1 Salt-Free Water Softeninging Process using WAC Resins	158
7.1.2 Salt-Free Water Softening Process Using SAC Resins in Polyvalent Form	160
7.2 Water Softening using Weak Acid Cation (WAC) Exchange Resins	163
7.2.1 Hardness Removal using Two WAC Exchangers at Influent Ca <sup>2+</sup> 400 mg/L	163
7.2.2 Comparison of Solid CO <sub>2</sub> Sparged Water and Acetic Acid Regeneration	164

7.2.3 Hardness Removal using Two WAC Exchangers at Influent Ca <sup>2+</sup> 200 mg/L	165
7.2.4 Hardness Removal using Two WAC Exchangers at Influent Ca <sup>2+</sup> 150 mg/L	167
7.2.5 Hardness Removal at Ca <sup>2+</sup> 70 mg/L and 2% Acetic Acid	170
7.3 Water Softening Using Strong Acid Cation Exchanger in Al <sup>3+</sup> form	173
7.3.1 Hardness Removal at Initial Ca <sup>2+</sup> 100 and 50 mg/L	173
7.3.2 Fluoride Removal	177
<b>CHAPTER 8: CONCLUSIONS</b>	179
8.1 The hybrid polymeric ion exchangers supported hydrated zirconium oxide (HZO) nanoparticles	179
8.1.1 Synthesis and Characterization of Hybrid Sorbents	179
8.1.2 Development of Hybrid Anion Exchanger Supported HZO Nanoparticles (HAIX-Zr) for Removal of Trace Anionic Ligands (i.e., arsenic and fluoride)	182
8.1.3 Development of Hybrid Cation Exchange Fibers Supported HZO Nanoparticles (HCIXF-Zr) for Removal of Heavy Metals (i.e. Zinc)	184
8.2 Salt-free water softening processes	185
<b>APPENDIX</b>	188
<b>REFERENCES</b>	191
<b>VITA</b>	201

## List of Figures

Description	Page no.
<b>Figure 1.1</b> Organic cation-exchanger bead comprising polystyrene polymer cross-linked with divinylbenzene with fixed co-ions (negatively charges) balanced by mobile positively charged counter-ions	6
<b>Figure 1.2</b> Chemical structures of four major types of polymeric ion exchangers	8
<b>Figure 1.3</b> An effluent history of an As(V) contaminated water for a fixed-bed column run using a strong-base anion exchanger (IRA-958)	12
<b>Figure 1.4</b> The $\text{Na}^+$ - $\text{Ca}^{2+}$ equilibrium for sulfonic acid cation exchange resin	15
<b>Figure 1.5</b> Distribution of As(V) and As(III) oxyacids and their conjugate anions as a function of pH	18
<b>Figure 1.6</b> Worldwide distributions of arsenic contaminated regions, showing source of arsenic and numbers of people at risk of chronic exposure	19
<b>Figure 1.7</b> Model global probability of fluoride concentration in groundwater exceeding the WHO guideline for drinking water of 1.5 mg/L	20
<b>Figure 1.8</b> A schematic diagram illustrating the binding of several of solutes onto hydrated metal oxides at circum-neutral pH	25
<b>Figure 1.9</b> The concept of polymer-supported inorganic metal oxide nanoparticles or hybrid ion exchanger	27
<b>Figure 1.10</b> Donnan membrane effect from the parent ion exchanger	29
<b>Figure 1.11</b> Composite predominant diagram, Fe- As and Zr-As	31
<b>Figure 1.12</b> Speciation of zirconium hydrolysis products as a function of solution pH	33

<b>Figure 1.13</b> Distribution of hard water as milligram per liter as CaCO <sub>3</sub> in the United States	35
<b>Figure 1.14</b> Laboratory set-up depicting the CO <sub>2</sub> in water used in the hardness removal cycles of fiber and resin ion exchange materials	40
<b>Figure 1.15</b> (A) Weak acid ion exchange fibers with carboxylate functional groups (B) Virgin fiber materials photographed at x10 magnification. (C) SEM photograph of a single fiber (x2000)	40
<b>Figure 1.16</b> (A) Schematic depicting the regeneration of weak-acid cation exchange beads. (B) Schematic depicting the regeneration of weak-acid cation exchange fibers	41
<b>Figure 1.17</b> Comparison of different structure of weak acid cation exchangers (A) Purolite C104, (B) Purolite SST 104, and (C) Fiban K4	41
<b>Figure 1.18</b> Scope of research on the topic of heterogeneous polymeric ion exchangers	46
<b>Figure 2.1</b> Rotary shaker for material preparation and batch test	56
<b>Figure 2.2</b> An illustration of the set up for the fixed bed column experiment	58
<b>Figure 2.3</b> Schematic of the batch kinetic test apparatus and stirrer assembly	60
<b>Figures 3.1</b> Report numbers of citation indexed within Web of Science from year 2004-2013	62
<b>Figure 3.2</b> The major steps of the process for HCIX-Fe synthesis	64
<b>Figure 3.3</b> Schematic diagrams illustrating first and second steps in the preparation of HAIX-Fe	66

<b>Figure 3.4</b> Schematic diagrams for batch (top) and column preparation method (bottom) for HIX-Zr synthesis	71
<b>Figure 3.5</b> Batch equilibrium test for arsenic removal: $C_{As0} = 158.8$ ppb, background anion of $SO_4^{2-}$ , $HCO_3^{2-}$ , $Cl^- = 100$ mg/L, mass of resin 0.1 g, volume 100 ml, pH 7.0, shaking time 5 days	73
<b>Figure 3.6</b> Batch equilibrium test for fluoride removal: $C_{F0} = 22$ mg/L, background anion of $SO_4^{2-}$ , $HCO_3^{2-}$ , $Cl^- = 100$ mg/L, mass of resin 0.2 g, volume 100 ml, pH 5.0	74
<b>Figure 3.7</b> Batch equilibrium test for arsenic removal by using HAIX-Ti at initial arsenic concentration 225 ppb: $C_{As0} = 225$ ppb, background anion of $SO_4^{2-}$ , $HCO_3^{2-}$ , $Cl^- = 100$ mg/L, mass of resin 0.2 g, volume 100 ml, pH 7.0	76
<b>Figure 3.8</b> Batch equilibrium test for arsenic removal by using HAIX-Ti at initial arsenic concentration 1000 ppb : $C_{As0} = 1000$ ppb, background anion of $SO_4^{2-}$ , $HCO_3^{2-}$ , $Cl^- = 100$ mg/L, mass of resin 0.3 g, volume 200 ml, pH 5.0	77
<b>Figure 3.9</b> Batch equilibrium test for arsenic removal using HAIX-Zr prepared from batch method: $C_{As0} = 1000$ ppb, background ions as appear in the challenge water with $SiO_2$ 10 mg/L, mass of resin 0.3 g, volume 1,000 ml, pH 7.0	79
<b>Figure 3.10</b> Batch equilibrium test for arsenic removal using HAIX-Zr prepared from column method : $C_{As0} = 1000$ ppb, background ions as appear in the challenge water with $SiO_2$ 10 mg/L, mass of resin 0.1 g, volume 200 ml, pH 7.0	81
<b>Figure 3.11</b> Zirconium content in the HAIX-Zr by (A) double digestion with 50% $H_2SO_4$ , HAIX-Zr 0.5 gram digested in 50% $H_2SO_4$ and (B) zirconium content (from Sample A500P-Zr from $ZrO_2$ (MEL) obtained semi-quantitatively by	

SEM/EDX method, shown 10% zirconium content within the material	83
<b>Figure 3.12</b> SEM, TEM, and EDX spectrum and elemental mapping of Purolite A500P-Zr	86
<b>Figure 3.13</b> SEM, TEM, and EDX spectrum and elemental mapping of Purolite A400-Zr	88
<b>Figure 3.14</b> SEM, TEM, and EDX spectrum and elemental mapping of Purolite A500P-Ti	90
<b>Figure 3.15</b> SEM, TEM, and EDX spectrum and elemental mapping of Amberlite XAD4-Zr	92
<b>Figure 3.16</b> SEM, TEM, and EDX spectrum and elemental mapping of commercial Iron-based sorbent (ArsenX-Fe)	94
<b>Figure 4.1</b> (A) HAIX-Zr beads with the size range of 0.4-1.2 mm in diameter (B) Photograph (40X) of enlarged view of the hybrid anion exchanger impregnated with hydrated Zr(IV) oxide nanoparticles (HAIX-Zr), (C) Scanning electron micrograph (SEM) of macro-porous type of HAIX-Zr (40,000X), (D) Energy dispersive X-ray spectroscopy (EDX) spectrum of the HAIX-Zr (10 % of elemental zirconium by mass basis)	98
<b>Figure 4.2</b> High resolution transmission electron microscopy (HRTEM) photograph of HAIX-Zr	99
<b>Figure 4.3</b> Effluent histories of As(V) during column runs with HAIX-Zr and Purolite A500P	102
<b>Figure 4.4</b> Effluent history of As(III) during a column run with HAIX-Zr	104

<b>Figure 4.5</b> A schematic diagram illustrating the binding of several of solutes onto hydrated zirconium oxides (HZO) at circum-neutral pH	108
<b>Figure 4.6</b> Effluent histories of As(V) during a column runs with HAIX-Zr and HCIX-Zr	109
<b>Figure 4.7</b> Donnan membrane effect exerted by parent anion exchange supported	111
<b>Figure 4.8</b> Dissolved arsenic concentration profiles during desorption of HAIX-Zr using 3% NaOH and 3% as the regenerate solution	113
<b>Figure 4.9</b> Composite predominance diagrams of Fe-As and Zr-As	115
<b>Figure 4.10</b> Arsenic sorption isotherm plot at pH 7.0 with background anions at 20 °C	117
<b>Figure 4.11</b> Effect of pH for arsenic removal using HAIX-Zr	118
<b>Figure 4.12</b> Effect of silica to the arsenic removal using HAIX-Zr	120
<b>Figure 4.13</b> Effect of phosphate to the arsenic removal using HAIX-Zr	121
<b>Figure 4.14</b> Effect of sulfate to the arsenic removal using HAIX-Zr	123
<b>Figure 4.15</b> Interruption test during the experimental column run on arsenic removal by HAIX-Zr	124
<b>Figure 4.16</b> Fractional uptake rate (F) versus time (t) plots for HAIX-Zr during batch kinetic test of arsenic removal	127
<b>Figure 5.1</b> Effluent histories of fluoride during column run between HAIX-Zr, LayneRT, and AA	129
<b>Figure 5.2</b> Effluent histories of fluoride during column runs with HAIX-Zr and HCIX-Zr	131



<b>Figure 5.3</b> Fluoride effluent histories and regeneration for the first run using HAIX-Zr and activated alumina (AA)	132
<b>Figure 5.4</b> Fluoride effluent histories and regeneration for the second run using the same HAIX-Zr and AA	133
<b>Figure 5.5</b> Fluoride sorption isotherms with other background ions at room Temperature	138
<b>Figure 5.6</b> Effect of pH for fluoride sorption for HAIX-Zr and AA	139
<b>Figure 5.7</b> Concentration of aluminum and zirconium in treated water coming from dissolution of AA and HAIX-Zr at different influent pH	140
<b>Figure 5.8</b> (A) Interruption test during the experimental column runs on fluoride removal by HAIX-Zr, (B) Fractional uptake (F) versus time (t) plots for HAIX-Zr during batch kinetic test of fluoride removal	142
<b>Figure 5.9</b> Comparison of mechanical strength and XRD diffractograms between used HAIX-Zr and activated alumina (AA) after 3 cycles of sorption/desorption for fluoride removal column run experiment	144
<b>Figure 5.10</b> Comparison of mechanical strength and XRD diffractograms between used HAIX-Zr and activated alumina (AA) after 3 cycles of sorption/desorption for fluoride removal column run experiment.	143
<b>Figure 6.1</b> (A) strong acid ion exchange fibers with sulfonic acid functional group, (B) Virgin fiber materials photographed at x10 magnification. (C) SEM photograph of a single fiber (x2000)	147

<b>Figure 6.2</b> A schematic diagram and the experimental apparatus used for both service cycles and regeneration cycles while using fiber and resin materials	150
<b>Figure 6.3</b> The results of Zn <sup>2+</sup> removal on fixed-bed column runs using four different ion exchange materials, namely, hybrid cation exchange fibers (HCIXF-Zr) , hybrid ion exchange resins (HCIX-Zr) loaded with Hydrated Zr (IV) oxide (HZO), commercial cation exchange resin bead C145, and commercial cation exchange fiber K1	152
<b>Figure 6.4</b> Comparison of zinc elution between HCIXF-Zr (Fiban K1) and HCIX-Zr (Purolite C145) loaded with HZO	153
<b>Figure 6.5</b> Schematic illustration of sorption/desorption of toxic metal zinc on HZO	154
<b>Figure 6.6</b> A schematic depicting the progress of regeneration for HCIXF-Zr materials, the progress of regeneration for HCIXF-Zr materials	155
<b>Figure 7.1</b> The results of Ca <sup>2+</sup> removal on fixed bed column runs using two different WAC resins ( SST104 and C104) at influent Ca <sup>2+</sup> 400 mg/L	163
<b>Figure 7.2</b> Comparison of water softening regeneration between the solid carbon dioxide sparged water @150 psi and dilute 0.5% acetic acid regeneration	164
<b>Figure 7.3</b> The results of Ca <sup>2+</sup> removal on fixed bed column runs using two different WAC resins ( SST104 and C104) at influent Ca <sup>2+</sup> 200 mg/L	166
<b>Figure 7.4</b> Diluted acetic acid regeneration (0.5% acetic acid) of traditional weak acid cation exchanger C104 and shallow shell technology (SST 104)	166

<b>Figure 7.5</b> The results of Ca <sup>2+</sup> removal on fixed bed column runs using WAC resins (SST104) at influent Ca <sup>2+</sup> 150 mg/L	168
<b>Figure 7.6</b> Diluted acetic acid regeneration (2% acetic acid) of the shallow shell technology (SST 104)	168
<b>Figure 7.7</b> The results of Ca <sup>2+</sup> removal on fixed bed column runs using WAC resins ( C106) at influent Ca <sup>2+</sup> 150 mg/L	169
<b>Figure 7.8</b> Diluted acetic acid regeneration (2% acetic acid) of traditional weak acid cation exchanger C106	169
<b>Figure 7.9</b> The results of Ca <sup>2+</sup> removal on fixed bed column runs using WAC resins( SST104 at influent Ca <sup>2+</sup> 70 mg/L	171
<b>Figure 7.10</b> Diluted acetic acid regeneration (2% acetic acid) of shallow shell technology WAC resin (SST 104)	171
<b>Figure 7.11</b> The results of Ca <sup>2+</sup> removal on fixed bed column runs using WAC resins(C106) at influent Ca <sup>2+</sup> 70 mg/L	172
<b>Figure 7.12</b> Diluted acetic acid regeneration (2% acetic acid) of traditional weak acid cation exchanger C106	172
<b>Figure 7.13</b> Effluent calcium history for hardness removal with high calcium in feed (100 mg/L) during column runs using macroporous strong acid cation exchanger in Al <sup>3+</sup> form	173
<b>Figure 7.14</b> Effluent history for hardness removal with low calcium in the feed (50 mg/L) during column runs using macroporous strong acid cation exchanger in Al <sup>3+</sup> form	174

<b>Figure 7.15</b> Concentration profiles of aluminum in treated water during column runs using macroporous strong acid cation exchanger in Al <sup>3+</sup> form	175
<b>Figure 7.16</b> Breakthrough profile of treated water conductivity during column runs using macroporous strong acid cation exchanger in Al <sup>3+</sup> form	176
<b>Figure 7.17</b> Effluent history for fluoride removal during column runs using macroporous strong acid cation exchanger that started in Al <sup>3+</sup> form	177
<b>Figure 7.18</b> SEM-EDX elemental mapping of Purolite C145 after the end of hardness removal and before regeneration	178
<b>Figure A1</b> Fluoride effluent histories and regeneration profiles using HAIX-Zr and AA	190
<b>Figure A2</b> Flow scheme for fluoride treatment plant and on-site regeneration facility	190

## List of Tables

Description	Page no.
<b>Table 1.1</b> Relative affinities of ion for resins	10
<b>Table 1.2</b> Oxyacids and Conjugate Anions of As(V) and As(III)	18
<b>Table 1.3</b> Advantages and Disadvantages of ion exchange and metal oxide adsorption adapt from Clifford	22
<b>Table 1.4</b> Comparison of Material Properties and Synergy Effect of Hybrid Ion Exchanger	28
<b>Table 2.1</b> Salient property of ion exchange resins used for synthesis of zirconium oxide based hybrid nanosorbents	49
<b>Table 2.2</b> Property of polymeric ion exchange fibers used for HCIXF-Zr for removal of zinc and other transition metals	50
<b>Table 3.1</b> Zirconium content from the acid digestion method	82
<b>Table 4.1</b> Property of polymeric ion exchangers	96
<b>Table 4.2</b> Characteristic of NSF Std. 53 Challenge Water formula	100
<b>Table 4.3</b> Chemical similarity between oxyacid of As(V) and P(V)	122
<b>Table 6.1</b> Salient property of ion exchange materials	148

## ABSTRACT

The study involves the development of two environmental applications using hybrid polymeric/ inorganic ion exchangers. First, the hybrid polymeric ion exchangers supported hydrated zirconium oxide (HZO) nanoparticles, referred to as HIX-Zr were developed for selective removal of heavy metals and anionic ligands. Second, salt-free water softening processes were presented using three different heterogeneous cation exchanger resins along with novel regeneration schemes.

The HIX-Zr nanosorbents have been prepared, characterized, and extensively studied in relation to heavy metal (i.e., zinc) and anionic ligand (i.e., arsenate and fluoride) removal in fixed-bed processes at trace concentrations with the presence of high concentrations of innocuous competing ions. The HIX-Zr adsorbents are essentially nanoparticles of HZO irreversibly dispersed onto the polymeric phase of either anion exchangers containing quaternary ammonium functional ( $R_4N^+$ ) groups or cation exchangers containing sulfonate ( $SO_3^-$ ) functional groups which are referred to as HAIX-Zr and HCIX-Zr, respectively. The new class of hybrid nanosorbents provides a synergy unattainable separately by either inorganic metal oxide nanoparticles or polymeric ion exchangers alone. HZO particles have long been known for their high chemical stability under varying conditions of pH and redox and exhibit amphoteric sorption properties near neutral pH. Besides providing high durability, the Donnan membrane effect from the polymeric ion exchanger plays an important role to enhance the permeation of target contaminants. HIX-Zr nano-adsorbents were characterized by scanning electron microscopy equipped with energy dispersive X-ray spectroscopy (SEM/ EDX), high

resolution transmission electron microscopy (HRTEM), and X-ray diffraction (XRD). The HZO nanoparticles were uniformly distributed throughout the polymeric ion exchanger phases at an approximately 12% (w/w) with sizes well below 50 nm, while the material's high surface area from the amorphous structure of HZO still remains even after 5 cycles of sorption-desorption as confirmed by XRD. From the equilibrium batch isothermal test, the arsenic and fluoride sorption behaviors follow the Langmuir isotherm with the maximum sorption capacity of 20 mg As(V)/g at pH 7 and 35 mg F/g at pH 5, respectively. The sorption capacity of the HAIX-Zr for both arsenic and fluoride is three times higher than the most commonly used activated alumina (AA). Kinetic studies on arsenate and fluoride adsorption onto the HAIX-Zr confirmed that intraparticle diffusion was the rate limiting step. The HAIX-Zr nanosorbents are amendable to efficient regeneration with more than 90% recovery within 15 bed volumes and can be reused for many cycles of sorption-desorption. The regenerable nature of HAIX-Zr reduces the volume of disposable waste more than 100-fold versus the commercially available granulated metal oxide adsorbents. Due to the high chemical stability of HZO nanoparticles, the HAIX-Zr can be disposed of safely in a landfill without risk of toxic leaching.

In general water softening processes, lime soda and ion exchange are the most widely used techniques for removal of hardness (e.g.,  $\text{Ca}^{2+}$ ,  $\text{Mg}^{2+}$ , etc.) from hard water, however, these technologies generate voluminous sludge and concentrated brine/mineral acid as waste stream, respectively. Residual management and long-term sustainability issues will continue to be major concerns with these processes. In this study, three

different salt-free water softening processes using different cation exchangers and regeneration schemes are developed. First, the shallow shell technology (SST) resins with dry-ice regeneration; second, a weak acid cation exchanger (WAC) with biodegradable organic acid regeneration (i.e., diluted acetic acid); and third, a strong acid cation exchanger in the aluminum form (SAC-Al) and stoichiometric of aluminium salt regeneration are evaluated for simultaneous softening of hard water and removal of fluoride at high pH.

For the commercially available SST resins, the process takes advantage of the shorter diffusion path length due to the inert core of the resin similar to the ion exchange fibers used previously and the high preference of hydrogen ions from the weak acid cation (WAC) exchanger. From the experimental hardness removal column runs and solid CO<sub>2</sub> (dry ice) regeneration study, we found that the solid CO<sub>2</sub> sparged in DI water was not effective for desorption of hardness (i.e., Ca<sup>2+</sup>) from the SST resins as expected. Although, the solid CO<sub>2</sub> (dry ice) is available, there are some difficulties to control the flow rate of CO<sub>2</sub> dissolved in water as regenerant solution at high pressure including the CO<sub>2</sub> gas in solution tend to disturb the resin bed.

For the second salt-free water softening scheme, we decided to use the traditional spherical weak acid cation (WAC) exchange resins which have high affinity toward hydrogen ions and using the diluted biodegradable organic acid such as 2% acetic acid instead of aggressive 5% inorganic HCl acid as hydrogen source as a regenerant. From the hardness regeneration studies, we found that the calcium recoveries as high as 98% were achieved with only 10 bed volumes by using stoichiometric amounts of dilute acetic



acid. The novel water softening process by using WAC resins and stoichiometric amounts of dilute biodegradable organic acids (i.e., acetic acid) results in two main attributes; first the WAC have higher capacity than the traditional SAC resins, and the second benefit is that the waste acid generated from the process is much less (near stoichiometric efficiency) than the brine solution (only 30% efficiency). Moreover the organic acids are biodegradable while the brine solution is permanently present in the environment.

The third salt-free water softening process uses polymeric cation exchangers pre-loaded with aluminum (SAC-Al) or other polyvalent cations (i.e., SAC-Fe). The process uses close to stoichiometric amounts of aluminum salts (i.e.,  $\text{Al}_2(\text{SO}_4)_3$ ,  $\text{AlCl}_3$ ) for regeneration and significantly less volume of waste brine is generated compared to traditional brine regeneration for strong acid cation exchange processes. Since no NaCl is added during regeneration, sodium is virtually absent in the disposable waste regenerant. The spent regenerant essentially contains only salts of hardness (e.g.  $\text{Ca}^{2+}$ ,  $\text{Mg}^{2+}$ ) removed during the regeneration cycle. Also, no mineral acid is needed for regeneration. Along with hardness, the process also removes fluoride when the bed is initially in the  $\text{Al}^{3+}$  form or contains precipitated aluminum (hydr) oxide.

# CHAPTER 1

## INTRODUCTION

### 1.1 Polymeric Ion Exchanger

Ion exchange is a heterogeneous process, defined as the interchange of ions between a solid phase (ion exchanger) and a liquid surrounding the solid. Ion exchange materials can vary from natural materials such as zeolites (alumino silicates), kaolinite, montmorillonite or synthetic materials such as polymeric ion exchange resins, fibers, and membranes. Ion exchange technology has been applied for the separation of ionic compounds in many fields for nearly a century. Natural ion exchange dates back to biblical times when Moses sweetened the waters of Mariah during their journey using a tree (Exodus 15:23-25). It can be inferred that the oxidized cellulose of the tree undergoes an ion exchange reaction with the bitter electrolytes of the water. (1) The first systematic study on ion exchange was reported in 1854 by H.S. Thomson and J. Thomas Way, English agricultural chemists, which related the exchange of calcium and ammonium ions in soil. In 1906, Robert Gans, a German chemist, used natural and synthetic aluminium silicates (zeolite) for industrial purposes to soften water. In 1935, Leibknecht developed a sulfonated coal exchanger in Germany, and Adams and Homes synthesized the first high capacity phenol-formaldehyde exchangers in England. In 1945, D' Alelio in the United States developed and patented sulfonated crosslinked polystyrene resin. In 1946, the first large-scale water softening plant was built in California by using synthetic silica-based media, and then was later changed to polymeric polystyrene divinyl

benzene cation exchange resin. (1-5) Modern ion exchangers are synthesized from a polymer matrix, usually a polystyrene crosslinked with 3 to 8% divinylbenzene (DVB), which offer improvement in faster exchange kinetics, higher capacity, and longer lifetimes than the natural ion exchange materials. Polymeric ion exchangers consist of a solid phase where a number of functional groups (fixed coions) are covalently attached to a polymer matrix. Ions in the aqueous phase with the same charge as the fixed functional groups are called “co-ions” and the ions with the opposite charges are referred to as “counter-ions” The counter-ions can permeate in and out of the resin, but the co-ions are excluded from the polymer phase by the phenomenon called “Donnan membrane effect”(2). Figure 1.1 represents a two-dimensional bead consisting of polystyrene polymer chains held together by divinylbenzene crosslinking.

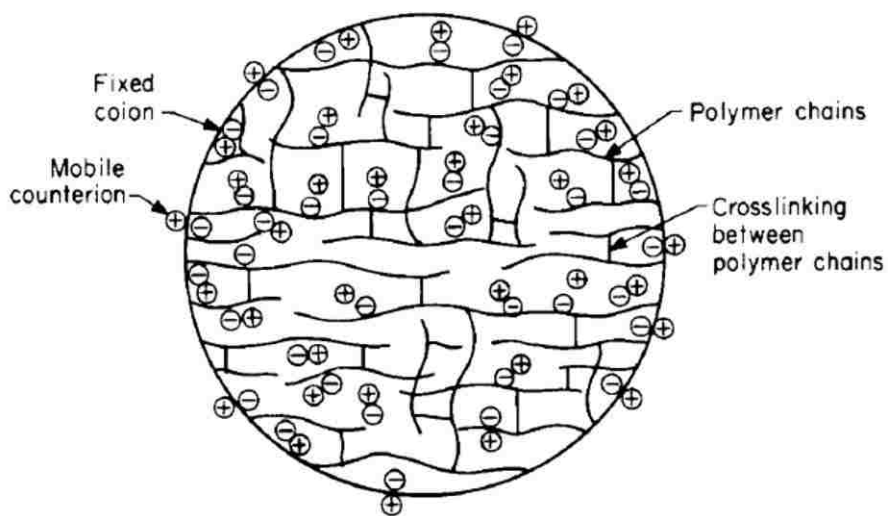


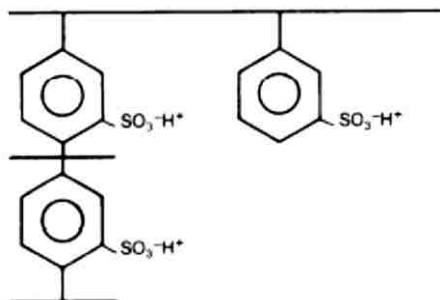
**Figure 1.1** Organic cation-exchanger bead comprising polystyrene polymer cross-linked with divinylbenzene with fixed co-ions (negatively charges) balanced by mobile positively charged counter-ions (2).

Traditional ion exchange resins can be classified based on their functional groups, which consist of four main categories: strong acid cation (SAC) exchanger (e.g., sulfonate,  $-\text{SO}_3^-$ ); weak acid cation (WAC) exchanger (e.g., carboxylate,  $-\text{COO}^-$ ); strong base anion (SBA) exchanger (e.g., quaternary amine,  $-\text{N}^+(\text{CH}_3)_3$ ) and weak base anion (WBA) exchanger (e.g., tertiary amine,  $-\text{N}(\text{CH}_3)_2$ ). Special types of polymeric ion exchangers such as chelating ion exchangers are not mentioned in this study because they were developed for specific purposes and have a high cost of implementation on a large scale. Four different types of polymeric ion exchangers with different functional groups are focused in this research and are shown in figure 1.2. **(6)**

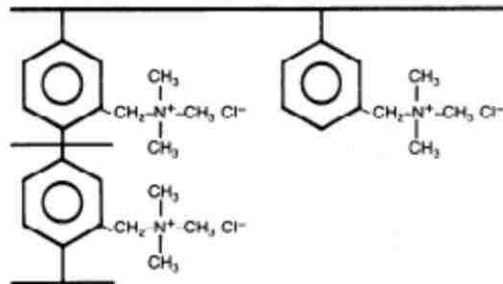
Polymeric ion exchangers are suitable for use in fixed-bed columns because they exhibit a high mechanical strength and are attrition resistant. The ion exchange technology is simple, reversible (i.e., reusable), has high capacity, and is efficient. Also, it is able to operate at a relatively high flow rate with a small footprint, to operate without electricity, and can withstand fluctuations in the feed flow rate or concentration. Nowadays, hundreds of different ion exchange materials are synthesized and used in many processes, including water softening, water demineralization, environmental remediation, wastewater treatment, hydrometallurgy, chromatography, biomolecular separation, catalysis, etc. **(3)**. For environmental applications, ion exchange is a powerful technology for removing many ionic impurities from water and wastewater. Ion exchange technology is primarily used for water softening and demineralization. Moreover, it is usually used to remove nitrate, barium, radium, chromate, perchlorate **(4, 7)**.

However, for complex problems, the concentration of background nontoxic cations (e.g.,  $\text{Ca}^{2+}$ ,  $\text{Na}^+$ ) and anions (e.g.,  $\text{SO}_4^{2-}$ ,  $\text{Cl}^-$ ,  $\text{HCO}_3^-$ ) are at much higher

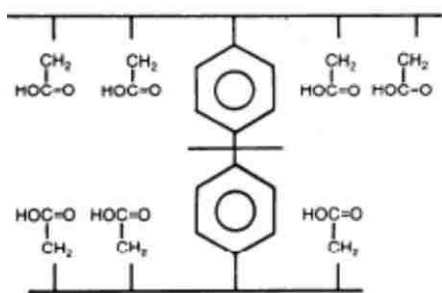
concentrations than the target toxic heavy metals (e.g.,  $Zn^{2+}$ ,  $Cu^{2+}$ ) and/or anionic ligands (e.g., arsenate, phosphate, fluoride, etc.). The ion exchange resins are unable to selectively remove those trace species. The limitations and challenges of applying ion exchange for the removal of trace ionic species are mentioned in section 1.1.1.



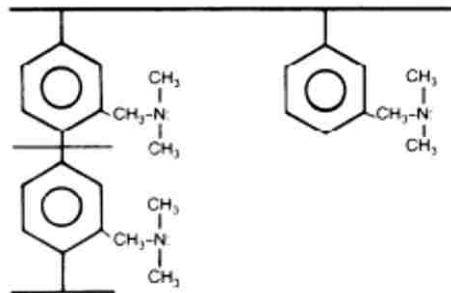
**Strong Acid Cation (SAC) Exchanger**  
(Styrene-DVB matrix  
with sulfonate ( $-SO_3^-$ ) functional groups)



**Strong Base Anion (SBA) Exchanger**  
(Styrene-DVB matrix with quaternary  
ammonium ( $-N^+(CH_3)_3$ ) functional groups)



**Weakly Acidic Cation (WAC) Exchanger**  
(Acrylic-DVB matrix with carboxylate  
( $-COO^-$ ) functional groups)



**Weakly Basic Anion (WBA) Exchanger**  
(Styrene-DVB matrix with tertiary amine,  
( $-N(CH_3)_2$ ) functional groups)

**Figure 1.2** Chemical structures of the four major types of polymeric ion exchangers (6)

Moreover, although the ion exchange process can be reversible, high concentrations or aggressive chemicals have to be used to overcome the selectivity reversal. For example, a high concentration of salt (12-15% NaCl) or acid (5% HCl) solution have to use for hardness regeneration by using strong acid cation (SAC) exchanger in the  $\text{Na}^+$  form or weak acid cation exchanger in the  $\text{H}^+$  form, respectively. Both limitations and challenges are discussed in section 1.1.2.

### **1.1.1 Inability to Selectively Remove Trace Ionic Species**

The preference of ion exchangers for one specific ion over another can be expressed qualitatively by a selectivity sequence as shown in the table 1.1 and quantitatively by the separation factor ( $\alpha$ ) or a selectivity coefficient (K) for binary exchange. Table 1.1 shows the selectivity sequence (from the bottom to the top) and the separation factor ( $\alpha_{i/\text{Na}}$  and  $\alpha_{j/\text{Cl}}$ ) of the strong acid cation (SAC) and strong base anion (SBA) exchangers with respect to the sodium and chloride ions, respectively. Weak acid cation (WAC) exchangers with carboxylic acid functional groups have the same selectivity sequence (not the selectivity value) as SAC resins except that hydrogen ion ( $\text{H}^+$ ) is the most preferred for WAC resins. Similarly, WBA and SBA resins exhibit the same selectivity sequence, except that hydroxide ions ( $\text{OH}^-$ ) are the most preferred by WBA resins. Note that special resins such as chelating resins exhibit a different selectivity sequence and values from the traditional resins, and are not mentioned for this study. (2) For dilute solutions, the ion exchange resins prefer counter ions of higher charge, atomic number, or ionic radius (4). However, some exceptions may apply and will not be discussed in this research.

**Table 1.1** Relative affinities of ion for resins (2)

Strong acid cation (SAC) ** resins		Strong base anion (SBA) *** resins	
Cation, i	$\alpha_{i/Na}$	Anion, j	$\alpha_{j/Cl}$
H <sup>+</sup>	0.67	F <sup>-</sup>	0.07
Na <sup>+</sup>	1.0	CH <sub>3</sub> COO <sup>-</sup>	0.14
NH <sub>4</sub> <sup>+</sup>	1.3	HCO <sub>3</sub> <sup>-</sup>	0.27
Mn <sup>2+</sup>	1.6	BrO <sub>3</sub> <sup>-</sup>	0.9
K <sup>+</sup>	1.67	Cl <sup>-</sup>	1.0
Mg <sup>2+</sup>	1.67	NO <sub>2</sub> <sup>-</sup>	1.1
Fe <sup>2+</sup>	1.7	HSO <sub>3</sub> <sup>-</sup>	1.2
Zn <sup>2+</sup>	1.8	SeO <sub>3</sub> <sup>2-</sup>	1.3
Ca <sup>2+</sup>	1.9	Br <sup>-</sup>	2.3
Cu <sup>2+</sup>	2.6	NO <sub>3</sub> <sup>-</sup>	3.2
Sr <sup>2+</sup>	4.8	HSO <sub>4</sub> <sup>-</sup>	4.1
Pb <sup>2+</sup>	5.0	HAsO <sub>4</sub> <sup>2-</sup>	4.5
Ba <sup>2+</sup>	5.8	SO <sub>4</sub> <sup>2-</sup>	9.1
Ra <sup>2+</sup>	13.0	SeO <sub>4</sub> <sup>2-</sup>	17
		CrO <sub>4</sub> <sup>2-</sup>	100
		ClO <sub>4</sub> <sup>-</sup>	150
		UO <sub>2</sub> (CO <sub>3</sub> ) <sub>3</sub> <sup>4-</sup>	3200

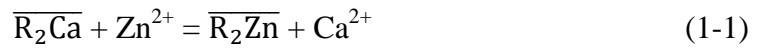
\*The above values are approximate separation factors for 0.005-0.010 N solution

(TDS = 250-500 mg/L as CaCO<sub>3</sub>).

\*\*SAC resin is polystyrene divinylbenzene matrix with sulfonate functional groups.

\*\*\*SBA resin is polystyrene divinylbenzene matrix with -N<sup>+</sup>(CH<sub>3</sub>)<sub>3</sub> functional groups

The inability of ion exchangers to remove trace species out of high concentrations of innocuous ionic species inevitably present in the water can be explained by using the concepts of separation factor and selectivity coefficient. For example, there are difficulties in removing trace concentrations of toxic heavy metals such as  $Zn^{2+}$ ,  $Cd^{2+}$ ,  $Cu^{2+}$ , etc. from the aqueous phase where the high concentrations of innocuous  $Ca^{2+}$  or other polyvalent species are inevitably present can be explained as follows:



where the overbar represents the cation exchange phase and R represents the polymer matrix with fixed anionic charged (e.g.,  $-SO_3^-$ ) functional groups. Assuming ideality, the equilibrium constant or selectivity coefficient of  $Zn^{2+}$  over  $Ca^{2+}$  ( $K_{Zn/Ca}$ ) of the equation 1-2 is as follows:

$$K_{Zn/Ca} = \frac{[\overline{R_2Zn}][Ca^{2+}]}{[Zn^{2+}][\overline{R_2Ca}]} = \frac{q_{Zn}C_{Ca}}{q_{Ca}C_{Zn}} \quad (1-2)$$

where  $q_{Zn}$  and  $q_{Ca}$  represent the concentration of  $Zn^{2+}$ ,  $Ca^{2+}$  in the resin phase and  $C_{Ca}$ , and  $C_{Zn}$  represent the concentration of  $Ca^{2+}$  and  $Zn^{2+}$  of the liquid. The ratio of  $Zn^{2+}$  to  $Ca^{2+}$  in the aqueous phase is much less thus in order to selectively remove  $Zn^{2+}$  over  $Ca^{2+}$  (high  $q_{Zn}$ ), the equilibrium constant or selectivity coefficient ( $K_{Zn/Ca}$ ) has to be very high. However, the traditional ion exchange processes are based on Coulombic (electrostatic) type interactions, thus they are unable to attain a high selectivity toward zinc. **(8)**



Similarly, trace arsenate ( $\text{HASO}_4^{2-}$ ), fluoride ( $\text{F}^-$ ), phosphate ( $\text{HPO}_4^{2-}$ ), and chromate ( $\text{CrO}_4^{2-}$ ) are not selectively removed by traditional anion exchangers under the presence of competing high concentration ions such as  $\text{SO}_4^{2-}$ . From figure 1.3, it can be inferred that arsenate or As(V) is poorly removed by traditional anion exchangers under the presence of sulfate.

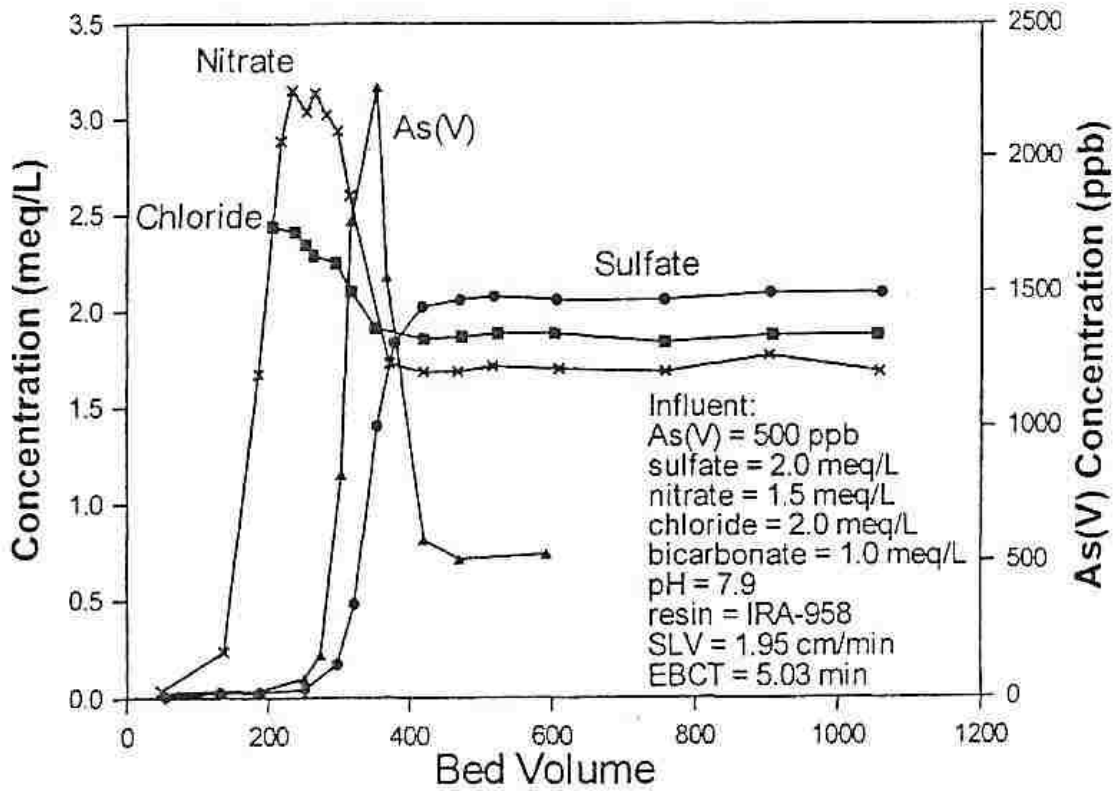


**Figure 1.3** An effluent history of an As(V) contaminated water for a fixed-bed column run using a strong-base anion exchanger (IRA-958)

### 1.1.2 High Concentration of Waste Generated from the Regeneration of Ion Exchange Processes

The selectivity values shown in table 1.1 were carried out at a general dilute concentration. For traditional ion exchange processes, the concentration of the solute also has a strong effect toward the selectivity of the target contaminants. If the system is dealing with the same charge (monovalent/monovalent or divalent/divalent), the selectivity coefficient (K) from eq. 1-2 and separation factor ( $\alpha_{i/j}$ ) from eq.1-5 are equal. For exchange ions of different valence, the separation factor ( $\alpha_{i/j}$ ) is not equivalent to the selectivity coefficient (K). For example, the water softening process where  $\text{Ca}^{2+}$  or other polyvalent cations from the water are exchanged with  $\text{Na}^+$  ion from the SAC resin is shown as (2):



$$K_{\text{Ca/Na}} = \frac{q_{\text{Ca}} C_{\text{Na}}^2}{q_{\text{Na}}^2 C_{\text{Ca}}} \quad (1-4)$$

The binary separation factor ( $\alpha_{i/j}$ ) is defined as the ratio of distribution of ion i between phases and the distribution of ion j between phases. For this case, the separation factor between  $\text{Ca}^{2+}$  and  $\text{Na}^+$  is;

$$\alpha_{\text{Ca/Na}} = \frac{(Y_{\text{Ca}})/(X_{\text{Ca}})}{(Y_{\text{Na}})/(X_{\text{Na}})} = \frac{Y_{\text{Ca}} X_{\text{Na}}}{Y_{\text{Na}} X_{\text{Ca}}} = \frac{(q_{\text{Ca}}/q)(C_{\text{Na}}/C)}{(q_{\text{Na}}/q)(C_{\text{Ca}}/C)} = \frac{q_{\text{Ca}} C_{\text{Na}}}{q_{\text{Na}} C_{\text{Ca}}} \quad (1-5)$$

where  $Y_{\text{Na}}$  and  $Y_{\text{Ca}}$  are the equivalent fraction of  $\text{Na}^+$  and  $\text{Ca}^{2+}$  in the resin phase

$X_{\text{Na}}$  and  $X_{\text{Ca}}$  are the equivalent fraction of  $\text{Na}^+$  and  $\text{Ca}^{2+}$  in the liquid phase,

$q_{Na}$ ,  $q_{Ca}$ , and  $q$  represent the concentration of  $Na^+$ ,  $Ca^{2+}$ , and total capacity in the resin,  $C_{Na}$ ,  $C_{Ca}$ , and  $C$  represent the concentration of  $Na^+$ ,  $Ca^{2+}$ , and total ionic concentration of the liquid.

Using the combination of eq. 1-4 and eq. 1-5 gives:

$$\alpha_{Ca/Na} = K_{Ca/Na} \frac{q_{Na}}{C_{Na}} \quad (1-6)$$

For heterovalent exchange (divalent/monovalent), the separation factor ( $\alpha_{i/j}$ ) depends inversely on solution concentration  $C$  and directly on the distribution ratio  $Y_{Na}/X_{Na}$  or  $q_{Na}$  between the resin and the water, with  $q$  constant. The higher concentration  $C$ , the lower the divalent/monovalent separation factor (i.e., selectivity will reverse in favor of the monovalent  $Na^+$  ion). That is why a traditional water softening process using SAC can be regenerated with high concentration of salt (10-12% NaCl) as the concentration is high enough to cause selectivity reversal. From figure 1.4, the high concentration of  $Na^+$  ion is concentrated in the resin (y axis) at high TDS of the solution (150,000 mg/L or 15%).

For water softening processes, high concentrations of salt (12-15% NaCl) or aggressive acid (5% HCl) are usually used to regenerate the resin resulting in high concentration of waste discharged from the process. High concentration of brine or acid is needed to drive the reaction to overcome the selectivity reversal. Waste brine solutions correspond with high total dissolved solids (TDS) in aquatic systems, which is harmful to aquatic life. There are regulations for salt-free regeneration of water softeners throughout the US, notably with recent legislation in California, Texas, and Florida. Effluents with high sodium or TDS also cause significant problems to water reclamation and reuse

facilities and septic systems. There is a need for clean technology that avoids discharge of high concentrations of salt into natural waters or using a mild acid solution for regeneration of WAC resins that can be used for household water softeners.

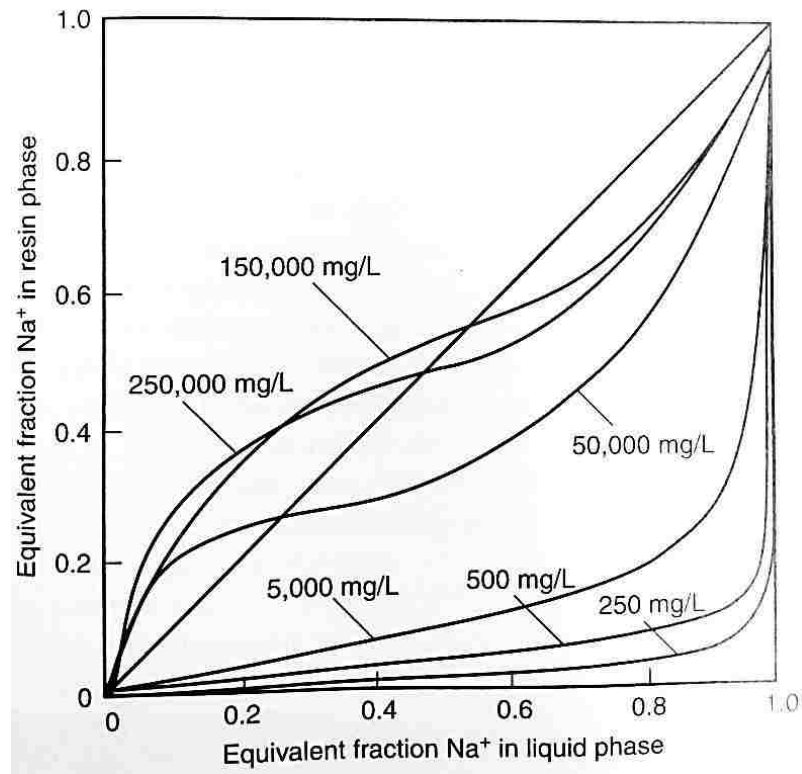


**Figure 1.4** The Na<sup>+</sup>-Ca<sup>2+</sup> equilibrium for sulfonic acid cation exchange resin (4)

## **1.2 Hybrid Polymeric Ion Exchanger Supported Hydrated Zr(IV) Oxide Nanoparticles for Selective Removal of Trace Anionic Ligands and Heavy Metals**

### **1.2.1 Trace Environmental Contaminants: Ligands and Heavy Metals**

Many environmental ionic contaminants of concern such as heavy metals (e.g.,  $\text{Zn}^{2+}$ ,  $\text{Pb}^{2+}$ ,  $\text{Cd}^{2+}$ ,  $\text{Ni}^{2+}$ , etc.) and anionic ligands (e.g., arsenate, phosphate, fluoride, selenite, etc.) are very toxic and present in water body at trace concentration (typically in the range of ppm and may be as low as ppb level). As mentioned earlier, traditional cation and anion exchangers cannot remove these contaminants if high concentrations of innocuous cations (i.e.,  $\text{Ca}^{2+}$ ,  $\text{Mg}^{2+}$ , etc.) and anions (i.e.,  $\text{SO}_4^{2-}$ ,  $\text{Cl}^-$ ,  $\text{HCO}_3^-$ , etc.) are also present in the aqueous phase. Important trace anionic contaminants can be categorized as anionic ligands (Lewis bases) or anions that can form strong complexes with metal ions (Lewis acids). Examples of the Lewis-base type contaminants include phosphate, arsenate, chromate, selenite, cyanide, oxalate, and phthalate. Because of the associated environmental impacts and health risks, these Lewis-base type contaminants are often subject to stringent environmental regulations. Arsenic and fluoride are selected for the sorption study due to the massive-scale of health problems. There are several hundred million people mainly in Asia (e.g., India, Bangladesh, China, Vietnam, and Cambodia), South America (e.g., Argentina, Mexico), Africa, including many states in the US that are contaminated with arsenic and fluoride in the groundwater (9-14).

Many technologies have been used to remove these contaminants such as chemical precipitation/ co-precipitation, membrane processes (e.g., reverse osmosis (RO)

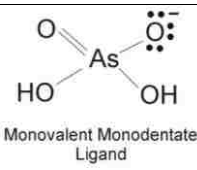
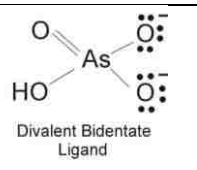
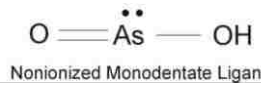
and nanofiltration (NF)), but removal of such low concentrations are faced with many challenges to meet the stringent standards, be cost effective, and remain a sustainable processes. For example, the chemical precipitation techniques result in residual contaminants (cannot meet the standard) due to the solubility limit and generate a large quantity of sludge which is both environmental and economic issues. Similarly, most of the membrane processes are complex and require a high investment and operating cost and thus are not suitable for use in certain areas. Fixed-bed adsorption processes or ion exchange technology can remove contaminants to near zero concentration, are simple to operate, and open the possibility for concentrating these toxic compounds and/or reuse for some industries. Two main technologies that are compatible and suitable for the fixed-bed configuration are ion exchange and adsorption onto metal oxide particles.

### **1.2.2 Arsenic and Fluoride Problems**

Arsenic is a metalloid mostly found in groundwater due to natural weathering reactions. The speciation of arsenic depends on the pH and redox of the water body. Arsenic is present mostly as inorganic arsenate or As(V) and arsenite or As(III) as shown in the table 1.2 and figure 1.5. Studies have demonstrated that chronic exposure to arsenic can lead to liver, lung, kidney, bladder, and skin cancer cause cardio vascular system problems, and affect the mental development in children. **(15, 16)** Accordingly, the United States Environmental Protection Agency (USEPA) revised the maximum contaminated levels (MCL) for arsenic in drinking water from 50 to 10 µg/L in 2001, and required compliance with this level since January 2006. Note that estimates of people at risk of poisoning are very difficult to quantify, particularly in areas where geochemical

surveys are limited. The worldwide distribution of arsenic contaminated regions is provided in the figure 1.6. (17)

**Table 1.2** Oxyacids and Conjugate Anions of As(V) and As(III) (15, 16)

Parent oxyacids	pKa values	Predominant dissolved species at pH 6.0	Predominant dissolved species at pH 8.0	Sorption interaction
As(V): $\text{H}_3\text{AsO}_4$	$\text{pK}_{a1} = 2.2$ $\text{pK}_{a2} = 6.98$ $\text{pK}_{a3} = 11.6$	 Monovalent Monodentate Ligand	 Divalent Bidentate Ligand	Undergo Coulombic and Lewis acid-base interaction
As(III): $\text{HAsO}_2$	$\text{pK}_{a1} = 9.2$	 Nonionized Monodentate Ligand		Only Lewis acid-base interaction

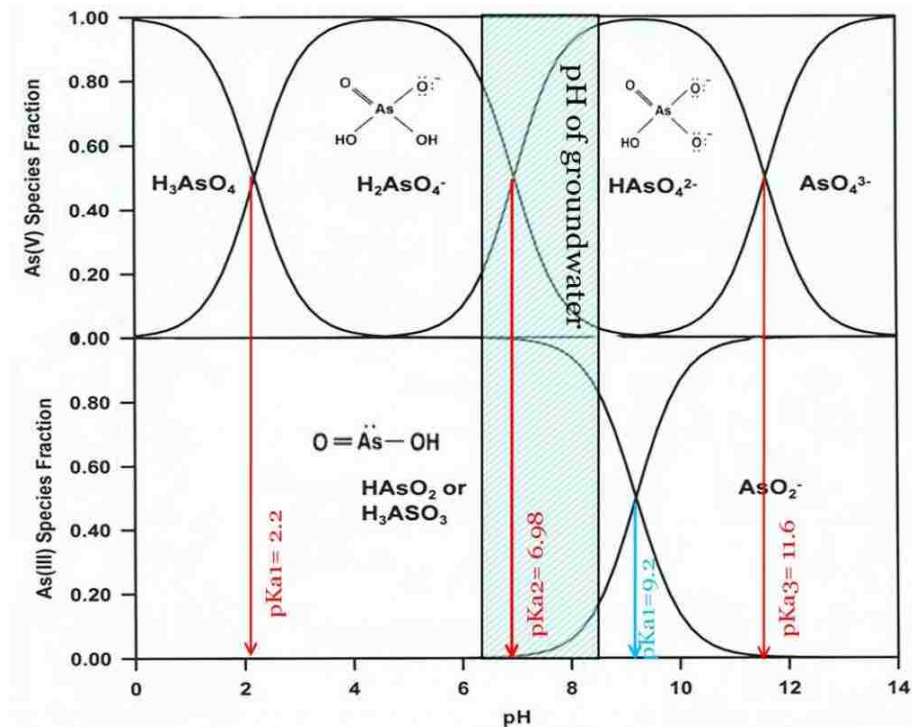


**Figure 1.5** Distribution of As(V) and As(III) oxyacids and their conjugate anions as a function of pH (16)

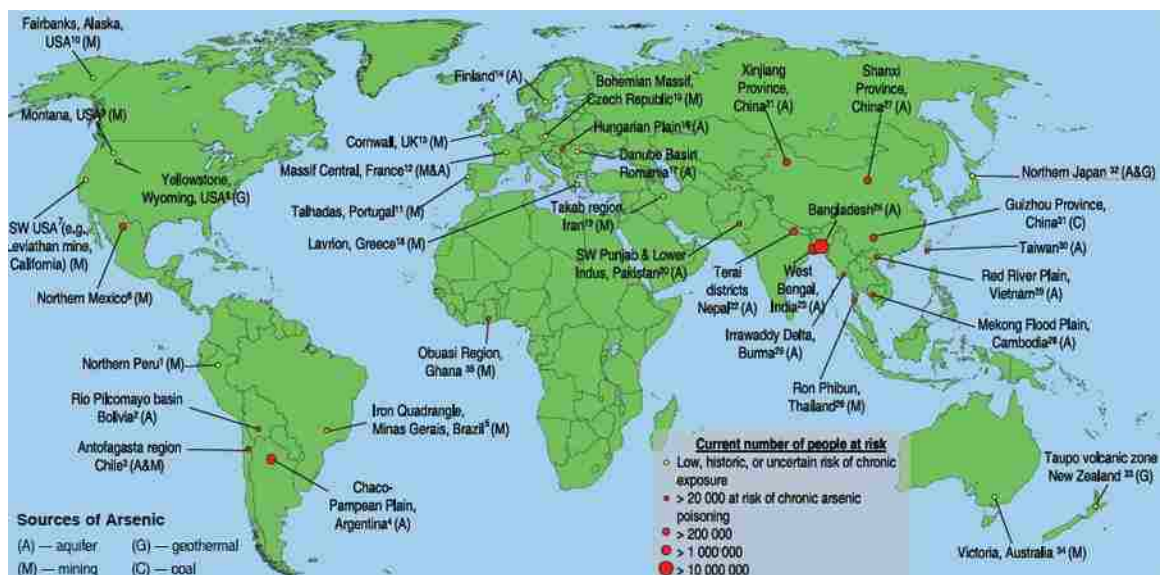


**Figure 1.6** Worldwide distributions of arsenic contaminated regions, showing source of arsenic and numbers of people at risk of chronic exposure (17)

Fluoride contamination in drinking water sources has also attracted attention in relation to its adverse health effects such as dental and skeletal fluorosis. More than 70 million people are suffering with fluorosis globally. The MCL from USEPA is 4 mg/L. However, the World Health Organization (WHO) recommended guideline is only 1.5 mg/L (18). Globally, high fluoride levels are found in belts that stretch from Syria through Jordan, Egypt, Libya, Algeria, Sudan, Kenya, Tanzania and from Turkey through Iraq, Iran, Afghanistan, India, Thailand and China.(19) The fluoride probability model in groundwater exceeding WHO guideline of 1.5 ppm is shown in the figure 1.7A (14) and the fluoride map for the affecting countries is also given in the figure 1.7B (20).



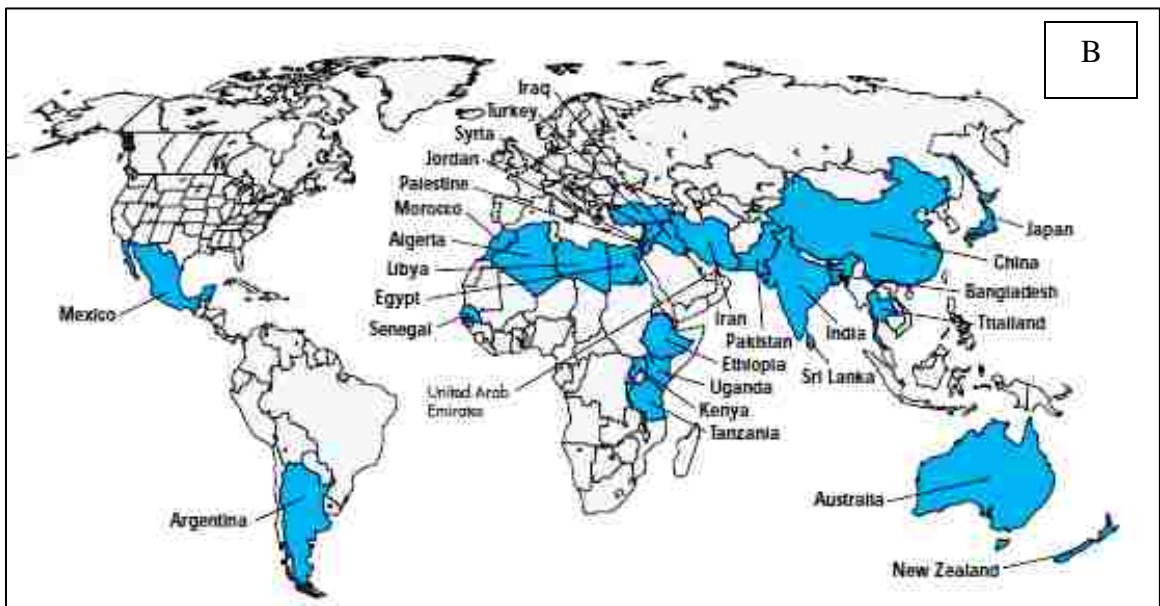
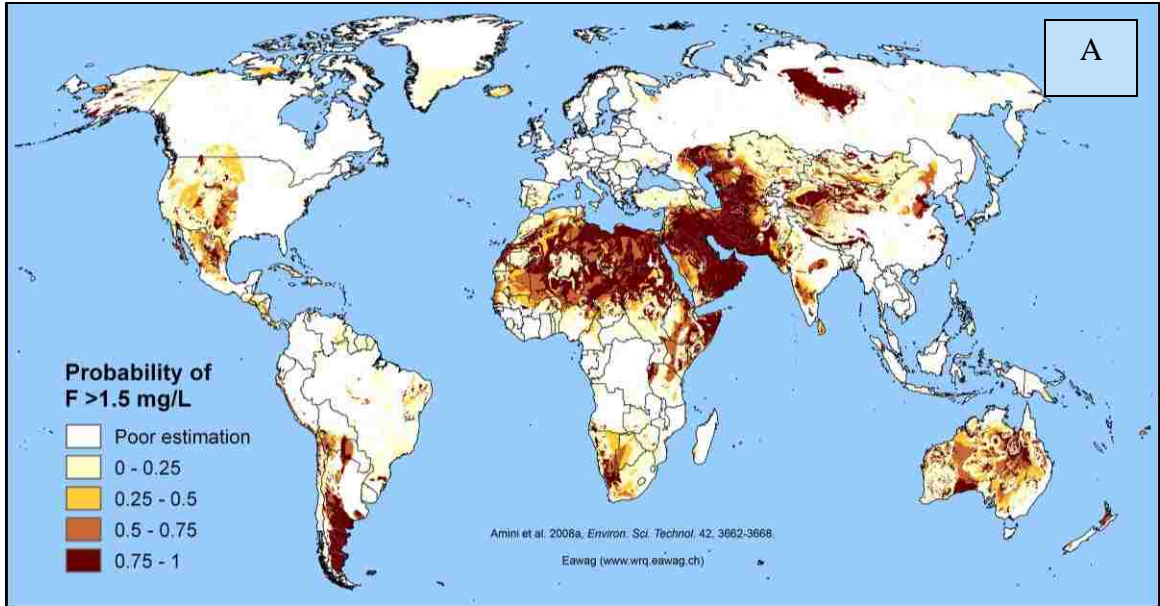


**Figure 1.7** Model global probability of fluoride concentration in groundwater exceeding the WHO guideline for drinking water of 1.5 mg/L (14, 20)

### 1.2.3 Adsorption by Metal Oxide Particles and Their Limitation

Oxides of some polyvalent metals such as Al(III), Fe(III), Si(IV), Ti(IV), Zr(IV), etc. are environmentally benign, and exhibit amphoteric sorption properties near neutral pH(21). They can selectively bind both Lewis acid or transition metal cations (e.g.,  $Zn^{2+}$ ,  $Cu^{2+}$ , etc.) and Lewis bases or anionic ligands (e.g., arsenic, phosphorus, fluoride, etc.) through the formation of inner-sphere complexes (19, 22-30). Unlike traditional cation exchangers, these metal oxide particles can selectively sorb trace toxic concentrations of transition metal cations (e.g.  $Zn^{2+}$ ,  $Cu^{2+}$ , etc.) in preference to other competing high concentrations of innocuous alkaline or alkaline earth metals such as  $Ca^{2+}$ ,  $Mg^{2+}$ ,  $Na^{+}$ . Similarly, these metal oxides can selectively bind with trace anionic ligands (e.g., arsenic, phosphorus, fluoride, etc.) within the presence of high concentrations of competing anions such as sulfate, nitrate, chloride, and bicarbonate. The advantages and disadvantages between the tradition polymeric ion exchangers and the metal oxide particles are summarized in the table 1.3.

The methodology of preparation of these inorganic metal oxide nanoparticles is environmentally safe, operationally simple, and inexpensive. Because sorption sites reside predominantly on the surface, the nano-scale metal oxide particles offer very high sorption capacity and rapid kinetics. However, the metal oxide particles cannot be used in fixed-bed columns, in groundwater reactive barriers, or in any plug flow type configurations due to excessive pressure drops. Also, these inorganic nanoparticles are not durable and lack mechanical strength.

**Table 1.3** Advantages and disadvantages of ion exchange and metal oxide adsorption  
adapt from Clifford (2)

---

### **Polymeric Ion Exchange Process**

#### **Advantages**

- Essentially zero level of effluent concentration possible
- Relatively insensitive to flow variations, operate on demand, influent concentration
- Be able to operate without electricity
- Large variety of specific resins available for specific applications
- Beneficial selectivity reversal commonly occurs upon regeneration

#### **Disadvantages**

- Not selective toward trace concentration at high levels of competing ions
  - Not feasible at high level of total dissolved solids
  - Potential for chromatographic elution
  - Large volumes and high concentration of TDS from spent regeneration solution
- 

### **Adsorption by Polyvalent Metal Oxide Particles**

#### **Advantages**

- Essentially zero level of effluent concentration possible
- Relatively insensitive to flow variations, operate on demand, influent concentration
- Relatively insensitive to the presence of competing ions and total dissolved solids
- Highly selective toward trace concentration of transition metals and anionic ligands such as arsenic, phosphate, and fluoride

#### **Disadvantages**

- Media tend to dissolve (some metal oxide exhibit chemical instability), producing fine particles (low mechanical strength and attrition resistant)
  - Inefficient to regeneration (for granulated type metal oxide adsorbents )
-

Many studies attempt to develop metal oxide based hybrid sorbents such as activated carbon, alginate, chitosan, cellulose and polymer beads doped with metal oxide nanoparticles. These hybrid sorbents improve the permeability in the fixed-bed systems, but most of them have low sorption capacity and unreliable results. The granulated typed metal oxide sorbents such as granulated ferric oxide (GFO), granulated titanium oxide (GTO), mesoporous zirconium oxide particles, and activated alumina (AA), etc. have been developed, and are currently available in the market for the removal of arsenic, fluoride and other contaminants (31, 32). Although these commercial granulated metal oxide adsorbents offer higher sorption capacity than the previously mentioned hybrid sorbents, they also have improved permeation in the fixed-bed systems. However, they exhibit a low attritional resistance (i.e., fine particles are formed) and are not effectively regenerated, thus they are mostly recommended for a single usage (23, 33). Note that the commercially mesoporous zirconium oxide sorbents cannot be directly used in the fixed-bed column, and a high pressure pump is needed to operate the system.

Activated alumina has been reported to have low mechanical strength (i.e. it turns into fine particles after several cycles), low sorption capacity at neutral pH, and is unable to remove As(III) effectively. Moreover, the exhausted materials generate a waste contaminated with high concentrations of toxic arsenic and pose a significant risk to the environment (i.e., iron based sorbents) (34, 35). Currently, there is no sustainable, long term adsorbent for both contaminants. There is the need to develop sorbents that exhibit high affinity and have high capacity toward target anionic ligands, able to be regenerated to reduce the cost of operation, minimize the waste generated from the process, and it

should be safe to dispose the exhausted sorbent into a landfill without a risk of toxic materials leaching into the environment.

### 1.2.4 Mechanism of Ligand and Heavy Metal Sorption onto the Surface of Metal Oxide Particles

The hydrated metal oxides show strong Lewis acid-base characteristics; the central metal atom exhibits Lewis acid character (electron pair acceptor) while the oxygen exhibits Lewis base behavior (electron donor). They can selectively bind transition metal cations (Lewis acids) e.g.,  $Zn^{2+}$ ,  $Cu^{2+}$ ,  $Cd^{2+}$  and anionic ligands (Lewis bases) e.g.,  $HAsO_4^{2-}$ ,  $CrO_4^{2-}$ ,  $HPO_4^{2-}$ ,  $F^-$  through the formation of innersphere complexes both individually and simultaneously.(36)

The hydrated metal oxides can be viewed as diprotic weak acids that can deprotonate as follows:



Depending on pH, the hydrated metal oxide surface may exhibit fixed positive charges, negatively charges, or be electrically neutral. At a pH lower than the point of zero charge (PZC), the metal oxides are protonated ( $\overline{MOH_2^+}$ ) to have positive charges and behave as a Lewis acid (electron pair acceptor). These metal oxides can selectively sorb anionic ligands (arsenic, phosphorus, fluoride, etc.) which act as a Lewis base (electron donor). At a pH greater than their PZC, the surface of metal oxides are deprotonated ( $\overline{MO^-}$ ) to have negative charges and exhibit Lewis base characteristics which can selectively bind with Lewis acid contaminants such as transition metals (e.g.  $Zn^{2+}$ ,  $Cu^{2+}$ ,

$\text{Ni}^{2+}$ ,  $\text{Pb}^{2+}$ , etc.). Note that other competing cations (e.g.,  $\text{Na}^+$ ,  $\text{K}^+$ ,  $\text{Ca}^{2+}$ , etc.) and anions (e.g.  $\text{SO}_4^{2-}$ ,  $\text{HCO}_3^-$ ,  $\text{Cl}^-$ ) form only weak outer sphere complexes through electrostatic (Coulombic) interactions, thus they poorly bind onto the surface of metal oxides.(36) Since sorption or binding sites reside only on the surface, nanoscale metal oxide particles with very high surface area to volume ratio offer significantly enhanced sorption capacity. Figure 1.8 shows the binding of various contaminants on the hydrated metal oxide particles through the formation of inner-sphere complexes.

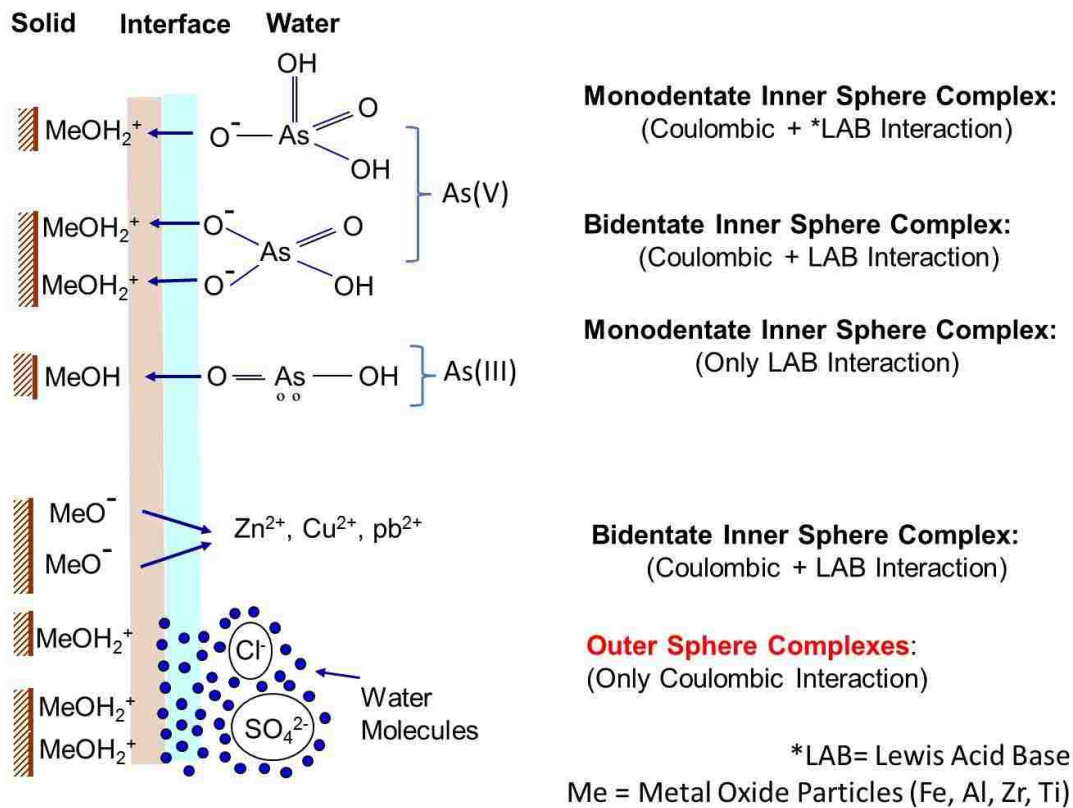


**Figure 1.8** A schematic diagram illustrating the binding of several of solutes onto hydrated metal oxides at circum-neutral pH

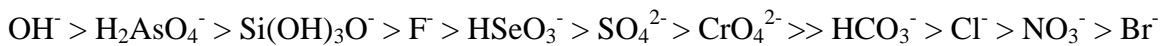
The selective sorption of transition metal cations and anionic ligands onto the surface of the metal oxide can be expressed according to the complexation model adsorption reaction. At the standard state, the overall free energy at equilibrium between surface of metal oxide and transition metals or anionic ligands is given by the following **(8, 16)**:

$$\Delta G_{\text{Overall}}^0 = \Delta G_{\text{Cou}}^0 + \Delta G_{\text{LAB}}^0 \quad (1-9)$$

$$-RT \ln K_{\text{Overall}} = -RT \ln K_{\text{Cou}} - RT \ln K_{\text{LAB}} \quad (1-10)$$

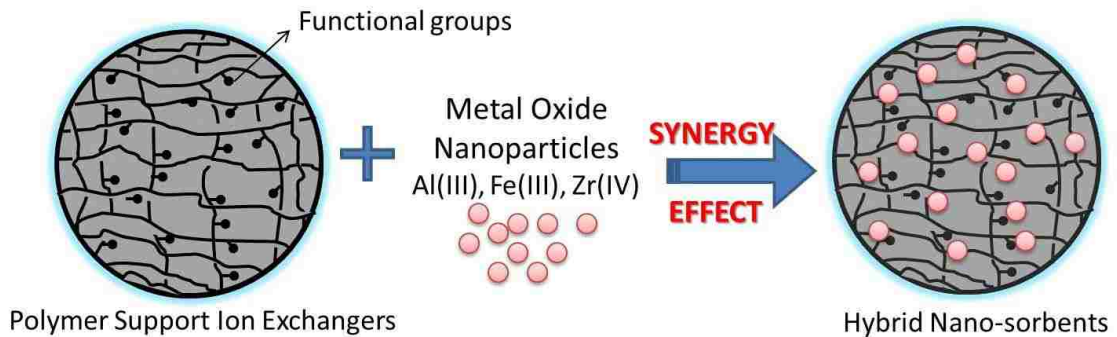
$$K_{\text{Overall}} = K_{\text{Cou}} * K_{\text{LAB}} \quad (1-11)$$

For the metal oxide,  $K_{\text{LAB}}$  is very high for most of the heavy metals and anionic ligands due to their Lewis acid base characteristics. Therefore  $K_{\text{Overall}}$  is very high. In contrast with other competing cations (e.g.,  $\text{Na}^+$ ,  $\text{K}^+$ ,  $\text{Ca}^{2+}$ , etc.) and anions (e.g.  $\text{SO}_4^{2-}$ ,  $\text{HCO}_3^-$ ,  $\text{Cl}^-$ ), the Lewis acid-base (LAB) is absent so  $K_{\text{Overall}}$  is equal to the  $K_{\text{Cou}}$ . Based on this concept, there are many applications based on the Lewis acid base interaction for selective removal of trace concentrations of toxic heavy metals and anionic ligands such as chelating resins for trace metal removal, granulated metal oxides for selective removal of arsenate, phosphate, fluoride, etc. With  $K_{\text{Overall}} \gg K_{\text{Cou}}$ , the selectivity sequence will change dramatically compares to the traditional exchange. For example, the sorption of many contaminants using activated alumina (AA) operated in the pH range of 5.5 to 8.5 prefers anions in the following order **(2)**:



### 1.2.5 Concept of Hybrid Polymeric/ Inorganic Ion Exchanger

To overcome the disadvantageous of nano-scale metal oxide particles, it would be desirable to encapsulate these nanoparticles within robust support materials which can offer excellent mechanical strength, durability, and favorable hydraulic properties. A hybrid ion exchanger essentially contains two phases: a functionalized polymeric ion exchanger host and metal oxide nanoparticles dispersed within the polymer phase as illustrated in figure 1.9.



Polymer support Ion Exchanger	Metal Oxide Nanoparticles
<b>Pros</b>	
High mechanical strength, Improve water permeation, Exert "Donnan membrane effect" (enhanced sorption capacity and kinetics)	High sorption capacity, Regenerable (due to amphoteric properties), Selective toward anionic ligands (i.e. arsenate, phosphate)
<b>Cons</b>	
Not selective toward trace anionic ligands (i.e. arsenate, phosphate)	Low mechanical strength, Impermeable in fixed bed systems

**Figure 1.9** The concept of polymer-supported inorganic metal oxide nanoparticles or hybrid ion exchanger



These hybrid nanosorbents incorporate some of the advantageous properties of several current anionic ligand (e.g., arsenate, phosphate, etc.) or heavy metal (e.g. zinc, copper, etc.) removal technologies. While traditional anion/cation exchange resins offer excellent hydraulic properties, the target contaminant (trace anionic ligands and transition metals) selectivity is relatively poor, especially in the presence of competing ions. Also, ion exchange resins show no affinity toward nonionic species such as As(III) at circum-neutral pH. Conversely, metal oxides such as hydrated Fe(III) oxide particles or HFO offer excellent heavy metals and anionic ligands such as arsenic selectivity for both anionic As(V) and non-ionized As(III) species, but perform poorly in terms of hydraulic properties and mechanical strength. By dispersing metal oxide nanoparticles into the ion exchanger, excellent hydraulic properties and heavy metals or anionic ligands e.g. arsenic, phosphorus, fluoride selectivity can be effectively integrated. These advantages and disadvantages are summarized in table 1.4.

**Table 1.4** Synergy Effect of Hybrid Ion Exchanger

<b>Properties</b>	<b>Polymer Support Ion Exchangers</b>	<b>Metal Oxide Nanoparticles</b>	<b>Hybrid Ion Exchangers</b>
Environmental safe	Yes	Yes	Yes
Suitable for fixed bed	Yes	No	Yes
Ability to regenerate/reuse	Yes	No	Yes
Mechanical strength	High	Low	High
Enhanced kinetics/ capacity by exert Donnan membrane effect	Yes	No	Yes
Surface area	Medium	High	High
Selectivity toward arsenic and toxic metal	Low	High	High

### 1.2.6 Role of Donnan Membrane Effect

In the past, hydrated ferric oxide (HFO) nanoparticles were dispersed in both spherical polymeric cation and anion exchanger beads containing sulfonic acid and quaternary ammonium functional groups, respectively (15, 29, 37). These hybrid cation and anion exchangers containing impregnated HFO nanoparticles have distinctly different sorption properties. Due to the Donnan membrane effect, the hybrid anion exchanger (HAIX) allows enhanced permeation of arsenate oxyanions inside the anion exchanger, and subsequently selectively bind onto dispersed HFO nanoparticles.

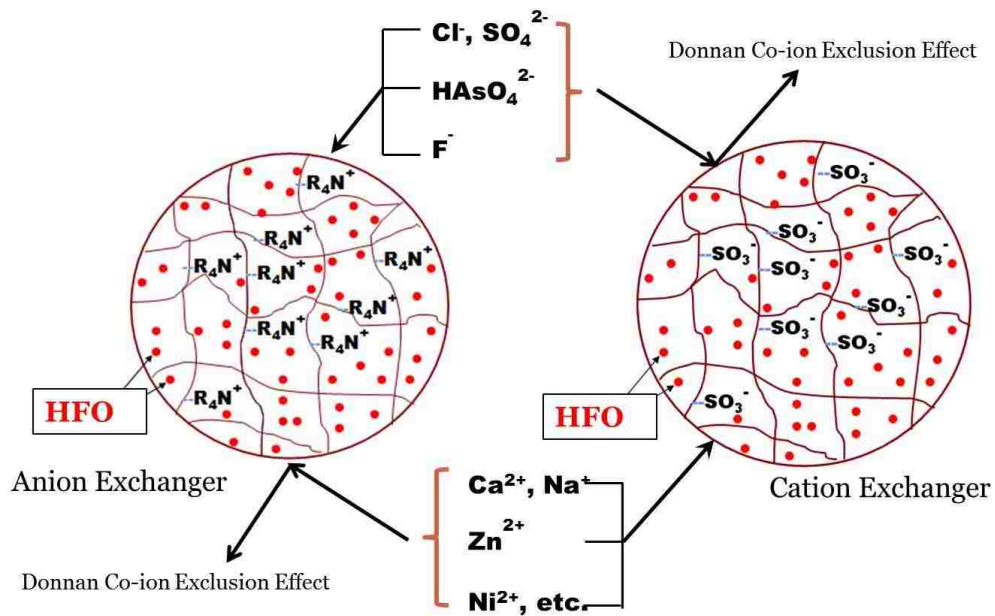


**Figure 1.10** Donnan membrane effect from the parent ion exchanger

Activated carbon, alginate, and porous polymers have also been used as host materials for doping HFO, but the favorable Donnan membrane effect is absent in these

hybrid materials (**38, 39**). The HAIX-Fe, now commercially available as LayneRT, offers a very high selectivity for sorption of arsenic due to the Donnan membrane effect as illustrated in figure 1.10. The choice of the ion exchanger host material for HFO nanoparticles can completely reject the transition-metal cations while allowing enhanced selective sorption of anionic ligands and vice versa. Thus, in principle, an amphoteric metal oxide nanoparticle can be tailored to behave either as a strictly metal-selective sorbent or as a ligand-selective exchanger. The HFO particles which are dispersed within the hybrid nanosorbents efficiently remove dissolved ligands such as oxyacids and oxyanions of As(III), As(IV), and phosphorus from the background of commonly occurring anions namely  $\text{Cl}^-$ ,  $\text{SO}_4^{2-}$ ,  $\text{NO}_3^-$ , etc. They are also capable of selectively removing heavy metal cations such as  $\text{Zn}^{2+}$ ,  $\text{Cu}^{2+}$ , and  $\text{Cd}^{2+}$  from the background of cations including  $\text{Na}^+$ ,  $\text{K}^+$ ,  $\text{Mg}^{2+}$ ,  $\text{Ca}^{2+}$ , etc.

### **1.2.7 Disadvantages of Hydrated Fe(III) Oxide (HFO) Nanoparticles**

Currently in developed western nations, toxic materials such as arsenic-laden sludge and/or adsorbents are routinely disposed of in landfills. However, several recent investigations have revealed that leaching of arsenic is stimulated or enhanced in a landfill or a hazardous waste site environment (**34, 35**). Both pH and redox conditions uniquely determine speciation of arsenic and iron that in turn controls arsenic leachability. From the composite predominant diagram (pe-pH diagram) as illustrated in figure 1.11, Fe(II) and As(III) are practically the sole species in the reducing landfill environment. The relatively high solubility of Fe(II) and low sorption affinity of As(III)

would always render the iron-laden sludge more susceptible to rapid leaching under the oxygen-starved environment of the landfill or underground waste site.

### 1.2.8 Use of Chemically Stable Hydrated Zirconium Oxide (HZO) Nanoparticles

For this study, new hybrid polymeric ion exchangers were developed by using the hydrated zirconium oxide (HZO) nanoparticles instead of previously used hydrated ferric oxide (HFO). The HZO nanoparticles also exhibit high selectivity toward both transition metals and anionic ligands. The HZO have higher chemical stability than the HFO. Therefore, the used sorbents can be disposed of safely in landfills without the chance of metal reduction, and toxic leaching which can occur with the HFO based nanosorbents. Moreover, the HZO particles also exhibit fluoride sorption property while HFO particles are not.

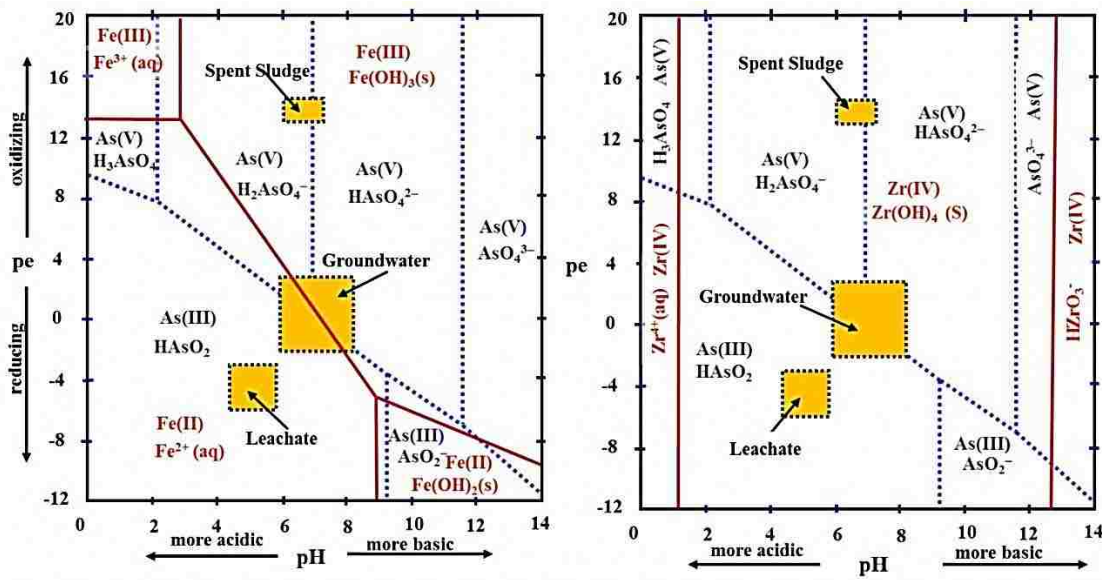


**Figure 1.11** Composite predominant diagram, Fe- As and Zr-As (adapt from (40))

Unlike HFO, HZO particles are chemically stable under the reducing environment of landfills. Figure 1.11 (RHS) shows the composite predominance diagram for various arsenic and zirconium species. Zr(IV) species are the sole species in both oxidizing and reducing environments. It will be safe to dispose of the materials laden with arsenic in the reducing environment such as in landfills. Both amorphous and crystalline HZO exhibit strong sorption affinity toward both As(III) and As(V) oxyacids and oxyanions through ligand exchange in the coordination spheres of structural Zr atoms **(23)**. Figure 1.11 (LHS) represents the composite pe-pH diagram for arsenic-iron. Note that Fe(III) and As(III) predominate in the oxidizing environment while reduced Fe(II) and As(III) are practically the sole species in the reducing environments such as in a landfill. Unlike Fe(III), Zr(IV) is chemically stable under reducing environment such as landfill. In general tetravalent metals bind to oxygen so strongly that dissolved complexes are partly deprotonated in aqueous solution. Corresponding zirconia ( $ZrO_2$ ) is virtually insoluble in aqueous solution as shown in figure 1.12.**(41)** The major environmental challenge lies not just in removing dissolved arsenic or other contaminants from contaminated groundwater but also in attaining safe, long term disposal of toxic-laden sludge. The volume of sludge is often small, but disposal of used iron based sorbent laden arsenic in the reducing environment of a landfill will stimulate iron reduction and release arsenic into environment.

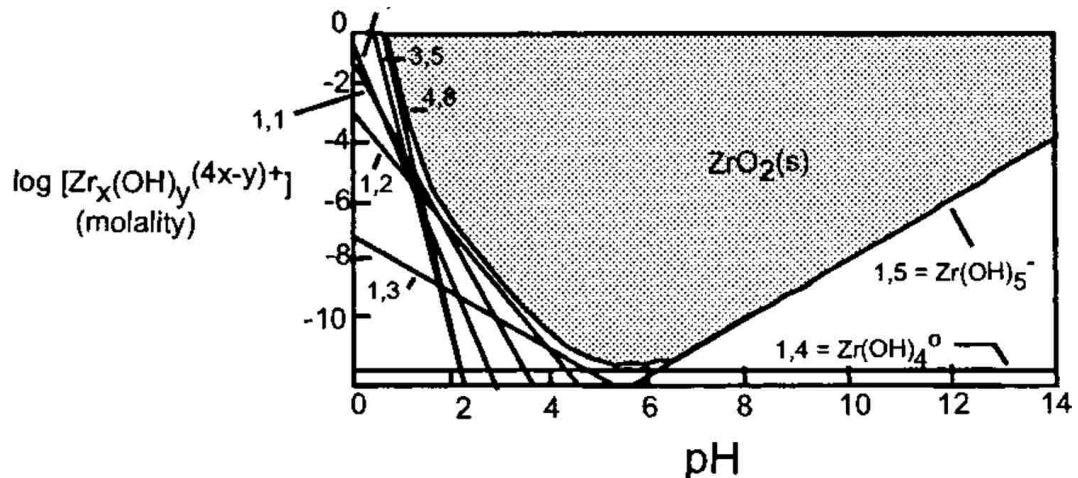


**Figure 1.12** Speciation of zirconium products as a function of solution pH (41).

### 1.3 Water Softening: Problems, Challenges, and New Opportunities

Hardness is caused by the presence of polyvalent cations mainly divalent cations such as calcium, magnesium, and iron. The hardness is usually expressed as milligrams per liter as  $\text{CaCO}_3$  and classified into soft water (0-60 mg/L), moderately hard water (61-120 mg/L), hard water (121-250 mg/L), and very hard water (250+ mg/L) as  $\text{CaCO}_3$  (42, 43). Many industrial unit operations and unit processes require near-complete removal of hardness (e.g., to minimize scale in heat transfer equipment, to prevent fouling in membranes, high concentrations of detergents and sequestering chemicals in cooling and wash water). The scale ( $\text{CaCO}_3$ ) precipitated in heating pipes is shown in the figure 1.13A. The distribution of hard water throughout the United States is shown in figure 1.13B.

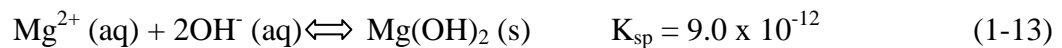
Hardness can be classified based on the anions associated with the cations (2):

- **Carbonate hardness:** Carbonate hardness or temporary hardness is caused by cations from the dissolution of calcium and magnesium carbonate and bicarbonate in the water.
- **Non-carbonate hardness:** Non-carbonate hardness or permanent hardness is caused by cations from calcium and magnesium compounds of sulfate, chloride, or silicate that are dissolved in the water.
- **Total hardness:** Total hardness represents the sum of multivalent cations which are mainly calcium and magnesium.

### 1.3.1 Current Technology: Problems and Challenges

#### 1.3.1.1 Lime–Soda Softening

Lime soda softening removes hardness through chemical addition. This process is operationally simple and suitable for large scale softening unit operations. In general, the chemicals required are inexpensive. However, calcium removal is limited to 35 mg/L as CaCO<sub>3</sub> and magnesium removal is 12 mg/L due to the solubility of the product species listed in the following reactions. The following precipitation reactions govern this process:



The disposal of residuals produced as a byproduct in the water treatment processes represents a significant portion of the overall treatment cost. To minimize the weight of these solids, the water content is often reduced through the use of a vacuum

filter, or belt press. Such unit processes add significant operating cost, space, and complexity to any treatment process scheme.

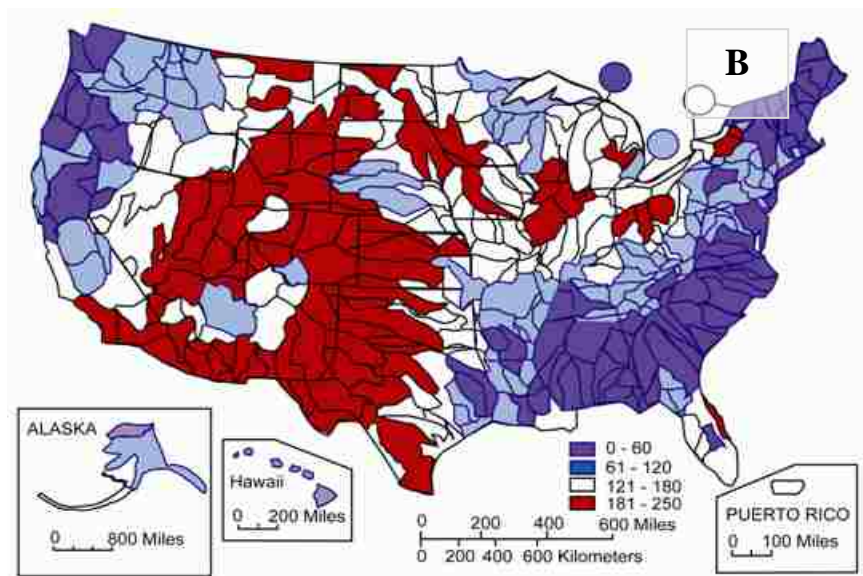


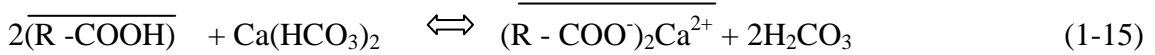
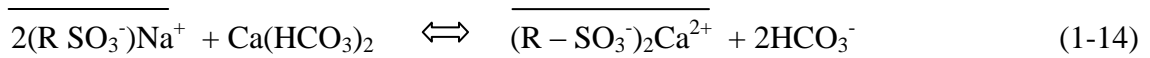
**Figure 1.13 (A) pipe scaling due to the presence of hardness in water (42)**

**(B) Distribution of hard water as milligram per liter as CaCO<sub>3</sub> in the United States (43)**

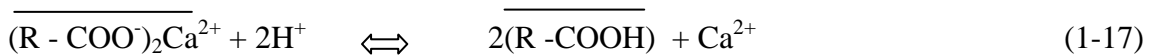
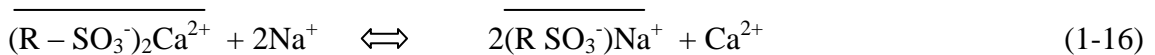


### 1.3.1.2 Ion Exchange Processes

Ion exchange softening processes are common at both industrial and residential scales. The calcium or magnesium ions that constitute hardness are exchanged with sodium or hydrogen ions from the ion exchanger phases. The following reactions are representative of the sorption steps in a traditional strong and weak acid ion exchange processes for removal of temporary hardness, respectively:



where the overbar represents the ion exchange phase of the strong acid cation exchanger in a sodium form containing sulfonic acid ( $-\text{SO}_3^-$ ) functional groups and the weak acid cation exchanger in a hydrogen form containing carboxylic ( $-\text{COO}^-$ ) functional groups. Once the exchange capacity of the resin has been exhausted, the material must be either regenerated using a concentrated sodium chloride solution at approximately 10-12% (for SAC resins) or an inorganic acid solution around 5% HCl (for WAC resins):



The strong acid cation (SAC) exchange resins have been widely used in both household and industrial softening processes. Regeneration is accomplished by passing a concentrated 10-12% brine solution through the calcium and magnesium saturated bed. At these high salt concentrations, the resin undergoes a phenomenon called “selectivity reversal”, allowing the sorbed calcium or magnesium to be exchanged for sodium. These

salt concentrations are greatly in excess of the ion exchange stoichiometry, which results in the formation of the brine-laden waste (containing sodium, calcium, magnesium, and chlorine). In certain areas, these salt discharges can pose an environmental threat. For example, in California and Arizona, where there is a significant level of evaporation, salt discharged can add to the already high total dissolved solids (TDS) content for receiving water bodies. Under such circumstances, any increase in TDS can pose a distinct threat to aquatic lives, plants, and agricultural production.

### **1.3.2 Need for Salt/Acid Free Water Softening Processes**

Traditional hardness removal processes use strong acid cation (SAC) exchangers in the  $\text{Na}^+$  form. Calcium, magnesium, and other polyvalent cations corresponding to the hardness are exchanged with the sodium in resin phase. Exhausted resins are typically regenerated with brine solution such as sodium chloride, potassium chloride with high concentration approximately 10-12 % to overcome selectivity reversal. This process is inefficient and requires an excess amount of brine solution resulting in excess brine discharge of nearly 50%. Both waste brine solution corresponds to high TDS in aquatic system and harmful for aquatic life, there are regulations for “salt ban regeneration water softening processes” mainly in California and other states throughout the United States. Moreover, sodium ions which exchanged with hard ions (i.e.  $\text{Ca}^{2+}$ ,  $\text{Mg}^{2+}$ ) from water are added into treated water with the same amount (meq.) of the calcium being exchanged. The adding of sodium to treated water may cause a problem especially for the people who have heart-related diseases. There is a need for salt free technology.

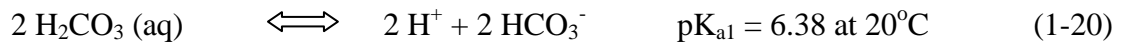
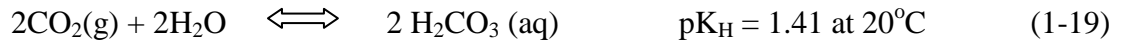
### 1.3.3 Previous Development of Salt-Free Water Softening Process Using IX-Fibers and CO<sub>2</sub> Regeneration

Based on an earlier study, an environmentally benign hardness removal process using IX fibers has been developed (44, 45). The process is illustrated in figure 1.14. Ion exchange fibers from the heart of the process offer unique opportunities to use and consume CO<sub>2</sub> for efficient regeneration. The fibers are essentially long polypropylene cylinders with an average diameter of approximately 25 μm as illustrated in figure 1.15. Ion exchange fibers containing carboxylate (-COOH) functional groups are the sorbent for the process, and the following steps constitute the softening process. F represents the fiber matrix and the overbar denotes the solid phase:

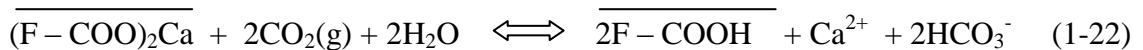
#### 1. Hardness removal by ion exchange fibers



#### 2. Regeneration with CO<sub>2</sub> sparged water



#### 3. Overall:



**IX-Fibers vs. IX Resins: Regeneration Mechanism:** The affinity sequence for WAC fibers with carboxylic functional groups can be described as follows: H<sup>+</sup> >> Ca<sup>2+</sup> > Na<sup>+</sup>. For this reason, hydrogen ions as provided by the carbonate system (eq. 1-20) can be

an effective regenerant for IX-fibers used in the removal of hardness. The above mentioned reactions (eqs.1-18-22) are equally applicable for commercial weak-acid cation exchange resins. However, the mechanism of sorption/desorption kinetics is intrinsically different between IX-fibers and commercial resin beads. That is why commercial ion exchange resins are not amenable to regeneration with carbon dioxide. In figure 1.16, the resin gradually shrinks during the regeneration progress through the exchange of  $\text{Ca}^{2+}$  and  $\text{H}^+$ . This exchange would thereby decrease the intra-particle diffusivity in the peripheral regions of the resin. On the contrary in ion exchange fibers, the functional groups essentially reside on the surface and they are readily accessible. Thus, intra-particle diffusion is nearly absent and protonation of weak-acid functional groups do not retard the regeneration process.

### **1.3.4 Development of Salt-free Water Softening Processes**

#### **1.3.4.1 Use of Shallow Shell Technology (SST) Resin and Solid $\text{CO}_2$ Regeneration**

Due to the limitation of IX fibers in regards to the commercial availability, price, and foreign dependence, the IX fibers cannot be easily applied to use at industrial and household scales. The new commercial available materials, SST, are a good candidate for this application. The SST IX resins have a unique physical configuration; the functional groups reside only on the outer shell resulting in reduced diffusion path lengths as shown in **figure 1.17**.

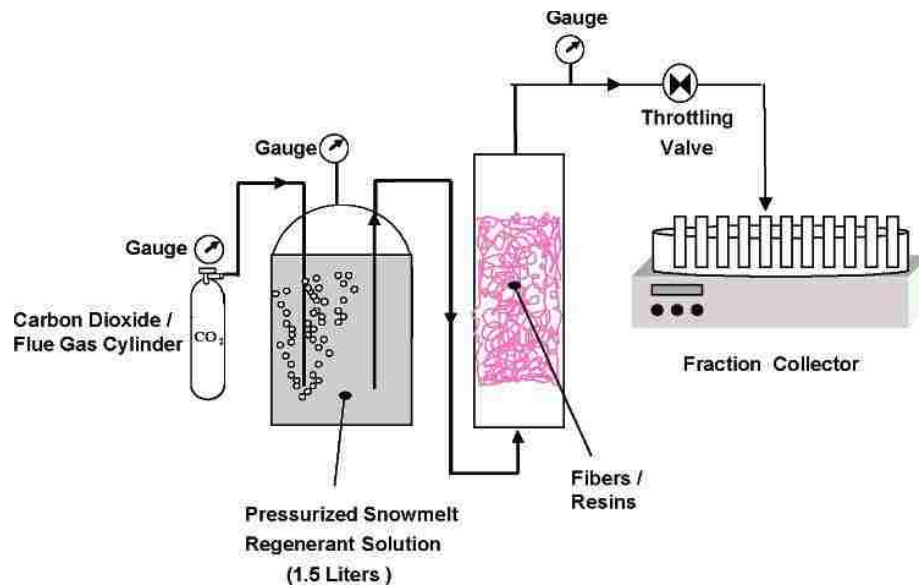


**Figure 1.14** Laboratory set-up depicting the CO<sub>2</sub> in water used in the hardness removal cycles of fiber and resin ion exchange materials (45).

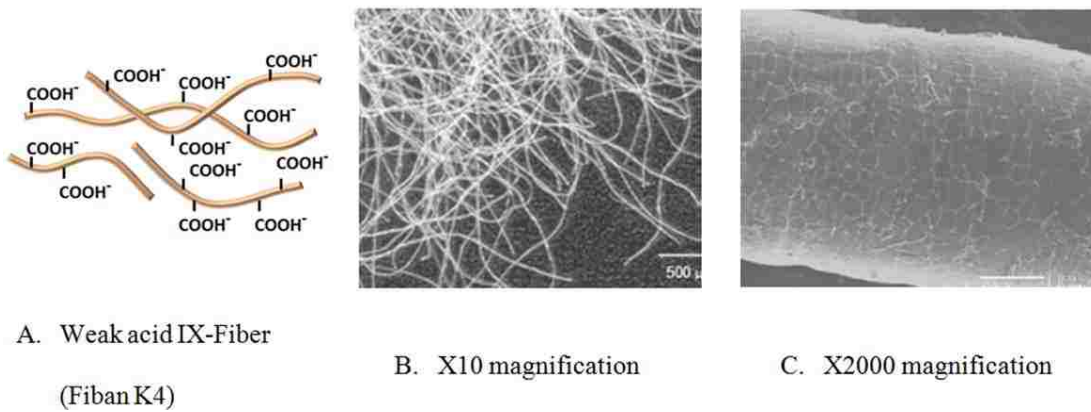


**Figure 1.15** (A) Weak acid ion exchange fibers with carboxylate functional groups (B) Virgin fiber materials photographed at x10 magnification. (C) SEM photograph of a single fiber (x2000) (46).

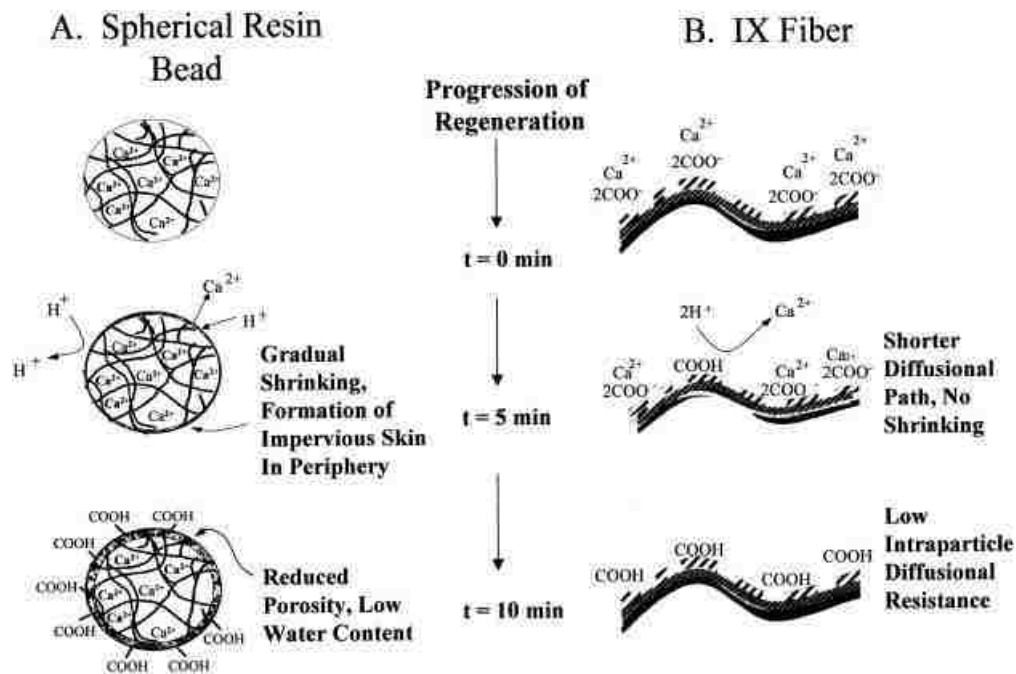


**Figure 1.16** (A) Schematic depicting the regeneration of weak-acid cation exchange beads. (B) Schematic depicting the regeneration of weak-acid cation exchange fibers.(45)

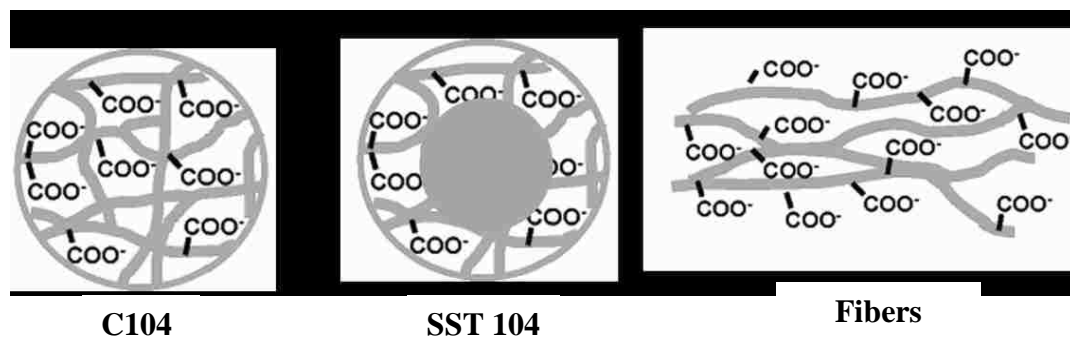


**Figure 1.17** Comparison of different structure of weak acid cation exchangers (A) Purolite C104, (B) Purolite SST 104, and (C) Fiban K4

Besides CO<sub>2</sub>, no other chemicals are required for the regeneration process. The waste regenerant streams do not contain any regulated chemicals or an unusually high

content of total dissolved solids (TDS). Rainwater, snowmelt, or any source of water with low alkalinity can be used for CO<sub>2</sub> dissolution. SST ion exchange resins are commercially available at competitive prices, chemically stable, and mechanically durable. Covalently attached functional groups reside primarily on the outer shell of spherical beads thus offering excellent sorption/desorption kinetics. SST can be conveniently used in fixed bed units and hence do not pose any operational problems.

#### **1.3.4.2 Use of Weak Acid Cation (WAC) Exchange Resin and Biodegradable Organic Acid Regeneration**

The hardness in water can be removed by using the weak acid cation (WAC) exchanger as shown in the equation 1-15. The traditional regeneration process can be achieved by using the inorganic acid solution such as 5% HCl. The advantage of using the WAC resin is that the resin has higher capacity than the SAC resin, and the resin has high affinity toward H<sup>+</sup> ions. The regeneration can be achieved easily by using dilute acid. However, the WAC resins are not widely used for household applications because the processes need acid storage which raises concern about safety issues and handling such an aggressive chemical. In this study, the biodegradable organic acid such as diluted acetic acid or vinegar will be used for regeneration. Dilute acetic acid is commonly available, inexpensive, and the waste generated from such a process is a minimum due to the favorable thermodynamics and biodegradability.

### **1.3.4.3 Simultaneous Hardness and Ligands Removal using Strong Acid Cation Exchange Resin in Polyvalent ( $\text{Al}^{3+}$ ) Form**

Traditional ion exchange hardness removal processes use a strong acid cation (SAC) exchanger in the sodium form. Calcium, magnesium, and other polyvalent cations corresponding to the hardness are exchanged on an equivalent basis with sodium in the resin phase as presented in the equation 1-14. Exhausted resins are typically regenerated with brine solution of 10-12% sodium chloride to achieve selectivity reversal in favor of sodium selectivity. This process is inefficient and the requirement of high concentrations of brine solution results in discharge of nearly 60-80% of the brine used. These traditional cation exchange water softeners still have a salt discharge problem due to unfavorable equilibrium i.e., 3-8 equivalents of  $\text{Na}^+$  are required to desorb one equivalent of hardness.

The novel salt-free water softening process replaces  $\text{NaCl}$  as the regenerant with a soluble salt of polyvalent cations such as  $\text{AlCl}_3$ . The strong acid cation exchangers are used in a polyvalent form, such as  $\text{Al}^{3+}$  or others, instead of  $\text{Na}^+$ . Since the resin bed is not in the  $\text{Na}^+$  form at the start of the service cycle, treated water has no sodium content compared to that for the conventional ion exchange softening process. Aluminum ions immediately precipitate upon exchange with hardness i.e.,  $\text{Ca}^{2+}$ ,  $\text{Mg}^{2+}$  and are not present in the treated water. The regeneration can be carried out at low concentrations of the regenerant (as low as 0.5%) at near-stoichiometric efficiency. Along with hardness, the process also removes fluoride or other ligands such as phosphate and arsenic when the bed is initially in the  $\text{Al}^{3+}$  form or contains precipitated aluminum (hydr)oxide.



## **1.4 Premise of the Study**

The study on the development of heterogeneous polymeric ion exchangers aims to engineer the traditional homogeneous ion exchangers into novel, heterogeneous hybrid ion exchangers. These heterogeneous ion exchangers are necessary for specific environmental processes for which the traditional ion exchanges are ineffective. The scope of research is shown in figure 1.18. The overall focus of this research is primarily on the development of HAIX-Zr for arsenic and fluoride removal. The other findings such as zinc removal and the development of environmentally benign hardness processes are present in the study for validation of the new processes and may not be fully investigated in every aspect.

### **1.4.1 Development of HIX-Zr for Selective Removal of Arsenic, Fluoride and Zinc**

The goal of this study is to investigate enhanced selectivity for anionic ligands (i.e., arsenate and fluoride) and heavy metals (i.e. zinc) sorption on the hydrated Zr(IV) oxide (HZO) nanoparticles which are irreversibly dispersed into the polymeric ion exchanger. As mentioned previously, the traditional ion exchanger cannot selectively remove these trace contaminants in the presence of a high concentration of inevitably present background innocuous ions. The study explores the use of HZO nanoparticles for selective adsorption of trace contaminants due to the Lewis acid-base or metal-ligand interaction. Unlike the previously used hydrated Fe(III) oxide (HFO), the HZO nanoparticles offer more chemical stability than HFO particles, which make HZO nanoparticles safe to dispose of into the landfill without toxic leaching.

- To develop the preparation techniques that use inexpensive startup materials. The resulting material should exhibit a high amount of metal oxide in the polymer ion exchanger supports, have small sized HZO particles, which are uniformly distributed in the material, and minimum loss of zirconium compounds during the regeneration.
- To quantify the maximum sorption capacity of the material (isotherm) and investigate the effect of the feed pH and competing anions such as sulfate, silica, phosphate on the uptake capacity of the HAIX-Zr.
- To investigate the performance of the hybrid nanosorbents for arsenic, fluoride, and zinc in terms of sorption/desorption in the column runs, removal capacity, and regeneration efficiency. Commercially available iron-based nanosorbents (LayneRT) and activated alumina (AA) will be used for comparison.
- To study the sorption kinetics of hybrid sorbents, identify the controlling-kinetic mechanism of As(V) and F<sup>-</sup> sorption on to HAIX-Zr ,and estimate the effective intra-particle diffusivity in order to understand the sorption/desorption mechanism.

#### **1.4.2 Development of Salt-Free Water Softening Process**

The main goal of this salt-free water softening process is to validate the three new alternatives for hardness removal processes by using heterogeneous cation exchange resins. All three processes should generate a less aggressive waste stream from the regeneration process. Each process is to be evaluated by the effectiveness of the softening process in terms of (1) hardness removal capacity and simplicity of operation, (2) regeneration efficiency (i.e., percent of hardness recovery and amount of regeneration

solution usage), and (3) the sustainability of the systems (i.e., ability to reuse in many cycles, toxic waste generation).

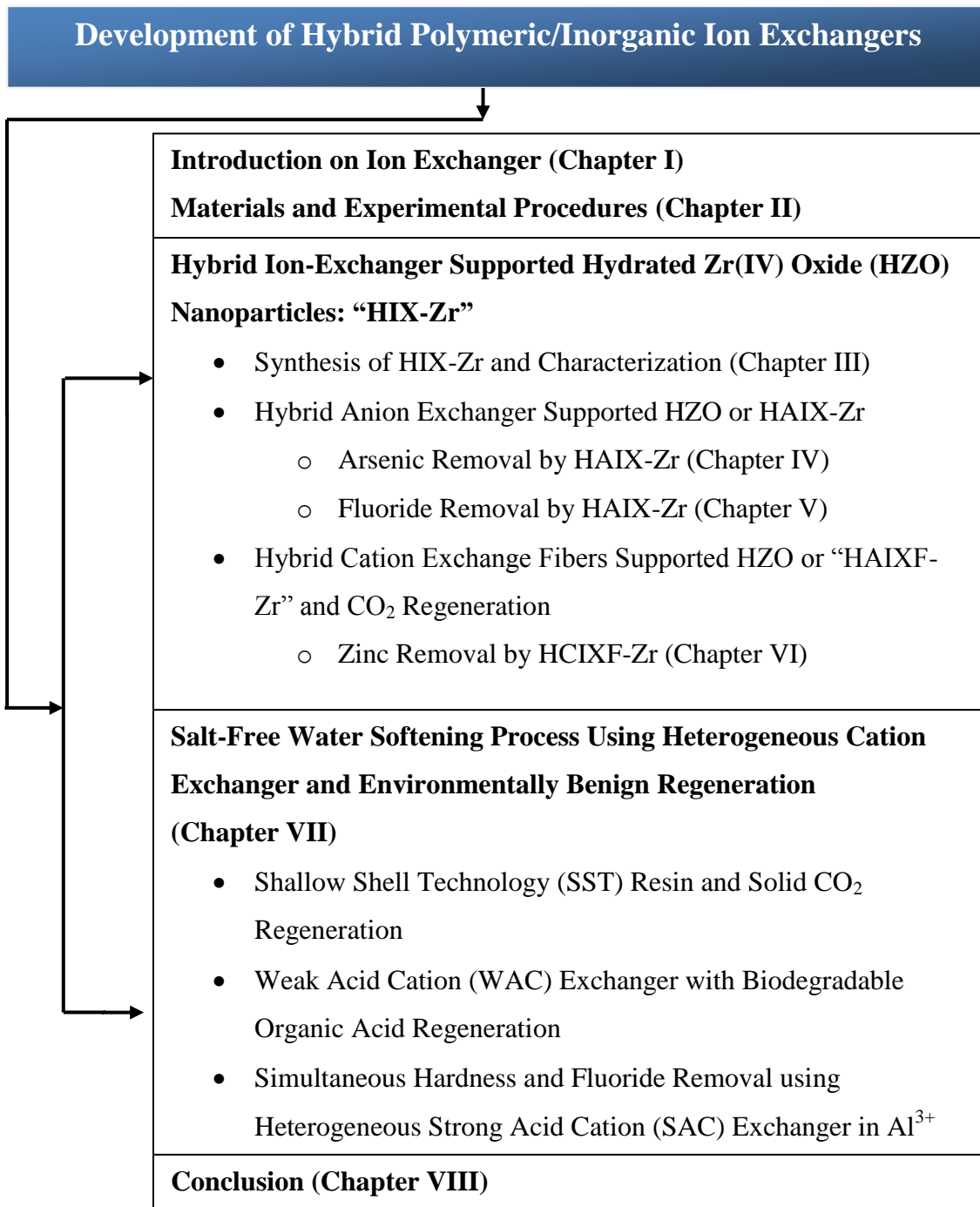


**Figure 1.18** Scope of research on the topic of heterogeneous polymeric ion exchangers

## CHAPTER 2

### MATERIALS AND EXPERIMENTAL PROCEDURES

#### 2.1 Materials and Chemicals

All chemicals used in this study are reagent grade purchased mainly from Fisher Scientific and Sigma Aldrich. Water used throughout the study is deionized (DI) water, which was purified by a two stage process (reverse osmosis system and mixed-bed of cation and anion exchanger cartridge). The DI water was used throughout the study for preparation of simulated influent water for arsenic, fluoride, zinc, and hardness (i.e.  $\text{Ca}^{2+}$ ) removal. Materials and chemicals used for both the hybrid polymeric/inorganic nanosorbent and the salt-free softening processes are listed in the following sections.

##### 2.1.1 Ion Exchange Resins and Fibers

The primary ion exchange resins were obtained mainly from Purolite (PA), Rohm and Hass (Dow chemical company), and Ion Exchange India.

- The main resins used for making hybrid zirconium oxide based nanosorbents are Purolite A500P, A500, A830, A400, and INDION 830. These include the strong acid resin Purolite C-145 and polymer beads without functional groups, Amberlite XAD4. The salient properties are summarized in table 2.1.

- Strong base cation exchange fibers (Fiban K1) obtained from the Institute of Physical Organic Chemistry of National Academy of Sciences of Belarus were used for preparing hybrid cation exchange fibers impregnated with hydrated Zr(IV) oxide

nanoparticles or referred as HCIXF-Zr. Table 2.2 is a list of properties of ion exchange fibers and resins used for making HCIXF-Zr and HCIX-Zr for transition metals (i.e. zinc) removal.

- For development of the salt-free water softening process, several cation exchange resins have been used for validation of the concept. The shallow shell technology weak acid type cation exchange resin (SST 104) and traditional weak acid cation exchange resins Purolite C104 and C106 were used for comparison of the performance of hardness removal and regeneration efficiency by using acetic acid as the regeneration solution. The properties of the materials used for the salt-free water softening process are summarized in table 2.3. Purolite C145, macroporous strong acid cation exchange resin, is used for the simultaneous fluoride and hardness removal process.

### **2.1.2 Zirconium Compounds and Other Chemicals**

Zirconium oxychloride ( $\text{ZrOCl}_2 \cdot 8\text{H}_2\text{O}$ ) and  $\text{TiCl}_4$  were purchased from Sigma Aldrich. Zirconium oxides (M 302), zirconium oxychloride 36% crystal were obtained from MEL chemical (Flemington, NJ). Zirconium oxychloride was also obtained as a test sample from Southern Ionic (West Point, MS). Other chemicals used to prepare feed solutions for experimental batch and column runs studies are reagent grade namely,  $\text{Na}_2\text{CO}_3$ ,  $\text{NaHCO}_3$ ,  $\text{CaCl}_2 \cdot 2\text{H}_2\text{O}$ ,  $\text{Mg}(\text{NO}_3)_6 \cdot 6\text{H}_2\text{O}$ ,  $\text{Na}_2\text{SO}_4$ ,  $\text{ZnCl}_2$ ,  $\text{Na}_2\text{HPO}_4$ ,  $\text{AlCl}_3 \cdot 6\text{H}_2\text{O}$ ,  $\text{Al}_2(\text{SO}_4)_3 \cdot 16\text{H}_2\text{O}$ ,  $\text{Na}_2\text{SiO}_3 \cdot 9\text{H}_2\text{O}$ ,  $\text{Zn}(\text{SO}_4) \cdot 7\text{H}_2\text{O}$  purchased from Sigma Aldrich, Fisher Scientific, and other suppliers. Arsenate, As(V), was prepared from sodium arsenate, dibasic heptahydrate ( $\text{Na}_2\text{HAsO}_4 \cdot 7\text{H}_2\text{O}$ ); arsenite or As(III) was prepared from sodium meta arsenite ( $\text{NaAsO}_2$ ). Fluoride solution was prepared from sodium fluoride (NaF).

**Table 2.1** Salient property of ion exchange resins used for synthesis of zirconium oxide based hybrid nanosorbents

<b>Ion exchange Resins</b>	<b>Matrix</b>	<b>Functional group</b>	<b>Capacity</b>
<b>Purolite A500P</b> <b>(Anion Exchanger)</b>	Macroporous Polystyrene Crosslinked with Divinylbenzene	Strong Base Type I Quaternary Ammonium	0.8 meq/ml (Cl <sup>-</sup> form)
<b>Purolite A500</b> <b>(Anion Exchanger)</b>	Macroporous Polystyrene Crosslinked with Divinylbenzene	Strong Base Type I Quaternary Ammonium	1.15 meq/ml (Cl <sup>-</sup> form)
<b>Purolite A830</b> <b>(Anion Exchanger)</b>	Macroporous Polyacrylic Crosslinked with Divinylbenzene	Weak Base Complex Amine	2.75 meq/ml (free base)
<b>DOWEX TAN-1</b> <b>(Anion Exchanger)</b>	Macroporous Polyacrylic Crosslinked with Divinylbenzene	Strong Base Type I Quaternary Ammonium	0.7 meq/ml (Cl <sup>-</sup> form)
<b>Ion Exchange India</b> <b>Indion 830 (Anion Exchanger)</b>	Macroporous Polystyrene Crosslinked with divinylbenzene	Strong Base Type I Quaternary Ammonium	0.95 meq/ml (Cl <sup>-</sup> form)
<b>Rohm and Hass</b> <b>Amberlite XAD4</b>	Macroreticular Crosslinked Aromatic Polymer	n/a	n/a

**Table 2.2** Property of polymeric ion exchange fibers used for HCIXF-Zr for removal of zinc and other transition metals

<b>Ion exchange Resins</b>	<b>Matrix</b>	<b>Functional group</b>	<b>Capacity</b>
<b>Fiban K1</b> (Cation Exchange Fibers)	Polypropylene fiber with graft copolymer of styrene and divinylbenzene	Strong Acid Sulfonic acid	3 meq/g (H <sup>+</sup> from)
<b>Purolite C145</b> (Cation Exchanger Resin )	Macroporous Polyacrylic Crosslinked with Divinylbenzene	Strong Acid Sulfonic acid	1.50 meq/ml or 3 meq/g (Na <sup>+</sup> form)

50

**Table 2.3** Property of polymeric cation exchange resin and fibers used for salt-free water softening process

<b>Ion exchange Resins</b>	<b>Matrix</b>	<b>Functional group</b>	<b>Capacity</b>
<b>Purolite C104</b>	Gel Polyacrylic Crosslinked with DVB	Weak Acid, (Carboxylic)	3.8 meq/ml, (H <sup>+</sup> from)
<b>Purolite SST104</b>	Porous Crosslinked Polyacrylic	Weak Acid, (Carboxylic)	3.3 meq/ml, (H <sup>+</sup> from)
<b>Purolite C145</b> (Cation Exchanger)	Macroporous Polyacrylic Crosslinked with Divinylbenzene	Strong Acid Sulfonic acid	1.50 meq/ml (Na <sup>+</sup> form)

## 2.2 Analytical Methods

### 2.2.1 Dissolve Metals and Metalloids

Dissolved metals in part per million ranges (ppm) (e.g.,  $\text{Na}^+$ ,  $\text{Ca}^{2+}$ ,  $\text{Mg}^{2+}$ ,  $\text{Zn}^{2+}$ ) were analyzed by using a Perkin Elmer AAnalyst 200 Atomic Absorption Spectrophotometer (AAS) with flame atomizer using hollow cathode lamps (HCL) at the appropriate wavelength. For the metalloids, i.e. arsenic, a Perkin Elmer AAnalyst 600 Graphite Furnace Atomic Absorption spectrophotometry (GFAA) with electrodeless discharge lamps (EDL) at wavelength of 193.7 nm was used to analyze arsenic at very low concentrations usually at less than 100 parts per billion (ppb) levels. Each sample was injected with a palladium/magnesium matrix modifier using auto sampler AS800. Note that a palladium matrix modifier helps to correct for general chemical interferences (47). The standard curve was prepared by using 5 standard arsenic solutions in the range 0-100 ppb purchased from Perkin Elmer and the correlation coefficient ( $R^2$ ) should be not less than 0.995 and two replicates of reading each sample was set in the measuring protocol.

As(III) concentration was analyzed by using the method developed by Ficklin (48). First, the sample was acidified immediately with concentrated hydrochloric acid to a pH of approximately 4. The 5.0 ml of acidified sample was passed through the mini column (10 cm height and 7 mm in diameter) containing a strong-base anion exchange resin in the chloride form (Bio-Rad AG 1-X8). At acidic pH, the effluent from the mini-column contains only As(III). The difference between the sample before and after passing through the column is As(V).



### **2.2.2 Anionic Species**

Anions (i.e.  $\text{Cl}^-$  and  $\text{SO}_4^{2-}$ ) were analyzed using a Dionex Ion Chromatography (IC) model DX-120 IC with High Performance Ion Chromatography (HPIC) AS 14 column, and a 4 mm separator column. The eluents contain a solution of 3.5 mM sodium carbonate and 1 mM sodium bicarbonate with a flow rate of 1.2 ml/min. The signal response and peak position were calculated using an Agilent 3395 integrator. A calibration curve was developed using 5 standards prepared from analytical grade standard from Fisher Scientific.

### **2.2.3 Fluoride and Aluminum Analysis**

Fluoride and aluminum concentrations were carried out by using a Hach UV-Vis spectrophotometer (model DR5000). Fluoride ion was analyzed by using SPADNS 2 reagent at a range of 0.02-2 mg/L  $\text{F}^-$ . Aluminum at concentration ranges 0.002-0.25 mg/L Al was analyzed using the Eriochrome Cyanine R reagent set by Hach. The results have to be corrected with fluoride concentration in the solution according to the manual. Both fluoride and aluminum analysis by using Hach spectrophotometer, which were developed from Standard Methods for Examination of Water and Wastewater (49).

#### **2.2.4 Zirconium and Silica Analysis**

Inductively Coupled Plasma Optical Emission Spectroscopy (ICP-OES) from a Perkin Elmer model Optima 2000 DV was used for zirconium and silica analysis. Radial and axial plasma view modes were used for trace concentrations (less than 1 ppm) and higher concentrations, respectively. The plasma aerosol type was wet with a sample flow rate of 1.5 mL/min and flush time of 10 seconds. Calibration standards were prepared from zirconium standard solution (1 mg/ml of Zr in 5% HF) purchased from Acros organic. The acid blank 5% (V/V) nitric acid from Ricca chemical was used as a blank solution. A calibration curve was plotted using 5 standards covering the range of samples with correlation coefficient of determination ( $R^2$ ) no less than 0.999.

#### **2.2.5 X-Ray Diffraction (XRD)**

Crystalline materials in this study were identified using a desktop X-ray diffractometer (XRD) from Rigaku MiniFlex II. X-ray diffraction data are radiation counts reflected from different planes within the different mineral species. The intensity of each reflection is a function of the composition and crystallography of the mineral species. The samples were ground into powder and place in the sample holder.

#### **2.2.6 Scanning Electron Microscopy with Energy Dispersive X-ray (SEM/EDX)**

**SEM and EDX at Lehigh University Laboratory:** Scanning electron microscope (SEM) images were obtained using an HITACHI Model 4300 combined with energy dispersive X-ray spectrometry (EDX) analysis to identify elemental compositions

of different samples. A conductive coating of iridium was deposited on each sample by a sputter coater to reduce surface charging before SEM analysis.

**The SEM and TEM from Singapore Laboratory:** For SEM, a JEOL JSM-6360A equipped with EDX system JED-2300 was operated at voltages in the range of 0.5-30 kV. The beads were embedded in a mixture of epoxy resin and hardener with a ratio of 10:1 to enhance the solidification process. The specimen disc was held parallel to the polishing surface to produce uniformly thin specimens. A conductive layer of platinum was deposited on the sample by a sputter coater to reduce surface charging during SEM analysis. A cross section of polymeric beads was prepared by embedding the beads into epoxy resin, which was then solidified by heating on a laboratory hot plate and subsequently ground carefully using a Gatan disc grinder in order to obtain the cross-sectional view.

For TEM, JEOL JEM-2010F equipped with an EDX system was setup at an acceleration voltage of 200 kV. A TEM image was captured instantaneously once selected area on sample has been identified to minimize the potential sample damage by the electron beam. The polymeric beads were carefully ground to a thickness suitable for observation under TEM. The samples were then dispersed in ethanol with ultrasonication for 10-20 min, and the droplet was a dropped on a copper grid coated with carbon film.

## 2.3 Experimental Procedures

### 2.3.1 Batch Equilibrium Test and Sorption Isotherm

All batch tests were conducted in a five chamber gyratory shaker, which was designed and built by the Environmental Engineering group at Lehigh University as illustrated in figure 2.1. The rotary shaker containing five chambers with a fixed speed motor (30 rpm) is the main equipment used for many batch studies including the material capacity screening test, the isotherm study, the effect of competing ions, the effect of pH, leaching test, etc.

**Batch Equilibrium Test:** The performance of each synthesized hybrid nanosorbent was compared by the simple test called a batch equilibrium test. In order to compare the removal capacity ( $q$ ) from different types of sorbents or from different preparation batches, the sorbent mass  $m$  (mg) was added into the contaminant solution volume  $V$  (L) with initial concentration  $C_0$  mg/L. Samples were shaken for three-five days in order to ensure equilibrium. The equilibrium capacity can be calculated from the mass balance equation (2-1). This technique is also applied for determination for the effect of pH and competing ions.

$$q(\text{mg/g}) = \frac{V(\text{L}) \times (C_0(\text{mg/L}) - C_e(\text{mg/L}))}{m(\text{g})} \quad (2-1)$$

**Sorption Isotherm:** The sorption of arsenate and fluoride onto the different adsorbents can be modeled by assuming the equilibrium partitioning of contaminants

between the aqueous phase and solid (adsorbent) phase. The equilibrium capacity,  $q$ , can be obtained by using equation 2-1.



**Figure 2.1** Rotary shaker for material preparation and batch test

### 2.3.2 Fixed-bed Column Runs

Fixed-bed column runs for all experiments were performed using an epoxy coated glass column (7 or 11 mm diameter) (Ace Glass), a constant flow pump (Fluid Metering) and a fraction collector (ELDEX). To avoid premature leakage due to the wall effects (50) the ratio of column diameter and sorbent particles diameters was maintained at more than 20:1. The influent was pumped through the column in a down-flow direction. Superficial liquid velocity (SLV) and empty bed contact time (EBCT) were recorded for each run. Figure 2.2 shows a schematic representation of the experimental set up along with a photograph of the actual setup. During fixed-bed column experiments with HAIX-Zr, interruption tests were performed to identify the rate limiting step of the process. The run was deliberately stopped for 24 hours. When the flow rate was resumed, the effluent

samples were analyzed for pH and contaminant concentrations for comparison with the results immediately before the interruption.

Typically column studies are plotted in normalized fashion,  $C/C_0$  vs. bed volumes (BV).  $C$  of both  $C$  and  $C_0$  relates to concentration,  $C_0$  is equivalent to the initial concentration. Most graphs include the feed, experimental information, and salient hydrodynamic properties such as Superficial Liquid Velocity (SLV) and Empty Bed Contact Time (EBCT).

- $BV = \text{Milliliters of influent solution passed through the column} / \text{milliliters of solution displaced by sorbents material.}$
- $SLV \text{ (m/hr.)} = (\text{Flow rate (m}^3\text{/hr)}) / (\text{column diameter (m}^2\text{)})$
- $EBCT \text{ (hr.)} = (SLV \text{ (m/hr)}) / (\text{length of sorbent (bed) within the column (m)})$

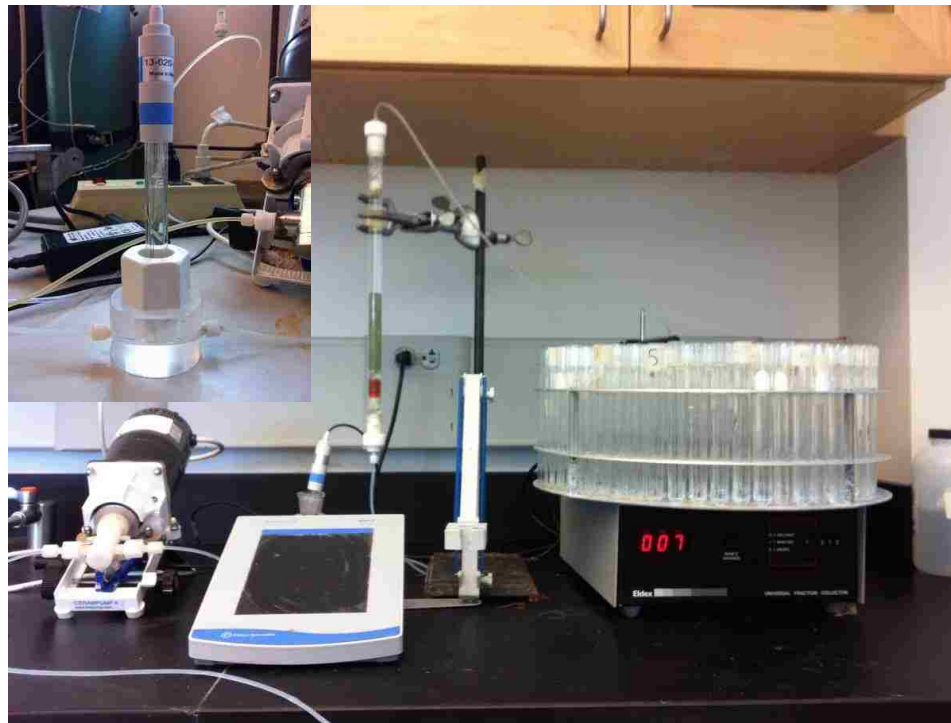
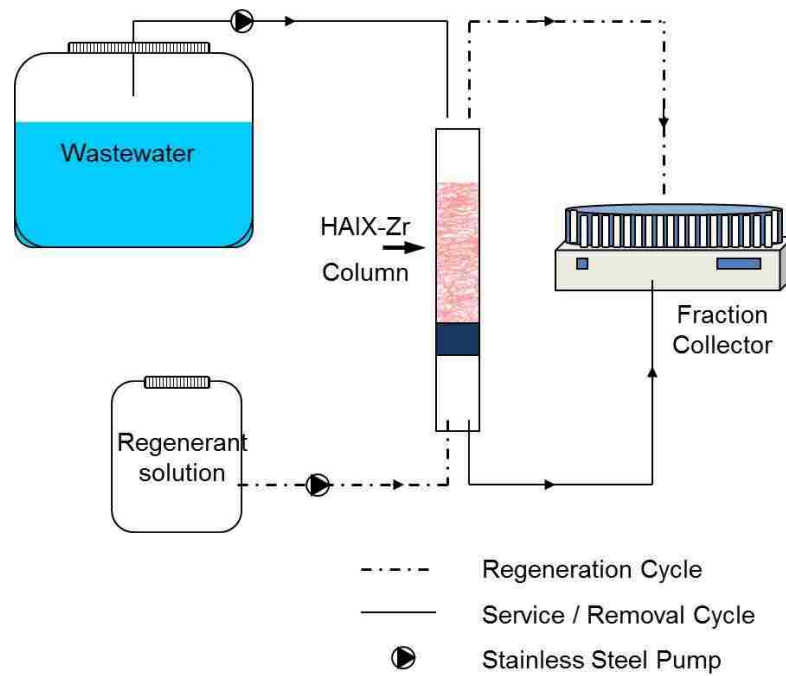


**Figure 2.2** An illustration of the set up for the fixed bed column experiment

### 2.3.3 Kinetic Tests

The batch kinetic studies were carried out to determine the intra-particle diffusion rates (diffusivity coefficient). Figure 2.3 illustrates the schematic of the kinetic test setup along with the actual setup. This apparatus was originally developed by Kressman (51) and mentioned by Helfferich (5) for the measurement of ion-exchange rates. The kinetic experiments for arsenate and fluoride uptake by HAIX-Zr were conducted with a constant background sulfate, chloride and bicarbonate concentrations of 100 mg/L. The initial arsenate or As(V) and fluoride concentrations were 100 µg/L and 10 mg/L, respectively.

The solution pH was 7.5 for arsenate and 5.5 for fluoride during the course of the kinetic tests. The hybrid materials (HAIX-Zr) were sieved to 500 µm using USA Standard Testing Sieves (Fisher Scientific Company). The sorbent was placed inside a polypropylene-membrane (fine mesh) cage. The stirrer was immersed and started in a solution of the substance of interest. The sorbent particles placed inside the apparatus were subjected to a rapid circulating flow of solution. The fresh solution was passed in from the bottom of the case, contacted with the sorbent, and forced out radially as explained in the drawing of the stirrer assembly. The vigorous agitation was maintained by a motor driven stirrer at 1,500 rpm. The diffusional resistances in the liquid film were absent under this condition. At different time intervals, a small volume of sample was collected from the solution and analyzed. The fraction of arsenate or fluoride (F) versus time was plotted and diffusivity coefficients ( $\overline{D}_{eff}$ ) were obtained by fitting with a mathematical model. The mathematical model and the experimental results are discussed in Chapter 4.



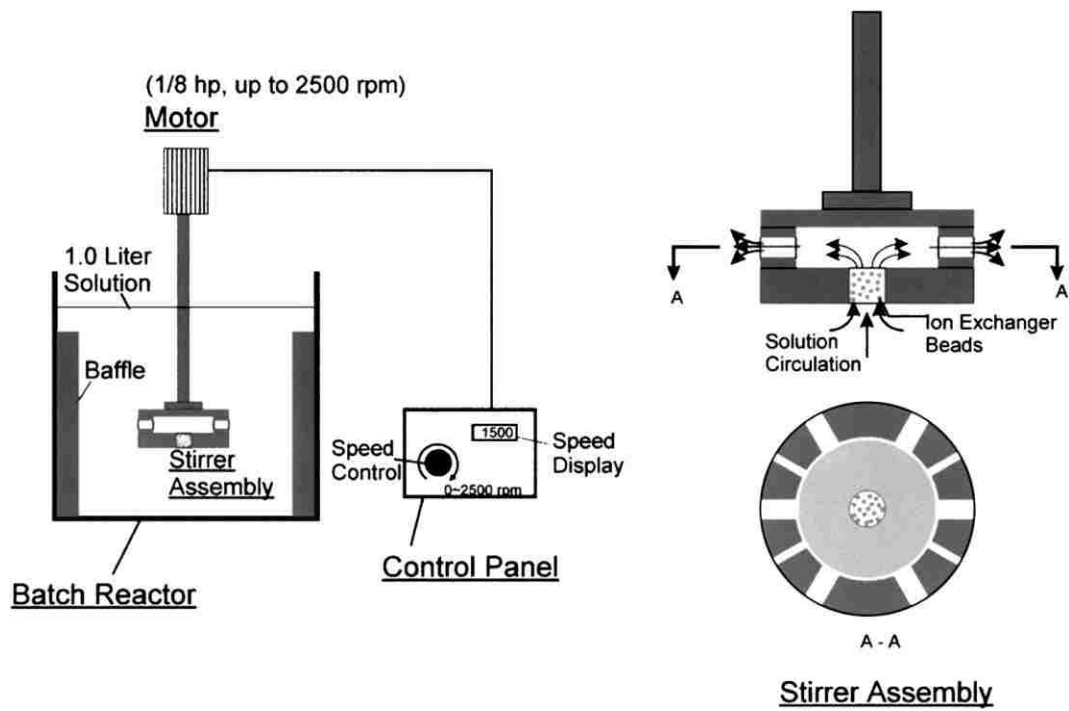


**Figure 2.3** Schematic of the batch kinetic test apparatus and stirrer assembly

## CHAPTER 3

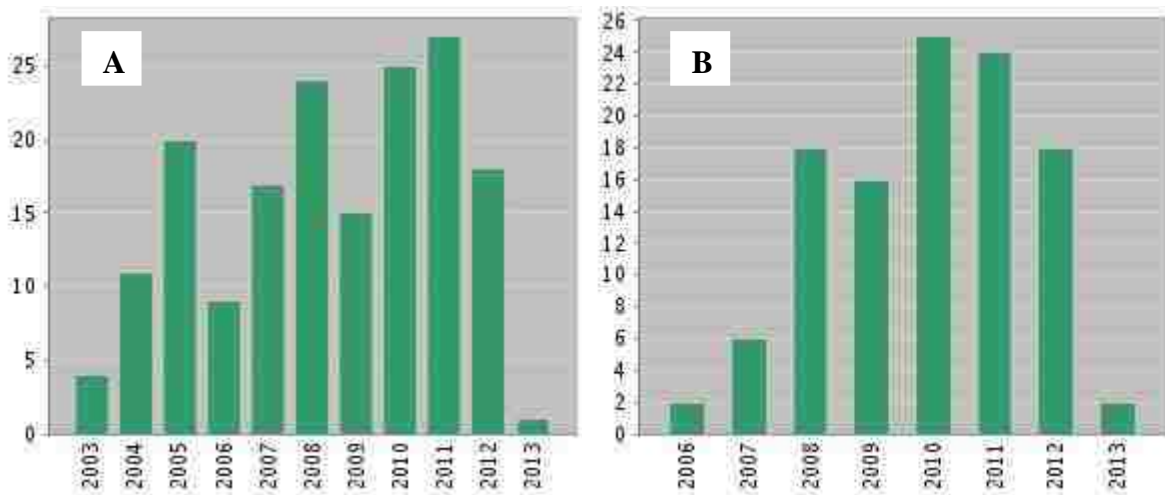
### HAIX-Zr SYNTHESIS & CHARACTERIZATION

The goal is to develop arsenic and fluoride selective sorbents which are environmentally benign, high capacity, reusable, and dispose of safely into a landfill. The synthesis processes should be simple (i.e., be able to prepare close to the affected area), inexpensive, locally available, and generate as little waste as possible. The development of hybrid anion exchanger supported hydrated Zr(IV) oxide nanoparticles or HAIX-Zr are discussed with respect to the following aspects:

1. Previous development of hybrid ion exchangers using hydrated Fe(III) oxide (HFO).
2. Investigation of different preparation methods (batch vs. column method), type of parent ion exchangers, different formulas of startup zirconium solution, types of precipitation agents, preparation order, and various techniques.
3. Results and discussion of arsenic and fluoride removal using (1) HAIX-Zr prepared from reagent grade  $ZrOCl_2 \cdot 8H_2O$ , (2) HAIX-Ti prepared from reagent grade  $TiCl_4$ , (3) HAIX-Zr from industrial grade inexpensive zirconium oxide ( $ZrO_2$ ) by batch and column methods.
4. Determination of zirconium contents in the HAIX-Zr and characterization of the prepared hybrid sorbents by using SEM/EDX and HR-TEM. The details of the instruments are provided in the Chapter 2.

The most suitable materials which were prepared from inexpensive industrial grade zirconium oxide by a batch method were further investigated for arsenic and fluoride removal. The results and discussion are mentioned in chapters 4 and 5.

### 3.1 Previous Development of Hybrid Ion Exchanger (HIX)



**A:** Arsenic removal using a polymeric/inorganic hybrid sorbent, published in Water Research Journal. (15)

**B:** Arsenic removal using polymer-supported hydrated iron(III) oxide nanoparticles: role of Donnan membrane effect, Published in Environmental Science & Technology Journal (29)

**Figure 3.1** Report numbers of citation indexed within the Web of Science (access on Jan 2013)

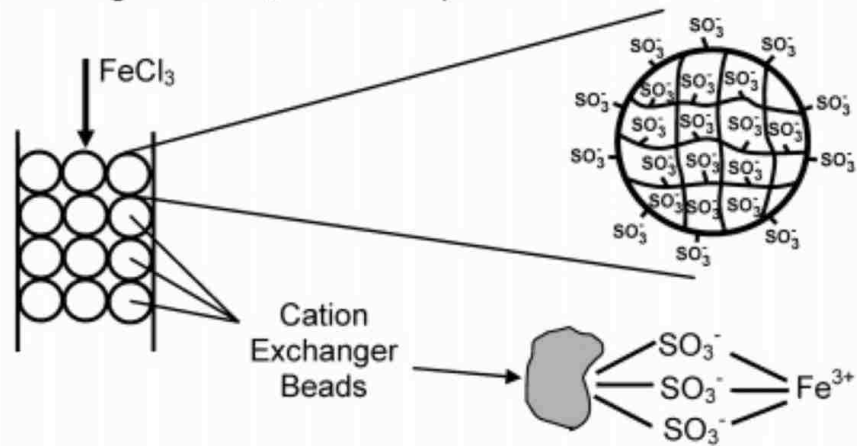
The polymeric ion exchangers supported metal oxide nanoparticle (HIX) have been developed at Lehigh University and published in the scientific papers since 2003. The HIX can remove target transition metals and anionic ligands effectively. The HIX can be tailored to specifically remove either transition metals, anionic ligands, or both

types simultaneously by using the Donnan membrane effect from the parent ion exchangers. The HIX nanosorbents can also be efficient for regeneration and be reused for many cycles of sorption/desorption yet exhibit strong mechanical strength and attrition resistance. (15, 21, 29, 37, 52, 53)The report as shown in the figure 3.1 reflects citations to source items indexed within the Web of Science.

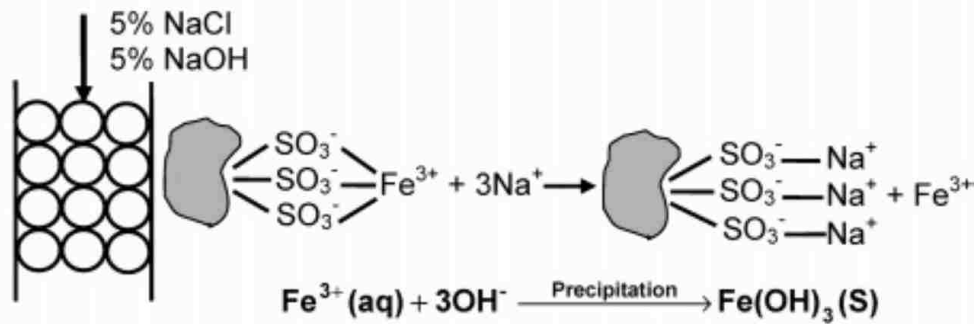
### **3.1.1 Hybrid Cation Exchangers Support Fe(III) Oxide Nanoparticles: HCIX-Fe**

These materials were developed in the Environmental Engineering Laboratory at Lehigh University by Demarco, Cumbal, Greenleaf, Leun with the supervision of professor SenGupta, and scientific papers have been published since 2003 (15, 29, 37). The preparation of the hybrid cation exchanger supported hydrated ferric oxide(HFO) nanoparticles or HCIX-Fe consisted of the following three steps as shown in figure 3.2: first, loading of Fe(III) onto the sulfonic acid sites of the cation exchanger by passing 4% FeCl<sub>3</sub> solution at an approximate pH of 2.0; second, desorption of Fe(III) and simultaneous precipitation of iron(III) hydroxides within the gel phase of the exchanger through passage of a solution containing both NaCl and NaOH, each at 5% w/v concentration; and third, rinsing and washing with a 50/50 ethanol-water solution followed by a mild thermal treatment (50-60 °C) for 60 min. Use of ethanol lowered the dielectric constant of water and supposedly enhanced the agglomeration of submicron particles through suppression of surface charges.

Step 1. Loading with FeCl<sub>3</sub> Solution at pH < 2.0



Step 2. Desorption and simultaneous hydroxide precipitation in the gel phase and pore surface



Step 3. Alcohol wash and mild thermal treatment

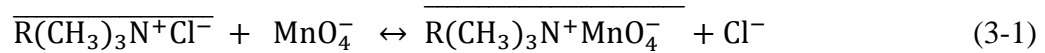


**Figures 3.2** The major steps of the process for HCIX-Fe synthesis (15)

### 3.1.2 Hybrid Anion Exchanger Supported Fe(III) Oxide Nanoparticle : HAIX-Fe

Unlike cation exchangers, anion exchangers have fixed positively charged functional groups. Thus forming hydrated Fe(III) oxides within an anion exchange resin poses a major challenge due to positively charged quaternary ammonium functional groups. The techniques for doping HFO nanoparticles onto the anion exchangers were developed and patented in 2007 (54). From the patent, the HFO particles can be dispersed in anion exchangers by a series of the following steps:

- Permanganate anion ( $\text{MnO}_4^-$ ) is loaded onto an anion exchange resin with quaternary ammonium functional groups (Purolite A500P). The loading of the resin with permanganate anion is carried out by passing potassium permanganate solution (500 mg/L  $\text{KMnO}_4$ ) through the bed to achieve the following reaction:

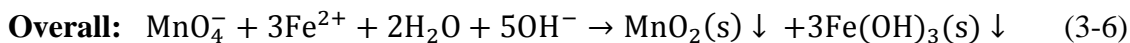
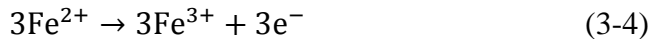
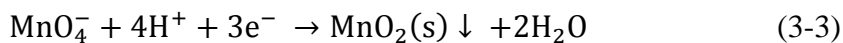


- The second step is simultaneous permanganate desorption, Fe(II) oxidation, and HFO formation within the anion exchanger. The permanganate loaded anion exchanger from the first step is contacted with 5% ferrous sulfate solution. The  $\text{MnO}_4^-$  is replaced by sulfate,  $\text{MnO}_4^{2-}$  is reduced to  $\text{MnO}_2$  (s), the  $\text{Fe}^{2+}$  is oxidized to  $\text{Fe}^{3+}$ , and finally, the  $\text{Fe}(\text{OH})_3$ (s) is precipitated within the anion exchange beads with the following reaction:

$\text{MnO}_4^-$  desorption:



Fe(II) oxidation and ferric hydroxide ( $\text{Fe}(\text{OH})_3$ ) precipitation:



- The third step is an acetone wash and drying. The overall procedures are summarized and shown in the **figure 3.3**.

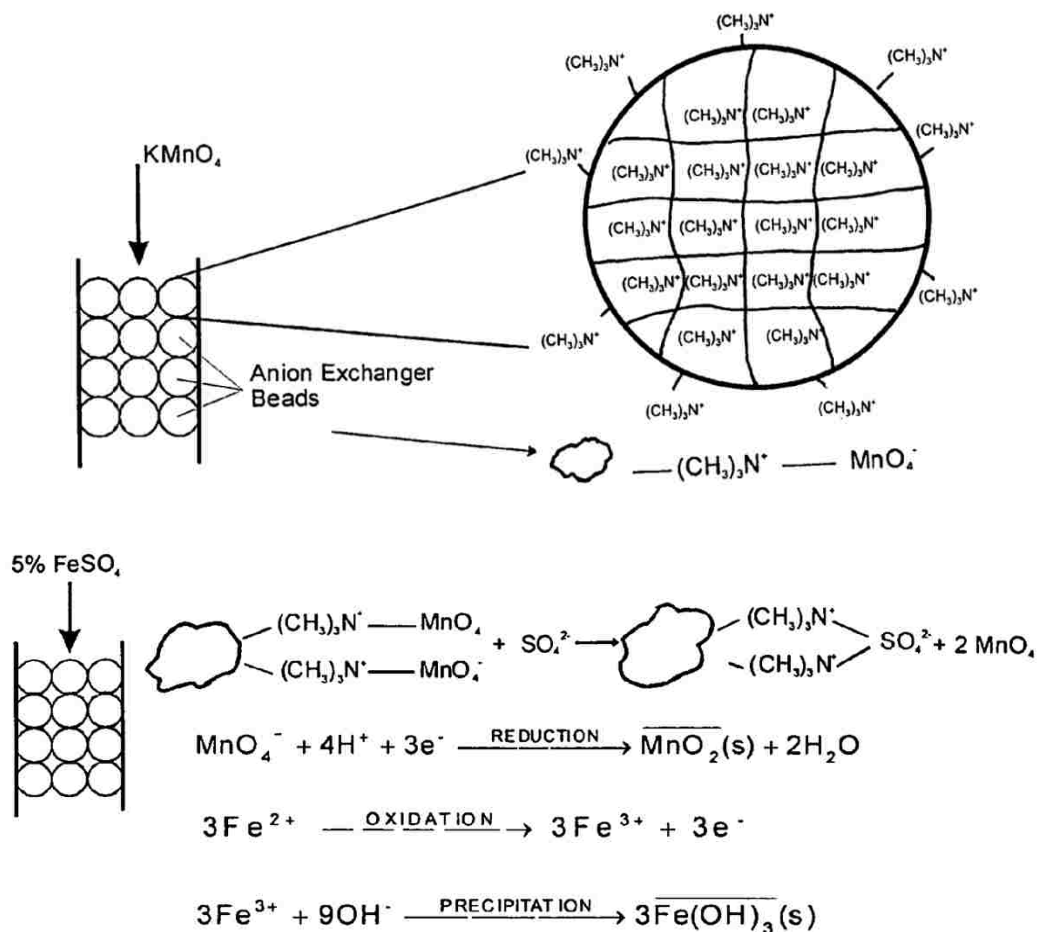


**Figure 3.3** Schematic diagrams illustrating first and second steps in the preparation of HAIX-Fe (54)

### **3.2 Synthesis of Hybrid Polymeric Ion Exchanger Supported Hydrated Zr(IV)**

#### **Oxide (HZO) Nanoparticles**

Unlike the HFO, the HZO nanoparticles offer several unique characteristics that make them safer to dispose of in landfills and they have higher selectivity toward fluoride than the iron based nanosorbents developed earlier in U.S. Pat. No. 7,7291,578 B2.(54) HZO particles are very stable over wide pH ranges in both oxidizing and reducing environments and therefore it becomes safe to dispose the used materials into landfills. Moreover, HZO can remove fluoride effectively while HFO based nanosorbents have very low affinity toward fluoride.

The general procedure for preparation of hybrid anion exchange resin impregnated with hydrated Zr(IV) oxide can be prepared by two different methods: batch and column methods. Note that the batch method is the first developed procedure to synthesize the hybrid materials because this method is simple and can be prepared even in remote locations. However, this method has a longer preparation time, consumes more chemicals, and generates more waste sludge than the column method. In general, batch preparation mode requires at least 2 repetitive cycles and usually takes nearly a week for preparation. The column method, on the other hand, was developed later, usually takes only 1 cycle and uses only 3-5 hours for preparation. Moreover, the chemical requirement and the waste generation are much less than the batch method.

The present study aims to develop methods to impregnate anion exchange resins with HZO nanoparticles. The synthesis methods for producing HAIX-Zr are modified from the previous method as described in section 3.1 and shown in figure 3.4. There are



multiple variables that affect the efficiency of the synthesized hybrid material. The following alternatives were tried and the resulting materials were validated for arsenic and fluoride removal efficiency by the batch tests as mentioned in the section 3.3-3.6:

- **Choice of various types of metals including the preparation of metal solutions:**
  - 5-15% of high purity reagent grade of zirconium oxychloride ( $\text{ZrOCl}_2 \cdot 8\text{H}_2\text{O}$ ) from Sigma-Aldrich, dissolved in either DI water or in a mixed solution of DI and methanol at 50:50 ratio
  - 10% of reagent grade titanium tetrachloride ( $\text{TiCl}_4$ ) from Fisher Scientific, dissolved in either 10% of HCl solution or a mixed solution of 20% of HCl and methanol at 50:50 ratio
  - 15% of zirconium oxide ( $\text{ZrO}_2$ ) from India and MEL Chemicals (Flemington, NJ), dissolved in either 10%  $\text{H}_2\text{SO}_4$  or a mixed solution of 20%  $\text{H}_2\text{SO}_4$  and methanol at 50:50 ratio
- **Choice of polymeric ion exchangers:**
  - Macroporous anion exchangers: Purolite A500P, Purolite A830, DOWEX TAN1, Indion 830 (Ion Exchange, India)
  - Gel-type anion exchangers: Purolite A400
  - Polymeric adsorbent without functional group: Amberlite XAD4
  - Polymeric cation exchanger resin and fibers: Purolite C145 and Fiban K1
- **Choice of precipitation reagents:** NaOH 5-20% or 28%  $\text{NH}_4\text{OH}$
- **Order of contacting polymeric anion exchangers with the solution (zirconium & alkaline solutions):**

○ The anion exchangers in the  $\text{Cl}^-$  form are used to contact with zirconium solution and then contact with alkaline solution

○ The anion exchangers in the  $\text{Cl}^-$  form are converted into  $\text{OH}^-$  form and then contacted with zirconium solutions (do not need to contact with alkaline solution again)

### 3.2.1 Batch Preparation Method

**Method #1:** As the first step, 50 mL of zirconium solution is loaded onto 25 grams of anion exchange resin with quaternary ammonium functional groups in the chloride form ( $\overline{\text{R}_4\text{N}^+\text{Cl}^-}$ ), where R and the overbar represent the polymer matrix of the anion exchanger and ion exchanger phase, respectively. The loading processes are carried out by shaking the mixed ion exchange resin and zirconium solution in the rotary shaker for 3 hours. The second step is impregnation of hydrated zirconium oxide (HZO) nanoparticles into the matrix of the resin. During this step, the decanted resin from the first step is brought into contact with 50 mL of alkaline solution and shaken for 1 hour. The third step is washing and drying. The resulting HZO loaded resin was washed with tap water and air dried at room temperature for 24 hours. These whole process was repeated for 3 cycles to achieve greater Zr(IV) loading.

**Method #2:** Unlike method #1, the startup anion exchange resin with quaternary ammonium functional groups in the chloride form ( $\overline{\text{R}_4\text{N}^+\text{Cl}^-}$ ) is converted into the hydroxide form ( $\overline{\text{R}_4\text{N}^+\text{OH}^-}$ ) by mixing 25 grams of the anion exchange resin in the chloride form with the 5% NaOH solution for 1 hour, and then washed with DI water until the pH goes down to neutral pH. The anion exchanger in the hydroxide form was contacted with 50 mL of zirconium solution and shaken for 3 hours. During this step, HZO is precipitated onto the resin matrix. The resulting HZO loaded resin is washed with

tap water and air dried at room temperature for 24 hours. The whole process was repeated for 3 cycles to achieve greater Zr(IV) loading.

### **3.2.2 Column Preparation Method**

**Method #1:** 15 grams of anion exchange resin in the chloride form were packed into a glass column (11 mm diameter) and 30 mL of zirconium solution was pumped down flow through the resin bed with a very low flow rate (1 mL/min) for approximately 1 hour. The zirconium solution was recycled within the container. Then all of the liquid in the column was vacuumed, and the new alkaline solution was pumped up-flow at the same volume and flow rate. After 1 hour, the resulting hybrid materials were washed in-situ by rinsing with DI water for 15 bed volumes. The resin was removed from the column and air dried for 24 hours.

**Method#2:** The experimental setup for this method is the same as mentioned in method #1. The commercially available anion exchange resin in the chloride form was packed inside the column. The 5% of NaOH was used for converting the resin into the hydroxide form by passing 30 mL down-flow into the 15 grams of resin at a flow rate of 1 mL/min. The solution inside the column was removed by vacuum followed by a short rinse with 10 BV of DI water. After removing all of the liquid inside the column, the zirconium solution was pumped in contact with the resin in the up-flow direction and all 30 mL of zirconium were recycled within the column around 1 hour. The column was stopped and all of the liquid was drained out of the column, followed by rinsing with DI water for 15 bed volumes. The material was removed from the column and air-dried for 24 hours.

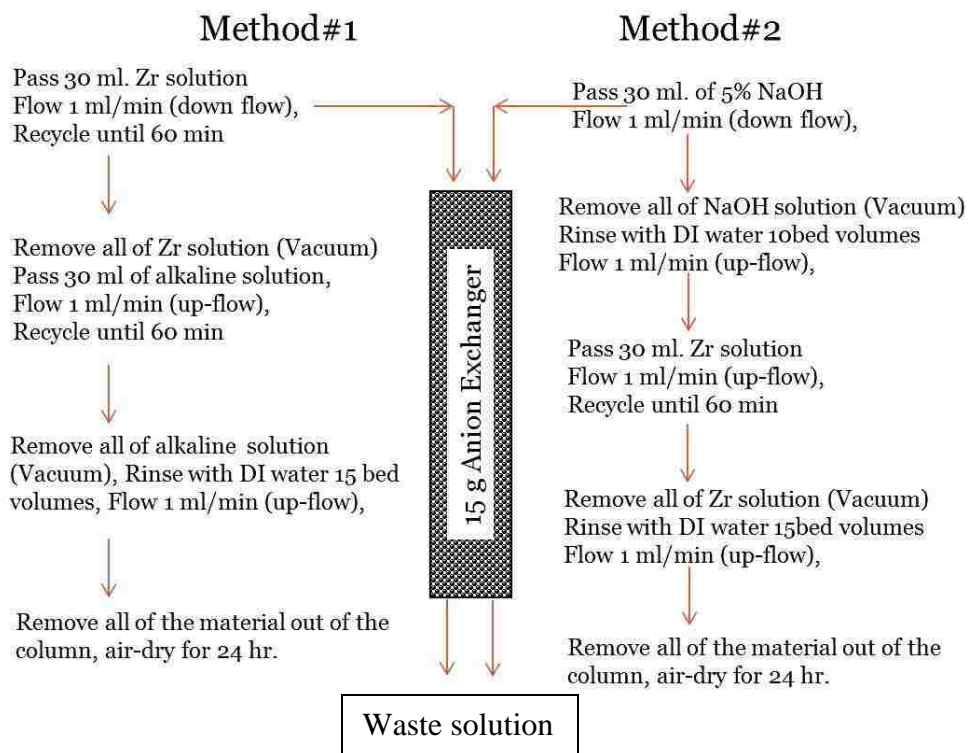
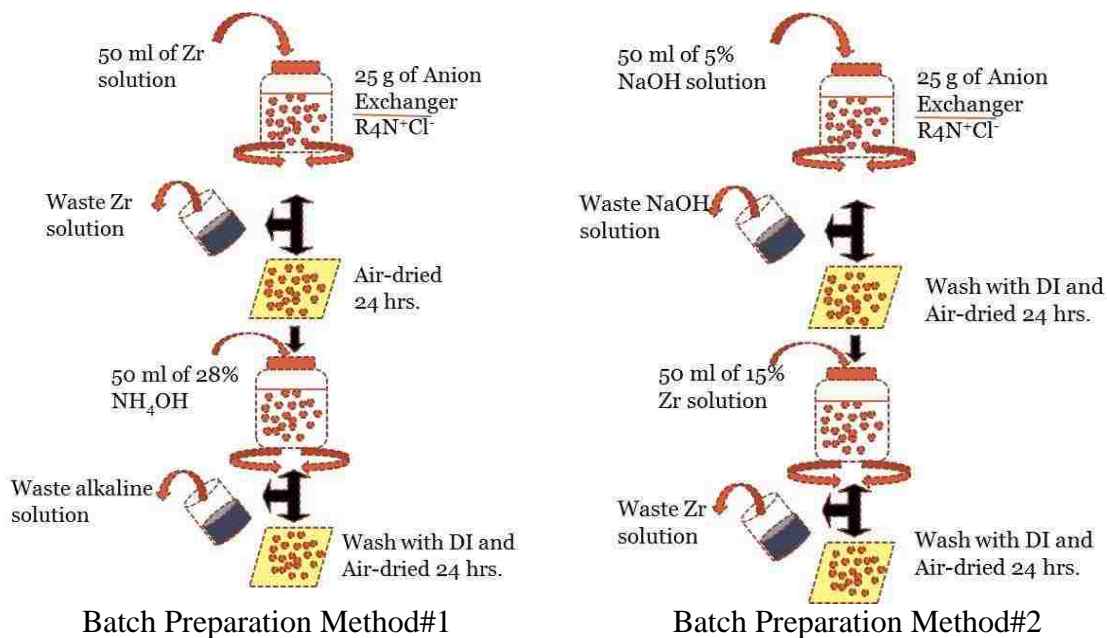


**Figure 3.4** HIX-Zr synthesis by batch (top) and column methods (bottom)

### **3.3 Arsenic and Fluoride Removal using HAIX-Zr Prepared from Reagent Grade $ZrOCl_2 \cdot 8H_2O$ by Batch Method #1**

Zirconium oxychloride purchased from Sigma-Aldrich was the first zirconium salt for producing the hybrid zirconium based adsorbent. These materials were prepared by the batch method as mentioned in the section 3.2.1. The 5% of zirconium oxychloride solution was prepared by adding zirconium salt into a mixed solution of DI water and methanol at 50:50 ratios. The goal of this study was to evaluate several factors which affect the efficiency of the hybrid material for arsenic and fluoride removal. Three different polymeric sorbents were used in this experiment: gel type strong base anion exchanger (Purolite A400), macroporous strong base cation exchanger (Purolite A500P), and the polymeric sorbent without functional groups (Amberlite XAD4). The shaking times for both zirconium loading and hydrated zirconium oxide (HZO) precipitation steps were 6 hours. Two different precipitating agents were applied: 20% NaOH and 28%  $NH_4OH$ . Other procedures are followed such as the batch method #1, as mentioned in the section 3.2.1.

The resulting materials are tested for arsenic and fluoride sorption capacity by the batch equilibrium test. 100 mg of hybrid adsorbents were added into 100 mL of test solutions which contain either arsenic 160  $\mu g$  As(V)/L or fluoride 22 mg  $F^-$ /L along with background ions:  $SO_4^{2-}$ ,  $Cl^-$ ,  $HCO_3^-$  at 100 mg/L. The commercially available iron based hybrid adsorbent “ArsenX” was used for comparison of arsenic removal while activated alumina (AA) was used for comparison of the fluoride removal. The results of arsenic and fluoride removal capacities were obtained from the mass balance equation:

$$q(\text{mg/g}) = \frac{V(\text{L}) \times (C_0(\text{mg/L}) - C_e(\text{mg/L}))}{m(\text{g})} \quad (3-7)$$

where  $q$  (mg/g) is the contaminant removal capacity,  $m$  (mg) is the mass of the sorbent,  $V$  (L) is the volume of test solution with initial concentration  $C_0$  (mg/L).  $C_e$  (mg/L) is the equilibrium concentration after shaking the samples for three-five days in order to ensure equilibrium.

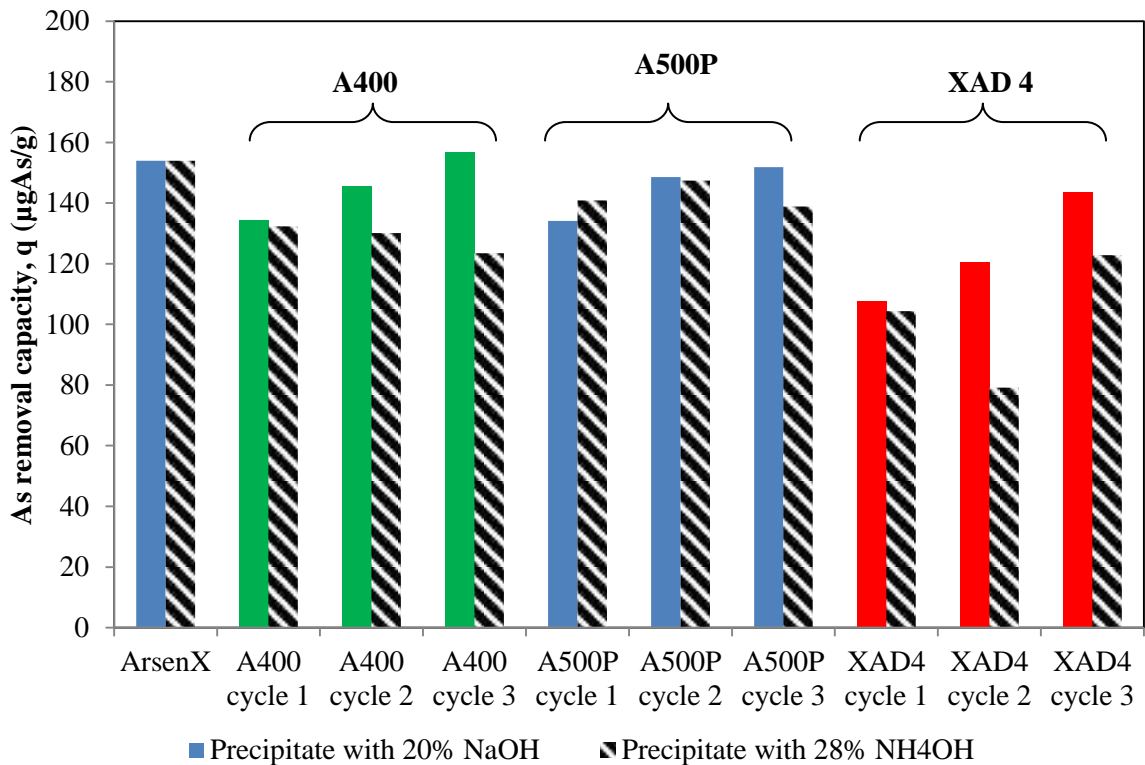


**Figure 3.5** Batch equilibrium test for arsenic removal:  $C_{As0}$  = 158.8 ppb, background anion of  $\text{SO}_4^{2-}$ ,  $\text{HCO}_3^{2-}$ ,  $\text{Cl}^-$  = 100 mg/L, mass of resin 0.1 g, volume 100 mL, pH 7.0, shaking time 5 days

From figure 3.5, we found that zirconium oxychloride can be used as startup zirconium for hybrid nanosorbent preparation. Macroporous strong based anion

exchanger (Purolite A500P) and gel type I strong base anion exchanger (Purolite A400) can also give high arsenic removal capacity. In contrast, Amberlite XAD4 which is a polymeric adsorbent without functional groups gives the lowest arsenic removal capacity. Precipitation with sodium hydroxide seems to give higher capacity than ammonium hydroxide and the number of loading cycles can enhance the arsenic removal capacity.

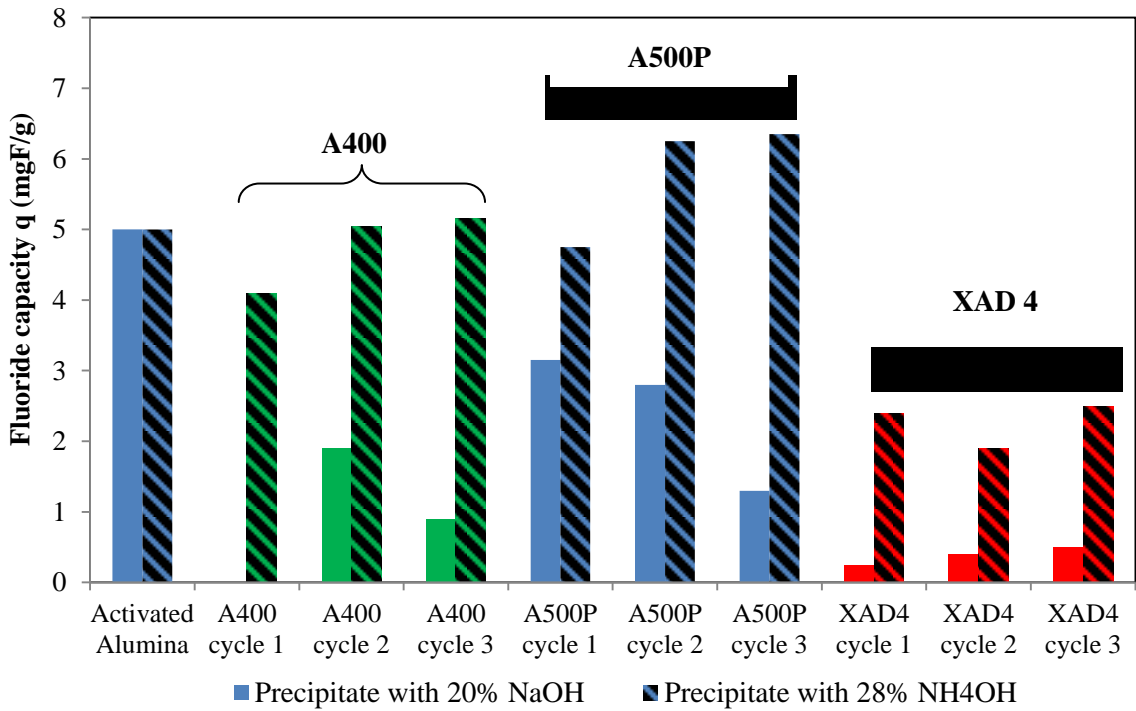


**Figure 3.6** Batch equilibrium test for fluoride removal:  $C_{F0} = 22$  mg/L, background anion of  $SO_4^{2-}$ ,  $HCO_3^{2-}$ ,  $Cl^- = 100$  mg/L, mass of resin 0.2 g, volume 100 mL, pH 5.0, shaking time 5 days

Figure 3.6 presents fluoride removal capacity from different prepared hybrid nanosorbents. Precipitation with ammonium hydroxide solution is found to give a significantly higher fluoride capacity than using sodium hydroxide. Purolite A500P is

again found to be the most suitable support material compared to A400 and XAD4. The number of loading cycles is also a minor impact the removal capacity.

### **3.4 Arsenic Removal using the HAIX-Ti Prepared from Titanium Tetrachloride (TiCl<sub>4</sub>) by Batch Method#1**

Titanium oxide particles are also known for their high affinity toward arsenic removal. In this study, titanium oxide based hybrid nanosorbents were synthesized by using a reagent grade titanium tetrachloride (TiCl<sub>4</sub>) from Fisher Scientific as a startup reagent. The TiCl<sub>4</sub> is an unusual metal halide which is highly volatile. When TiCl<sub>4</sub> contacts humid air, it will form a cloudy smoke of TiO<sub>2</sub> and hydrogen chloride (HCl). In order to prepare the titanium solution, 10% (v/v) of TiCl<sub>4</sub> solution was prepared by adding liquid TiCl<sub>4</sub> into concentrated (30%) HCl acid. Then the titanium solution dissolved in concentrated HCl solution was mixed with methanol 50:50 ratios.

The five different types of materials were used for synthesis of hybrid materials: strong base macroporous anion exchanger, Purolite A500P (normal size), sieved ( $\phi$  500  $\mu$ m) Purolite A500P, DOWEX TAN1, gel type strong based anion exchangers (Purolite A400), and polymeric sorbent without functional group (Amberlite XAD4). The resin was mixed with the titanium solution and shaken for 6 hours, dried overnight, and then precipitated with 28% NH<sub>4</sub>OH solution by shaking for 6 hours. The resulting hydrated titanium oxide (HTO) nanoparticles loaded resin was washed with tap water and air dried at room temperature for 24 hours. The whole process was repeated for 3 cycles to achieved greater Ti(IV) oxide loading.



Figures 3.7 and 3.8 show the sorption arsenic removal capacity from equilibrium batch test experiments using different initial As(V) concentrations and experimental conditions. Titanium oxide based hybrid nanosorbents also give good results for arsenic removal. From the results, A500P and A400 give a good result for arsenic removal while XAD4 has lower removing capacity. The number of loading cycles did not help to improve arsenic removal capacity. As compared with the zirconium based hybrid material, both titanium and zirconium can be used for removal of arsenic effectively.

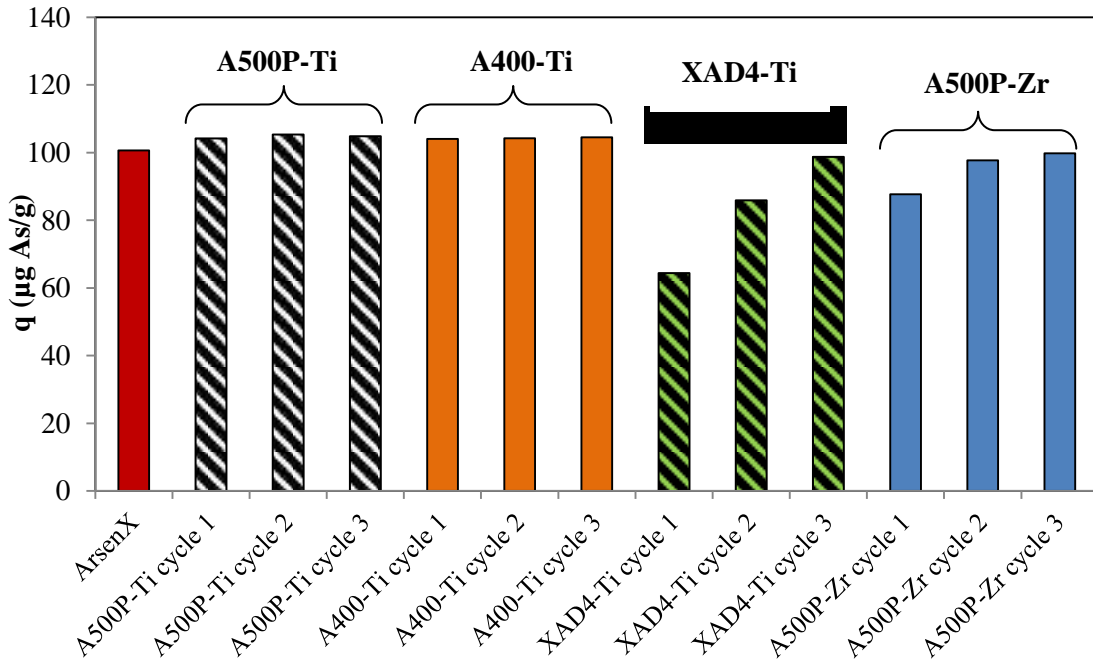


**Figure 3.7** Batch equilibrium test for arsenic removal by using HAIX-Ti at initial arsenic concentration 225 ppb:  $C_{As0} = 225$  ppb, background anion of  $SO_4^{2-}$ ,  $HCO_3^{2-}$ ,  $Cl^- = 100$  mg/L, mass of resin 0.2 g, volume 100 mL, pH 7.0

For the second experiment as shown in figure 3.8, we were interested to see the effect of particle size and try another resin called DOWEX TAN1 from DOW chemical.

DOWEX TAN-1 is a macroporous strong base anion exchange resins which is similar to the Purolite A500P. From the result, both DOWEX TAN1 and Purolite A500P can be effectively used as supports for producing hybrid nanosorbents. The particles size seems not to affect the removal capacity; however, it may help to improve the kinetics.

From this experiment, we found that titanium based hybrid nanosorbents can be used for arsenic removal. However, the cost and difficulty of handling titanium tetrachloride as startup titanium sources are limited for practical applications.

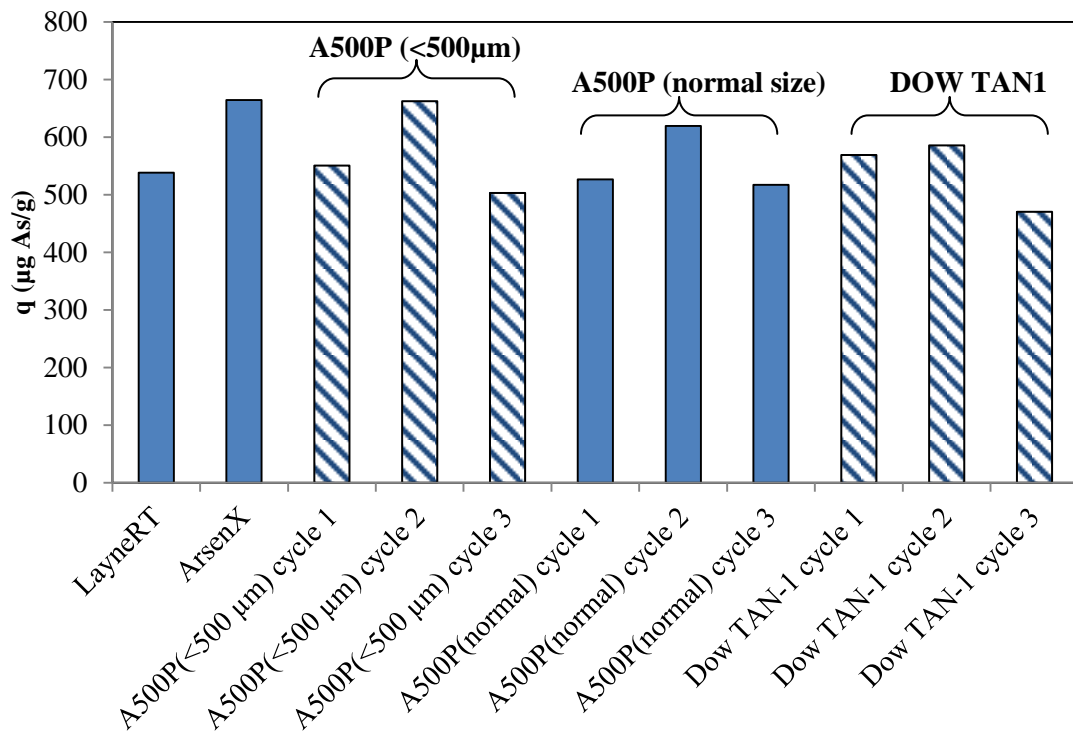
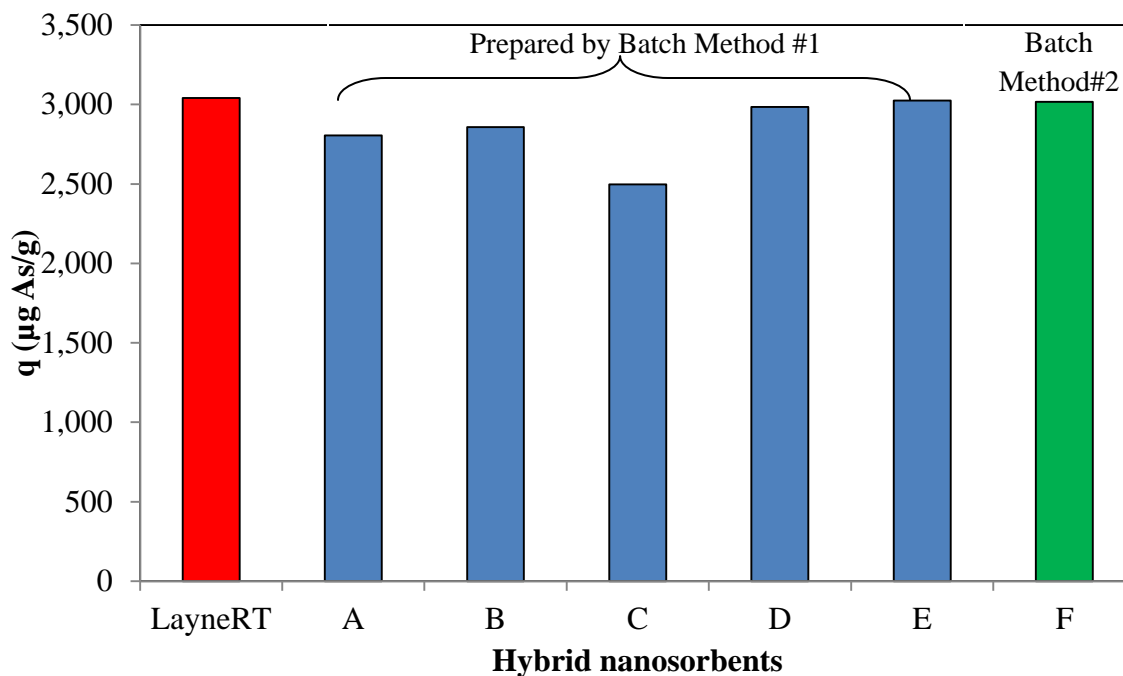


**Figure 3.8** Batch equilibrium test for arsenic removal by using HAIX-Ti at initial arsenic concentration 1000 ppb :  $C_{As0} = 1000$  ppb, background anion of  $SO_4^{2-}$ ,  $HCO_3^{2-}$ ,  $Cl^- = 100$  mg/L, mass of resin 0.3 g, volume 200 mL, and pH 5.0

### **3.5 HAIX-Zr from Inexpensive Industrial Grade Zirconium Oxide (ZrO<sub>2</sub>) by Batch Method**

For this study, various HAIX-Zr nanosorbents were prepared from zirconium oxide (ZrO<sub>2</sub>) obtained from MEL Chemicals (Flemington, NJ). Note that the cost of zirconium oxide as a startup material is much cheaper than the previous zirconium obtained from MEL Company, approximate \$7 per lb., while the reagent grade zirconium oxychloride and titanium tetrachloride from Sigma-Aldrich cost approximately \$100 per 100 grams. The zirconium solution was prepared by dissolving zirconium oxide at 15% in a mixed solution of 20% H<sub>2</sub>SO<sub>4</sub> solution and methanol at a 1:1 ratio.

Figure 3.9 shows the arsenic sorption capacity using both batch method # 1 (materials A-E) and method #2 (material F) as mentioned in section 3.2.1. The batch test experiment uses initial arsenic concentrations of 1,000 µg/L, pH 7.0 along with many background ions following by NSF standard 53 for challenge water (detail can be found in Chapter 4, table 4.2). From the table below figure 3.9, we can see that material F exhibits high arsenic sorption capacity which was prepared by batch method # 2 in only 1 cycle. This technique can significantly reduce preparation time and amount of waste generation. The used zirconium and alkaline solutions are clean and can be reused many times. Note that for the batch method #1, the alkaline waste tends to have a cloud of zirconium oxide precipitate, thus it is difficult to reuse.



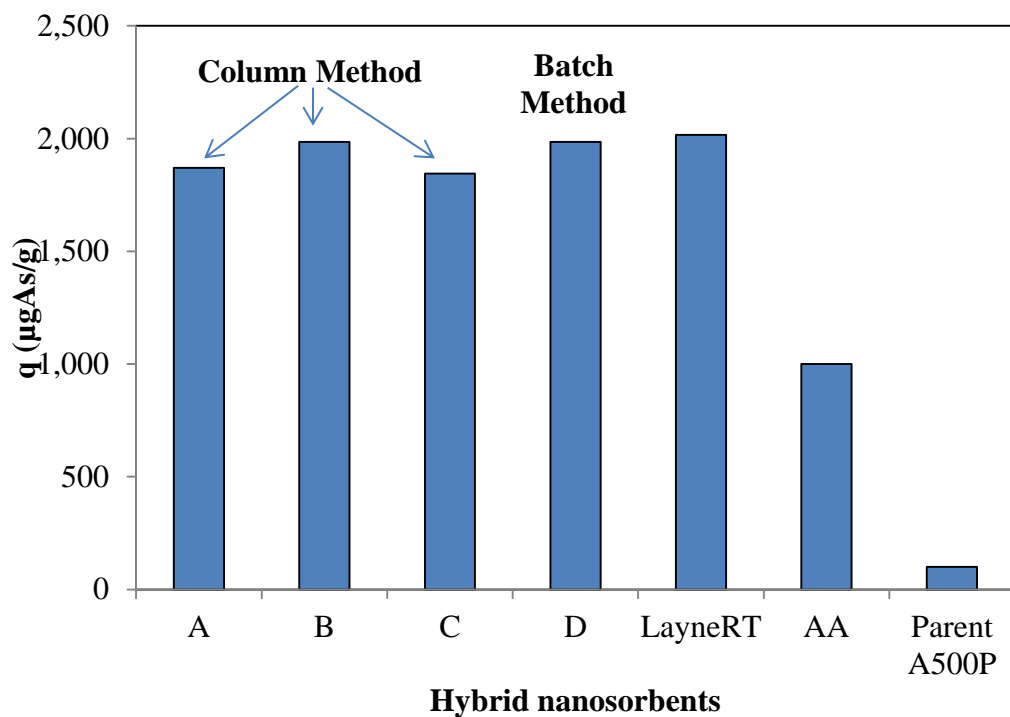
Ion Exchange Support	Metal Solution	Precipitating agents	Number of cycles	HAI-X-Zr
A500P in Cl <sup>-</sup> form	15% Zr (MEL) with MeOH	28% NH <sub>4</sub> OH	3	<b>A</b>
"	"	5% NaOH	3	<b>B</b>
"	15% Zr (MEL) without MeOH	28% NH <sub>4</sub> OH	3	<b>C</b>
"	15%Zr + 8% Fe with MeOH	"	3	<b>D</b>
"	8% Fe with MeOH	"	3	<b>E</b>
A500P in OH <sup>-</sup> form	15% Zr (MEL) with MeOH	-	1	<b>F</b>

**Figure 3.9** Batch equilibrium test for arsenic removal using HAI-X-Zr prepared from batch method:  $C_{As0} = 1,000$  ppb, background ions as appear in the challenge water with SiO<sub>2</sub> 10 mg/L, mass of resin 0.3 g, volume 1,000 mL, pH 7.0

### **3.6 HAIX-Zr Prepared from Zirconium Oxide by Column Method**

From previous batch method #2 techniques (material F in the figure 3.9), we think that it might be very convenient and possible to obtain higher zirconium oxide loading if the material can be prepared using the column method. The column methods offer many advantages over the batch methods such as reducing rinsing time and volume of water, less chance to contact with the material and reagent directly, and not dealing with the material transfer which is suitable for large-scale production. For this study, material A was prepared by using column method # 1. Materials B and C were synthesized by using column method #2. Two different resins were converted into the OH<sup>-</sup> form by passing a 5% NaOH solution, followed by rinsing and passing the zirconium solution. Unlike material B, material C was repeated for the second cycle with the ferric chloride solution instead of zirconium oxide. Material D prepared by batch method #1, commercial activated alumina (AA), and parent Purolite A500P were used for comparison.

From figure 3.10, both batch and column methods can be used for preparation of high arsenic removal capacity adsorbents. Zirconium oxide and Indion 830 resin from India, which is similar to the zirconium from MEL Chemical and Purolite A500P can also be used and exhibit high arsenic sorption capacity the same as the material available in the United States. Depending on the situation, batch methods are suitable for using onsite preparation because of its simplicity. However, for manufacturing, the column methods are more efficient and have a cleaner process. Note that material D is further used for in depth performance testing for arsenic (chapter 4) and fluoride (chapter 5) removal.



Preparation Procedure/ Type of Resins		Source of Zirconium	Alkaline solution	HAIX- Zr
Column	A500P in Cl <sup>-</sup> form	ZrO <sub>2</sub> from India w/ MeOH	28%NH <sub>4</sub> OH	<b>A</b>
Column	Indion 830 in OH <sup>-</sup> form	ZrO <sub>2</sub> from India w/ MeOH	-	<b>B</b>
Column	A500P in OH <sup>-</sup> form	Zr (1 <sup>st</sup> cycle) then convert to OH-form and Fe(2 <sup>nd</sup> cycle) w/ MeOH	-	<b>C</b>
Batch	A500P in Cl <sup>-</sup> form	ZrO <sub>2</sub> from MEL w/ MeOH (repeat 3 cycles)	28%NH <sub>4</sub> OH	<b>D</b>

**Figure 3.10** Batch equilibrium test for arsenic removal using HAIX-Zr prepared from column method :  $C_{As0} = 1,000$  ppb, background ions as appear in the challenge water with SiO<sub>2</sub> 10 mg/L, mass of resin 0.1 g, volume 200 ml, pH 7.0

### 3.7 Determination of Zirconium Contents from the HAIX-Zr

The amount of zirconium in the hybrid nanosorbent can be obtained quantitatively by a gravitational method by double acid digestion and a semi-quantitative method by using Energy Dispersive X-ray Spectroscopy (EDX or EDS). For the double acid digestion method, the hybrid materials were digested with 50% H<sub>2</sub>SO<sub>4</sub> for a week and the digested hybrid resins were again subjected to a new acid solution. Two fractions of acid contained zirconium were analyzed for zirconium content by ICP-OES as mentioned in chapter 2. Note that the polymeric ion exchanger supports are resistant to the acid, thus they do not breakdown under this condition. Under very acidic conditions zirconium oxide is dissolved from the hybrid material into the acid solution. The second digestion is a repetitive process to obtain higher zirconium dissolution from the material. The amount of zirconium (mg Zr/g adsorbent) for the first and second digestion was shown in figure 3.11. The zirconium content from the three different materials are very close to 10% which agree to the EDX techniques as shown in the table 3.1.

**Table 3.1** Zirconium content from the double acid digestion method

No	Materials	Conc. Zr (mg/L)	mg Zr /g resin	Total mg/g
1	A500P-Zr from ZrO <sub>2</sub> (MEI) , 1st leaching	1,049	104.9	109.6
	2st leaching	46.5	4.65	
2	A500P-Zr from ZrOCl <sub>2</sub> 8H <sub>2</sub> O, 1st leaching	1,095	109.5	113.7
	2st leaching	42	4.2	
3	TAN1-Zr from ZrOCl <sub>2</sub> 8H <sub>2</sub> O, 1st leaching	992	99.2	103.3
	2st leaching	41.4	4.1	

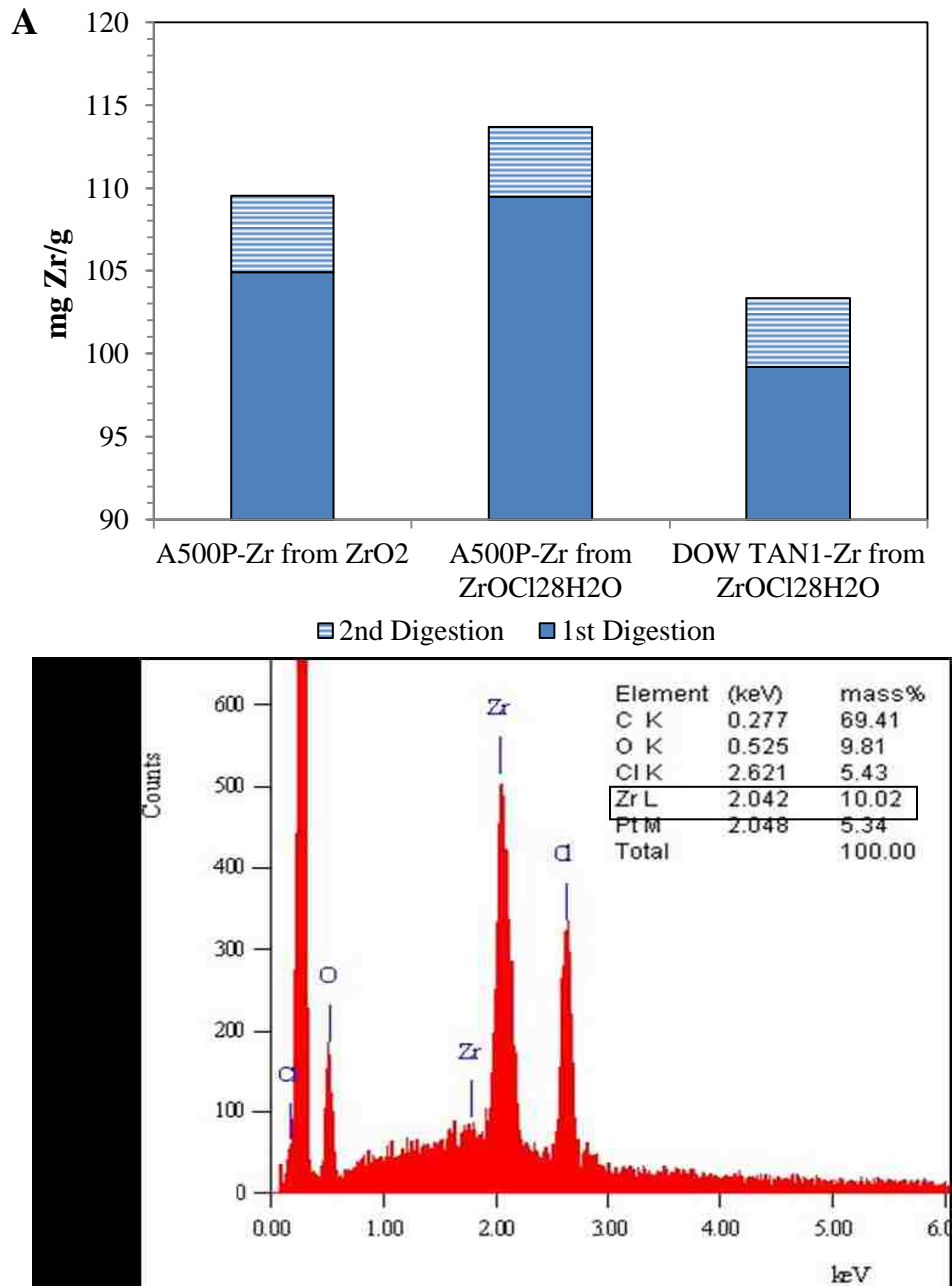


**Figure 3.11** Zirconium content in the HAIX-Zr by (A) double digestion with 50% H<sub>2</sub>SO<sub>4</sub>, HAIX-Zr 0.5 gram digested in 50% H<sub>2</sub>SO<sub>4</sub> and (B) zirconium content (from Sample A500P-Zr from ZrO<sub>2</sub> (MEL)) obtained semi-quantitatively by SEM/EDX method, shown 10% zirconium content within the material



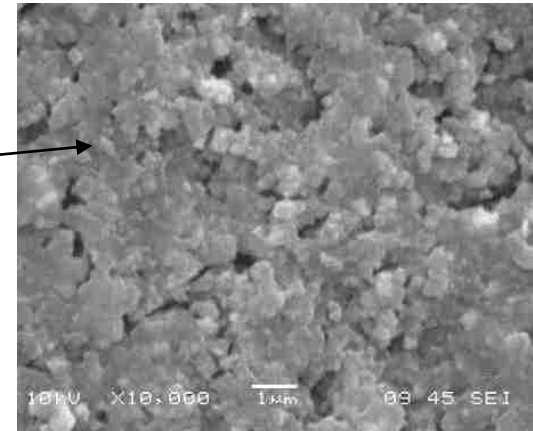
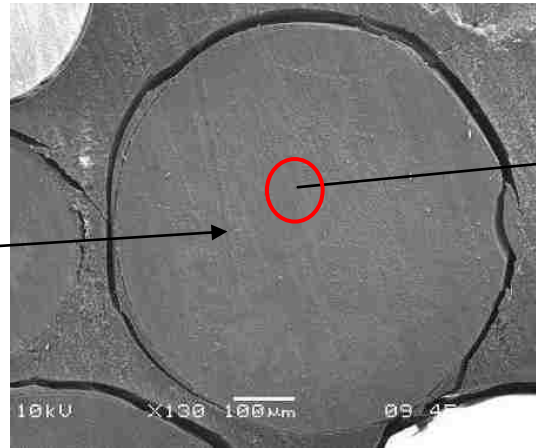
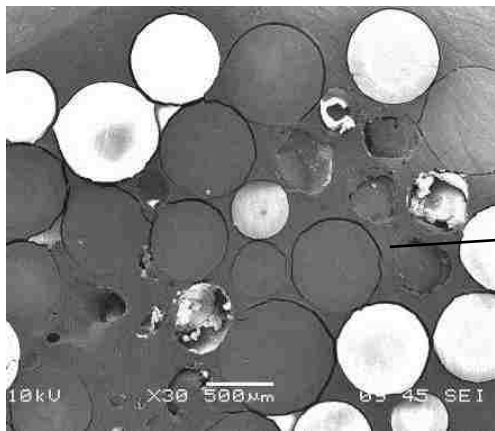
### 3.8 Characterization of HAIX-Zr

For this section, there are five different hybrid nanosorbents namely, Purolite A500P-Zr, Purolite A400-Zr, Purolite A500P-Ti, Amberlite XAD4-Zr, and commercially available iron based hybrid nanosorbent, ArsenX. These adsorbents were characterized by using Scanning Electron Microscopy (SEM), High Resolution Transmission Electron Microscopy (HRTEM), and Energy Dispersive X-ray Spectroscopy (EDX). EDX is an analytical techniques used for elemental analysis. The impact of an electron beam on the sample produces X-rays that are characteristic of the elements present on the sample. For this study, EDX was used to determine the elemental composition of image area mainly ion exchange beads. The SEM technique can provide a topographical detail of the material such as macro pores. HRTEM is a technique used to identify crystallographic structure of the sample at an atomic scale.

List of SEM, TEM, and EDX spectrum and elemental mapping of the hybrid nanosorbent prepared by batch method#1:

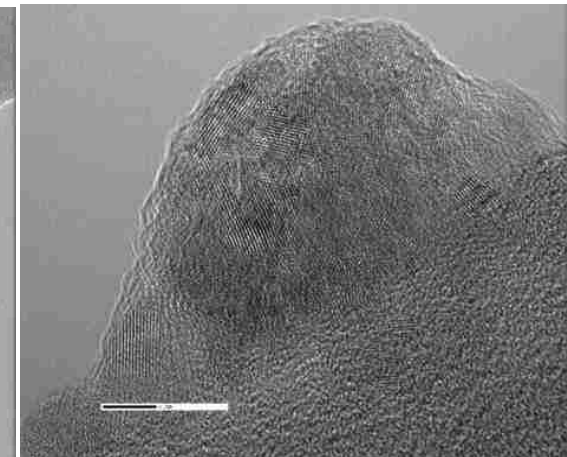
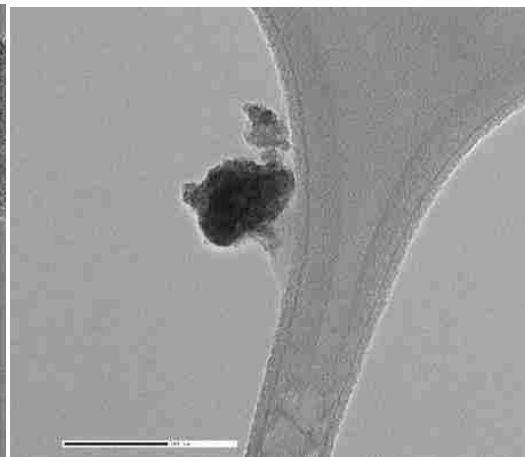
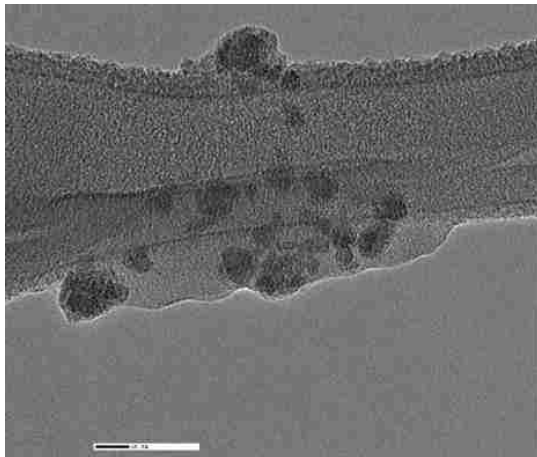
- Macroporous anion exchanger impregnated with HZO nanoparticles or A500P-Zr
- Gel strong based anion exchanger impregnated with HZO nanoparticles or A400-Zr
- Macroporous anion exchanger impregnated with HTO nanoparticles or A500P-Ti
- Polymeric adsorbent without functional group impregnated with HZO or XAD4-Zr
- Commercially available iron based nanosorbents or ArsenX<sup>np</sup>

**SEM of A500P-Zr**



85

**TEM of A500P-Zr**



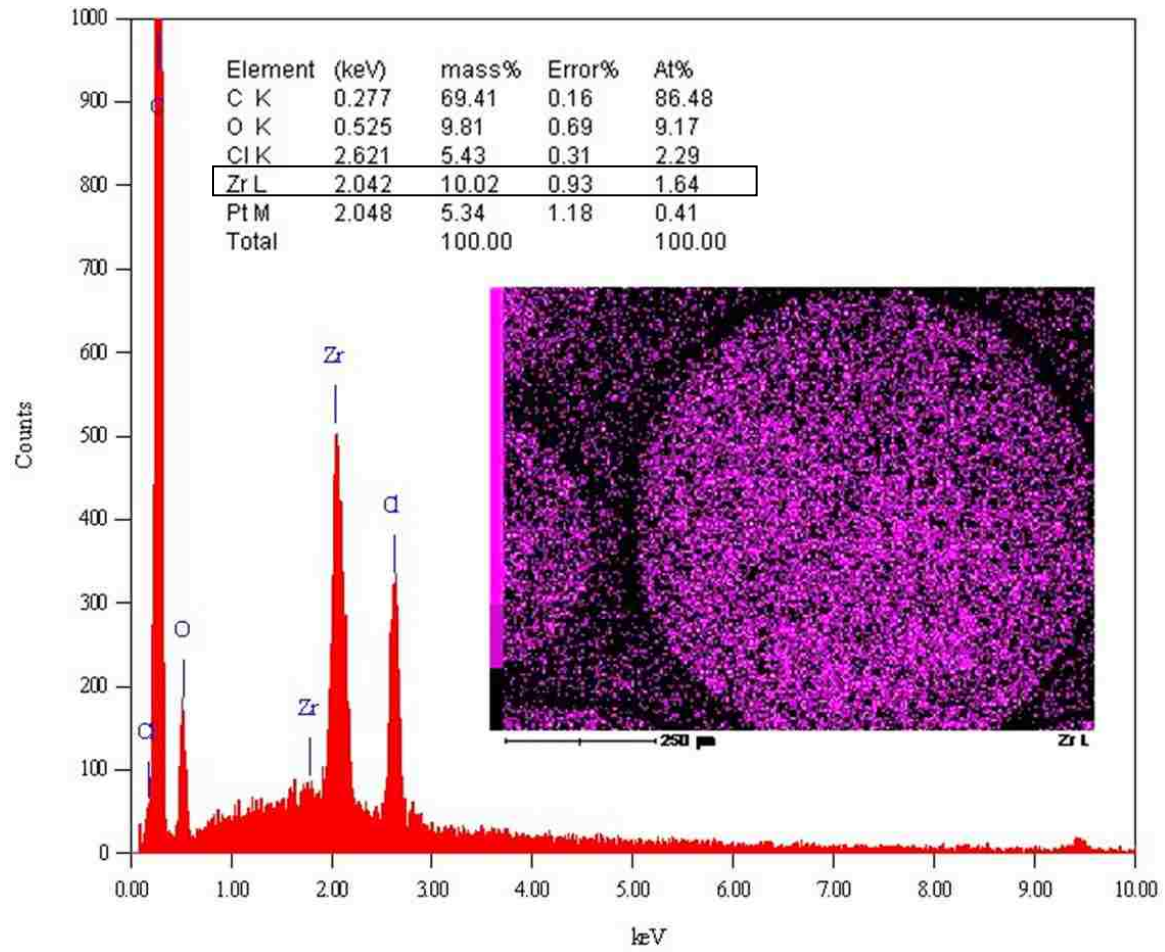
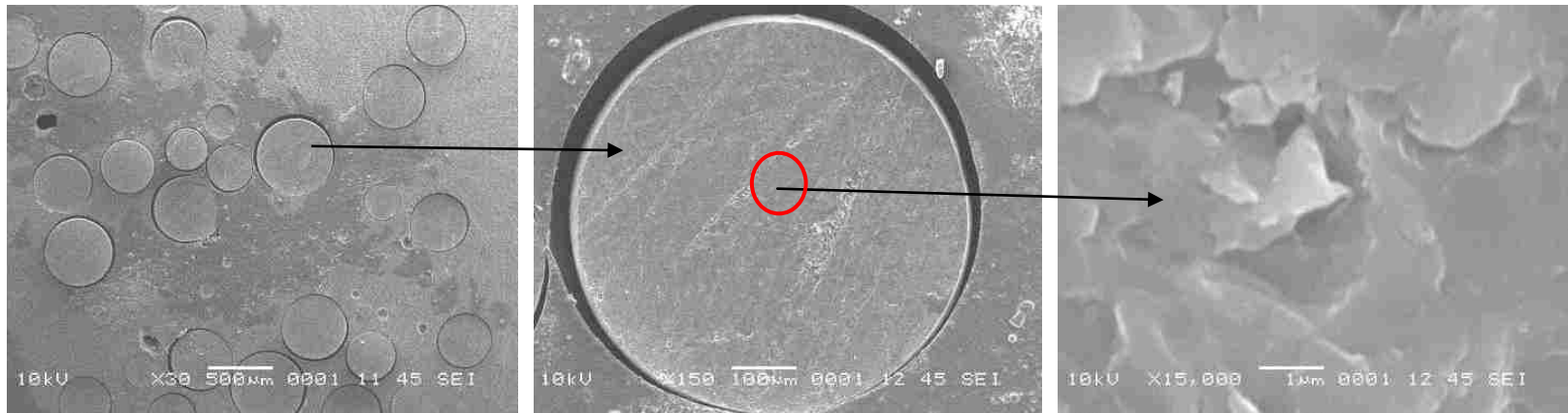


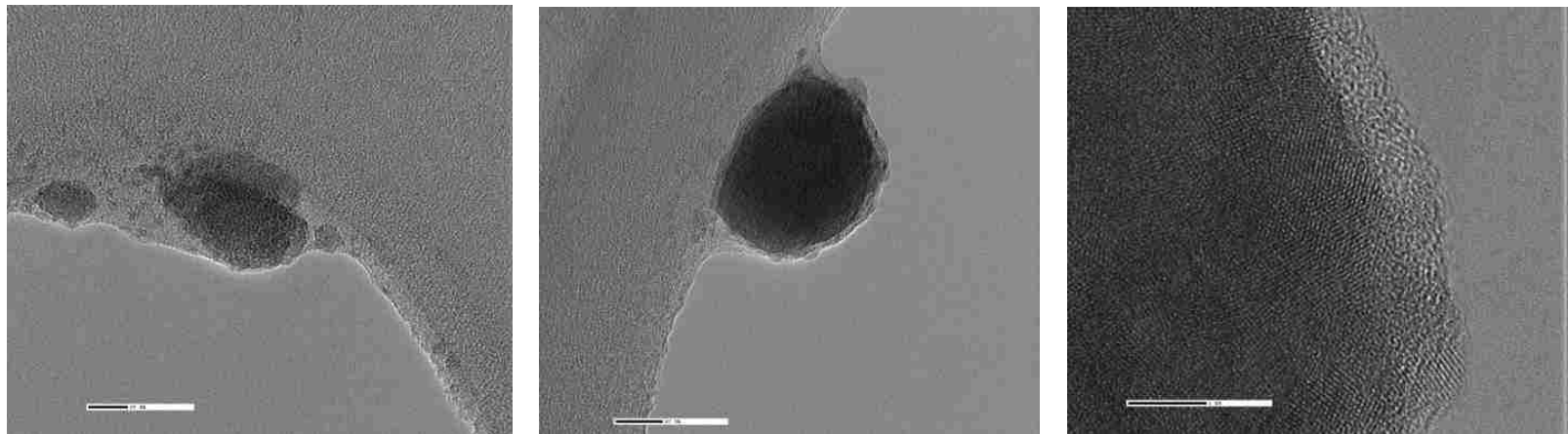
**Figure 3.12** SEM, TEM, and EDX spectrum and elemental mapping of Purolite A500P-Zr

**SEM of Purolite A400-Zr**



87

**TEM of Purolite A400-Zr**



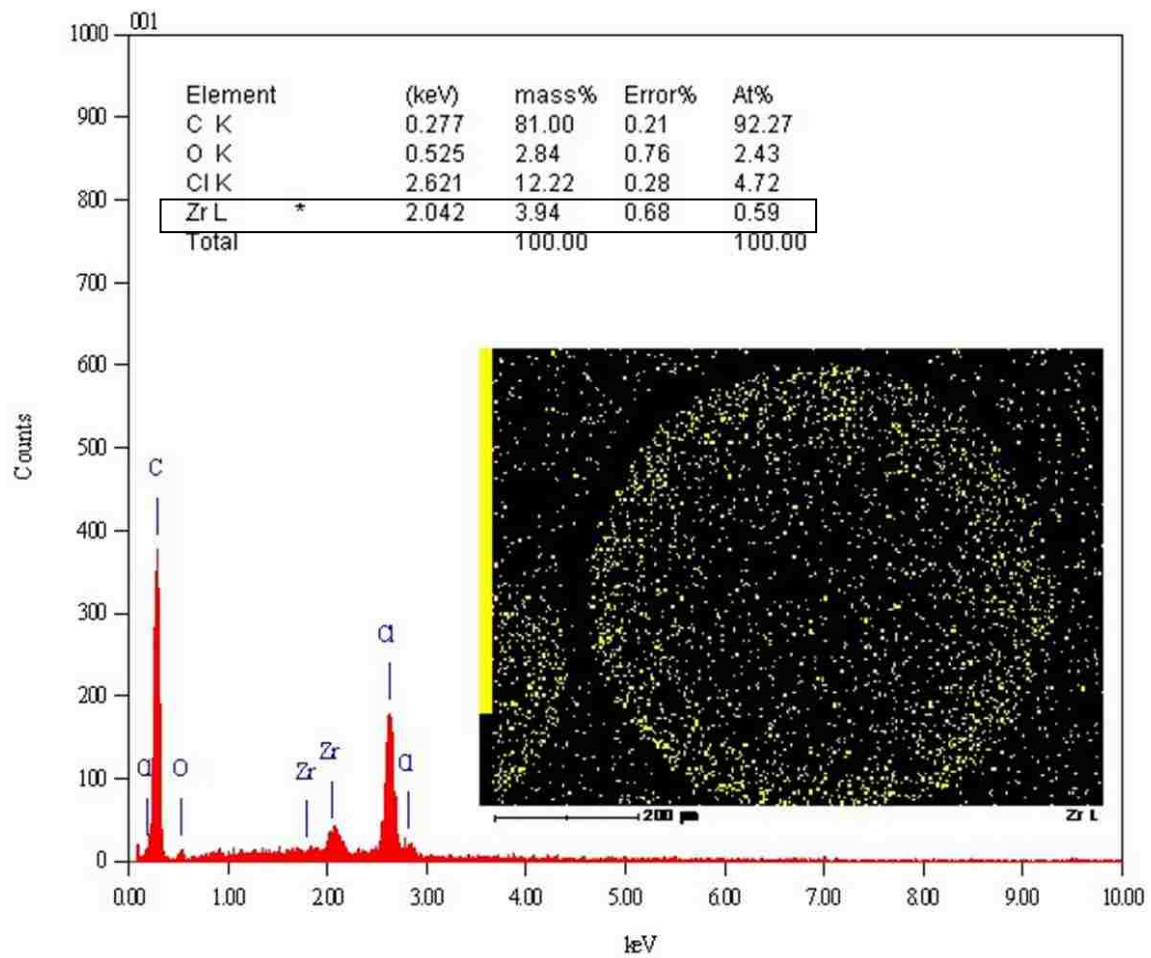
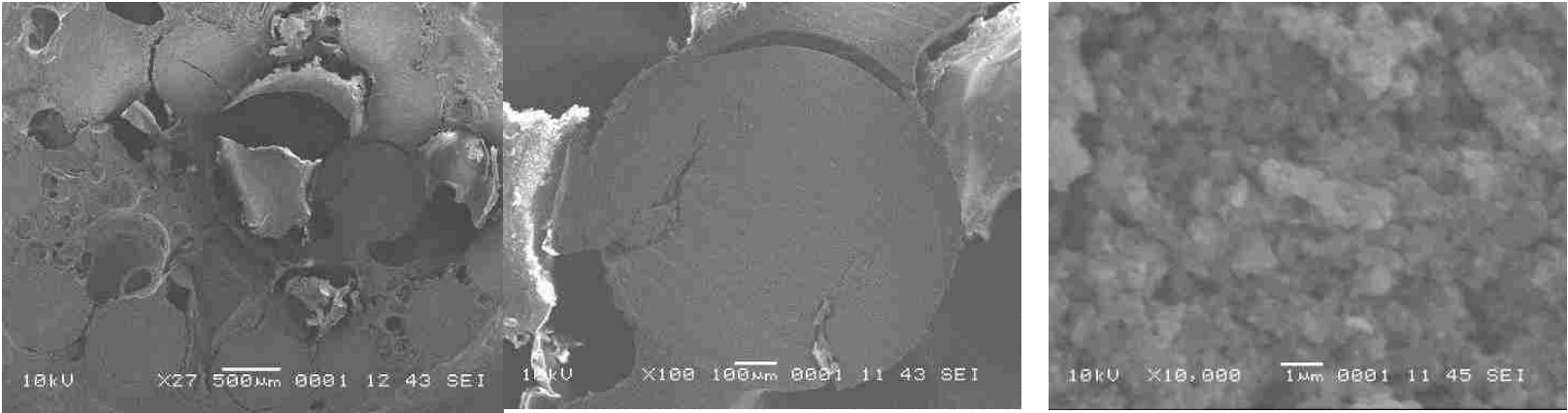
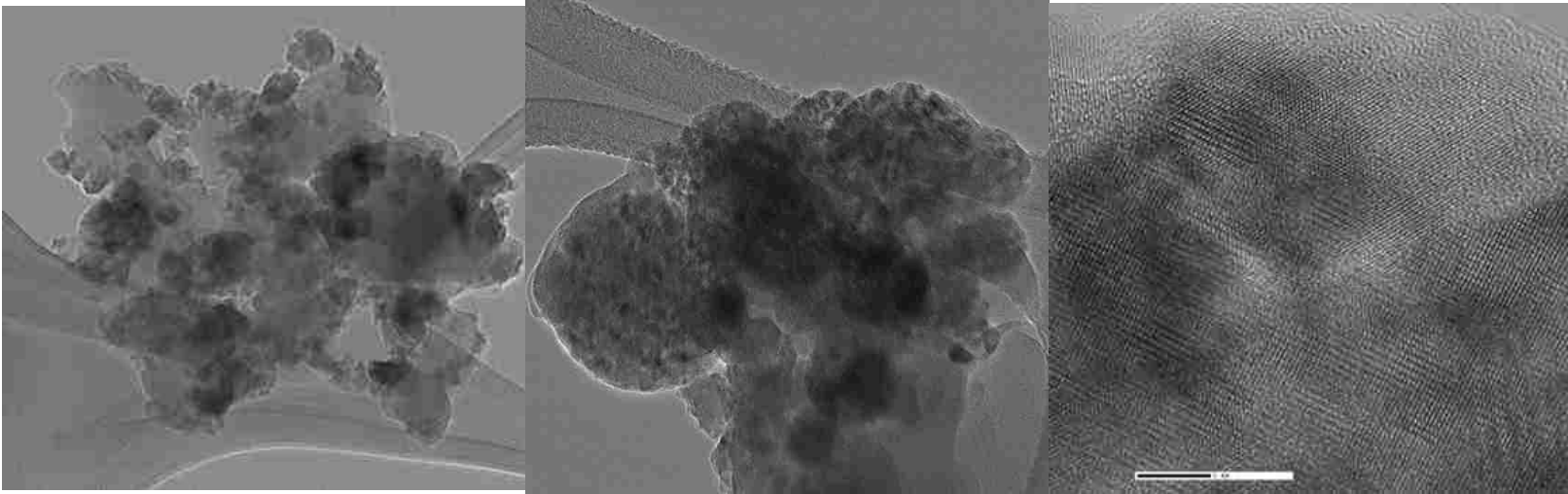


**Figure 3.13** SEM, TEM, and EDX spectrum and elemental mapping of Purolite A400-Zr

**SEM of Purolite A500P-Ti**



68 **TEM of Purolite A500P-Ti**



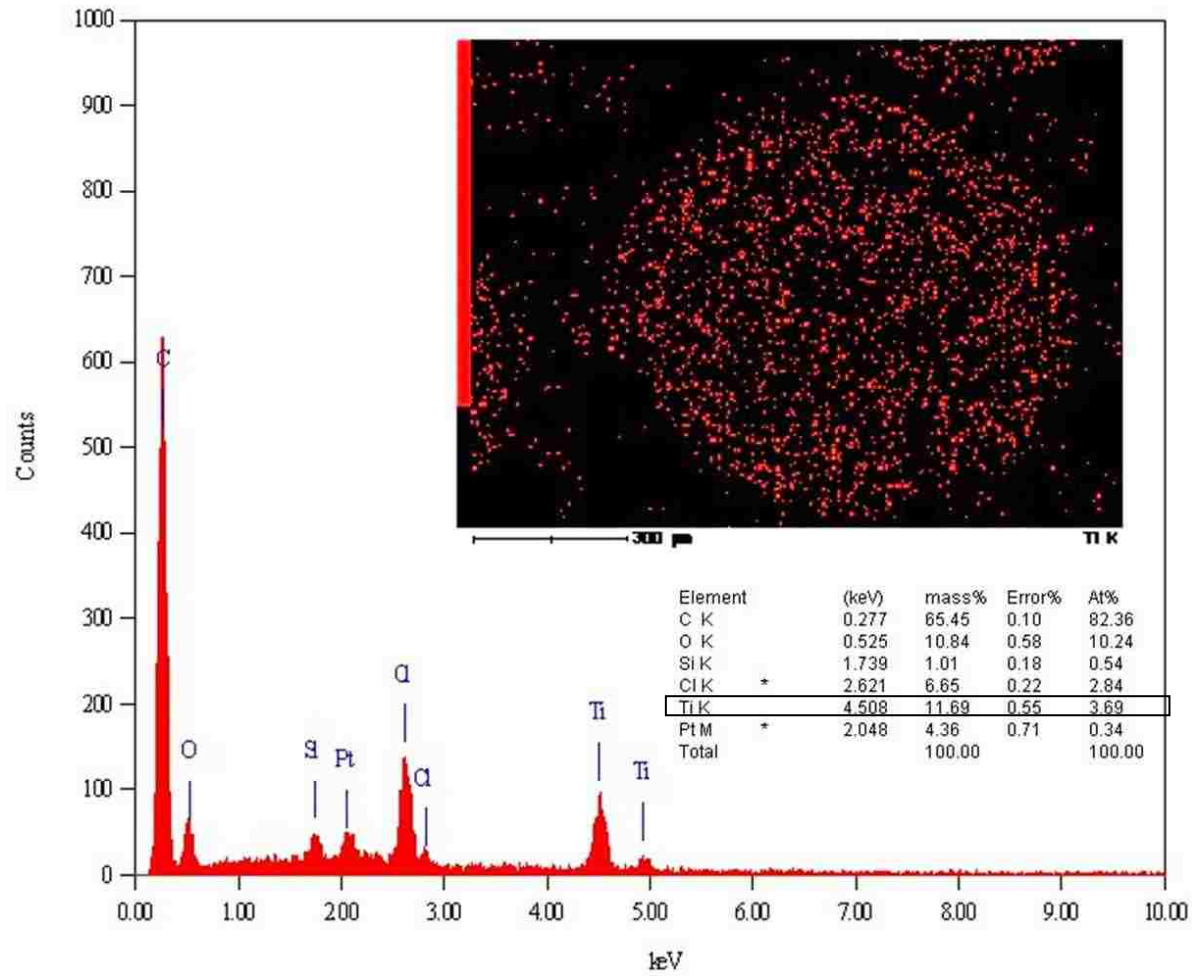
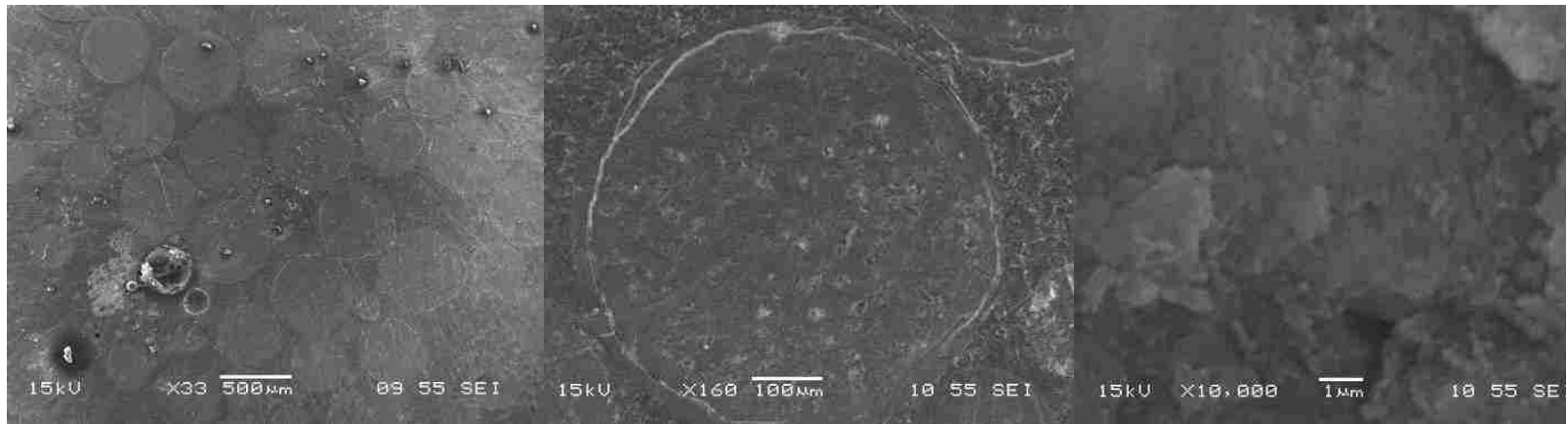


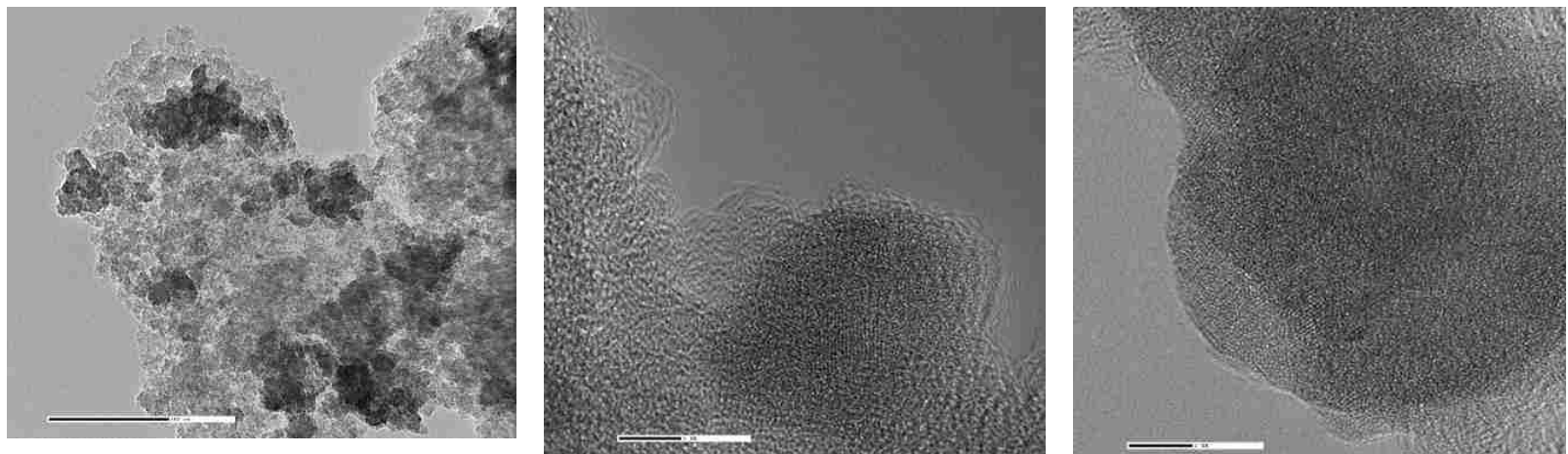
**Figure 3.14** SEM, TEM, and EDX spectrum and elemental mapping of Purolite A500P-Ti

**SEM of Amberlite XAD4-Zr**



16

**TEM of Amberlite XAD4-Zr**





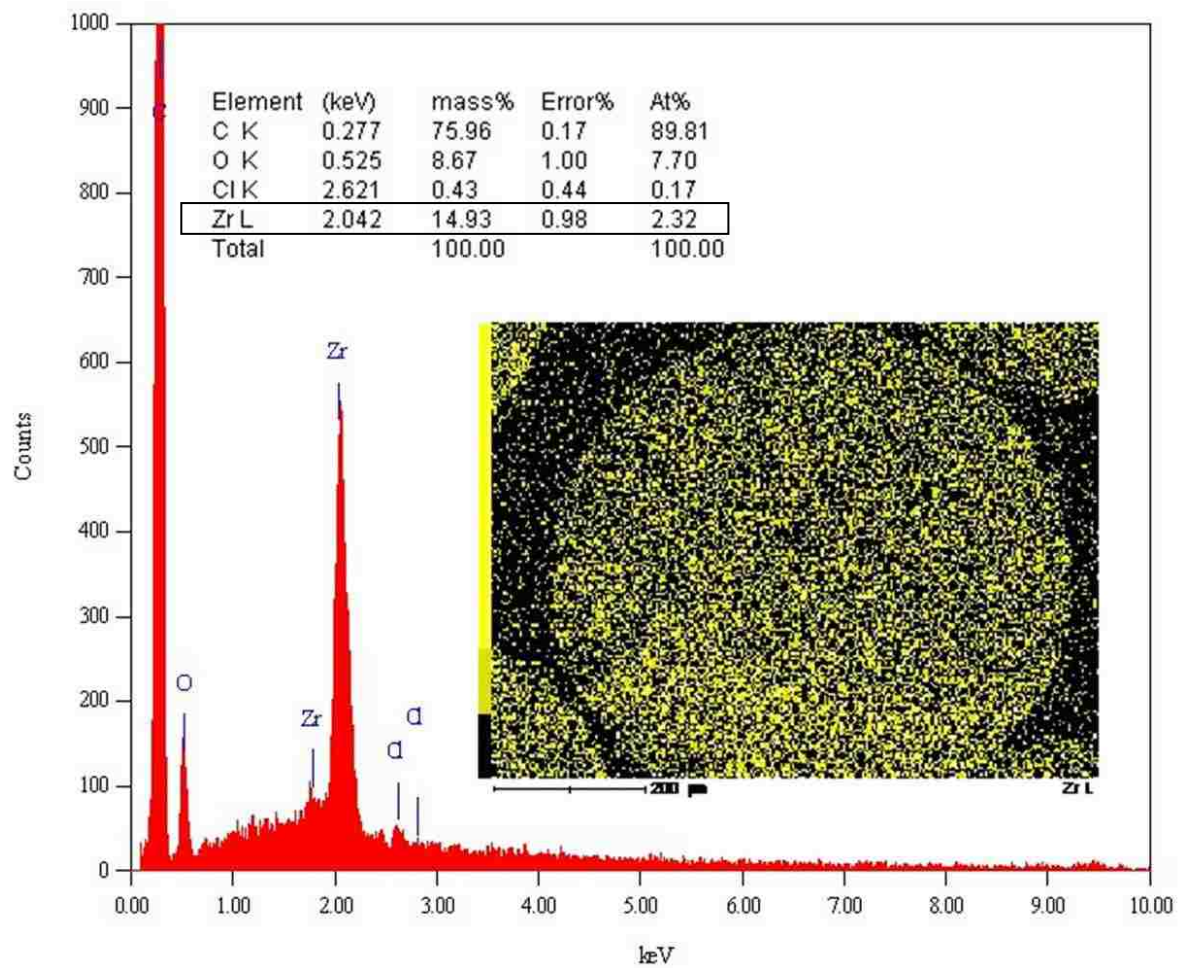


**Figure 3.15** SEM, TEM, and EDX spectrum and elemental mapping of Amberlite XAD4-Zr

**SEM of commercial Iron-based sorbent (ArsenX-Fe)**



**TEM of commercial Iron-based sorbent (ArsenX-Fe)**



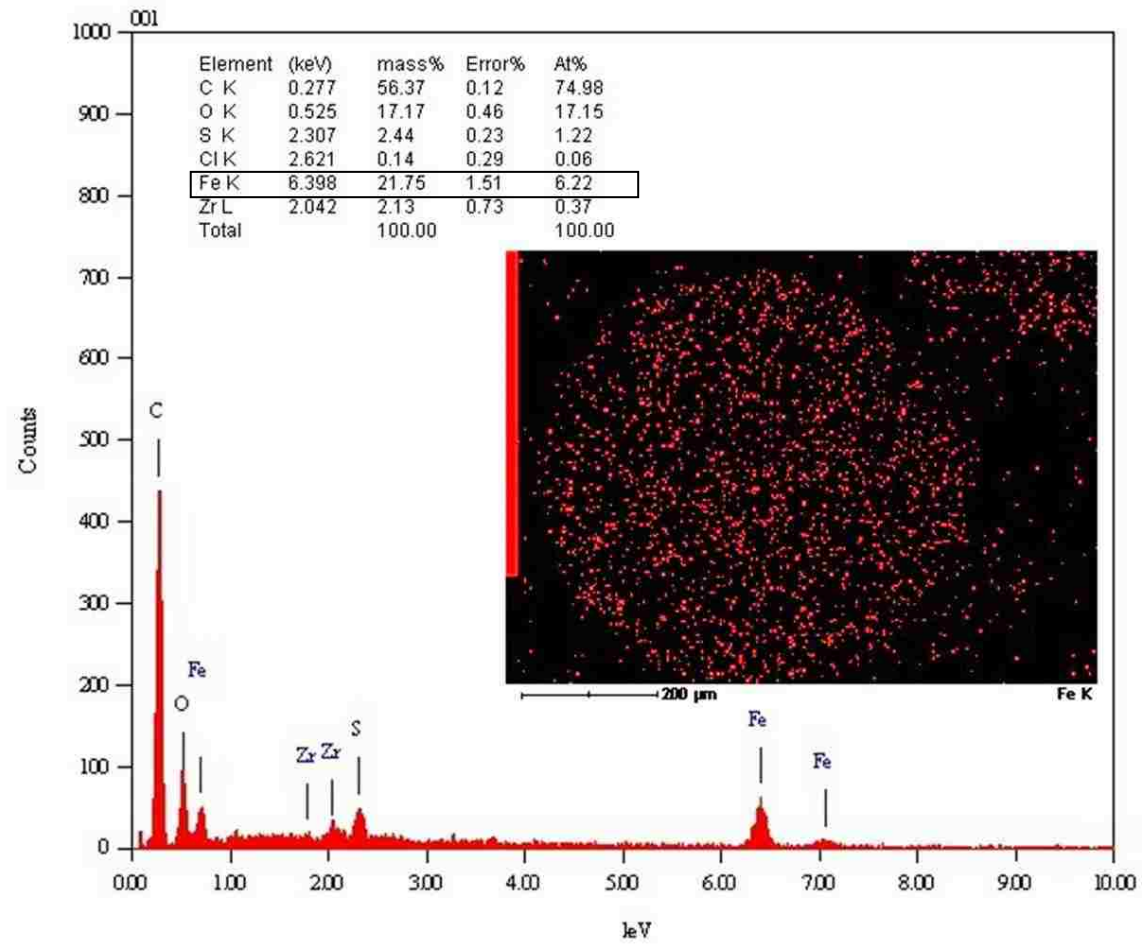


**Figure 3.16** SEM, TEM, and EDX spectrum and elemental mapping of commercial Iron-based sorbent (ArsenX-Fe)

## CHAPTER 4

### RESULTS AND DISCUSSION: ARSENIC REMOVAL BY HAIX-Zr

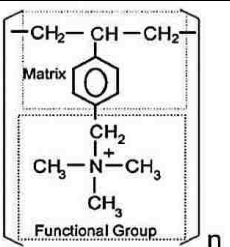
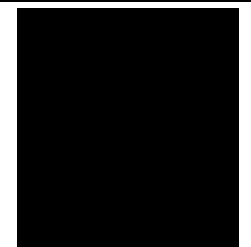
In this chapter, the best hybrid anion exchanger impregnated with hydrated Zr(IV) oxide (HZO) nanoparticles or HAIX-Zr as mentioned in the chapter 3 section 3.6, which was prepared from an inexpensive zirconium oxide by batch method #1 was used for further investigations for arsenic removal. The results and discussion of arsenic removal by the HAIX-Zr were investigated in the following aspects:

1. Material characterization and evidence of HZO nanoparticles dispersed in the HAIX-Zr. The zirconium content, size of nanoparticles, and the distribution of HZO throughout the resin phases were characterized using the combination of a gravitational method, SEM/ EDX, and HR-TEM.
2. Sorption/desorption of trace As(V) and As(III) by using NSF Std. 53 Challenge Water as a test influent. The arsenic removal mechanisms, role of the Donnan membrane effect from the functional groups of the ion exchangers, regeneration mechanisms, and waste containment are discussed in this section.
3. The various equilibrium sorption tests including sorption isotherms, effect of the influent pH to the sorption capacity, and effects of the main competing ions that change the sorption capacity of the HAIX-Zr namely, silica, phosphate, and sulfate.
4. Modeling of the As(V) sorption kinetics onto the HAIX-Zr.

## 4.1 Material Characterization and Evidences of HZO Nanoparticles

For this study, the hybrid materials were prepared by the batch method using zirconium oxide from MEL chemicals (Flemington, NJ) as the startup zirconium source. A macroporous strong-base anion exchanger (Purolite A500P) was used as the polymeric support. For comparison of the Donnan membrane effect resulting from the ion exchange support, the macroporous strong acid cation exchanger (Purolite C145) was also used for zirconium oxide impregnation. The salient properties of the parent resins are summarized in the table 4.1.

**Table 4.1** Property of polymeric ion exchangers

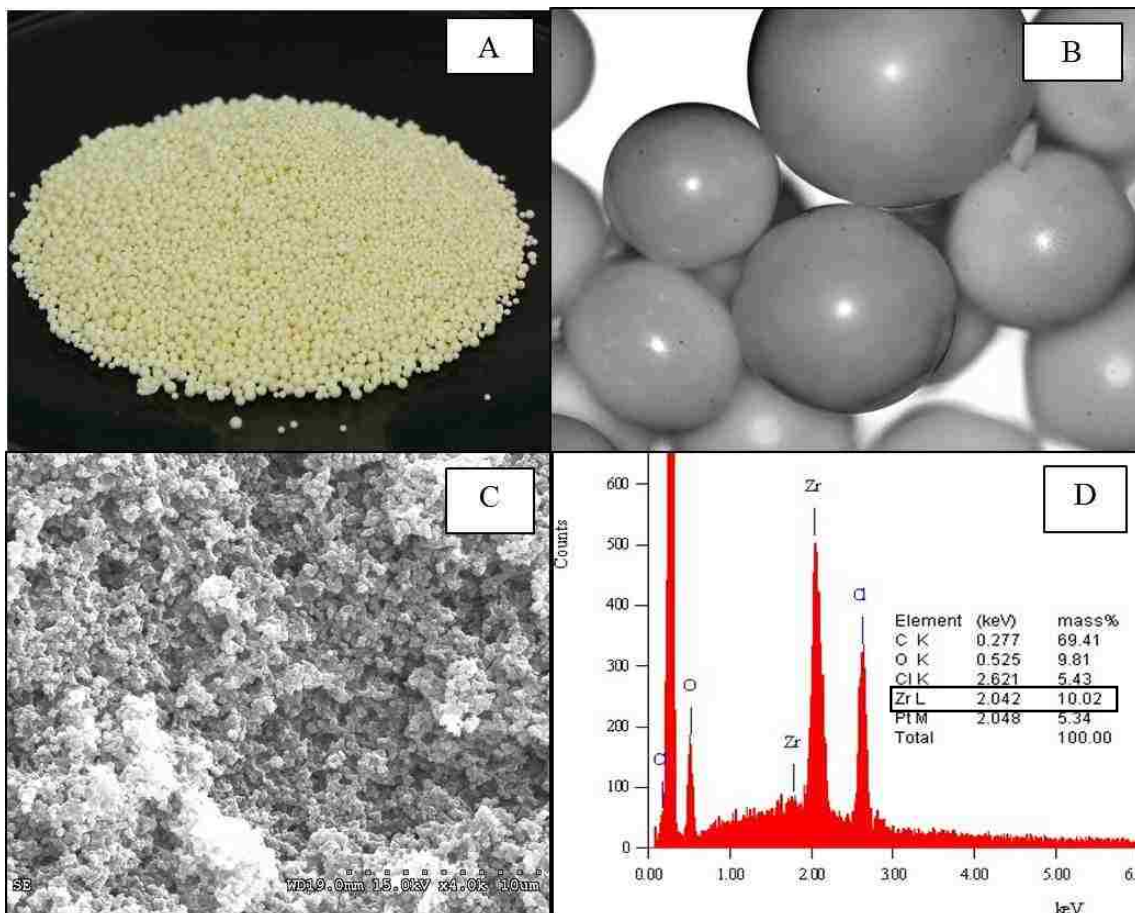
Ion Exchangers	Purolite A500P Anion Exchanger	Purolite C145 Cation Exchanger
<b>Structure</b>	 <p>The diagram shows a polymer chain segment <math>[-CH_2-CH-CH_2-]</math> where the central CH is bonded to a benzene ring labeled 'Matrix'. Below the benzene ring is a quaternary ammonium group: <math>CH_2</math> is bonded to a nitrogen atom (N) with a positive charge (+), which is also bonded to three methyl groups (<math>CH_3</math>). The entire structure is labeled 'Functional Group' and has a subscript 'n'.</p>	
<b>Functional groups</b>	Type I quaternary ammonium	Sulfonic acid
<b>Matrix</b>	Macroporous polystyrene cross linked with divinylbenzene	Macroporous polystyrene cross linked with divinylbenzene
<b>Capacity (meq./ml)</b>	0.8	1.5

The details and development techniques are discussed in chapter 3. For this study, the hybrid material was prepared by batch method #1 as mentioned in section 3.2.1. Briefly, as the first step, the zirconium solution was prepared by adding 15% of

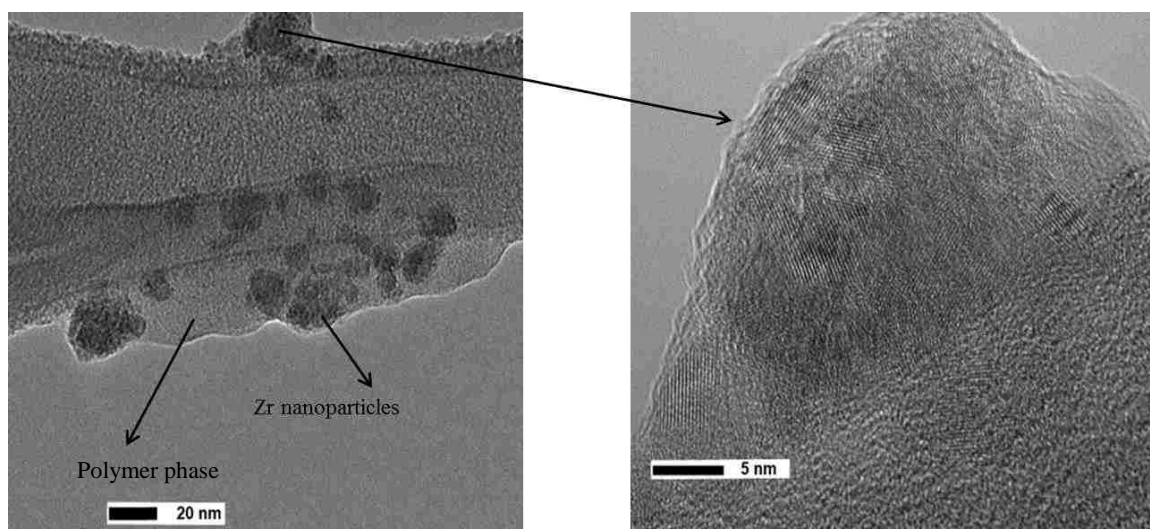
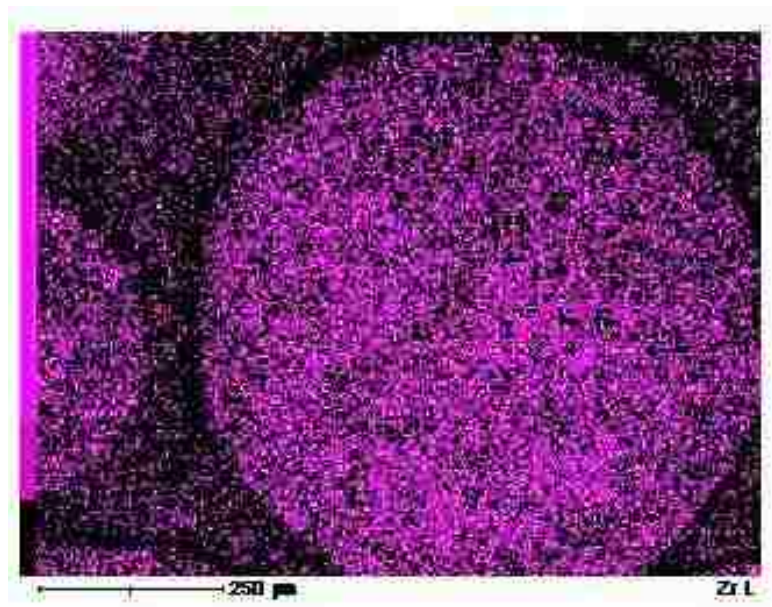
zirconium oxide into 20% of sulfuric acid solution and methanol at 50:50 ratios. Then the zirconium solution was mixed with parent macroporous anion exchange resins with quaternary ammonium ( $R_4N^+$ ) functional groups in the chloride form by shaking the resin and the zirconium solution in the rotary shaker for 3 hours. Second, the decanted resin from the first step was brought into contact with alkaline solution (28%  $NH_4OH$  solution) for 1 hour. Anion exchanger beads from the second step were washed with tap water followed by an acetone wash, and air dried for 24 hours. These steps were repeated for two more cycles to achieve greater Zr(IV) loading. HZO agglomerates were irreversibly encapsulated within the spherical anion exchanger beads and which were found to have 110-130 mg Zr/g. Total zirconium contents of the HAIX-Zr were determined by double 72 hours acid digestion with 50% sulfuric acid. The zirconium content was determined using ICP-OES (Perkin Elmer 2000 DV). The zirconium content in the hybrid material prepared from zirconium oxide (MEL Chemical, NJ) is 11% (w/w) as also mentioned in chapter 3, sections 3.7. The mass of zirconium in the hybrid material was confirmed semi-quantitatively by SEM/EDX and shown in the figure 4.1D.

Figure 4.1A-B shows a photo of HAIX-Zr beads with size approximately 300-1,200 micrometers in diameter and with an enlarged view (40X). The SEM micrograph of HAIX-Zr bead as illustrated in figure 4.1C, which shows the macroporous structure of the parent macroporous anion exchanger resin (Purolite A500P). The Zr content in the HAIX-Zr was determined semi-quantitatively as 10% by mass using the energy-dispersive X-ray (EDX) spectroscopy analysis as shown in figure 4.1D. The evidence of

hydrated Zr(IV) oxide nanoparticle deposited on the hybrid material is confirmed by using a high resolution TEM as shown in the figure 4.2



**Figure 4.1** (A) HAIX-Zr beads with the size range of 0.4-1.2 mm in diameter (B) Photograph (40X) of enlarged view of the hybrid anion exchanger impregnated with hydrated Zr(IV) oxide nanoparticles (HAIX-Zr), (C) Scanning electron micrograph (SEM) of macro-porous type of HAIX-Zr (40,000X), (D) Energy dispersive X-ray spectroscopy (EDX) spectrum of the HAIX-Zr (10 % of elemental zirconium by mass basis)



**Figure 4.2** High resolution transmission electron microscopy (HRTEM) photograph of HAIX-Zr



## 4.2 Fixed-Bed Column Runs using HAIX-Zr

Fixed-bed column runs for sorption-desorption of arsenate and arsenite were carried out using epoxy coated glass columns (Ace Glass) with 11 mm in diameter, a constant flow pump (Fluid Metering Inc.), and an Eldex fraction collector. The ratio of column diameter to the hybrid adsorbent bead diameter is more than 20:1; the previous work on chromate and phosphate removal with similar setups showed no premature leakage due to wall effects under identical conditions (50, 55). The empty bed contact time (EBCT) and the superficial liquid velocity (SLV) were recorded for each experimental column run. For testing arsenic removal, NSF Standard 53 Challenge Water was prepared which contained As(V) or As(III) 50 µg/L, pH 7.5, and other ions as shown the table 4.2.

**Table 4.2** Characteristic of NSF Std. 53 Challenge Water formula

Species	mg/l	Cations	mg/L	meq/L	Anions	mg/L	meq/L
Na <sub>2</sub> CO <sub>3</sub>	106	Na <sup>+</sup>	71.2	3.1	CO <sub>3</sub> <sup>2-</sup>	60	2
CaCl <sub>2</sub> 2H <sub>2</sub> O	147	Ca <sup>2+</sup>	40	2	Cl <sup>-</sup>	71	2
Mg(NO <sub>3</sub> ) <sub>2</sub> 6H <sub>2</sub> O	18.3	Mg <sup>2+</sup>	1.7	0.1	NO <sub>3</sub> <sup>-</sup>	8.9	0.14
NaF	2.2				F <sup>-</sup>	1	0.05
Na <sub>2</sub> SO <sub>4</sub>	74				SO <sub>4</sub> <sup>2-</sup>	50	1
P	0.12						
SiO <sub>2</sub>	10						
As(V)	50 ppb						
			total	5.2			
						total	5.2

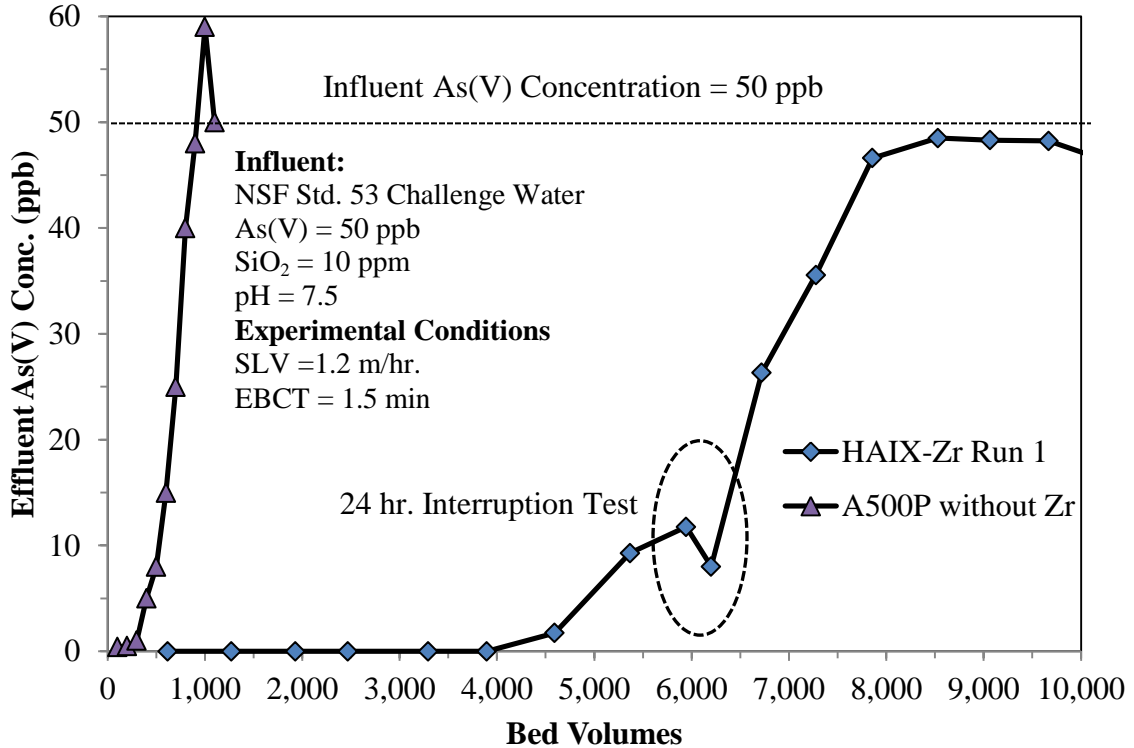
For As(III) in the feed, nitrogen gas was continuously sparged to guarantee that no As(III) was oxidized to As(V). Exhausted hybrid nanosorbents were regenerated using a mixed solution of 3% NaOH and 3% NaCl. Following regeneration, the bed was rinsed with CO<sub>2</sub> sparged water solution (pH =3.2) for about 10 bed volumes to bring the hybrid sorbent to working condition.

Figure 4.3-4.6 provide As(V) and As(III) effluent histories for four separate column runs under identical conditions using parent macroporous anion exchanger Purolite A500P in the chloride form, hybrid cation exchanger (Purolite C145) loaded HZO or HCIX-Zr, and hybrid anion exchanger (Purolite A500P) loaded with HZO or HAIX-Zr, respectively. For the HAIX-Zr, two different arsenic species were tested, arsenate (As(V)) and arsenite (As(III)). The abscissa represents the effluent arsenic concentration and treated bed volumes (mL water/mL sorbent). The influent composition and the hydrodynamic conditions, i.e. empty bed contact time (EBCT) and superficial liquid velocity (SLV) are also provided. NSF Standard 53 Challenge Water containing As (V) or As(III) 50 µg/L at pH 7.5 and other background ions was used as feed water for column experiments.

#### **4.2.1 Sorption of Trace As(V) under High Concentration of Competing Ions**

Figure 4.3 shows comparison of effluent histories of arsenate or As(V) during separate column runs between a strong base anion exchanger (A500P from Purolite) and the HAIX-Zr. HAIX-Zr can remove As(V) effectively with nearly 6,000 bed volumes before reaching the maximum contamination level (MCL) of arsenic at 10 ppb. In contrast, for Purolite A500P, arsenic breakthrough started at less than 300 bed volumes. It

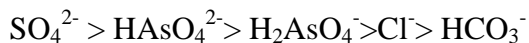
can be concluded that the arsenic removal capacity of the anion exchanger is greatly enhanced by HZO nanoparticles impregnated within the material.



**Figure 4.3** Effluent histories of As(V) during column runs with HAIX-Zr and Purolite A500P

The following observations are noteworthy: First, trace arsenate or As(V) were selectively removed by HAIX-Zr under the presence of high concentrations of competing anions such as sulfate, while the parent anion exchanger cannot remove much arsenate (arsenate breakthrough at only 300 bed volumes). Second, the effluent As(V) concentration from Purolite A500P was significantly greater than the influent concentration after breakthrough. This phenomenon is called “chromatographic elution” which implies that the anion exchanger exhibits greater selectivity toward sulfate over

As(V) oxyanions. The same observations were also seen in the literature (29). The selectivity for various anions toward anion exchangers are as follows and the column runs result was also mentioned in chapter 1 section 1.1.1:



Theoretically, As(V) can be removed by an anion exchanger. However, in real applications, there are many innocuous anions (i.e.  $\text{SO}_4^{2-}$ ,  $\text{HCO}_3^-$ ,  $\text{Cl}^-$ ) that appear at two or more order of magnitudes higher concentrations than arsenate. The arsenate removal capacity is significantly reduced in the presence of competing ions, especially sulfate ions. For arsenate contaminated waters with high concentrations of sulfate, the traditional anion exchanger is not an effective method.(16)

#### 4.2.2 Sorption of As(III)

For arsenite or As(III) removal, figure 4.4 shows As(III) effluent history for an HAIX-Zr column run. During the column run experiment, nitrogen gas was continuously sparged in the influent container to prevent the oxidation of As(III) to As(V). The effluent samples were processed by adding acid solution and separate As(III) out of the solution by using anion exchange resins as mentioned in chapter 2, section 2.2.1. From the results in figure 4.4, several observations are summarized as follows:

- Arsenite or As(III) was effectively removed by HAIX-Zr for close to 4,000 bed volumes before the effluent exceeded the MCL (10 ppb). Due to the  $\text{pK}_{\text{a}1}$  of As(III) oxyacid ( $\text{HAsO}_2$ ) of around 9.2 (16), the As(III) appears in the water as the non-ionized

from (HAsO<sub>2</sub>) thus non-ionized As(III) oxyacid cannot be removed by any type of Coulombic interactions.

- Compared with As(V) removal from figure 4.3, the removing capacity of HAIX-Zr for As(III) is lower than As(V). The As(V) breakthrough is at 6,000 bed volumes at the MCL 10 ppb while As(III) breakthrough was at 4,000 bed volumes.

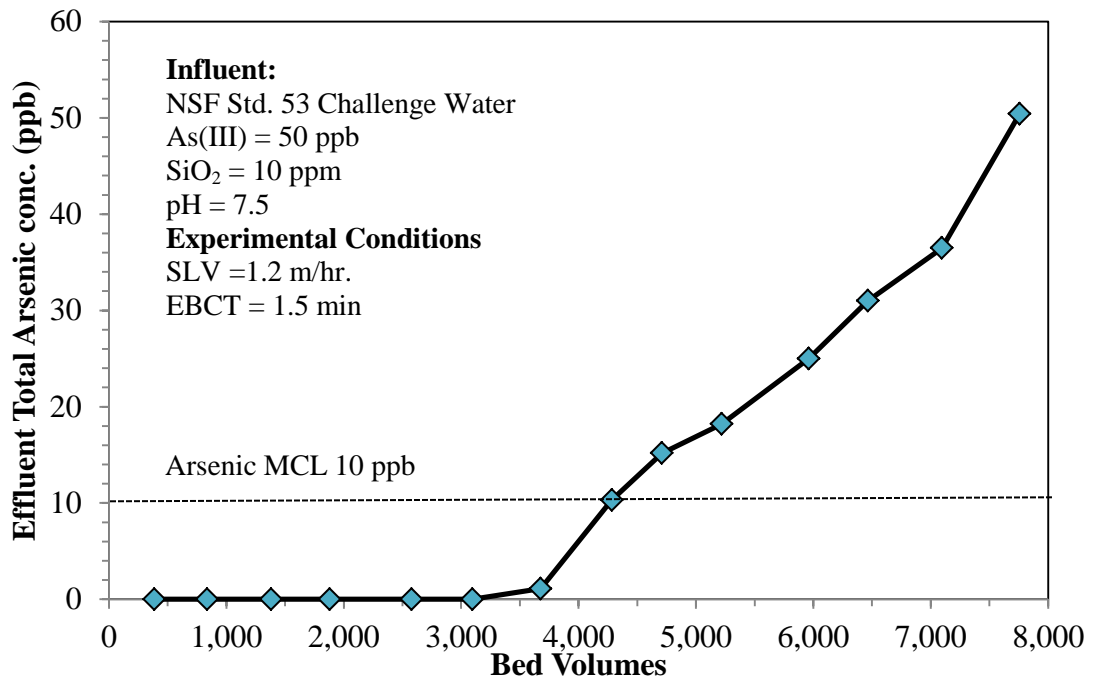


**Figure 4.4** Effluent history of As(III) during a column run with HAIX-Zr

#### 4.2.3 Arsenic Sorption Behaviors with Hydrated Zirconium Oxide in the HAIX-Zr

Under circum neutral pH of groundwater and natural water, arsenate or As(V) exists as mono (H<sub>2</sub>AsO<sub>4</sub><sup>-</sup>) and divalent (HAsO<sub>4</sub><sup>2-</sup>) anions in aqueous solution. At neutral pH, As(III) appears as non-ionized species, HAsO<sub>2</sub> or H<sub>3</sub>AsO<sub>3</sub>. The arsenic chemistry is the following (16):

### Arsenate or As(V) Species



### Arsenite or As(III) Species



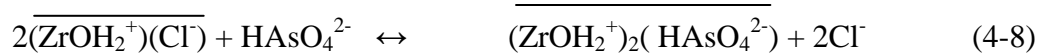
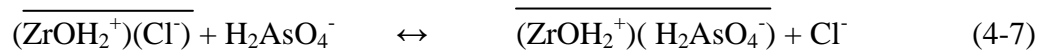
As mentioned in chapter 1, section 1.2.3, hydrated zirconium oxide particles are environmentally benign, inexpensive, and exhibit selective sorption properties toward both As (III) and As(V) through the formation of innersphere complexes.  $\text{HAsO}_4^{2-}$  is a bidentate ligand with two oxygen donor atoms while  $\text{H}_2\text{AsO}_4^-$  and  $\text{HAsO}_2$  are monodentate ligands, which have only one donor atom. Note that the commonly occurring competing ions such as sulfate and chloride can form only outer-sphere complex (46). Because  $\text{HAsO}_4^{2-}$  is a bidentate ligand, the innersphere complex between zirconium oxide (Lewis acid) and  $\text{HAsO}_4^{2-}$  (Lewis base) is stronger than the  $\text{H}_2\text{AsO}_4^-$  and  $\text{HAsO}_2$  that are only monodentate. From the result between As(V) and As(III) removal by HAIX-Zr at circum neutral pH in figures 4.3 and 4.4, the HAIX-Zr can remove As(V) better than the As(III) because As(V) can form a stronger complex with the HZO than the As(III). Moreover, As(V) is also bound to the zirconium oxide surface through the Coulombic interaction while As(III) binds with the zirconium oxide only through the Lewis Acid-Base (LAB) interaction.

In general, mechanisms of arsenic sorption at the surface of zirconium oxide are contributed to Coulombic and Lewis Acid-Based (LAB) interactions. The point of zero charge of zirconium (hydr)oxide averages 6.5 (56). The hydrated zirconium oxides can be viewed as diprotic weak acids that can be deprotonated as follows:



At a pH lower than the point of zero charge (PZC), the zirconium oxides are protonated ( $\overline{\text{ZrOH}_2^+}$ ) to have positive charges and behave as a Lewis acid (electron pair acceptor), and also act as anion exchangers. As(V) can be sorbed onto the surface sites through ion exchange reactions and at the same time can bind through the Lewis Acid Base (LAB) interactions. The reactions are shown as:

### Coulombic interactions



where the overbar represents the solid phase. At circum neutral pH, As(III) appears as non-ionized  $\text{HAsO}_2$ , thus it does not participate with the zirconium oxides via Coulombic interactions.

Sorption of arsenic onto the zirconium oxide nanoparticles is not only based on electrostatic (Coulombic) interactions similar to the ion exchange process but also mainly due to the Lewis Acid-Base (LAB) interaction. Thermodynamically, the overall free

energy change for the reaction of arsenic sorption onto the zirconium oxide nanoparticles come from both Coulombic (i.e., ion exchange) and Lewis Acid-Base (LAB) interactions as follows **(16)**:

$$\Delta G_{\text{Overall}}^0 = \Delta G_{\text{Cou}}^0 + \Delta G_{\text{LAB}}^0 \quad (4-9)$$

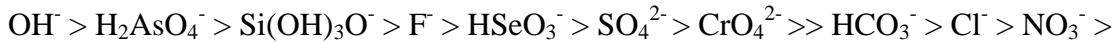
$$\text{or} \quad -RT \ln K_{\text{Overall}} = -RT \ln K_{\text{Cou}} - RT \ln K_{\text{LAB}} \quad (4-10)$$

$$\text{or} \quad K_{\text{Overall}} = K_{\text{Cou}} * K_{\text{LAB}} \quad (4-11)$$

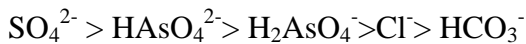
where  $\Delta G^0$  represents free energy changes at the standard state, R is the universal gas constant, T is the temperature in Kelvin and K is the equilibrium constant.

For the metal oxides such as zirconium, iron, aluminum,  $K_{\text{LAB}}$  is very high for most of the anionic ligands (i.e., arsenate) due to their Lewis acid base characteristics. Therefore, the  $K_{\text{Overall}}$  is very high. In contrast with other competing cations (e.g.,  $\text{Na}^+$ ,  $\text{K}^+$ ,  $\text{Ca}^{2+}$ , etc.) and anions (e.g.  $\text{SO}_4^{2-}$ ,  $\text{HCO}_3^-$ ,  $\text{Cl}^-$ ), the Lewis acid-base (LAB) is absent so the  $K_{\text{Overall}}$  is equal to the  $K_{\text{Cou}}$ .

Sorption with metal oxide **(2)**:



Removal by ion exchange (Coulombic):





## Lewis Acid-Based (LAB) interactions

LAB interactions play an important role for selective arsenic sorption onto the zirconium oxide nanoparticles. From figure 4.5, As(V) (both  $\text{H}_2\text{AsO}_4^-$  and  $\text{HAsO}_4^{2-}$ ) are sorbed on the surface of zirconium oxide particles through the combination of Coulombic and LAB interactions. The Lewis acid sites of zirconium oxides accept a lone pair of electron from oxygen donor atoms of  $\text{H}_2\text{AsO}_4^-$  and  $\text{HAsO}_4^{2-}$ . For arsenite or As(III), the Lewis acid sites of zirconium oxides accept lone pairs of electron from arsenic donor atoms of arsenite ( $\text{HAsO}_2$ ). The sulfate and chloride bind with zirconium oxide weakly through outer sphere complexes. Thus, for this study arsenate ( $\text{H}_2\text{AsO}_4^-$  and  $\text{HAsO}_4^{2-}$ ) with oxygen donor atoms and arsenite ( $\text{HAsO}_2$ ) with arsenic donor atoms are sorbed in preference to other commonly innocuous encounter anion namely, sulfate, chloride, and bicarbonate.

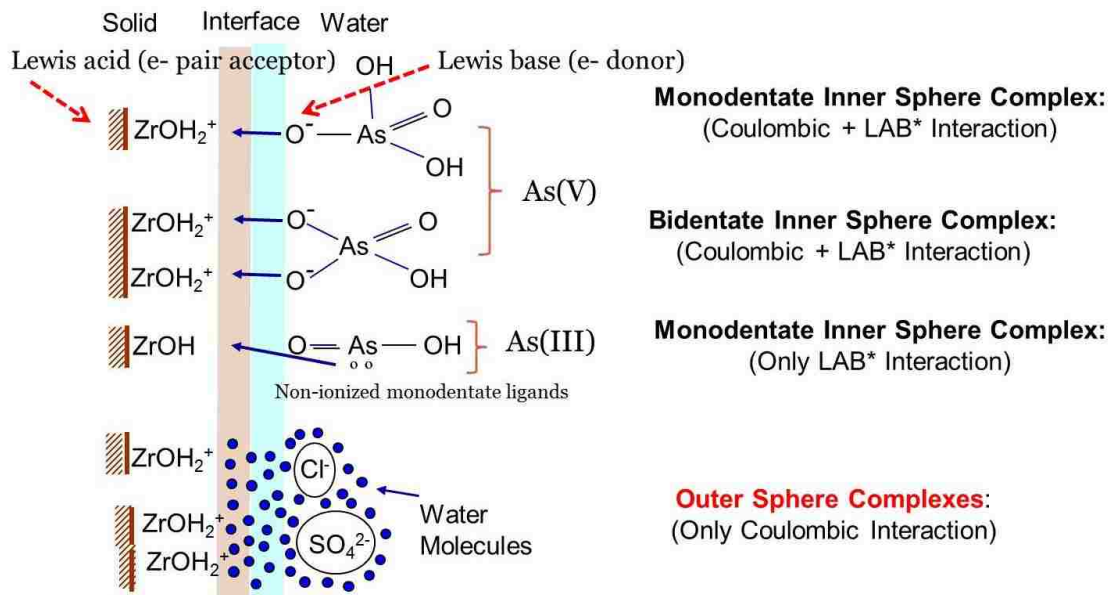


**Figure 4.5** A schematic diagram illustrating the binding of several of solutes onto hydrated zirconium oxides (HZO) at circum-neutral pH (adapt from (16))

#### 4.2.4 As(V) Removal from HAIX-Zr Vs. HCIX-Zr

From figure 4.6, there are marked differences in the performance of two different sorbents; HCIX-Zr and HAIX-Zr. Note that despite the same HZO contents, approximately 10-13% by mass in both HAIX-Zr and HCIX-Zr, HCIX-Zr was essentially unable to remove As(V), which broke through almost immediately. In contrast, HAIX-Zr exhibits excellent arsenic removal capacity. Arsenic started to breakthrough at MCL (10 ppb) after approximately 5,500 bed volumes.

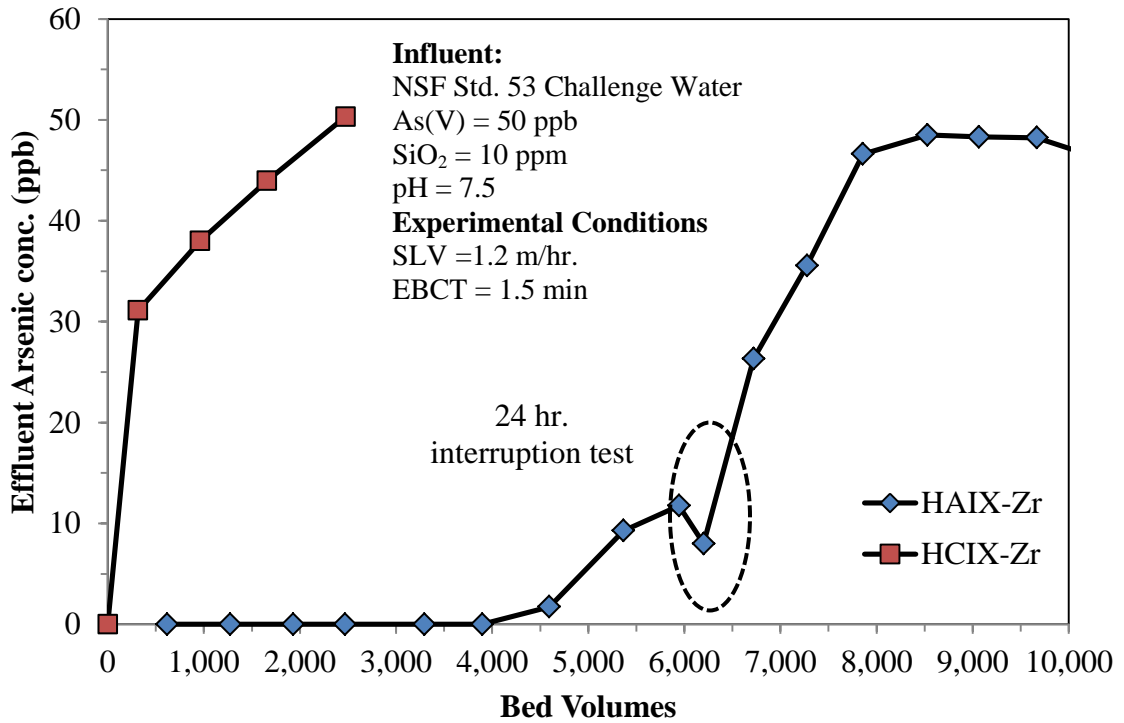


**Figure 4.6** Effluent histories of As(V) during a column runs with HAIX-Zr and HCIX-Zr

The following observations are noteworthy: for HAIX-Zr, the column run was deliberately stopped for 24 hours. The sharp decreases in effluent arsenic concentration occurred after the restart of the column run. The sharp drop in the effluent arsenic

concentration after restarting the column run suggested that the arsenic sorption onto the hybrid material is controlled by intraparticle diffusion within the material at this point in the run (50, 57).

#### 4.2.5 Donnan Membrane Effect

The submicron size HZO nanoparticles are easy to prepare, inexpensive, innocuous, and have very selective sorption toward both transition metals and anionic ligands. To improve mechanical strength and removal capacity, HZO have been loaded into many supports, namely chelating resins (58-60), collagen fibers, activated carbon, chitosan (61-64), polymers without functional groups (23, 65, 66), etc. Note that activated carbon, zeolite, alginate, cation exchangers, chelating resins, etc. also contain significant concentrations of negatively charge functional groups, namely, carboxylate and amino silicate. These substrates may be easily dispersed with HZO nanoparticles, but arsenic removal capacity will not be fully attained due to the Donnan exclusion effect. On the other hand, many reports confirmed that polymeric anion exchangers are an excellent substrate because it allows enhanced permeation of anions within the polymer phase due to its high concentration of fixed positively charges such as quaternary ammonium functional groups ( $R_4N^+$ ) in Purolite A500P (21, 29).

**Figure 4.7** provides a schematic illustrating the Donnan membrane effect for enhancing permeation of target anionic ligand contaminants. The presence of a high concentration of non-diffusing fixed positively charges in the polymer phase acts as a highly permeable interface for anionic species, thus influencing its sorption onto HZO particles embedded in the polymer phase. Because both Zr(IV) and quaternary

ammonium functional groups,  $R_4N^+$ , are positively charged, dispersing HZO nanoparticles within an anion exchanger faces a major scientific challenge.

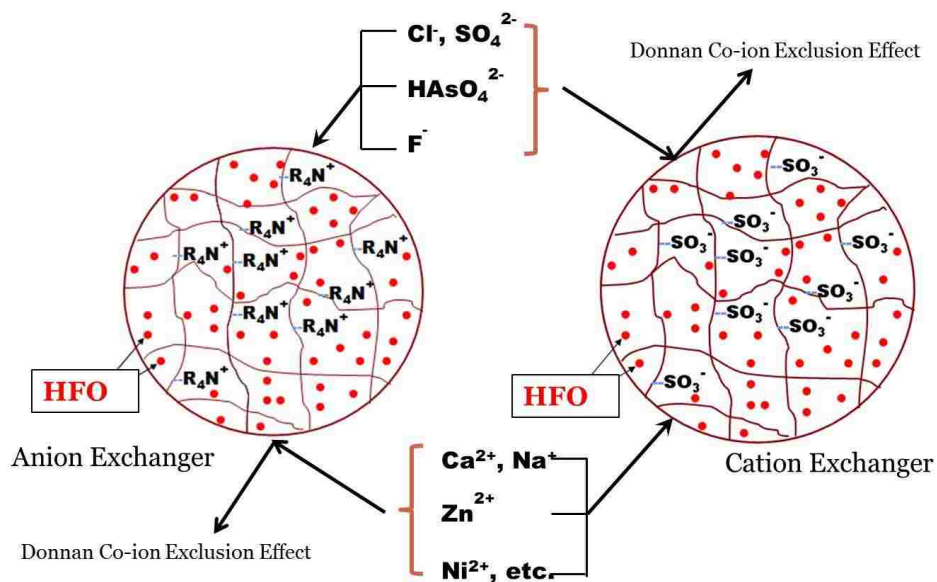


**Figure 4.7** Donnan membrane effect exerted by parent anion exchange supported

Several techniques for dispersing oxide nanoparticles into polymeric ion exchange supports including cation and anion resins have been discussed elsewhere (37, 53). Once the HZO are loaded into anion exchangers, the Donnan membrane effect caused by the polymeric anion exchanger support play an important role to remove target contaminants and enable tailoring of sorbents for intended applications. According to the information in the open literature, preparation and development of highly selective hybrid sorbent, HAIX-Zr, using HZO based on the Donnan membrane principle has not been reported to date.

#### **4.2.6 Regeneration and Reuse of HAIX-Zr**

After the column run, the exhausted HAIX-Zr was regenerated using a 3% NaCl and 3% NaOH mixed solution at pH of 12 and with an EBCT of 6.0 minutes. In less than 15 bed volumes, almost the entire amount of arsenate was desorbed from the HAIX-Zr. Over 90% of arsenic was desorbed within 15 bed volumes. Two successive As(V) sorption and regeneration runs are shown in figure 4.8 and clearly demonstrates that arsenate can be efficiently desorbed from HAIX-Zr effectively and the sorbent reused for multiple cycles without a significant loss in arsenic removal capacity. The spherical HAIX-Zr beads are robust and durable. There are no signs of particle breakdown into powder and XRD (XRD diffractograms were shown in chapter 5) show that the HZO are still amorphous after using three cycles of sorption/desorption.

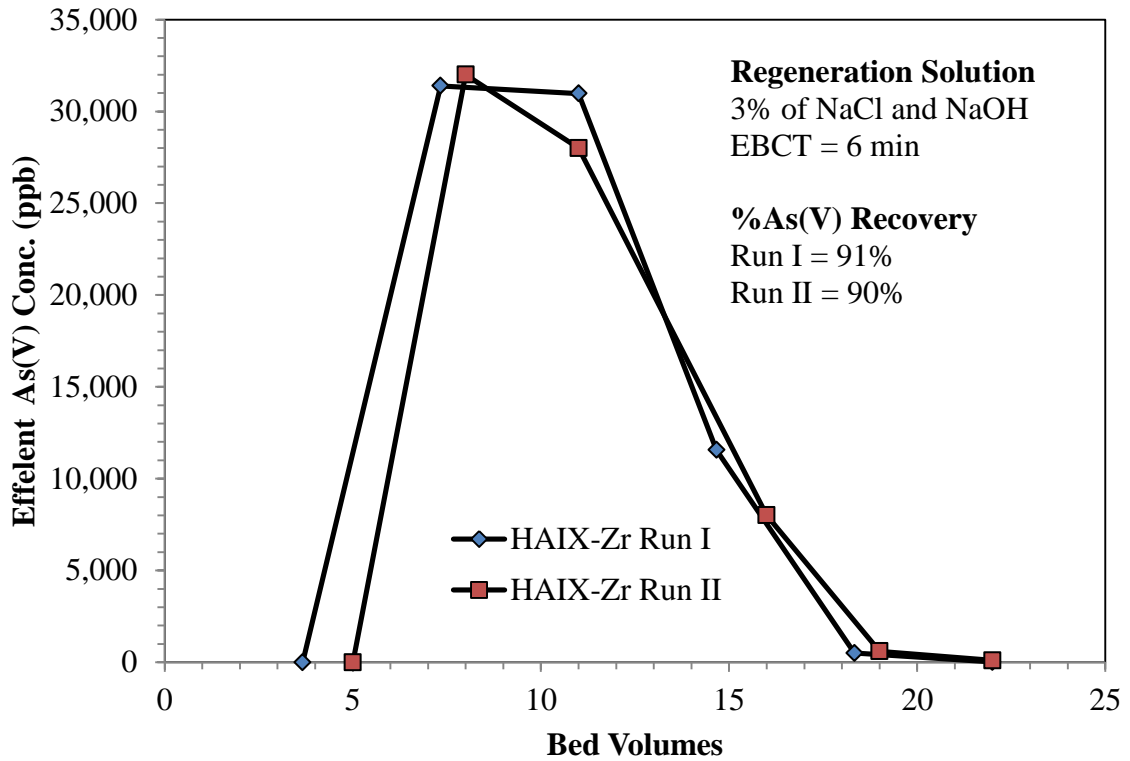
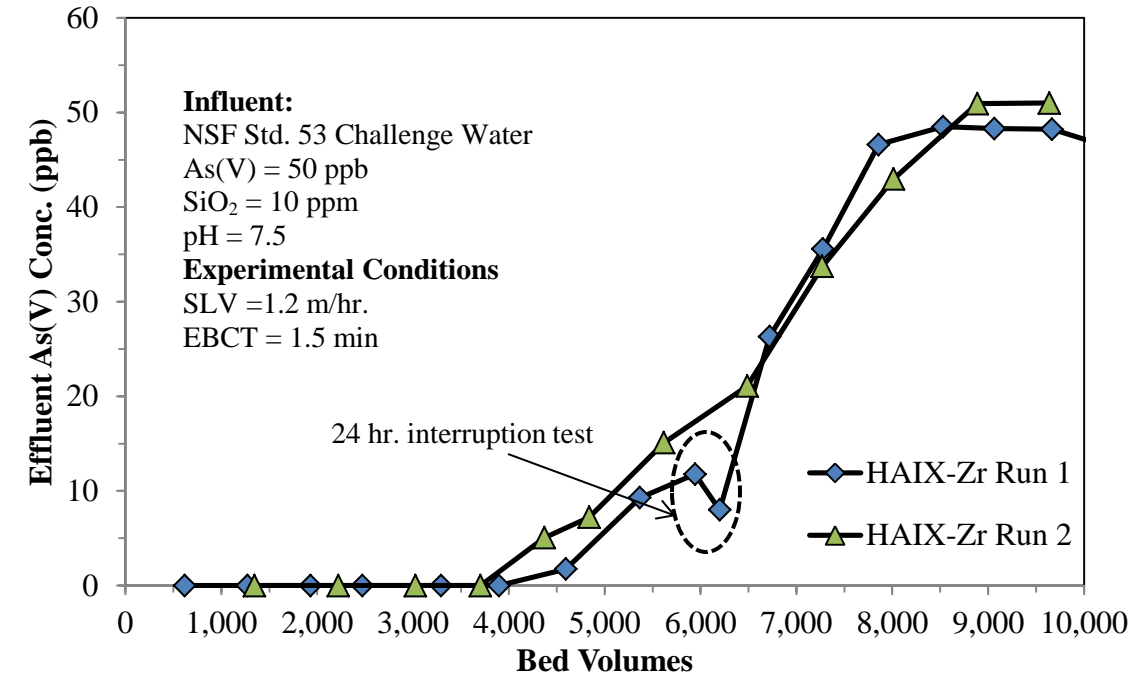
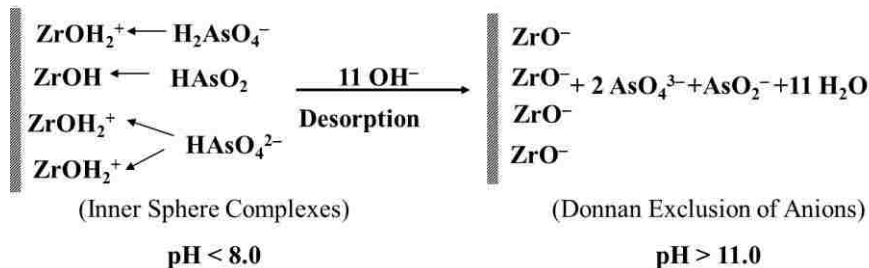
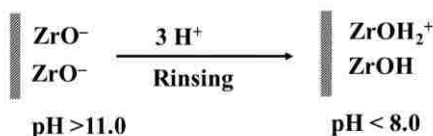


**Figure 4.8** Dissolved arsenic concentration profiles during desorption of HAIX-Zr using 3% NaOH and 3% as the regenerate solution.

**STEP 1. Mixed 3% NaOH and 3% NaCl**



**STEP 2. 0.5 N HCl or CO<sub>2</sub> sparged water**



The sorption/desorption mechanisms are illustrated in the above equation (15). During regeneration, when the pH was increased, the HZO sorption sites were deprotonated (negatively charge), so all arsenic oxyacid and oxyanion were desorbed from the HAIX-Zr at 3 orders of magnitude higher than feed concentration. The Donnan co-ion exclusion effect is predominant under regeneration conditions resulting in efficient desorption processes. Subsequently, the HAIX-Zr was reconditioned with dilute acid or CO<sub>2</sub> sparged water to adjust the pH from alkaline to nearly neutral, in less than 10 bed volumes. From this step, the surface charges of HZO in HAIX-Zr are protonated and ready for the next sorption cycle and no further pH adjustment was necessary during the service run.

The regenerable nature of HAIX-Zr can reduce the volume of toxic-laden waste by 100 times as compare to single-use adsorbent media (67). Most of single used media are routinely disposed of in landfills or hazardous waste sites. The phase diagrams of the

predominant arsenic, iron, and zirconium species are represented in figure 4.9. Note that even at slight anoxic and acidic condition ( $pe=0$ ,  $pH<7$ ),  $Fe(OH)_3(s)$  is thermodynamically unstable and soluble  $Fe^{2+}(aq)$  is predominates. Thus, the toxic metal or anionic toxic ligands sorbed onto Fe(III) oxide based adsorbents will gradually leach away under the reducing environment of a landfill. Al(III) based adsorbents (i.e., activated alumina (AA)), are thermodynamically stable under anoxic condition but As(V) species are not stable, and would be reduced to As(III) which is poorly adsorbable onto the AA (67). In contrast, HZO is chemically stable under wide pH and redox conditions. This unique characteristic of HZO makes HAIX-Zr it safe to dispose of the used material into the landfill.

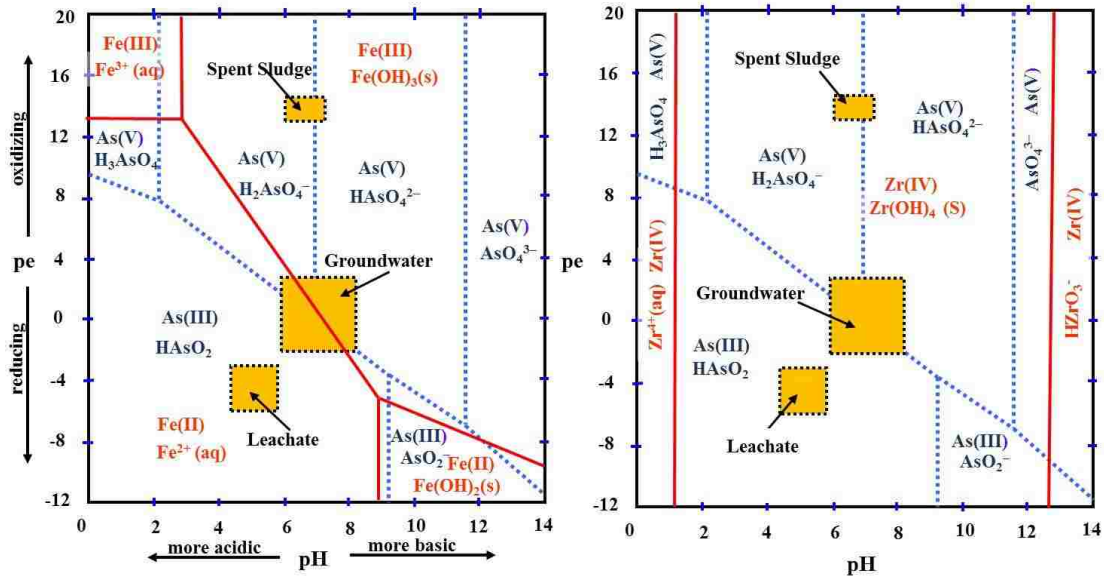


**Figure 4.9** Composite phase diagrams of Fe-As and Zr-As



## 4.3 Equilibrium Batch Test with HAIX-Zr

### 4.3.1 Sorption Isotherm of As(V) using HAIX-Zr

Batch equilibrium adsorption isotherm experiments were conducted to obtain the adsorption isotherms. Each point of the As(V) sorption isotherm was found by varying 6 initial arsenic concentrations. The samples were shaken for 5 days at room temperature to attain equilibrium. The supernatant was subsequently filtered through a 45 µm membrane filter. Arsenic concentration was measured using a graphite furnace atomic absorption spectrometer (Perkin Elmer model AAnalyst 600).

Langmuir and Freundlich adsorption isotherms are commonly used for adsorption studies. For this experiment, the sorption behavior of As(V) is fitted with the Langmuir model. The general and linear form of Langmuir adsorption model is given as:

$$\text{General form } q_e = \frac{QbC_e}{1+bC_e} \quad (4-12)$$

$$\text{Linear form } \frac{1}{q_e} = \frac{1}{QbC_e} + \frac{1}{Q} \quad (4-13)$$

where  $q_e$  and  $C_e$  represent the adsorption capacity (mg/g) and adsorbate concentration at equilibrium (mg/L),  $Q$  represents the maximum adsorption capacity (mg/g), and  $b$  (L/mg) is the Langmuir constant. From the equilibrium batch test, the arsenic sorption behaviors follow the Langmuir isotherm with maximum sorption capacity ( $Q$ ) of 20 mg As(V)/g (pH 7.5). The sorption capacity of HAIX-Zr towards arsenic is three times higher than commercially available activated alumina (AA).

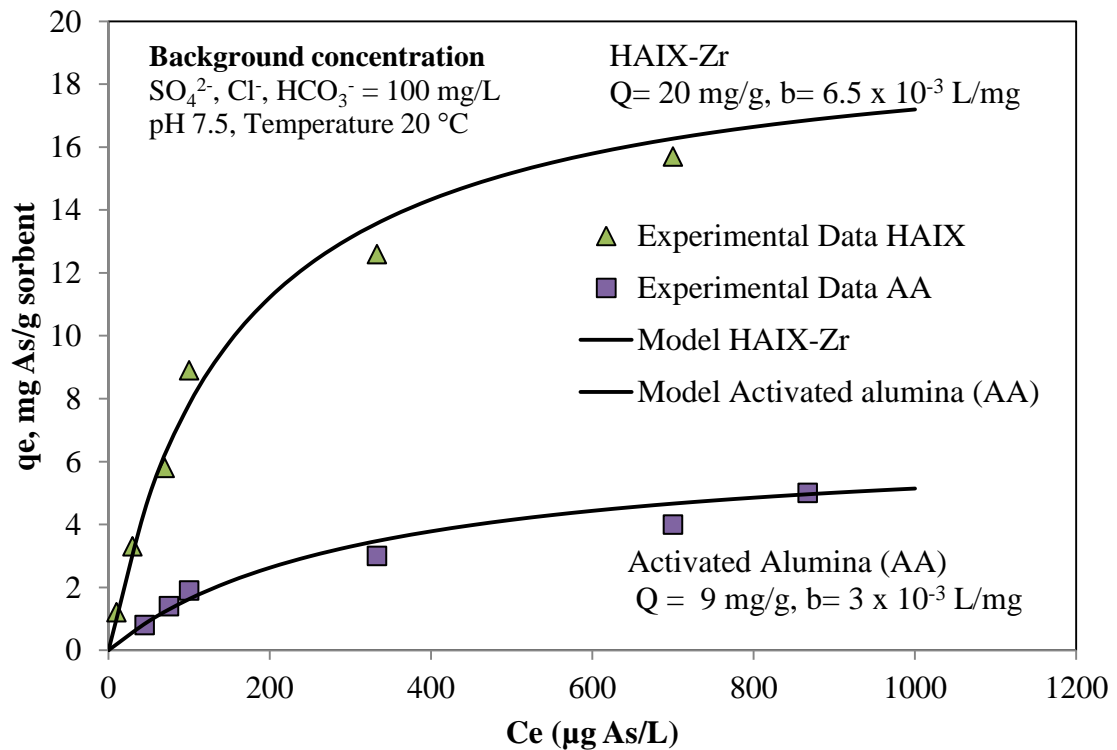
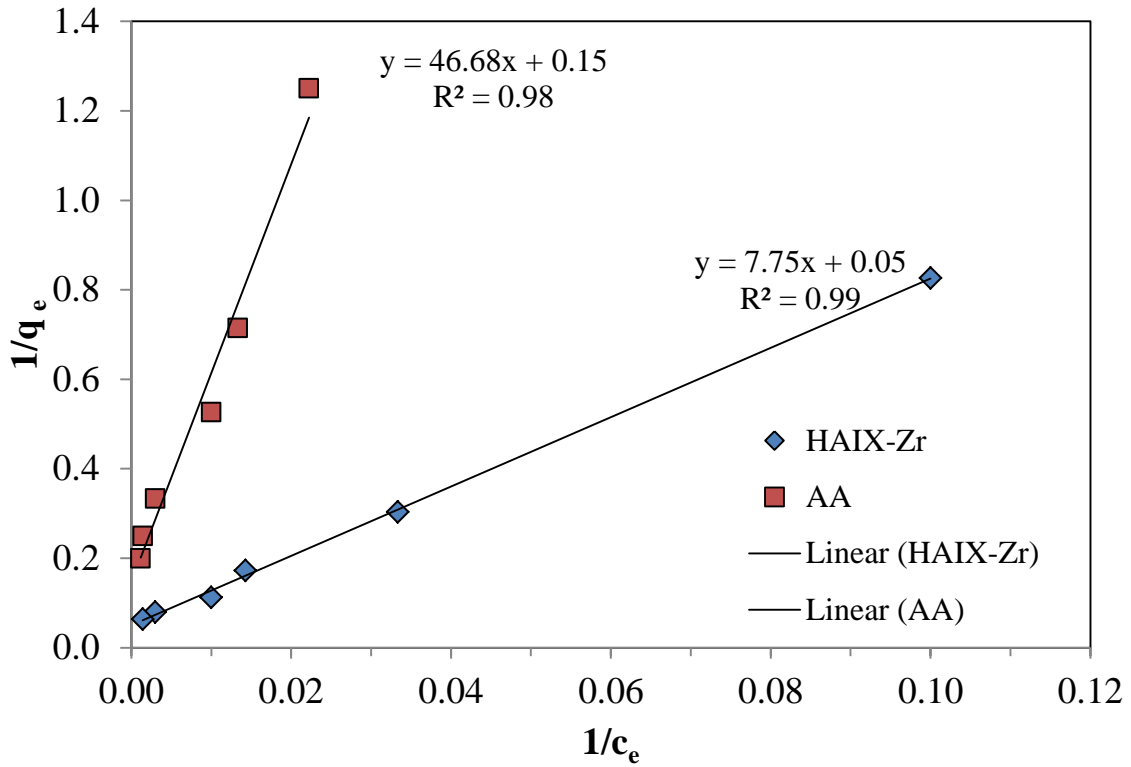


**Figure 4.10** Arsenic sorption isotherm plot at pH 7.5 with background anions at  $20^\circ\text{C}$

### 4.3.2 Effect of pH for the Sorption of As(V) using HAIX-Zr

In this test, 50 milligrams of HAIX-Zr were added into four different solutions containing As(V) with other background ions at different pHs. The solutions were shaken in the gyratory shaker for 5 days to attain equilibrium. The equilibrium arsenic removal capacity can be obtained by mass balance. Figure 4.11 shows the effect of pH for arsenic removal by HAIX-Zr. The equilibrium arsenic concentration is provided in the figure. Figure 4.11 implies that the pH affects the sorption capacity. The arsenic removal capacity dropped as the pH increases.

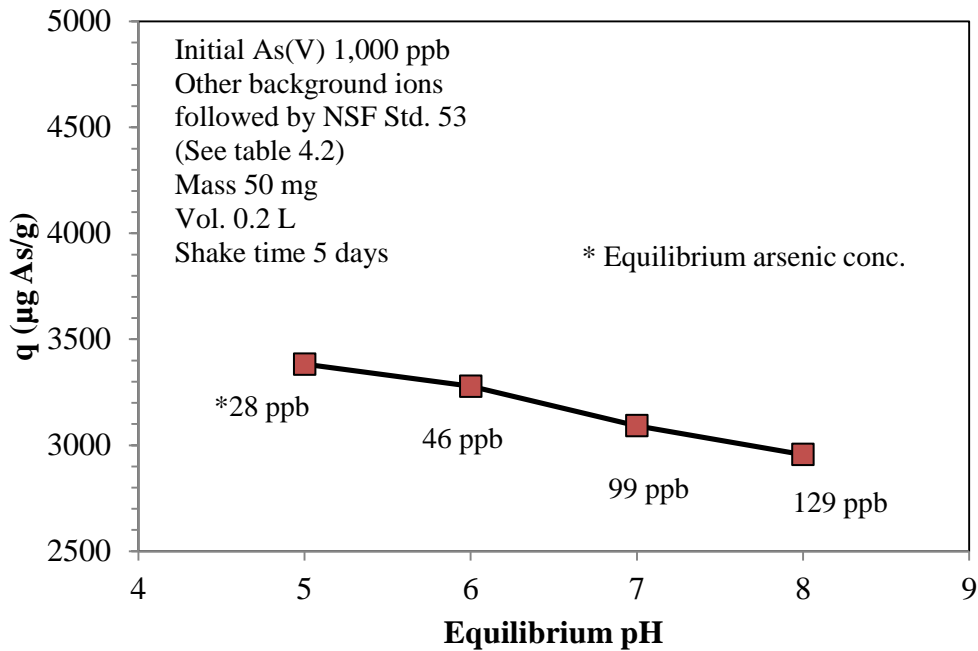


**Figure 4.11** Effect of pH for arsenic removal using HAIX-Zr

Arsenic and surface zirconium oxide species are pH dependent. As mentioned previously, the average point of zero charge (PZC) is around 6.5 (56). If the pH is greater

than the point of zero charge, most of the zirconium oxide surface charges appear as negatively charges ( $\text{ZrO}^-$ ) resulting in repulsion between the negative charge of  $\text{HAsO}_4^{2-}$  and  $\text{ZrO}^-$ . Moreover, at high pH the competition between hydroxyl ions ( $\text{OH}^-$ ) and  $\text{HAsO}_4^{2-}$  becomes fierce, and the metal oxides have high affinity toward  $\text{OH}^-$  resulting in decreasing of arsenic removal capacity as shown in figure 4.11.

### 4.3.3 Influence of Competing Ions

Dissolved anions such as phosphate, silicate, and sulfate have been reported to reduce the arsenic removal capacity. From the batch experimental data shown in figures 4.12-14, phosphate and silicate anions are strong competitors to the arsenic for HAIX-Zr sorption sites at high levels approximately greater than 30 ppm for  $\text{SiO}_2$  and 250 ppb for phosphate. However, the natural groundwater silica and phosphate concentration are found lower than the level that impact the performance of arsenic removal by HAIX-Zr.

#### 4.3.3.1 Effect of Silica

Silica is found in the natural surface and groundwater at the concentration range 1-20 mg/L in surface water and 7-45 mg/L as  $\text{SiO}_2$  in groundwater (68). Dissolved silica in water is usually written as  $\text{SiO}_2$ . When  $\text{SiO}_2$  depolymerizes in water, silicic acids ( $\text{Si(OH)}_4$ ) are formed. Many models are used to describe the chemistry of silica in water, but the best formula used to describe silicic acid is  $\text{Si(OH)}_4$ . In acidic and neutral pH, soluble silica is present mainly in nonionic silicic acid. Silica is highly soluble at high pH. The dissociation constants of silicic acids are as follows:



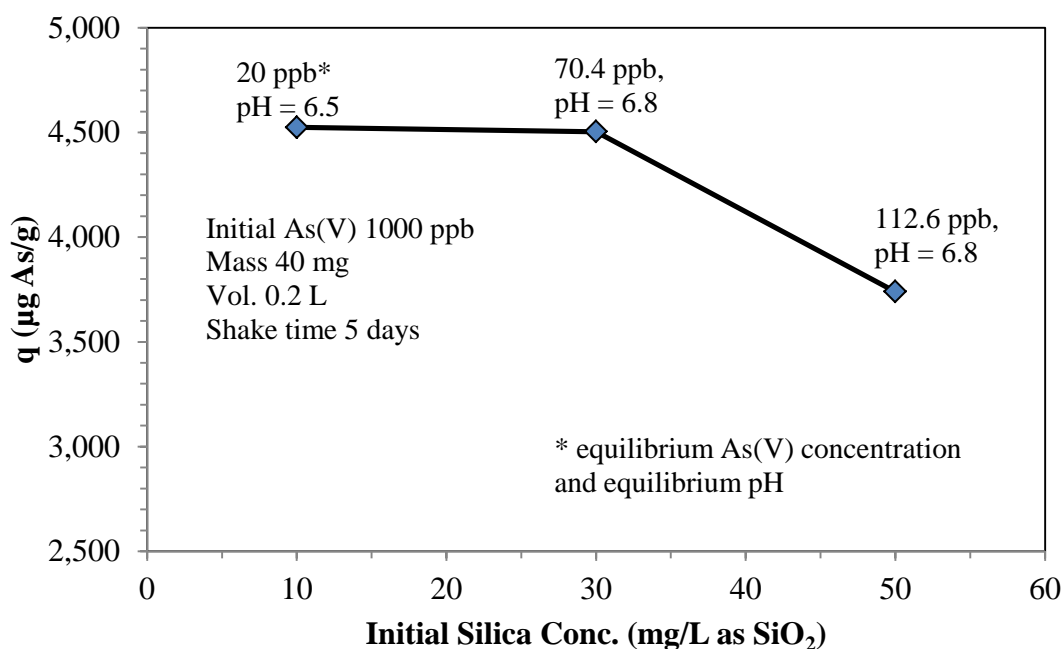
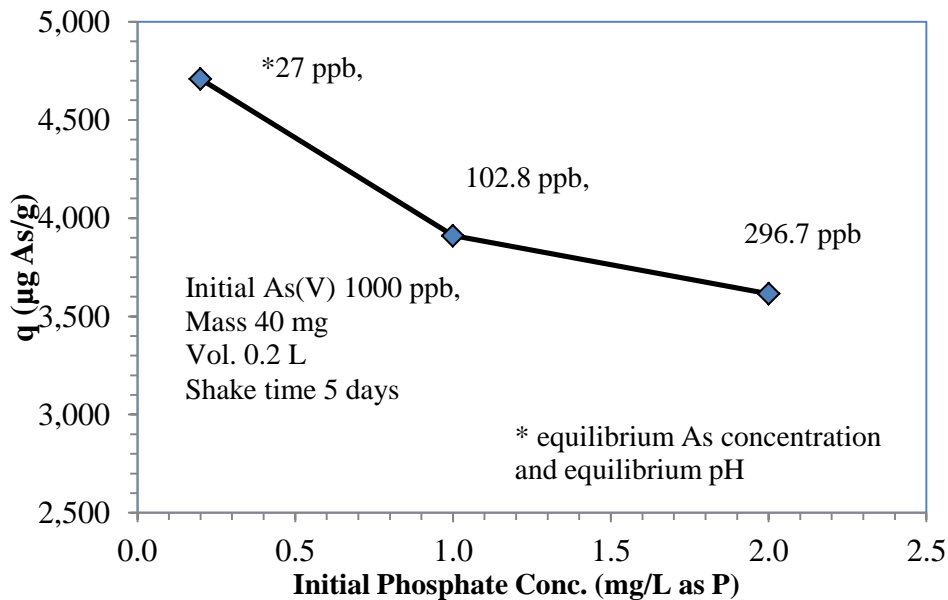


**Figure 4.12** Effect of silica to the arsenic removal using HAIX-Zr

Several studies reported that silica can interfere with arsenic uptake and results in decreasing of arsenic removal (68, 69). In this equilibrium batch study, different levels of silica was spiked into the test water along with arsenic at pH 7. The 40 milligrams of HAIX-Zr was added into 200 milliliters of test solution. The solution was shaken in the rotary shaker for 5 days to attain equilibrium. The arsenic removal capacity was calculated based on the mass balance. The results are shown in figure 4.12 and found that the arsenic removal capacity decreases significantly as the concentration of silica increases from 10 to 50 mg/L as SiO<sub>2</sub>.

### 4.3.3.2 Effect of Phosphates

Figure 4.13 shows the equilibrium batch test of arsenate removal capacity using HAIX-Zr under the presence of different phosphate concentrations. Initial phosphate concentrations were varied at 200, 1000, and 2000 ppb. From figure 4.13, the arsenic removal capacity was significantly decreased from 4700 to 3500  $\mu\text{gAs(V)}/\text{g}$  as the influent phosphate concentration increases from 200 to 2000 ppb. Undoubtedly, arsenic and phosphorus are chemically similar and both are in group 15 on the periodic table. The acid dissociation constants of orthophosphoric acid ( $\text{H}_3\text{PO}_4$ ) and arsenic acid ( $\text{H}_3\text{AsO}_4$ ) are shown in table 4.3.

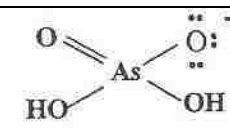
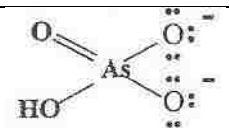
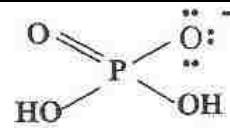
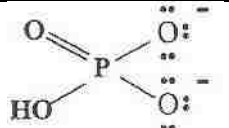


**Figure 4.13** Effect of phosphate to the arsenic removal using HAIX-Zr

The chemistry of phosphate and arsenate or As(V) are very similar. The acid dissociation constants of both oxyacids are very close to each other. The phosphate can

compete for the sorption sites with the arsenate resulting in a significant drop in arsenate removal capacity as shown in figure 4.13. Note that phosphate can be removed by the same mechanism as arsenate through the combination of Columbic interactions and formation of an innersphere complex. Previous study confirmed that hybrid polymeric anion exchanger supported metal oxide nanoparticles can remove phosphate effectively (28). Phosphate can be found mostly in the surface waters, and is rarely found in groundwater where the arsenic appears. In real applications, phosphate is not the main competing ion in removal of arsenic from groundwater.

**Table 4.3** Chemical similarity between oxyacid of As(V) and P(V) (16)

Oxyacid	pKa values	Predominant Species at pH 5.5	Predominant Species at pH 8.5
As(V): $\text{H}_3\text{AsO}_4$	pKa1 = 2.2 pKa2 = 6.98 pKa3 = 11.6	 monodentate ligand	 bidentate ligand
P(V): $\text{H}_3\text{PO}_4$	pKa1 = 2.12 pKa2 = 7.21 pKa3 = 12.7	 monodentate ligand	 bidentate ligand

### 4.3.3.3 Effect of Sulfate

The effect of sulfate to the arsenic removal capacity batch experiment was carried out the same way as the silica and phosphate as mentioned previously. From figure 1.14, arsenic removal is now affected by the level of sulfate in the water with the concentration range between 0-200 mg/L. The sulfate ions can form only weak outer-sphere complexes with the zirconium oxide particles, and are not competing with arsenic for the sorption sites. Moreover, since the HAIX-Zr is composed of hydrated zirconium oxide (HZO) nanoparticles dispersed in the parent macroporous strong base anion exchanger, the sulfate can also be removed by an ion exchange mechanism.

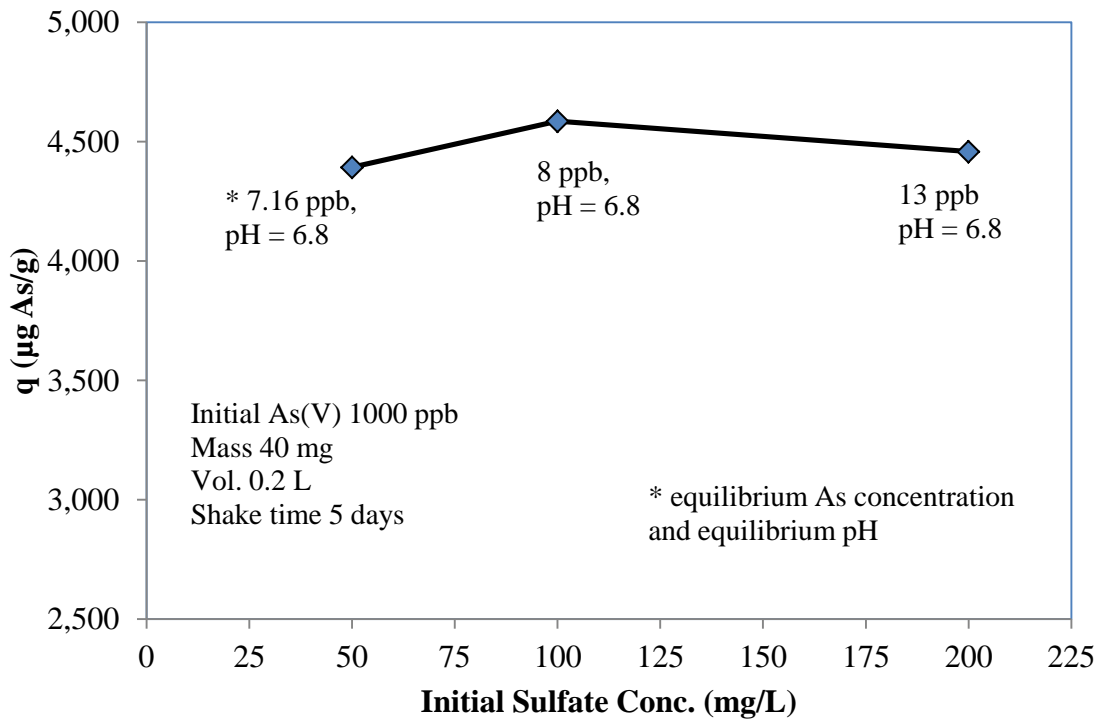


**Figure 4.14** Effect of sulfate to the arsenic removal using HAIX-Zr



## 4.4 Sorption Kinetics

Interruption tests were carried out during the fixed-bed HAIX-Zr column runs (run 1) as shown in figure 4.15 and are marked within circles. From figure 4.5, after 5,000, 6,000, and 8,000 bed volumes, the influent feed was deliberately stopped for 24 hours. When the flow was resumed, the effluent arsenic concentration decreased markedly and after 500 bed volumes, the effluent arsenic concentration reached the concentration prior to the interruption. This interruption test was mentioned by Helfferich as a technique for determination between particle and film diffusion control (5).

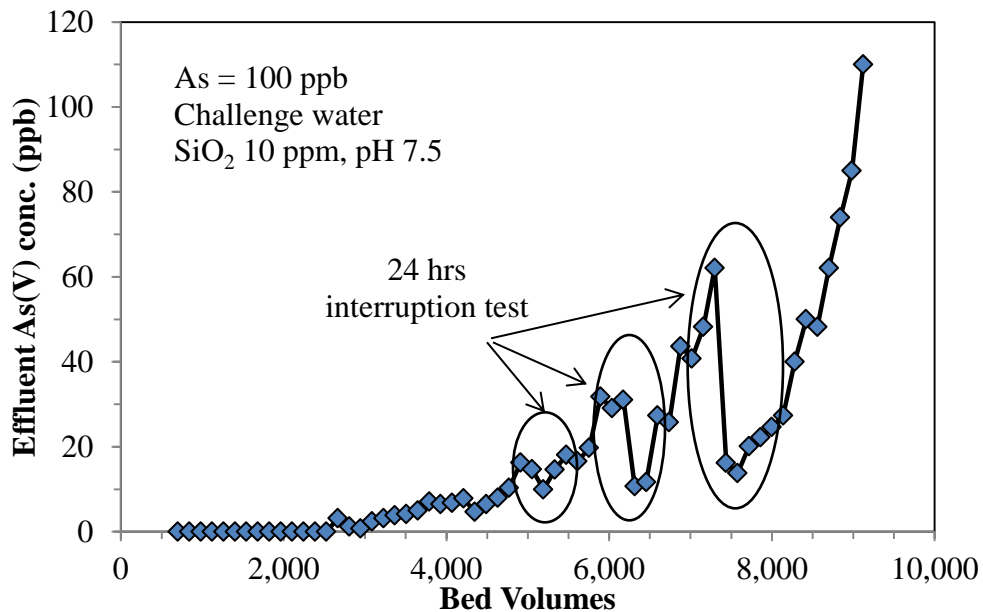


**Figure 4.15** Interruption test during the experimental column run on arsenic removal by HAIX-Zr

Many studies have reported that most selective sorption is controlled by intraparticle diffusion (15, 57, 70). When the reactions are controlled by intraparticle

diffusion mass transfer, the concentration gradient in the HAIX-Zr serves as a driving force and governs the overall ion exchange kinetic rate. The concentration gradient decreases when the column has a progress. The feed interruption allows the sorbed arsenic concentration to spread out in the spherical sorbents resulting in a high concentration gradient when the column is restarted. The arsenic uptake rate is then higher than the uptake rate before the interruption test. The details are also described in the literature (57, 70).

#### 4.4.1 Mathematical model

The effective diffusivity can be obtained by mathematical modeling. The diffusion in a spherical ion exchanger beads can be described by the partial differential equation (71):

$$\frac{\partial q}{\partial t} = \bar{D}_{eff} \left( \frac{\partial^2 q}{\partial r^2} + \frac{2\partial q}{r\partial r} \right) \quad (4-1)$$

where  $q$  is the arsenic concentration in the ion exchange phase,  $\bar{D}_{eff}$  is the intraparticle effective diffusivity,  $r$  is the radius of ion-exchanger beads, and  $t$  is time. Under the condition of the linear equilibrium relation ( $q=kC$ ) and finite volume, the solution for equation 4-1 can be written as:

$$F = \frac{q_{As,t}}{q_{As,\infty}} = 1 - \sum_{n=1}^{\infty} \frac{6\omega(\omega+1) \cdot \exp(-\bar{D}_{eff} \beta_n^2 t / R^2)}{9 + 9\omega + \beta_n^2 \omega^2} \quad (4-2)$$

where  $\beta_n$  is the non-zero root of

$$\tan \beta_n = \frac{3\beta_n}{3 + \omega\beta_n^2} \quad (4-3)$$

and  $\omega$  can be calculated from the relationship with the final fractional uptake;

$$\frac{q_{As,\infty}}{VC_{As,0}} = \frac{1}{1 + \omega} \quad (4-4)$$

where V is the volume of the batch reactor, and  $C_{As,0}$  is the initial concentration of As(V) in the batch reactor.  $q_{As,\infty}$  can be obtained from mass balance equation 4-5

$$mq_{As,\infty} = V (C_{As,0} - C_{As,\infty}) \quad (4-5)$$

where m is the mass of sorbent used for the test and  $C_{As,0}$  and  $C_{As,\infty}$  are concentrations of arsenic at  $t=0$  and  $\infty$  (equilibrium), respectively.

From the experimental data of the kinetic test, the graph of F versus time can be plotted as shown in figure 4.16. The fractional arsenic uptake (F) is dimensionless and is defined by the ratio of the arsenic uptake capacity at time t ( $q_t$ ) and the arsenic uptake capacity at equilibrium ( $q_\infty$ ). By fitting computed values of F to the experimental data of F, we can find the best fit profiles. From the best fit profiles, we can finally identify effective diffusivity,  $\overline{D}_{eff}$ . From the arsenate batch kinetic experiment using HAIX-Zr, the effective intraparticle diffusivity ( $\overline{D}_{eff}$ ) was computed and the result is  $2.3 \times 10^{-11}$  cm<sup>2</sup>/sec. The resulting  $\overline{D}_{eff}$  is comparable with other selective sorption process **(15)**.

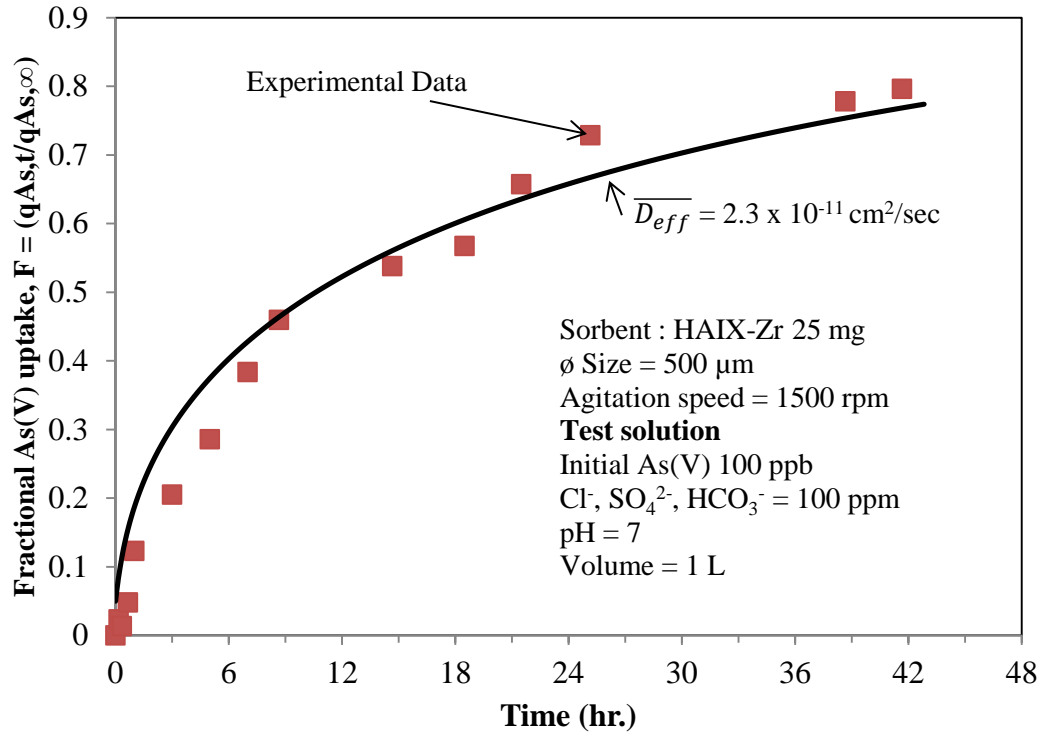


**Figure 4.16** Fractional uptake rate (F) versus time (t) plots for HAIX-Zr during batch kinetic test of arsenic removal

## CHAPTER 5

### RESULTS AND DISCUSSION: FLUORIDE REMOVAL BY HAIX-Zr

Zirconium oxide exhibits a high sorption selectivity toward fluoride ions while other known metal oxides such as Fe(III), Ti(IV), Al(III) are poorly sorbed with fluoride ions. For this study, the HAIX-Zr, the same material for removal of arsenic, was used to investigate the fluoride sorption/desorption properties. Unlike arsenic which appears in groundwater at the parts per billion (ppb) level, fluoride is usually found in parts per million (ppm), more than a thousand times higher than arsenic, resulting in low throughput per volume of adsorbent being used. These studies cover the following aspects:

- Comparison of various metal oxides sorbents (i.e., Al (III), Fe (III), and Zr (IV)) toward fluoride removal under identical conditions by column run experiments.
- Confirmation of the Donnan membrane effect resulting from the fixed functional groups of the parent polymeric ion exchange resins to enhance or exclude fluoride ion transport into the hybrid sorbents.
- Multiple fluoride sorption/desorption cycles by using HAIX-Zr.
- Equilibrium isothermal test, effect of feed pH on the fluoride sorption capacity and the stability of hybrid sorbents (mechanical strength of sorbent and metal leaching under different pH).
- Kinetic study of fluoride sorption by HAIX-Zr.

## 5.1 Fixed-Bed Column Runs Using HAIX-Zr

### 5.1.1 Comparison of Fluoride Removal Using Different Metal Oxides Sorbents

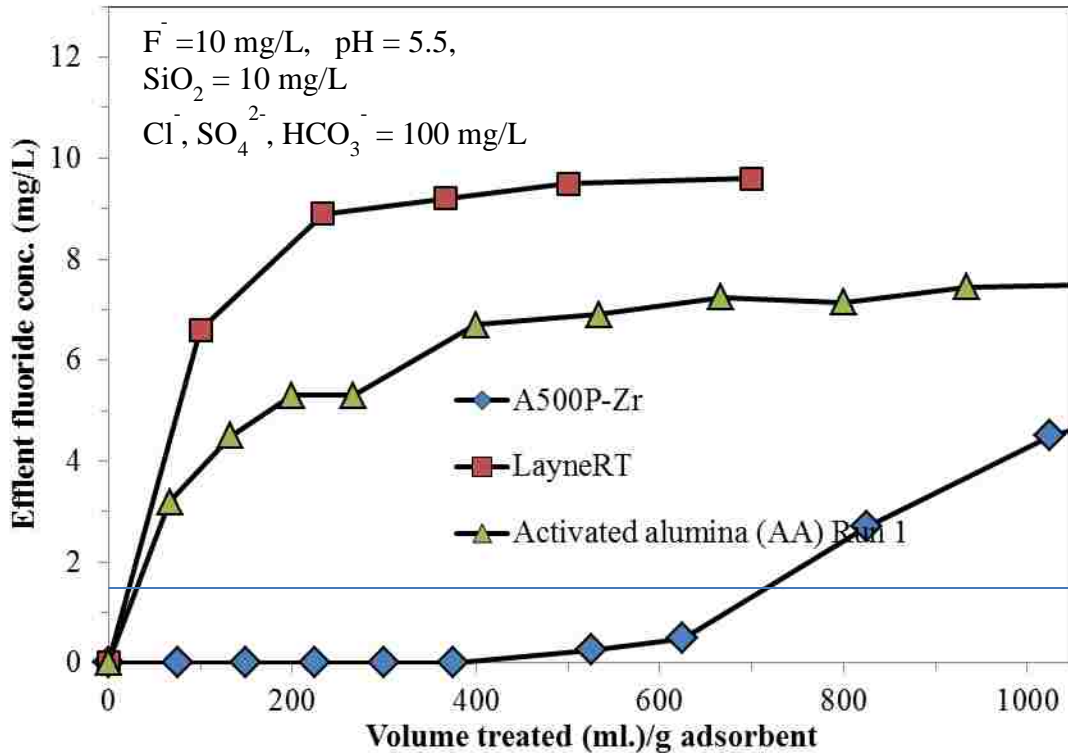


**Figure 5.1** Effluent histories of fluoride during column run between HAIX-Zr, LayneRT, and AA

From the effluent histories, HAIX-Zr can remove fluoride selectively more than 700 mL/g before the effluent exceeds the WHO recommendation for fluoride (1.5 mg/L). Activated alumina (AA) can remove fluoride, but the removal capacity was significantly lower than the HAIX-Zr. In contrast, iron based nanosorbents have very low affinity toward fluoride ions resulting in nearly immediate breakthrough. Moreover, after two runs of fluoride sorption/desorption, most of the activated alumina (AA) was degraded

into very fine particles that blocked the water flow through the column as shown in figure 5.9B.

Zirconium ions have a high charge to radius ratio characteristic of hard Lewis acid ions, so they can form very strong coordination complexes with hard Lewis bases such as fluoride ions according to the Hard and Soft Acids and Bases (HSAB) principles. Note that iron can be categorized as a transition metal which exhibits a weak interaction with fluoride. According the HSAB principles, hard acids prefer to bind with hard bases and soft acids prefer to bind with soft bases.(72, 73) Based on the classification, hard acids such as zirconium and aluminium are likely to bind with hard bases such as fluoride. Iron is categorized as a transition metal (borderline), thus it has less affinity toward fluoride ions. Fluoride ion forms one of the strongest zirconium complexes on the zirconium oxide surface (74). Many studies have also confirmed that zirconium oxide has a high affinity toward fluoride ions. Zirconium oxide is very chemically stable (as oxidation number +4) under wide pH and redox conditions.(22, 65, 66, 74, 75)

### **5.1.2 Effect of Donnan Membrane Effect**

Figure 5.2 illustrates two fluoride effluent histories during column runs using HAIX-Zr and HCIX-Zr. The HAIX-Zr can remove fluoride very well and fluoride started breakthrough after 1,800 mL/g at WHO fluoride recommended level at 1.5 mg/L. On the contrary, it can be seen that the polymeric cation exchanger supported zirconium oxide or HCIX-Zr exhibits low fluoride removal capacity. Fluoride was started to exit the column in less than 400 mL/g of HCIX-Zr. The details about the Donnan membrane effect used to explain this phenomenon was discussed in chapter 4.

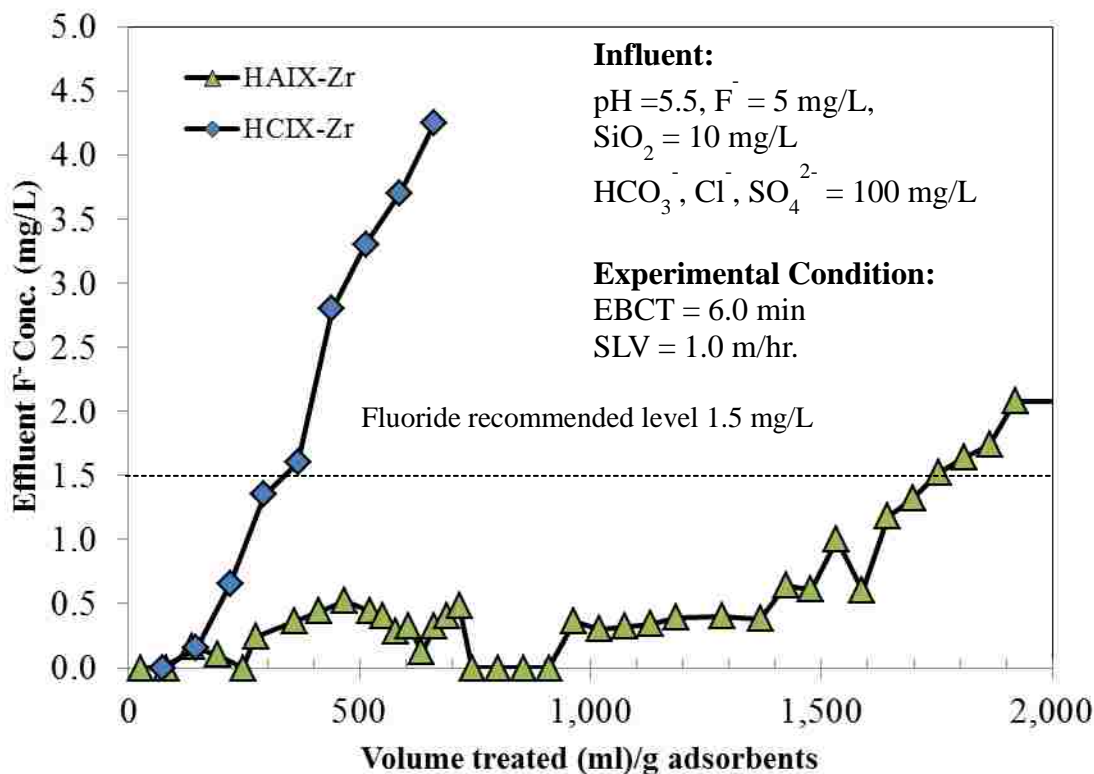


**Figure 5.2** Effluent histories of fluoride during column runs with HAIX-Zr and HCIX-Zr

### 5.1.3 Multiple Sorption-Desorption of Fluoride with HAIX-Zr and AA

Figures 5.3-5.4 show fluoride effluent histories including regeneration profiles for two separate column runs under identical conditions using HAIX-Zr and activated alumina (AA). The influent composition and the hydrodynamic conditions (i.e., empty bed contact time (EBCT) and superficial liquid velocity (SLV)) are also provided within the figure. The feed water contains fluoride at 5 mg/L and background ions of chloride, sulfate, and bicarbonate 100 mg/L and  $\text{SiO}_2$  10 mg/L at pH 5.5.



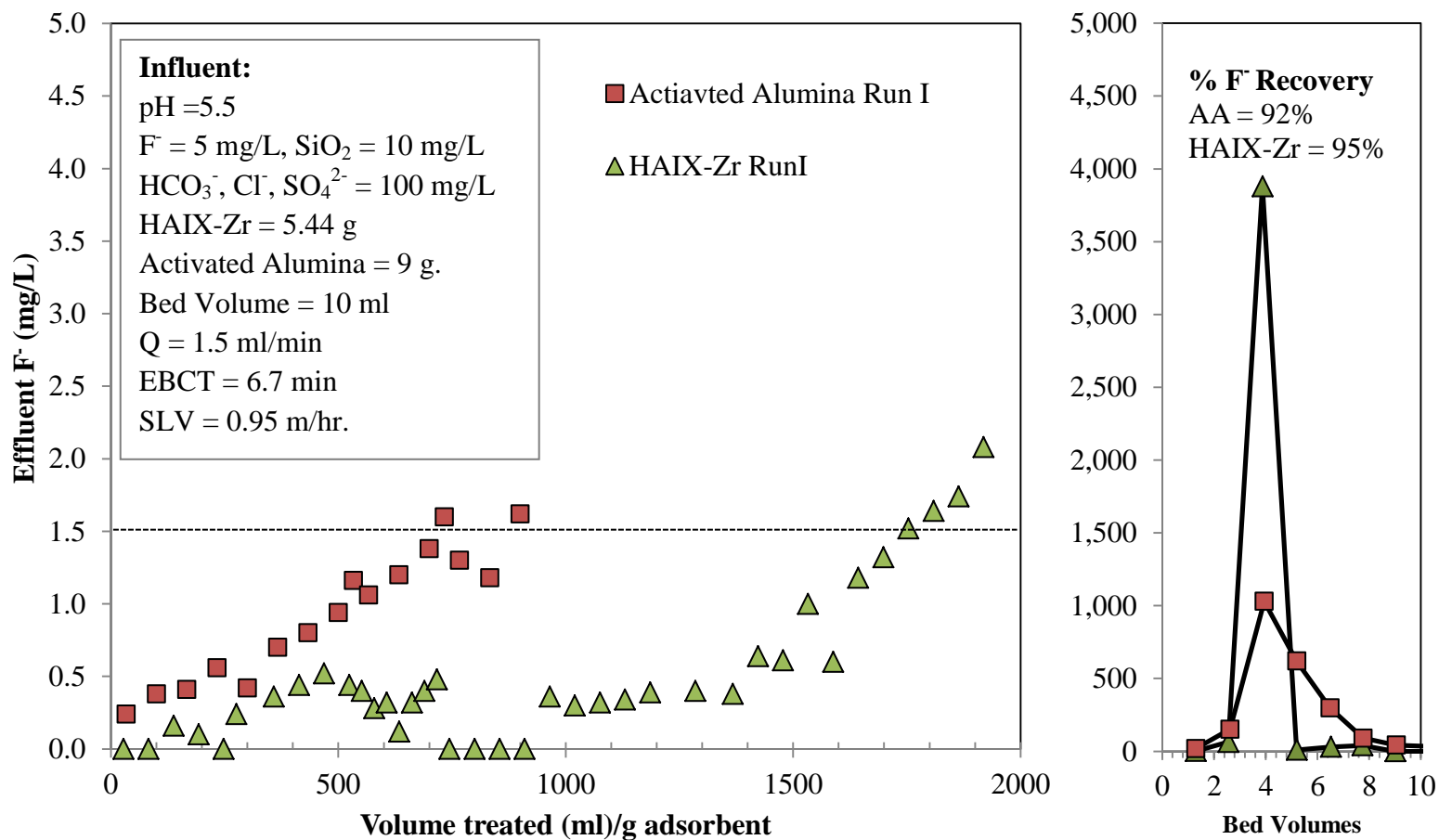


**Figure 5.3** Fluoride effluent histories and regeneration for the first run using HAIX-Zr and activated alumina (AA)

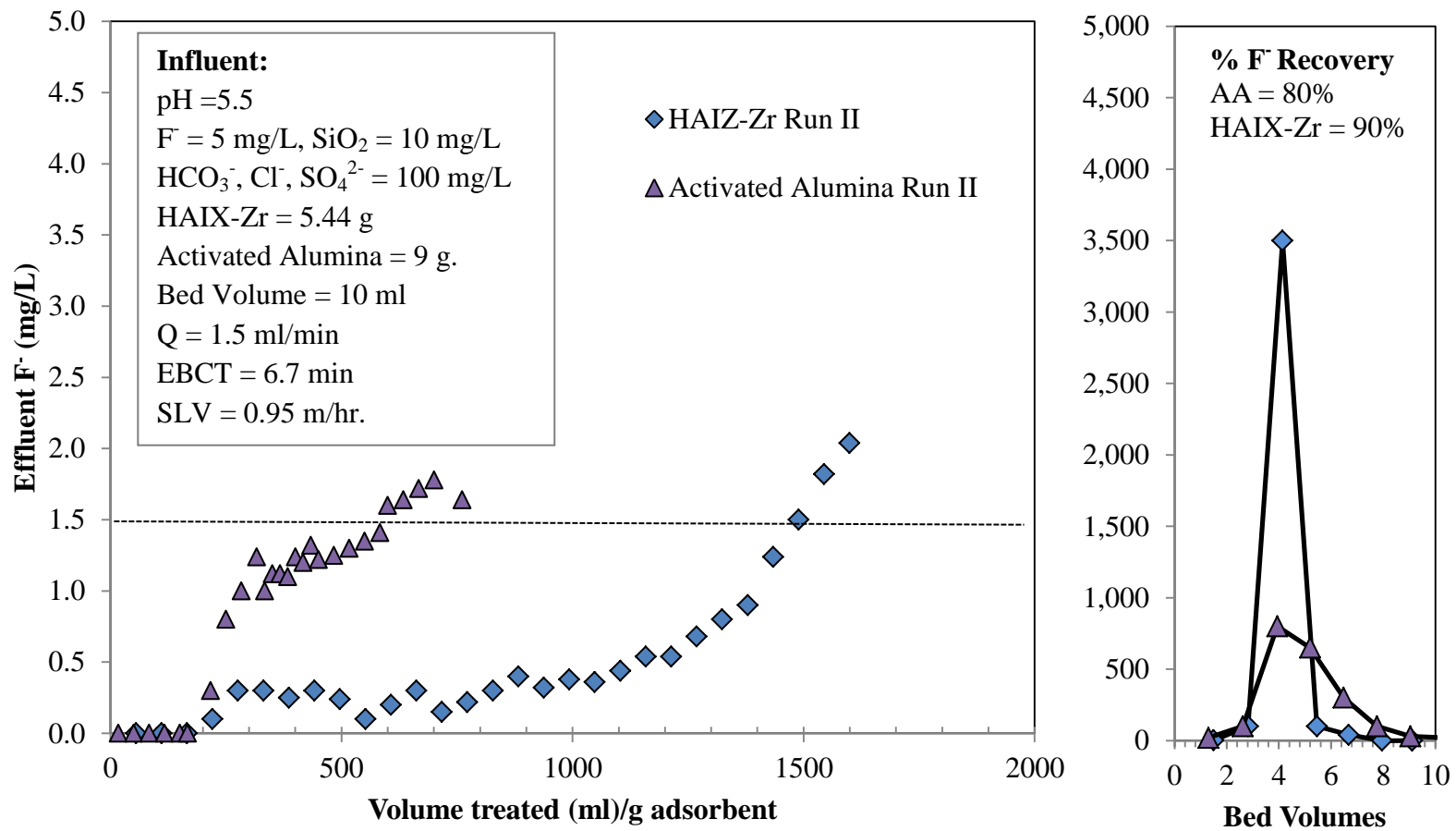


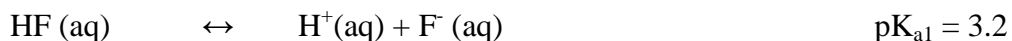
**Figure 5.4** Fluoride effluent histories and regeneration for the second run using the same HAIX-Zr and AA

Effluent histories in figures 5.3-5.4 demonstrate that HAIX-Zr can remove fluoride selectively under the presence of 20 times higher concentrations of background anions, namely sulfate, chloride, and bicarbonate. In comparison with traditional activated alumina, HAIX-Zr exhibits more than twice the capacity (considered breakthrough at 1.5 mg/L).

#### 5.1.4 Mechanism of Fluoride Sorption onto the HZO Nanoparticles

It is well established that the surface charge of metal oxide of polyvalent metals such as Al(III) and Zr(IV) are pH dependent. Hydrated zirconium oxides or HZO particles exhibit amphoteric sorption properties around neutral pH.(36) Theoretically, HZO can selectively bind Lewis acids or transition metals (e.g.  $Zn^{2+}$ ,  $Cu^{2+}$  and  $Pb^{2+}$ ) as well as Lewis bases of anionic ligands (e.g. arsenate, phosphate, fluoride) through formation of inner-sphere complexes. The point of zero charge (PZC) of zirconium (hydr)oxide is 6.5 on average (56).

Hydrofluoric acid (HF) can be viewed as a monoprotic acid which has a pKa of approximately 3.2, so at pH greater than 3.2, most of fluoride ions appear in the anionic form ( $F^-$  (aq)).



From figure 5.4, fluoride can also be removed due to a combination of the Coulombic interaction and a ligand exchange reaction (inner sphere complex). At pH greater than the point of zero charge (PZC), the surface charges exhibit a negative charge which is why fluoride can be desorbed during regeneration cycles using alkaline solution.

### 5.1.5 Regeneration and Reuse

In order for the fixed-bed sorption process to be economically viable and sustainable, the adsorbents have to be amenable to efficient regeneration and reuse for multiple cycles. Due to the amphoteric properties of HZO depending on the solution pH, the HAIX-Zr can efficiently be regenerated with only 10 bed volumes of a mixed solution of 3% NaOH and NaCl (pH 12) and an EBCT of 6 minutes. In less than 10 bed volumes, almost the entire amount of fluoride was desorbed from HAIX-Zr with over 90% of fluoride recovery confirmed by mass balance. During the regeneration, the pH increased to 12, the HZO sorption sites were deprotonated (negatively charged) all the fluoride anions get rejected from HAIX-Zr into the regeneration stream within less than 10 bed volumes at very high concentration as can be seen in figures 5.3-5.4. The Donnan co-ion exclusion effect is predominant under regeneration conditions resulting in an efficient desorption process. Subsequently, the HAIX-Zr was reconditioned with CO<sub>2</sub> sparged water to adjust the pH from alkaline to nearly neutral, in less than 10 bed volumes. From this step, the surface charges of the HZO are protonated and ready for next sorption cycles and no further pH adjustment was necessary during the service run.

The two successive runs shown in figures 5.3-5.4 clearly demonstrate that fluoride can be desorbed effectively with insignificant loss in fluoride removal capacity as shown in figures 5.3-5.4. The HAIX-Zr is robust and durable. There are no signs of particles breaking down into small particles or powder. Unlike HAIX-Zr, after 3 runs of fluoride sorption/desorption the activated alumina (AA) was degraded into small particles and create a head loss inside the column as shown in the figure 5.9B. The powder X-ray

diffractograms (XRD) show that zirconium inside the HAIX-Zr is in the amorphous form both before and after 3 sorption/desorption cycles, while the activated alumina exhibits crystalline structure both before and after 3 cycles. The amorphous structures usually have a higher surface area than crystalline structures so that the fluoride removal also improves in part for the HAIX-Zr because of amorphous structure. From figure 5.9, we can infer that the use of some chemical during the regeneration process such as NaOH and CO<sub>2</sub> sparged water solution are not resulting in changing of the zirconium oxide structure from amorphous to crystalline which can reduce in surface area.

The regenerable nature of HAIX-Zr can reduce the volume of toxic-laden waste by 100 times as compare to single-used adsorbent media. **(67)** There are many single-use fluoride adsorbents that have been adopted in many fluoride affected areas because of the low cost. However, the inexpensive adsorbent tends to have low capacity, unreliable quality and produce a large quantity of toxic-laden waste resulting in high risk of recontamination to the surface water. The regenerable HAIX-Zr can produce fluoride-free water with high capacity and reliable results. The regenerable property can reduce the cost for long-term operation and can reduce the risk of toxic leaching to the environment.

## 5.2 Equilibrium Isothermal Test

Langmuir and Freundlich adsorption isotherm are commonly used for the study of sorption behavior and quantify the maximum sorption capacity toward specific contaminants by the sorbent of interest. For the fluoride adsorption experiment, sorptions of fluoride using both HAIX-Zr and activated alumina follow the Langmuir isotherm model. The general and linear forms of Langmuir adsorption model are given as the following equation, respectively. **(2, 4)**

$$q_e = \frac{QbC_e}{1+bC_e} \quad \text{Eq. 1}$$

$$\frac{1}{q_e} = \frac{1}{QB} \frac{1}{C_e} + \frac{1}{Q} \quad \text{Eq. 2}$$

where  $q_e$  and  $C_e$  represent the adsorption capacity (mg F/g) and the fluoride concentration at equilibrium (mg F/L),  $Q$  represents the maximum adsorption capacity (mg F/g), and  $b$  (L/mg) is the Langmuir constant. The general Langmuir equation including experimental fluoride sorption data are plotted in figure 5.5. From the equilibrium isotherm test, the maximum fluoride sorption capacity from HAIX-Zr and activated alumina (AA) are 35 mg F/g and 10 mg F/g, respectively.

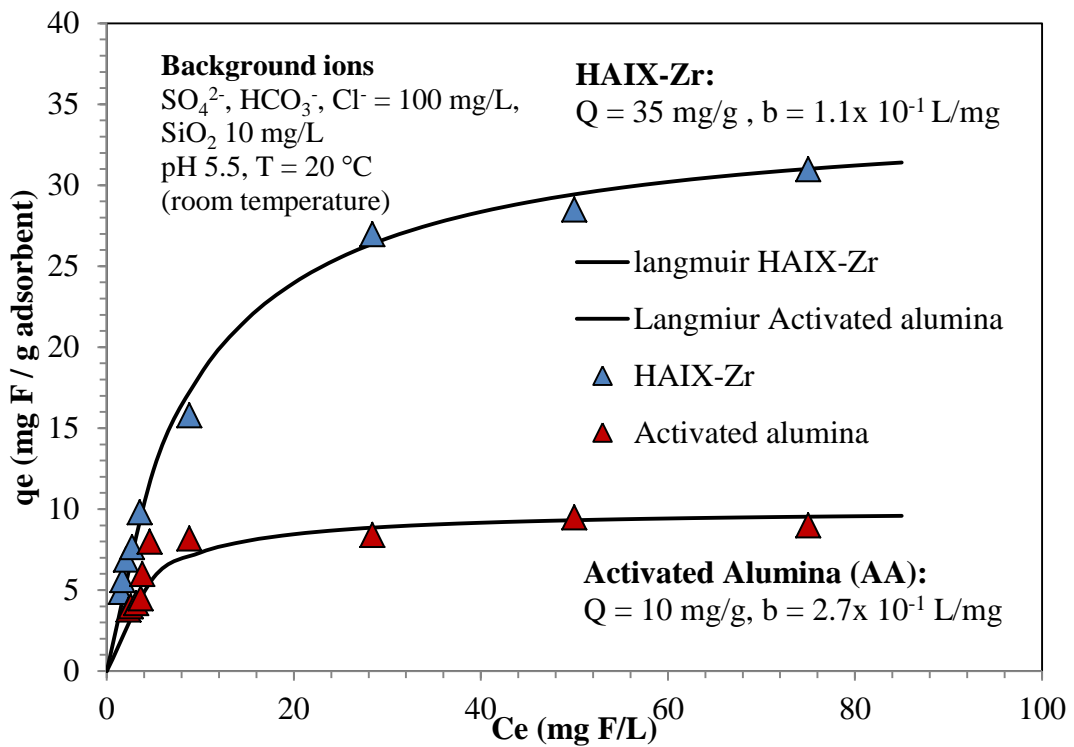
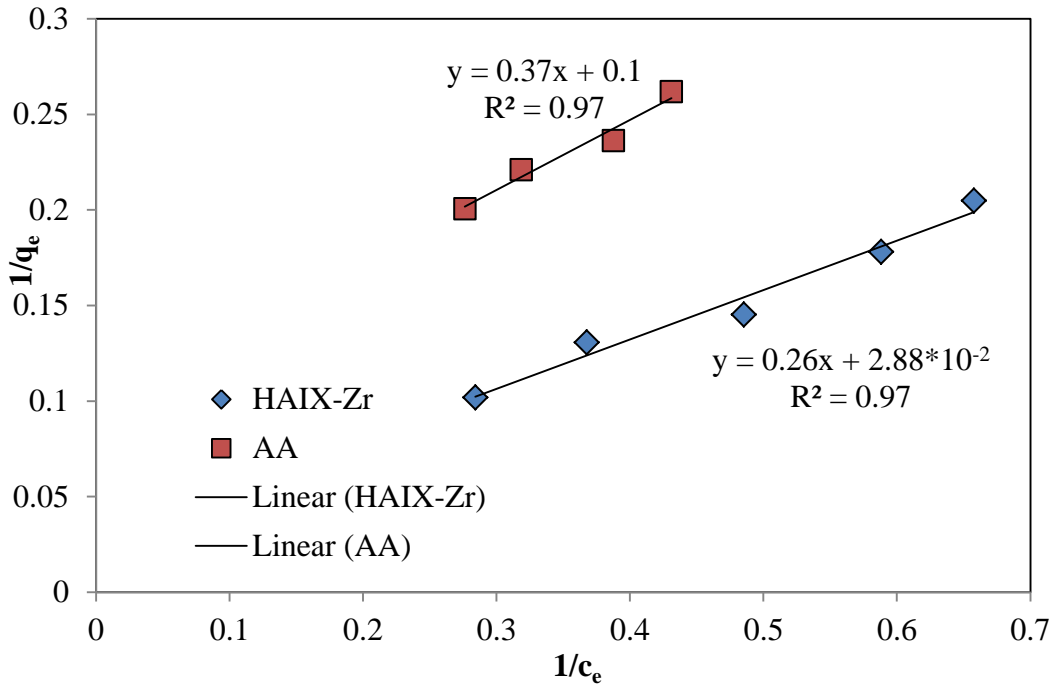


**Figure 5.5** Fluoride sorption isotherms with other background ions at room temperature

### 5.3 Effect of Feed pH and Stability of Hybrid Adsorbents

Fluoride sorption on the surface of oxides of Al(III) and Zr(IV) are pH dependent. Figure 5.6 shows the effect of pH of the feed solution on fluoride removal capacity. It was observed that the fluoride removal capacity was decreased significantly above pH 7.0. The acid dissociation constant of HF is approximately 3.2, thus in natural water fluoride presents as the anion (F<sup>-</sup>).

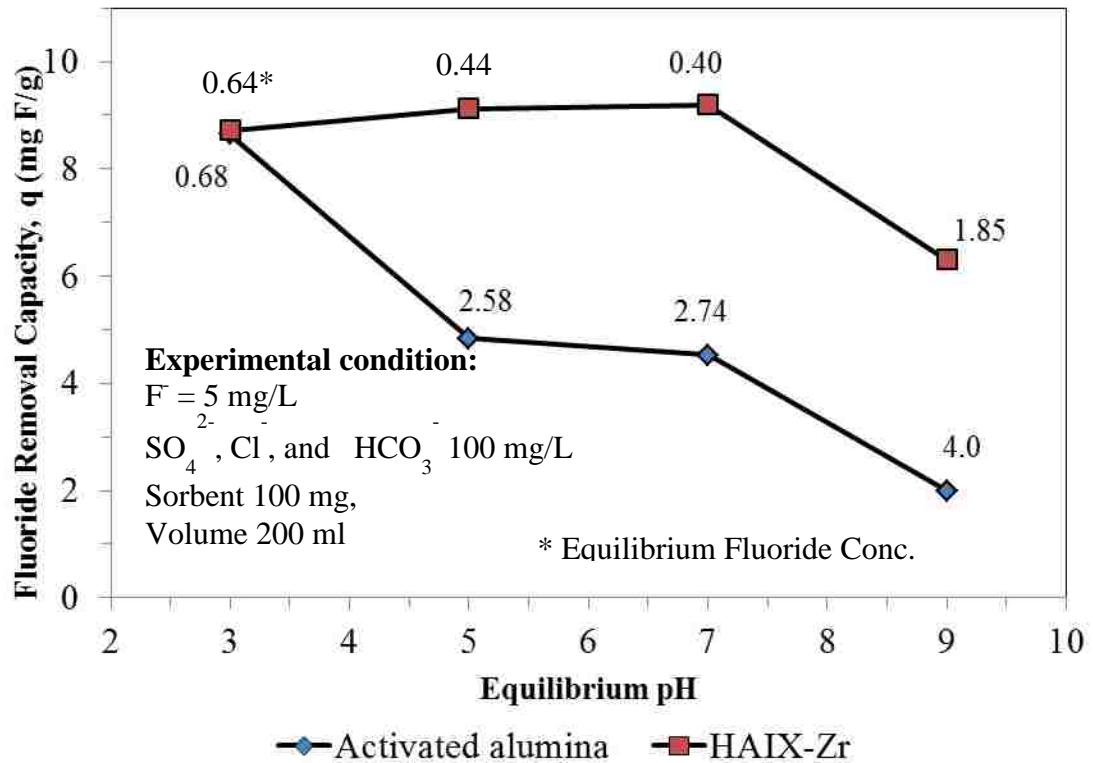


**Figure 5.6** Effect of pH for fluoride sorption for HAIX-Zr and AA



From chapter 4, the point of zero charge (PZC) of zirconium oxide is around 6.5 on average. At pH greater than neutral, most of the zirconium oxide surfaces are neutral ( $\text{ZrOH}$ ) and negatively charged ( $\text{ZrO}^-$ ), thus the sorption of fluoride ( $\text{F}^-$ ) due to the Coulombic interaction is diminished. Moreover, at high pH, the surfaces of metal oxides exhibit high affinity toward hydroxyl anions ( $\text{OH}^-$ ). The competition between  $\text{F}^-$  and  $\text{OH}^-$  is significant resulting in the reduced sorption capacity as illustrated in figure 5.6.(29)

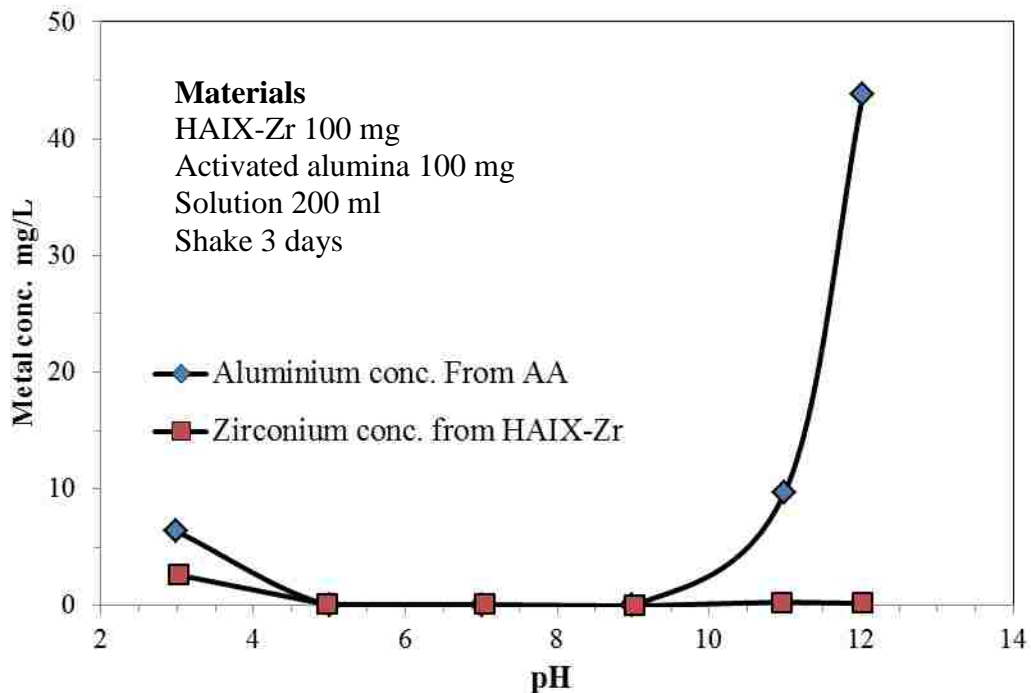


**Figure 5.7** Concentration of aluminum and zirconium in treated water coming from dissolution of AA and HAIX-Zr at different influent pH

There are many studies that use both aluminium and zirconium based adsorbents for fluoride removal. The zirconium oxide is chemically stable over wide pH and redox ranges and has a very low solubility product (76) while the aluminium are soluble both in acid and alkaline ranges. In most cases, aluminium ions tend to leach to the treated water

during regeneration with alkaline solution resulting in loss of capacity and mechanical strength of material. From figure 5.7, the metal aluminum and zirconium leaching from the sorbent into the water were monitored by adding the sorbents into different pH solutions. After shaking for 5 days, the concentrations of aluminum and zirconium were analyzed and plotted in figure 5.7. We found that zirconium concentrations in the water were very low while aluminum concentrations were very high at pH greater than 10. From many studies, Al(III) oxide based sorbents such as activated alumina (AA) have some disadvantages such as low capacity, the capacity is dropped significantly at neutral pH, and tend to degrade into small particles inside the fixed-bed column after several regenerations (16).

#### **5.4 Fluoride Sorption Kinetics**

The details of the kinetic study were already discussed in chapter 4. Figure 5.8A shows the evidence of intraparticle control by interruption tests as highlighted in the circle. Figure 5.8B shows the kinetic plot of fractional fluoride uptake (F) versus time during the batch kinetic study of fluoride sorption by HAIX-Zr. The diffusivity from the model that fit well with the experimental data is  $8 \times 10^{-11} \text{ cm}^2/\text{sec}$ . Note that the diffusivity coefficient for arsenic removal by the same material (HAIX-Zr) is  $2.3 \times 10^{-11} \text{ cm}^2/\text{sec}$ . The diffusivity coefficient for preferred ions (arsenate) will be lower than species that are less preferred (fluoride) by the sorbents. The details of the kinetic study are found in the literature.(57, 70)

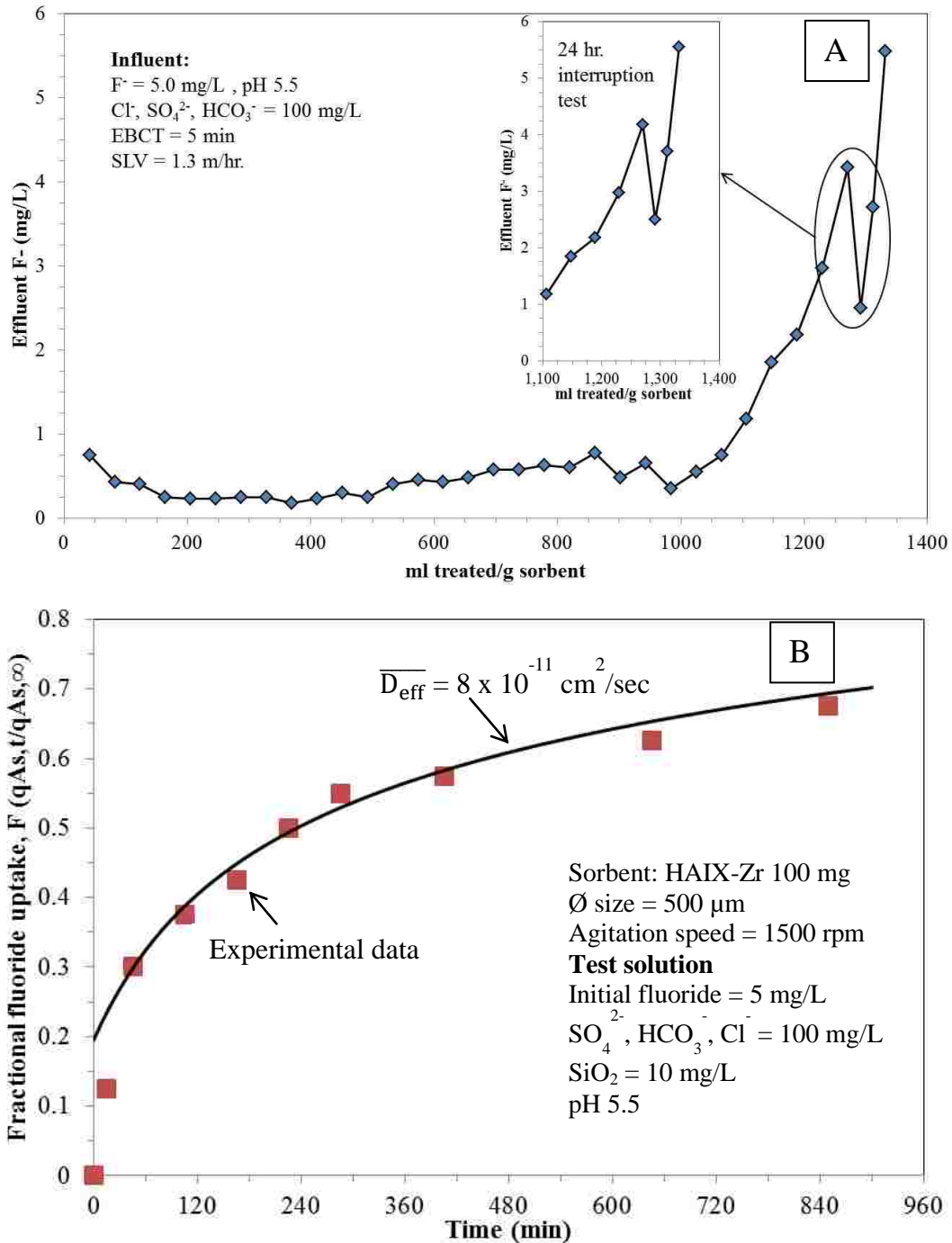


**Figure 5.8** (A) Interruption test during the experimental column runs on fluoride removal by HAIX-Zr, (B) Fractional uptake ( $F$ ) versus time ( $t$ ) plots for HAIX-Zr during batch kinetic test of fluoride removal

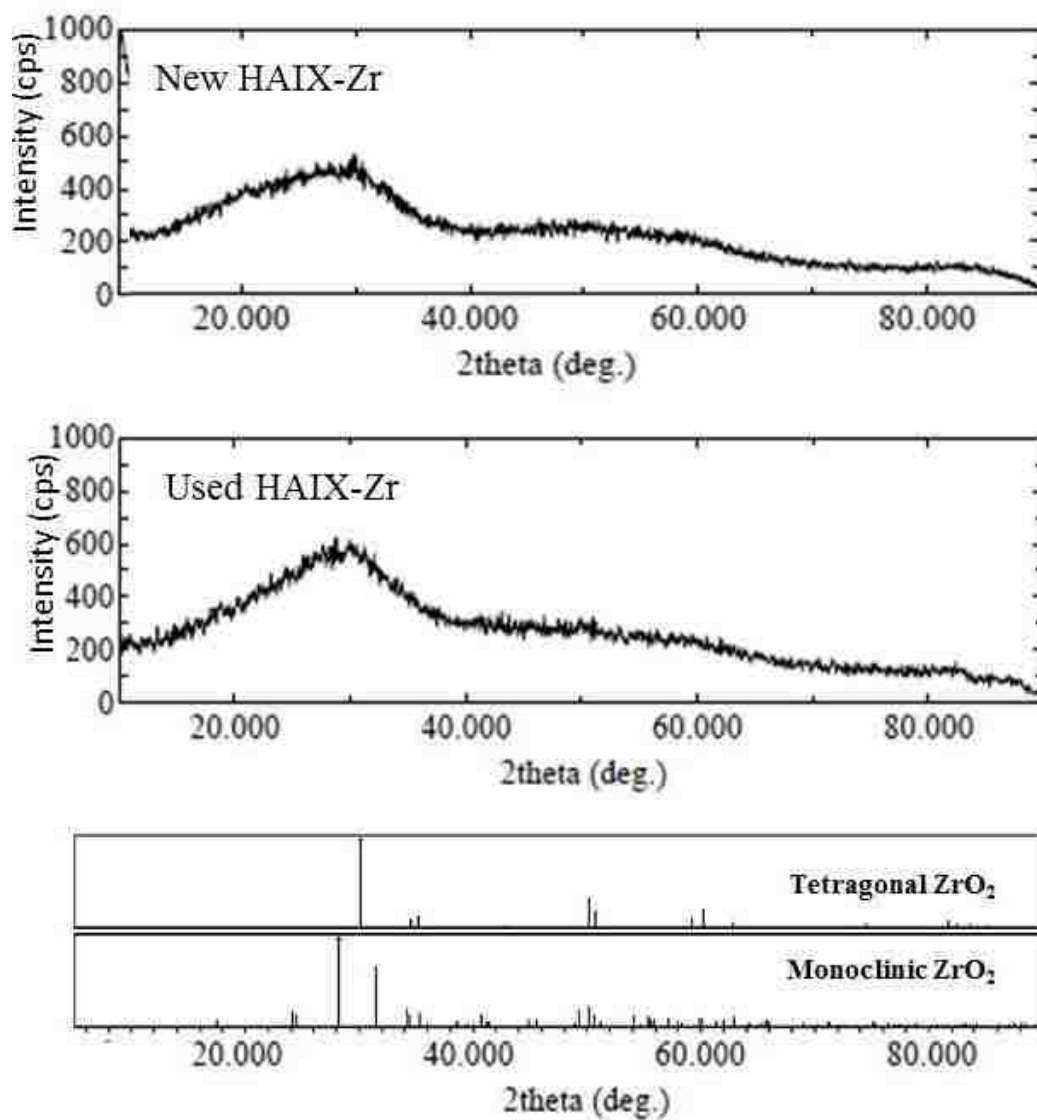


**Figure 5.9** Comparison of XRD diffractograms between used HAIX-Zr and activated alumina (AA) after 3 cycles of sorption/desorption for fluoride removal column run experiment and mechanical strength of used (A) HAIX-Zr and (B) Activated Alumina

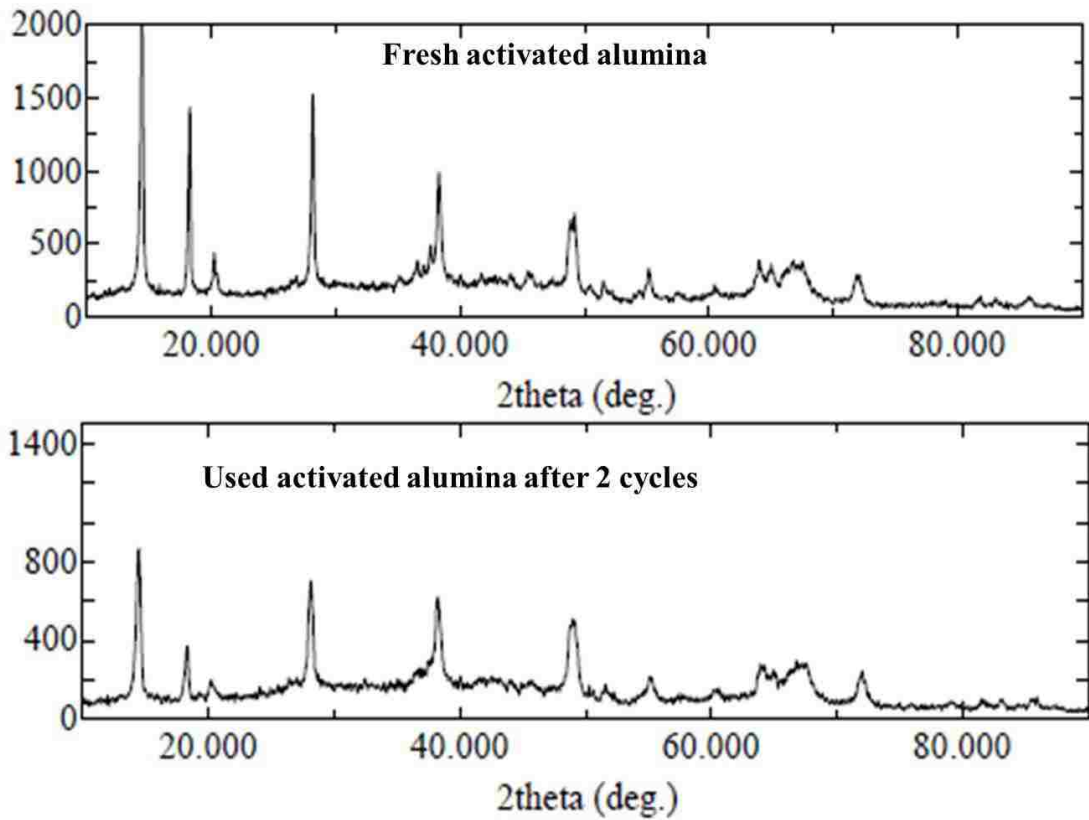


**Figure 5.9** Comparison of XRD diffractograms between used HAIX-Zr and activated alumina (AA) after 3 cycles of sorption/desorption for fluoride removal column run experiment and mechanical strength of used (A) HAIX-Zr and (B) Activated Alumina

## CHAPTER 6

### RESULTS AND DISCUSSION: ZINC REMOVAL BY HCIXF-Zr AND CO<sub>2</sub> REGENERATION

Toxic transition metals such as zinc, copper, lead, cadmium, etc. contaminants in water/ wastewater are among environmental concerns. Most transition metals are toxic and present as trace concentrations in the environment. The removals of these toxic substances to meet the stringent standards are very challenging. The general chemical precipitation technologies are suitable to treat high concentrations of toxic metals, and these techniques often cannot bring the toxic concentration down to meet the standard due to the solubility limit (4). Moreover, an additional problem related to handling the large quantities of waste sludge which is an environmental and economic issue. Selective removal of toxic metals using ion exchange technologies (i.e., chelating resins), or adsorption at the surface of polyvalent metal oxides (i.e. iron oxide, zirconium oxide) particles are more appropriate to remove such a trace concentration of these toxic metals (8). In this study, we are focusing on the use of metal oxide nanoparticles as a candidate to remove trace toxic contaminants in water. The special resins such as chelating resins are not discussed for this study. Note that the polyvalent metal oxide based sorbents are much cheaper than the chelating resins.

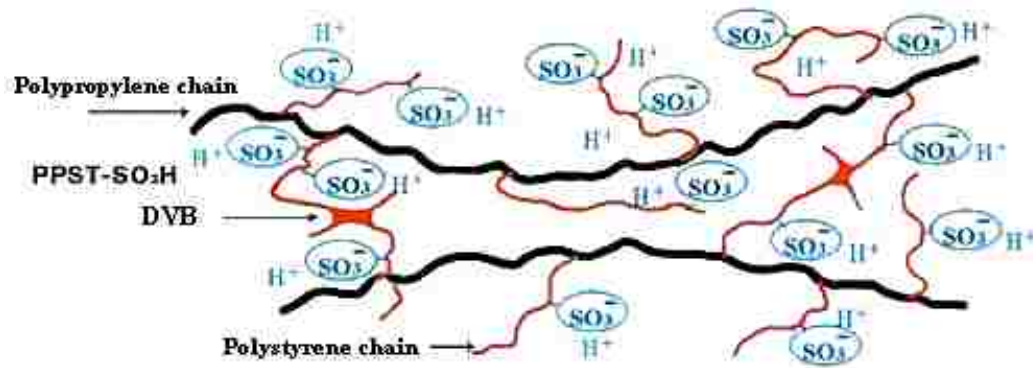
From a previous study, the hydrated iron oxide (HFO) nanoparticles were dispersed in the polymeric ion exchangers referred to as hybrid ion exchanger supported iron oxide or HIX-Fe (15, 29, 37, 52). Amphoteric sorption behaviors of metal oxide

nanoparticles can be maintained after dispersing metal oxide particles within the gel phases of ion exchangers. The hybrid nanosorbent can be tailored to be selective either toward transition-metal cations or anionic ligands while completely rejecting the other by selecting the appropriate type of polymeric ion exchangers. Such tunability of the hybrid material results from the Donnan effect exerted by the ion exchanger support **(21)**.

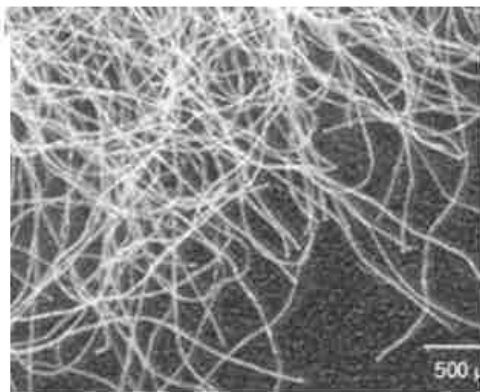
Instead of using the traditional cation spherical beads, ion exchange fibers (IX-F) were used as support materials where the hydrated zirconium oxide (HZO) nanoparticles were irreversibly dispersed into the polymer phase of cationic exchange fibers. Ion exchange fibers (IX-fibers) from the heart of the proposed processes; in essence, they offer unique opportunities to use and consume CO<sub>2</sub> for efficient regeneration compared to other commercial sorbent materials available to date.

The fibers are essentially long polypropylene cylinders with average diameter of approximately 25 μm. Figure 6.1A illustrates ion exchange fibers with strong-acid(-SO<sub>3</sub><sup>-</sup>) functional groups (Fiban K1); figure 6.1B presents virgin fiber materials photographed at x10 magnification and figure 6.1C shows the scanning electron microphotograph (SEM) of a single fiber (x2,000). The sulfonic acid functional groups of the IX-fibers do not have specific affinity for toxic metals, but due to the Donnan effect, toxic metals are concentrated within IX-fibers **(29)**. It should be noted that HZO nanoparticles are innocuous, inexpensive, and chemically more stable than the previously used HFO nanoparticles. The amorphous zirconium oxide exhibits very high sorption affinity for toxic metals as well as metalloids namely arsenic oxyanions and oxyacids as mentioned in chapters 4 and 5. Nano-scale HZO particles dispersed within the cation exchange

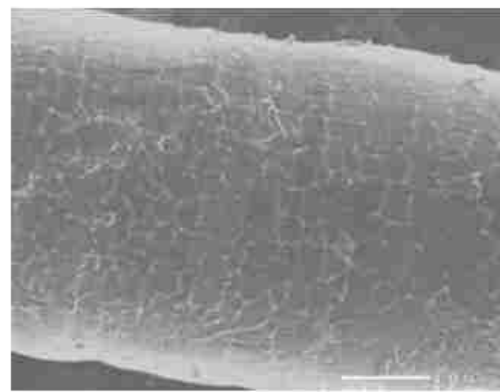
fibers offer selective sorption sites for toxic metals ( $M^{2+}$ ) through Lewis acid-base (metal-ligand) interactions where toxic metals (Lewis acid) accept lone pair of electrons from the oxygen donor atoms (Lewis base) of the HZO nanoparticles (36, 77).



A. Fiban K 1



B. X10 magnification



C. X2000 magnification

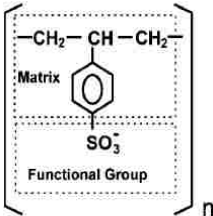
**Figure 6.1** (A) strong acid ion exchange fibers with sulfonic acid functional group, (B) Virgin fiber materials photographed at x10 magnification. (C) SEM photograph of a single fiber (x2,000) (44)



## 6.1 Synthesis of Hybrid Cation Exchange Fibers impregnated with HZO nanoparticles or HCIXF-Zr

Cylindrical strong-acid cation exchange fibers (Fiban K-1) and strong acid cation exchange resin beads (Purolite C145) were obtained from the Institute of Physical Organic Chemistry of the National Academy of Science in Belarus, and Purolite (PA), respectively. Similar materials are also produced by other manufacturers. Table 6.1 provides the salient information about the cation exchange fibers and resin beads used in the study. The method for impregnating host polymeric ion exchange materials with hydrated metal zirconium oxide nanoparticles was the same as the method for preparation of HAIX-Zr discussed in chapter 4.

**Table 6.1** Salient property of ion exchange materials

Property	Strong Acid Cation (SAC) Exchangers	
<b>Material</b>	Purolite C145	Fiban K1
<b>Shape</b>	Spherical	Cylindrical
<b>Size</b>	500-1200 $\mu\text{m}$ in diameter	10-50 $\mu\text{m}$ cross section
<b>Capacity</b>	3 meq/g dry	3 meq/g dry
<b>Functional groups</b>	R-SO <sub>3</sub> <sup>-</sup> H <sup>+</sup>	F-SO <sub>3</sub> <sup>-</sup> H <sup>+</sup>
<b>Chemical structure</b>		
		See figure 6.1A

## 6.2 Metals (Zinc) Removal during Fixed-bed Column Runs

Column runs were carried out using both hybrid cation exchange fibers (HCIXF-Zr) and resins (HCIX-Zr) material loaded with the same HZO nanoparticles. For comparison, both materials were run with identical influent concentrations of 2 mg/L  $\text{Zn}^{2+}$  in the presence of 100 mg/L of  $\text{Na}^+$ ,  $\text{Ca}^{2+}$ , and  $\text{HCO}_3^-$  at pH 7.5. Fixed-bed column runs with 1 g (around 3 cm<sup>3</sup>) of packed hybrid ion exchange fibers (HCIXF-Zr) were carried out using pressure-resistant epoxy coated glass columns (11 mm in diameter and 250 mm in length), constant-flow stainless steel pumps, and an Eldex fraction collector. Figure 6.2 provides the schematic of the laboratory apparatus used during fixed bed column run and CO<sub>2</sub> regeneration cycles for both IX-fibers and resins.

Two major processes are depicted in figure 6.2 including metal removal ( $\text{Zn}^{2+}$ ) using hybrid strong acid cation exchange fiber (HCIXF-Zr) loaded with hydrated Zr(IV) oxide (HZO) and the CO<sub>2</sub> regeneration process using 1% of  $\text{Ca}^{2+}$  solution sparged with solid CO<sub>2</sub>. The exhausted HCIXF-Zr column for metal (i.e.  $\text{Zn}^{2+}$ ) removal was regenerated by solid CO<sub>2</sub> sparged in 1% of calcium chloride at pH 3.7. The pressurized regenerant solution could be sparged with carbon dioxide by adding dry ice until the pressure reaches 100 psi. The throttling valves were used to control the flow rate of regenerant solution while an Eldex fraction collector collected samples at predetermined time intervals.

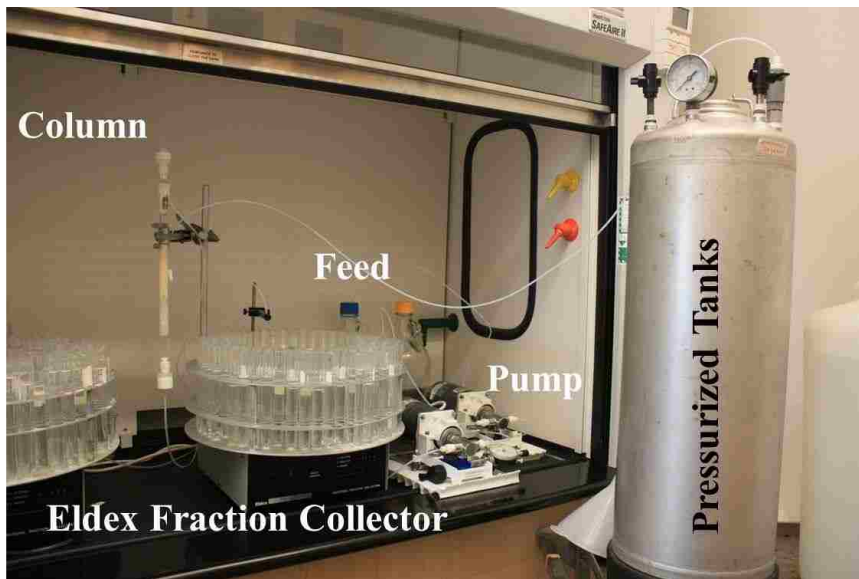
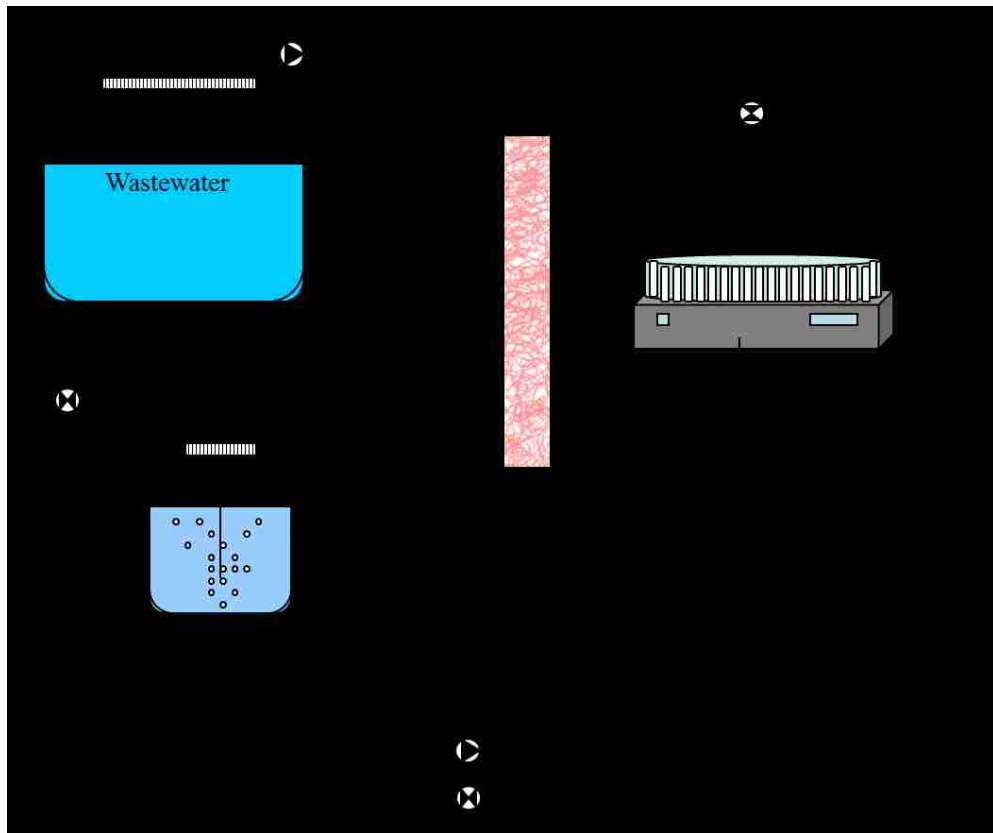


**Figure 6.2** A schematic diagram and the experimental apparatus used for both service cycles and regeneration cycles while using fiber and resin materials (46)

During the service cycles as shown in Figure 6.3, HCIXF-Zr demonstrates a high selectivity for the target contaminant (i.e.  $Zn^{2+}$ ) in the presence of competing ions. The hybrid fibers perform comparably to their hybrid resin counterparts in terms of both efficiency and overall capacity. From Figure 6.3, it can be observed that both materials effectively removed trace amounts of zinc in the presence of high concentrations (100 mg/L) of competing sodium and calcium cations. Sharper breakthroughs were seen for HCIXF-Zr materials with 10% breakthrough occurring at approximately 7,500 mL of volume throughput. The HCIX-Zr materials experienced 10 % breakthrough at less than 5,000 mL. One significant difference is that the breakthrough curves exhibit fairly “sharp” profiles as opposed to the more gradual breakthrough seen with traditional ion exchange resins. These sharp breakthroughs are indicative of the difference in physical and kinetic properties of the resin and fiber materials. Additional confirmation of these differing properties can be seen following the 24 hours interruption test as highlighted in Figure 6.3. Following a restart, monitoring of the effluent zinc concentration in the HCIX-Zr column showed a substantial decrease in the effluent zinc concentration. After the passage of several hundred bed volumes, the effluent concentration returns to pre-interruption levels. In contrast, very little change was observed in the HCIXF-Zr column during the interruption test. This phenomenon, as explained in previous studies, represents a predominance of intraparticle diffusional resistance within the resin beads (**53, 78, 79**). For the HCIXF-Zr, the drop of  $Zn^{2+}$  concentration in the column was negligible, suggesting relatively insignificant intraparticle diffusional resistance within the fibers.

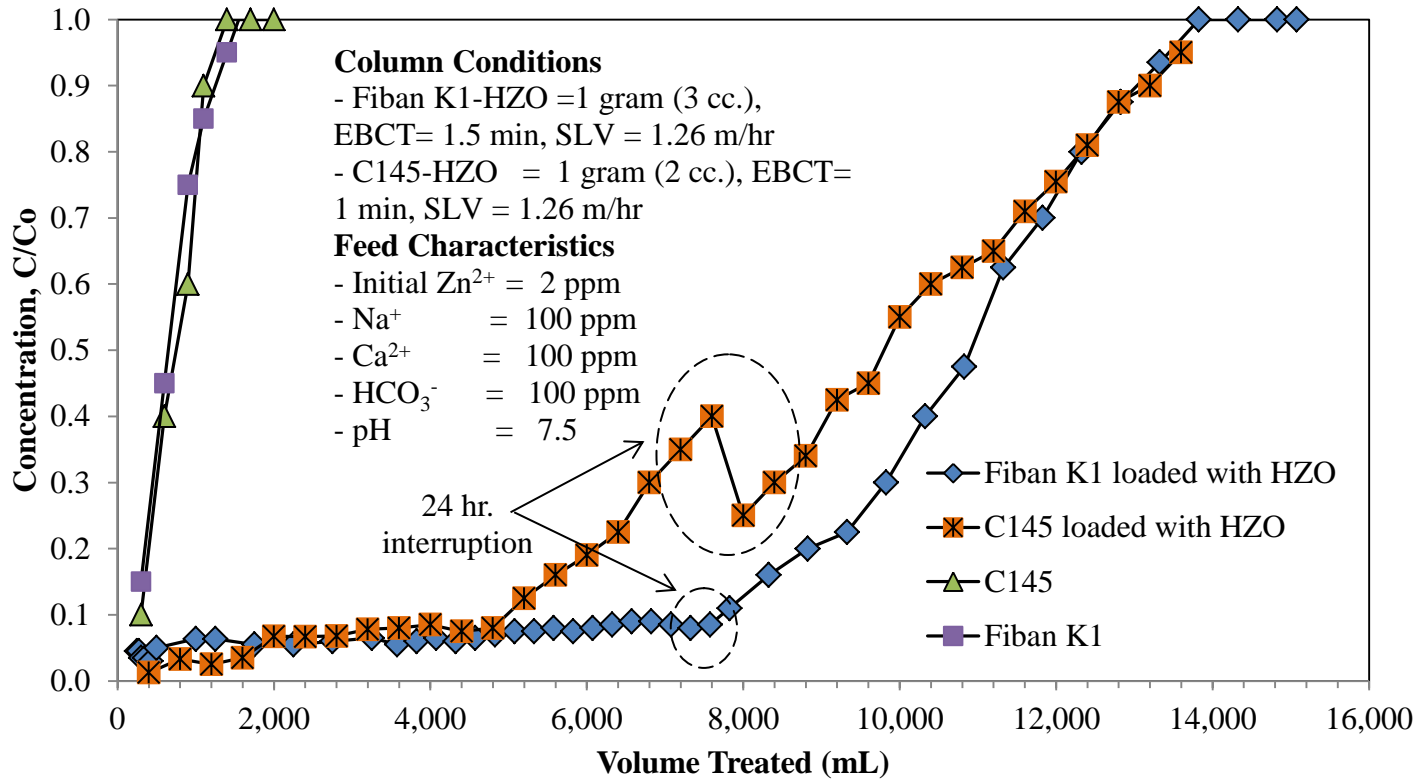


**Figure 6.3** The results of  $Zn^{2+}$  removal on fixed-bed column runs using four different ion exchange materials, namely, hybrid cation exchange fibers (HCIXF-Zr), hybrid ion exchange resins (HCIX-Zr) loaded with Hydrated Zr (IV) oxide (HZO), commercial cation exchange resin bead C145, and commercial cation exchange fiber K1

### 6.3 Regeneration using Solid CO<sub>2</sub> (Dry Ice) Sparged 1% Ca<sup>2+</sup> Solution

Figure 6.4 shows the results of two regeneration histories using both HCIX-Zr and HCIXF-Zr under otherwise similar conditions. It can be seen that HCIX-F outperforms its resin counterpart and is fully regenerated (> 98 % zinc recovered) in fewer than 100 bed volumes. The HCIX-Zr was poorly regenerated with only 30% zinc recovery. Fast and favorable kinetics of IX-fibers have also been reported in several studies. (80)

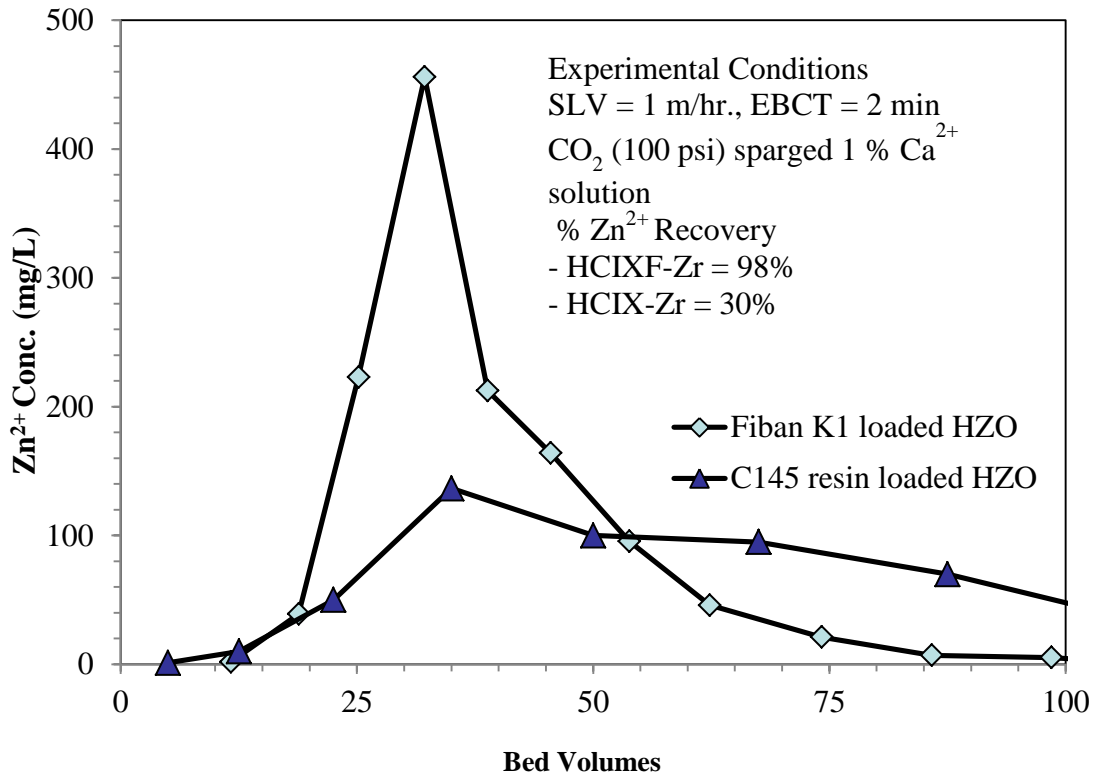


**Figure 6.4** Comparison of zinc elution between HCIXF-Zr (Fiban K1) and HCIX-Zr (Purolite C145) loaded with HZO

## 6.4 Fiber Morphology and Regeneration

The most significant difference between the resin and fiber materials can be observed during the carbon dioxide regeneration process as demonstrated in figures 6.5 and 6.6. In each instance, the fiber material is completely regenerated in less than 100 bed volumes while the resin material's performance is substantially inferior. The underlying reasons for these phenomena are largely morphological in nature for fiber materials (HCIXF-Zr). Earlier studies have also provided optical verification of shrinking resin cores during acid regeneration (81). On the contrary, for IX-fibers, the functional groups essentially reside on the surface, and they are readily accessible. Thus, intra-particle diffusion is nearly absent as illustrated in figure 6.6. Additional studies have shown the diffusional path length to be significantly less for fiber materials versus their resin counterparts. Consequently, a weak acid CO<sub>2</sub> solution works satisfactorily as a substitute for mineral acids, namely sulfuric and hydrochloric acid as regenerant. HZO surface binding sites are amphoteric; at an acidic pH, the binding sites are protonated and become positively charged. Consequently, positively charge Zn<sup>2+</sup> gets rejected due to the Donnan co-ion exclusion effect and thus desorption is thermodynamically favorable as illustrated in Figure 6.5.

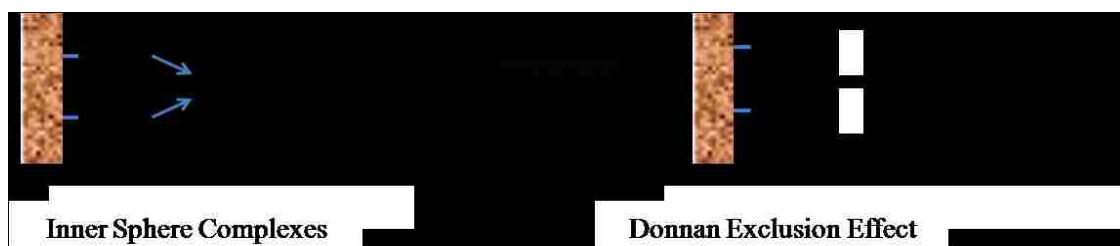


**Figure 6.5** Schematic illustration of sorption/desorption of toxic metal zinc on HZO

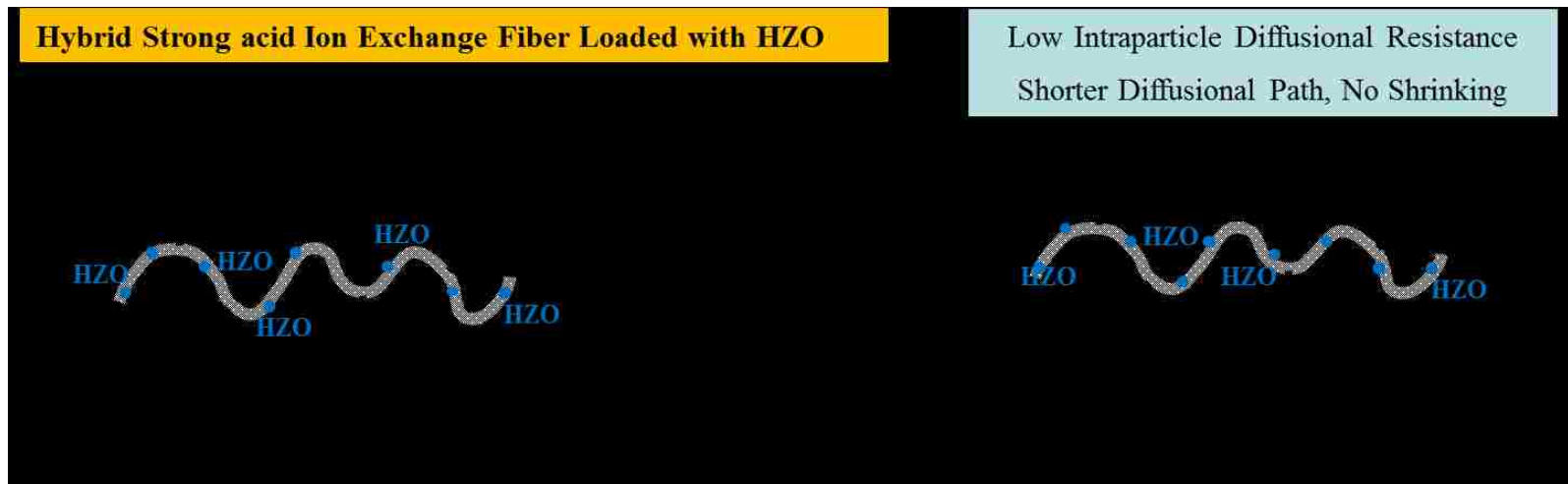


**Figure 6.6** A schematic depicting the progress of regeneration for HCIXF-Zr materials, the progress of regeneration for HCIXF-Zr materials



## 6.5 The Use and Sequestration of Carbon Dioxide

The use of carbon dioxide as an environmentally benign regenerant chemical has several notable advantages. First, the use of aggressive chemicals may be avoided entirely in the regeneration process. The waste regenerant streams do not contain any aggressive acid solution. Rain water, snowmelt or any source of water with low alkalinity can be used for CO<sub>2</sub> dissolution. Second, because regeneration efficiency is dependent only on the partial pressure of carbon dioxide, a number of alternative carbon dioxide sources may exist. Previous studies have demonstrated the use of captured flue gas ( $P_{\text{CO}_2} = 0.19 \text{ atm}$ ) as a viable regenerant (**44, 45, 82**). The reuse of such waste streams would represent a very inexpensive process input as opposed to the purchase of chemical regenerant. Third, the carbon dioxide used for regeneration would be permanently sequestered as carbonate alkalinity. This represents a net avoidance of carbon dioxide emissions that would otherwise be generated by the flue gas source or a traditional ion exchange process. Along the lines of using alternative carbon dioxide sources, this research demonstrated the effective use of dry ice as a carbon dioxide source. Some progress has recently been made in producing solid carbonic acid and dry ice economically from carbon dioxide gas (**83**). Dry ice may present some operational advantages over using carbon dioxide gas in terms of both use and storage. The condensed form of carbon dioxide can also serve as an excellent regenerant for HCIXF-Zr.

## CHAPTER 7

### SALT FREE WATER SOFTENING PROCESSES

The objective of this study is to validate novel salt free water softening processes using two types of heterogeneous cation exchangers along with regeneration techniques. First, the gel weak acid cation (WAC) exchangers preloaded in a sodium form were used for hardness removal. Both traditional WAC and Shallow Shell Technology (SST) resins were used to validate the efficiency of the regeneration processes with either CO<sub>2</sub> sparged DI water in a pressurized chamber or a diluted biodegradable organic acid (i.e., 2% acetic acid). Second, the macroporous strong acid cation (SAC) exchanger is used in polyvalent forms (i.e., Al<sup>3+</sup> and Fe<sup>3+</sup>) instead of the traditional water softening exchange process that uses a strong acid cation (SAC) exchanger in the sodium form. Regeneration of the novel material uses only stoichiometric amounts of polyvalent cation salts so that no excess salt from the regeneration solution is discharged from the process. The results and discussion cover the following topics:

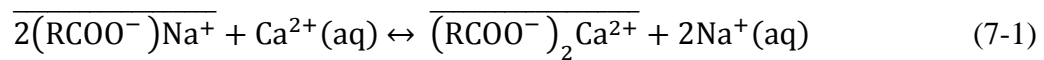
1. Underlying principal of the proposed processes by using two different types of heterogeneous cation exchangers and regeneration techniques.
2. Hardness removal by using weak acid cation exchangers for both traditional WAC and SST resins, and regeneration with solid CO<sub>2</sub> (dry ice) or dilute biodegradable organic acid (2% acetic acid).
3. Simultaneous removal of hardness and anionic ligands (i.e., fluoride) by using the SAC resin in the aluminum form.

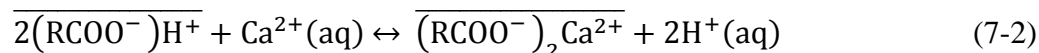
## 7.1 Underlying Principal of The Proposed Processes

The novel salt-free water softening processes (i.e., removal of  $\text{Ca}^{2+}$ ,  $\text{Mg}^{2+}$ ,  $\text{Fe}^{2+}$ , etc.) are presented in this study using two different cation exchangers. First, weak acid cation (WAC) exchangers were used for removal of hardness and either solid  $\text{CO}_2$  (dry ice) sparged in water in a pressurized chamber or diluted biodegradable organic acid (i.e., 2% of acetic acid) was used as a regenerant solution. The waste acetic acid is biodegradable, so it does not affect the environment after discharge into a natural waterway. Second, the macroporous strong acid cation (SAC) exchange resins preloaded in aluminum form and the use of stoichiometric amounts of Al(III) salts as the regeneration chemical. The waste is mainly from hardness (i.e.,  $\text{Ca}^{2+}$  or  $\text{Mg}^{2+}$ ) removed during softening and anionic species from regeneration chemicals, e.g., chloride, with no excess salts from regeneration being discharged during the process. No aluminum or other polyvalent cations leach into the treated water due to the formation of polyvalent cation (hydr)oxide particles and the deposition of the particles into the matrix of the resins. The process can also remove trace anionic ligands (i.e., fluoride, phosphate, etc.) due to the formation of oxides of the polyvalent cation particles, i.e., Al(III) oxide, through Lewis acid-base interactions.

### 7.1.1 Salt-Free Water Softening Process using WAC Resins

- Hardness ions are removed by weak acid ion exchanger (WAC) in hydrogen or sodium form;

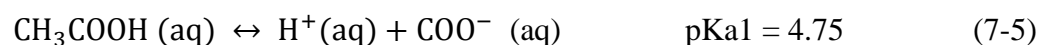




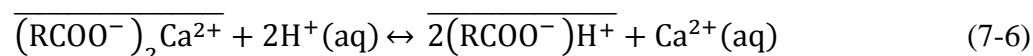
- Regeneration with solid CO<sub>2</sub> (dry ice) sparged water in pressurized chamber @120psi



- Regeneration by 2% acetic acid solution



- Regeneration of WAC resins using either CO<sub>2</sub> or acetic acid solution



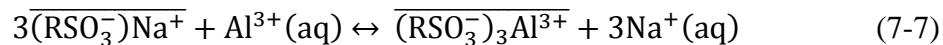
The affinity sequence of WAC resins with carboxylic functional groups can be described as follows:  $\text{H}^+ \gg \text{Ca}^{2+} > \text{Na}^+$ . For this reason, hydrogen ions as provided by the carbonate systems (eq 7-4) or the acetic acid dissociation (eq.7-5) can be effective regenerant for WAC resins. Note that from the previous study using ion exchange fibers which have much shorter diffusional path length than the tradition WAC resins were effective for CO<sub>2</sub> regeneration. (44, 45, 82) The hydrogen concentration from the carbonate systems (eq.7-4) are much less than the inorganic acid that is used to for regenerate traditional WAC resins. Due to the unavailability of commercial ion exchanger fibers, the commercially available SST resins from Purolite which have an inert core and the functional groups residing primarily on the outer shell similar to the former ion exchanger fibers were chosen to validate the concept. SST resins are believed

to be able to regenerate by CO<sub>2</sub> or dilute acetic acid because they have lower diffusional path lengths so that hydrogen ions can easily migrate into the pore and exchanged with the hardness.

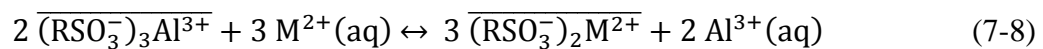
### 7.1.2 Salt Free Water Softening Process Using SAC Resins in Polyvalent Form

The second salt free water softening processes use macroporous strong acid cation (M-SAC) exchange resins in the aluminum form. Note that gel type SAC can also be used. However, M-SAC exchangers give higher fluoride or other anionic ligands removal capacity than gel type SAC due to the high possibility of metal oxide deposition. A cation exchanger in polyvalent cation form, namely Al(III), Fe(III), Zr(IV) or Ti(IV) can also be used.

First, the resins are changed into the aluminum form by passing stoichiometric amounts of aluminum salt, such as alum (Al<sub>2</sub>(SO<sub>4</sub>)<sub>3</sub> · 16 H<sub>2</sub>O) or aluminum chloride (AlCl<sub>3</sub> · 6 H<sub>2</sub>O) solution as shown in equation (7-7), where the overbar indicates the resin phase.

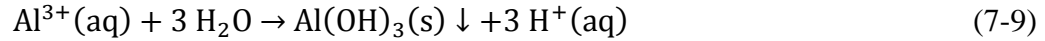


The hardness (i.e., Ca<sup>2+</sup> or Mg<sup>2+</sup>) in the water is removed by ion exchange with the Al<sup>3+</sup> in M-SAC as shown in equation (7-8), where M represents cation corresponding to hardness (e.g., Ca<sup>2+</sup>, Mg<sup>2+</sup>, Sr<sup>2+</sup>, Ba<sup>2+</sup>).

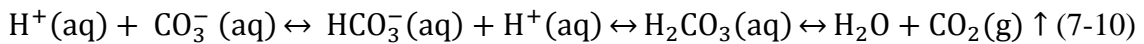


Aluminum ions, released from the cation exchange functional groups undergo

hydrolysis reactions with water to form aluminum (hydr)oxide (Al(OH)<sub>3</sub>(s)) particles that precipitate within a macroporous cation exchanger through the following reaction:

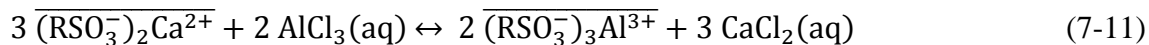


From equation (7-9), protons are produced from the precipitation reaction, which can then react with alkalinity in water by equation (7-10)



Overall, the ion exchange of hardness and polyvalent cations (i.e., Al<sup>3+</sup>) removes total dissolved solid (TDS) from the solution as bicarbonate (HCO<sub>3</sub><sup>-</sup>) and hardness (i.e., Ca<sup>2+</sup> and Mg<sup>2+</sup>) via acid-base neutralization and ion exchange mechanism reactions, respectively. Thus, changes in effluent TDS and pH are indicators of ion exchange activity and predictors of when the resin becomes exhausted. The exhausted resins are regenerated by passing only stoichiometric amounts of aluminum or other polyvalent cation salts, such as alum (Al<sub>2</sub>(SO<sub>4</sub>)<sub>3</sub>·16 H<sub>2</sub>O) or AlCl<sub>3</sub> solution through the macroporous strong acid cation exchange resin to reverse the reaction in equation (7-8). The aluminum hydroxide (Al(OH)<sub>3</sub>(s)) particles that were previously deposited are still retained in the resin phase without being disturbed by ion exchange or hardness removal. After the regeneration with AlCl<sub>3</sub> solution, the resins are again in the aluminum form and ready for the next service cycle of hardness removal as shown in equation (7-11). The waste regenerant stream contains small quantities of only CaCl<sub>2</sub> solution where calcium comes from hardness and chloride comes from the AlCl<sub>3</sub> regeneration solution. Due to adding

stoichiometric amounts of regenerant, there is no excess salt from the regeneration solution.



In general, the novel water softening process requires only stoichiometric amounts of polyvalent cations, namely Al(III), Fe(III), etc., during the regeneration process, which then exchange on an equivalent basis with the hardness (i.e.,  $\text{Ca}^{2+}$  or  $\text{Mg}^{2+}$ ). The process can be classified as a salt-free water softening process because the soft water effluent has lower sodium than traditional cation exchange and there are no NaCl being discharged in the waste regeneration stream. The waste regeneration stream contains low amounts of hardness (i.e.,  $\text{Ca}^{2+}$  and  $\text{Mg}^{2+}$ ) from the influent and anions from the salt of the polyvalent cations used for regeneration.

During the water softening process, transition metals and anionic ligands can be removed from the water simultaneously through the Lewis acid-base interaction with concurrent hardness removal due to the presence of freshly precipitated polyvalent cation oxides on the matrix of the cation exchanger. Every cycle of cation exchanger regeneration with polyvalent cations provides a new source for freshly precipitated polyvalent cation oxides that can take part in Lewis acid-base interactions.

## 7.2 Water Softening using Weak Acid Cation (WAC) Exchange Resins

### 7.2.1 Hardness Removal using Two WAC Exchangers at Influent $\text{Ca}^{2+}$ 400 mg/L

Figure 7.1 shows the results of two separate fixed-bed column runs using two different weak acid cation (WAC) exchangers, namely, shallow shell technology weak acid cation exchange resin with inert core (Purolite SST 104) and traditional weak acid cation exchange resin (Purolite C104). Besides the difference in physical configuration, the chemical properties are virtually identical for these two ion exchange materials. Note that in both cases, hardness was removed very efficiently for more than 55 bed volumes.

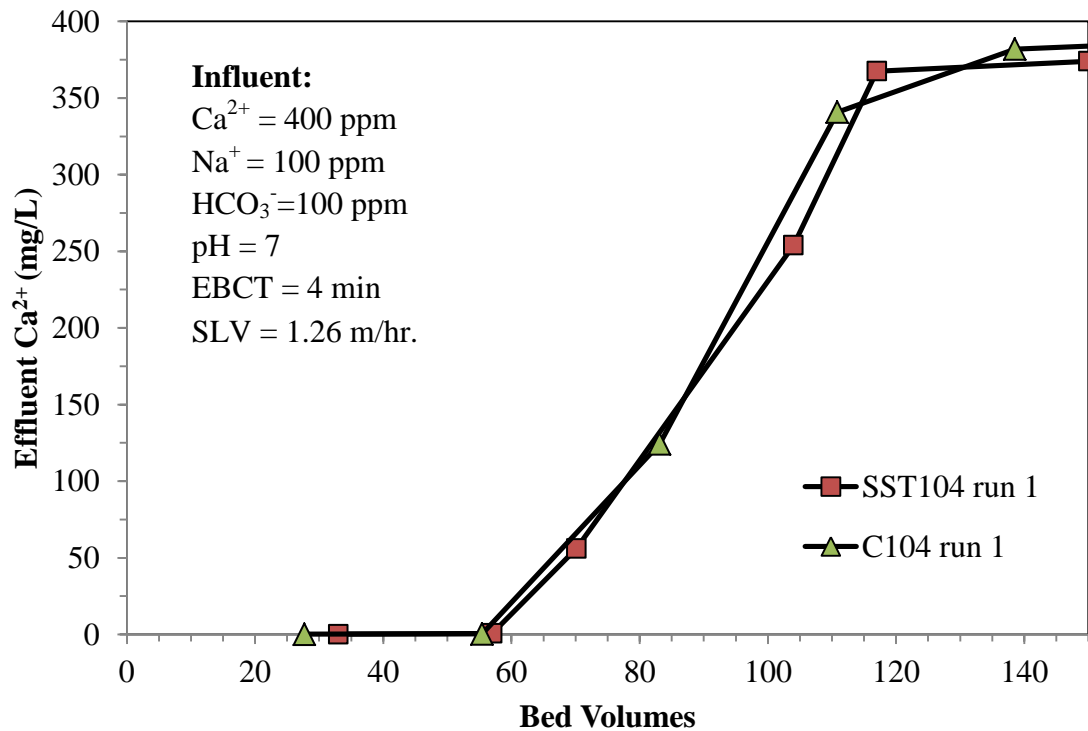


**Figure 7.1** The results of  $\text{Ca}^{2+}$  removal on fixed-bed column runs using two different WAC resins (SST104 and C104) at influent  $\text{Ca}^{2+}$  400 mg/L.



### 7.2.2 Comparison of Solid CO<sub>2</sub> Sparged Water and Acetic Acid Regeneration

Figure 7.2 shows the results of two hardness regeneration runs using two different regeneration schemes, namely CO<sub>2</sub> sparged in DI water at 150 psi and 0.5 % acetic acid. It can be seen that the diluted acetic acid (0.5%) resulted in high calcium desorption with more than 85% of calcium recovery, while the solid CO<sub>2</sub> sparged water was not effective for hardness regeneration with only 6-25 % of calcium recovery.

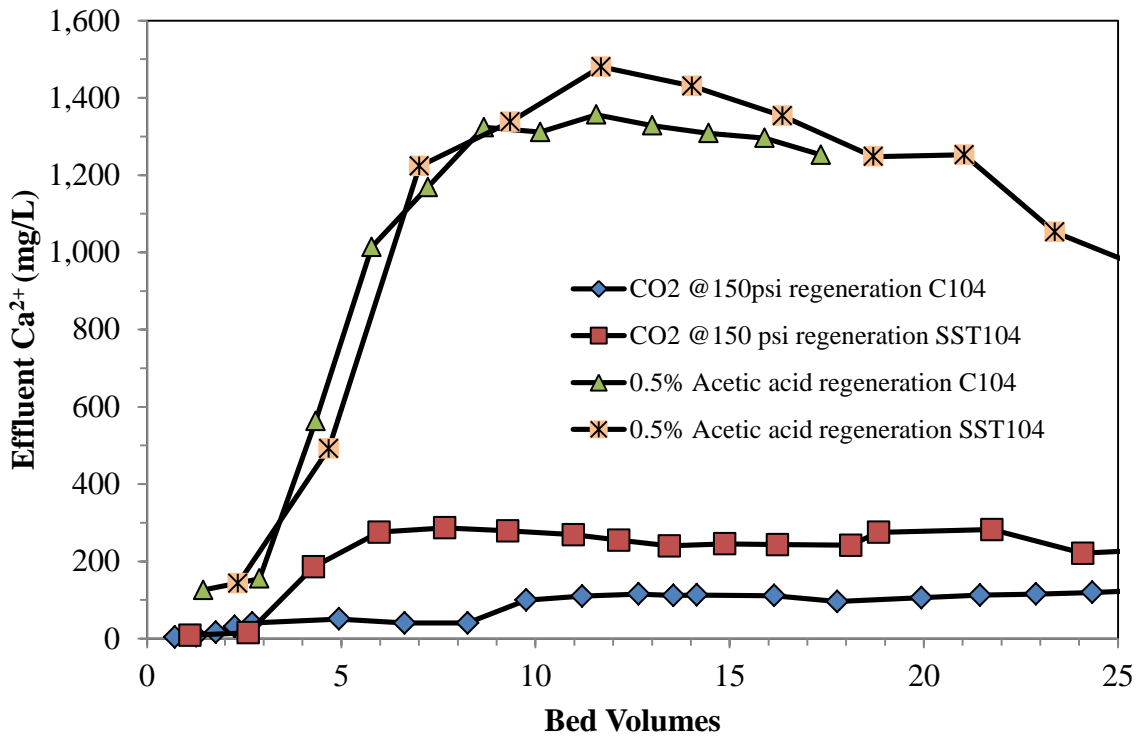


**Figure 7.2** Comparison of water softening regeneration between the solid carbon dioxide sparged water @150 psi and dilute 0.5% acetic acid regeneration

From the previous study (44, 45, 53, 82), CO<sub>2</sub> can be successfully used to regenerate hardness from ion exchange fibers due to the much shorter diffusion path length of the ion exchanger fibers compared to the traditional resin beads. For this experiment, we think that the reason may come from the insufficient hydrogen ions concentration provided by the carbonate systems (CO<sub>2</sub> sparged water at 150 psi) as well as the diffusion path length of the SST resin is still much higher than the ion exchange fibers. Note that the general ion exchange resins including the SST resins have diameters of approximately 500µm while the ion exchanger fibers have a cylindrical shape with diameter around 50 µm. Although the SST resin has an inert core so that the diffusion path length is shorter than the traditional resin, the SST resin still has a much longer diffusion pathlength than the ion exchanger fibers.

### **7.2.3 Hardness Removal using Two WAC Exchangers at Influent Ca<sup>2+</sup> 200 mg/L**

Two weak acid cation (WAC) exchangers with carboxylic functional groups were used for removal of hardness and the feed calcium concentration was reduced from 400 to 200 mg/L including other ions as shown in the figure 7.3. The calcium was removed from the feed influent effectively and calcium breakthrough from SST104 was a little earlier compared to the traditional C106. As observed from the previous study, acetic acid can be used for hardness regeneration more effectively than the CO<sub>2</sub> sparged DI water. For this experiment, 0.5% of acetic acid solution was used to regenerate both resins at stoichiometric amounts (i.e., no excess acid required). The amount of acetic acid is calculated based on the capacity of the resin.

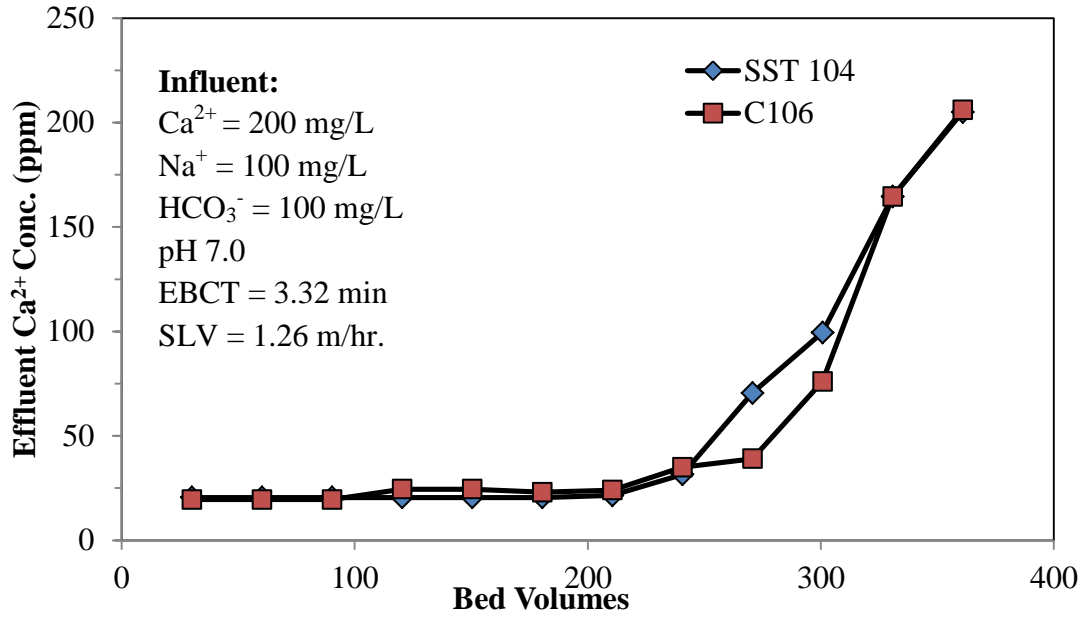


**Figure 7.3** The results of  $\text{Ca}^{2+}$  removal on fixed bed column runs using two different WAC resins (SST104 and C104) at influent  $\text{Ca}^{2+}$  200 mg/L.

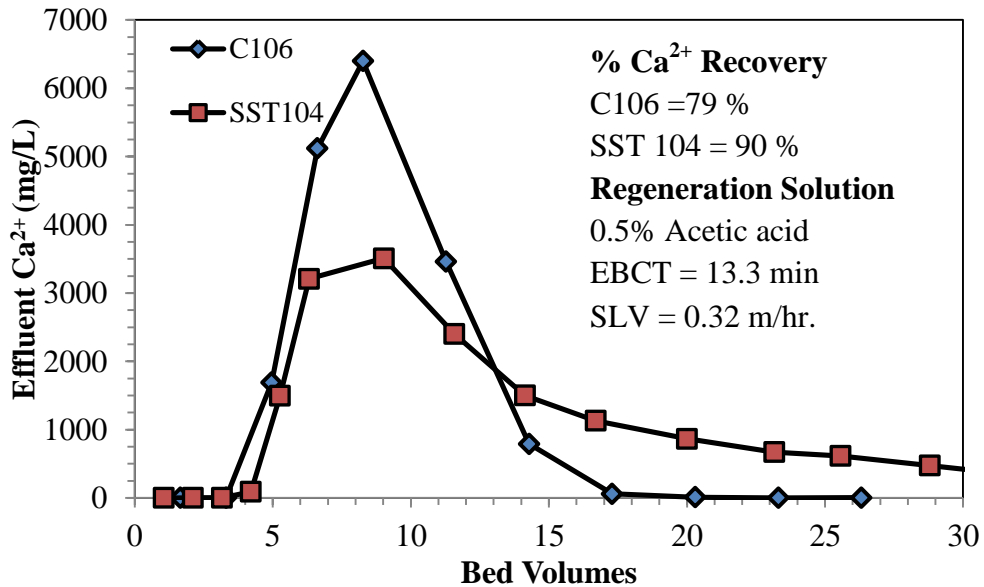


**Figure 7.4** Diluted acetic acid regeneration (0.5% acetic acid) of traditional weak acid cation exchanger C104 and shallow shell technology (SST 104)

From figure 7.4, two different regeneration curves are presented and high calcium recoveries (80-90%) are observed. Calcium can be recovered from the SST104 better than the C106 even though the SST104 takes a longer time than the C106. The concentration of acetic acid may affect the regeneration efficiency. For the next experiment, the concentration of acetic acid was increased from 0.5% to 2.0%.

#### **7.2.4 Hardness Removal using Two WAC Exchangers at Influent $\text{Ca}^{2+}$ 150 mg/L**

For this study, the influent calcium concentration was lower than the previous experiment and a higher concentration of acetic regenerant solution was used. Purolite SST104 and C106 were again used to validate the hardness removal and acetic acid regeneration. From the regeneration curve of the SST104 regeneration with 2% acetic acid, high calcium recovery from regeneration runs 2 and 3 can be achieved by reducing the flow rate that keeps the EBCT at 13.3 min. By increasing the acetic acid concentration from 0.5 to 2.0 %, high calcium recovery (87-100 %) can be achieved with less than 20 bed volumes as shown in the regenerations 2 and 3 from figure 7.6. For the traditional WAC resin (Purolite C106), high calcium recovery can be obtained by 2% acetic acid as shown in the figure 7.8. From the previous experiments in section 7.2.3, 0.5% of acetic acid can not fully regenerate all of the calcium with 79% recovery as mentioned in figure 7.4. By using 2% acetic acid, very high calcium recovery from the regeneration process can be attained in both traditional spherical WAC resin beads (Purolite C106) and the Shallow Shell Technology (inert core) and WAC resin (Purolite SST104).

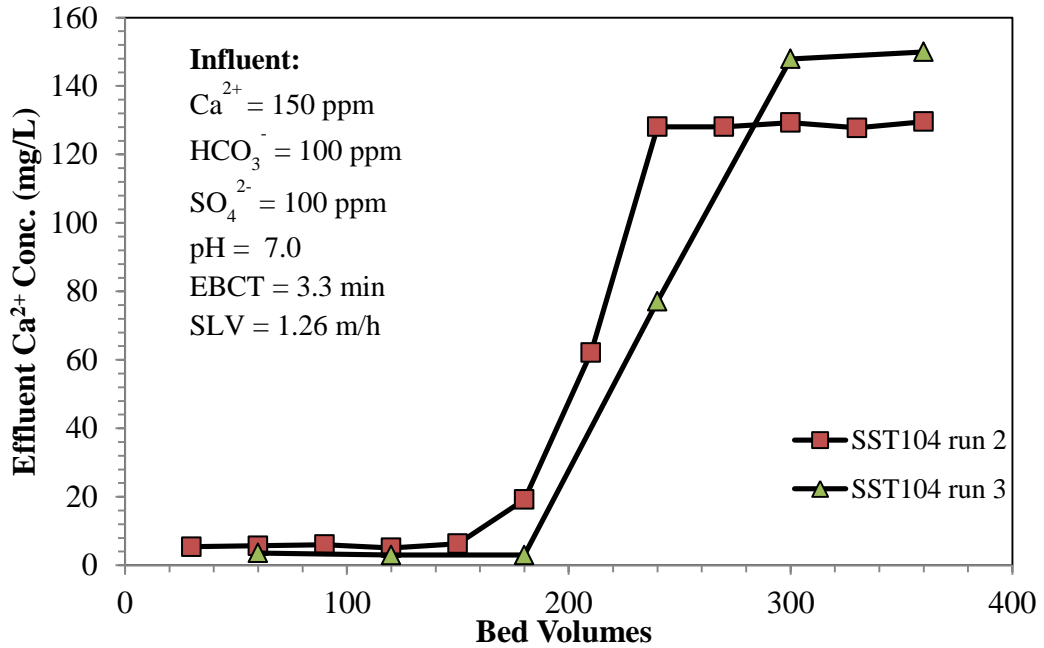


**Figure 7.5** The results of  $\text{Ca}^{2+}$  removal on fixed bed column runs using WAC resins (SST104) at influent  $\text{Ca}^{2+}$  150 mg/L

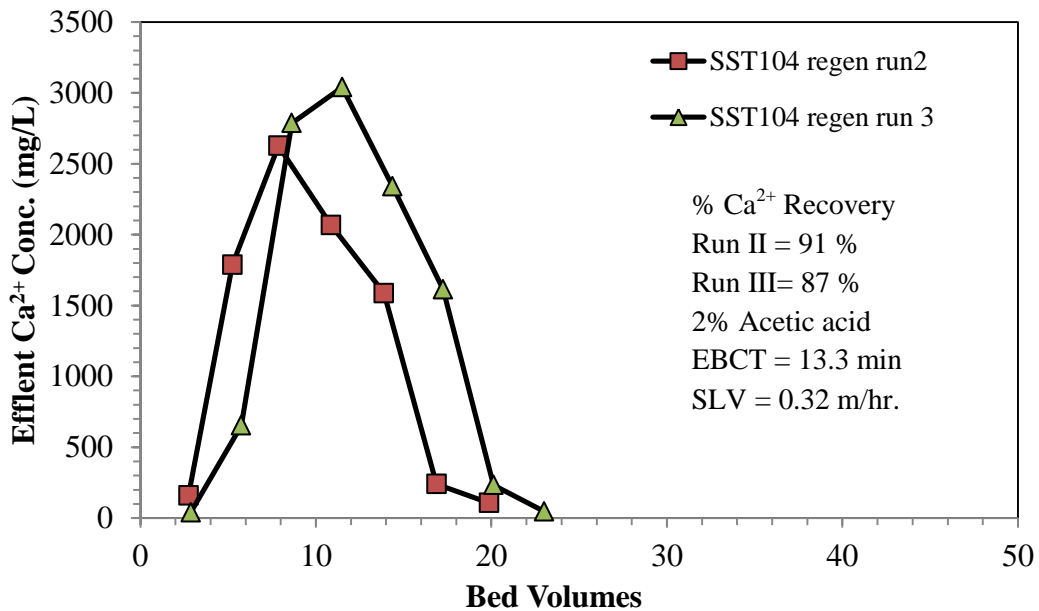


**Figure 7.6** Diluted acetic acid regeneration (2% acetic acid) of the shallow shell technology (SST 104)

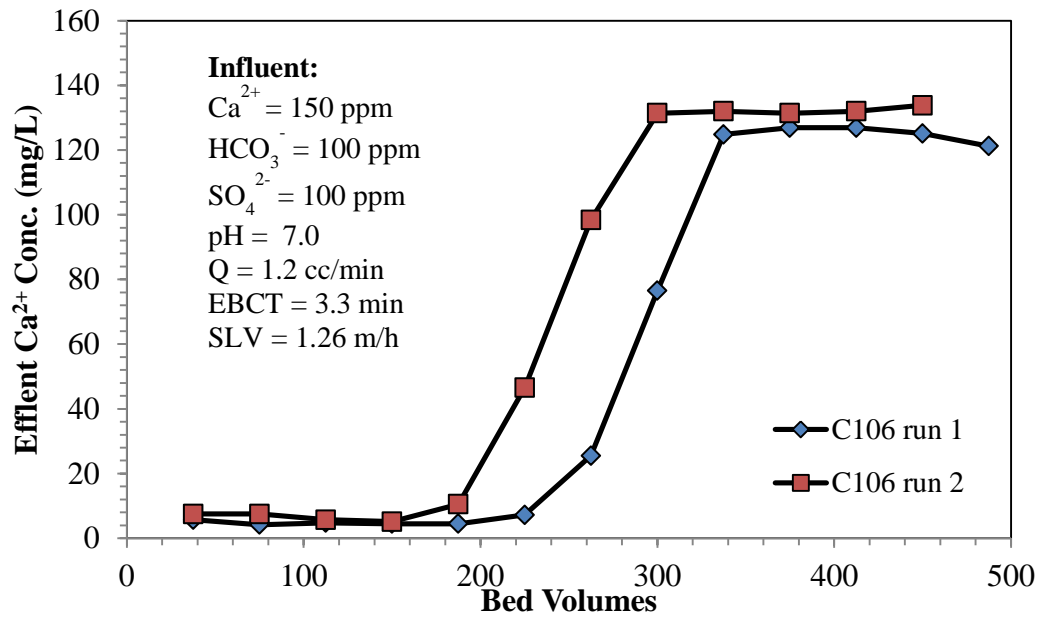


**Figure 7.7** The results of  $\text{Ca}^{2+}$  removal on fixed bed column runs using WAC resins ( C106) at influent  $\text{Ca}^{2+}$  150 mg/L

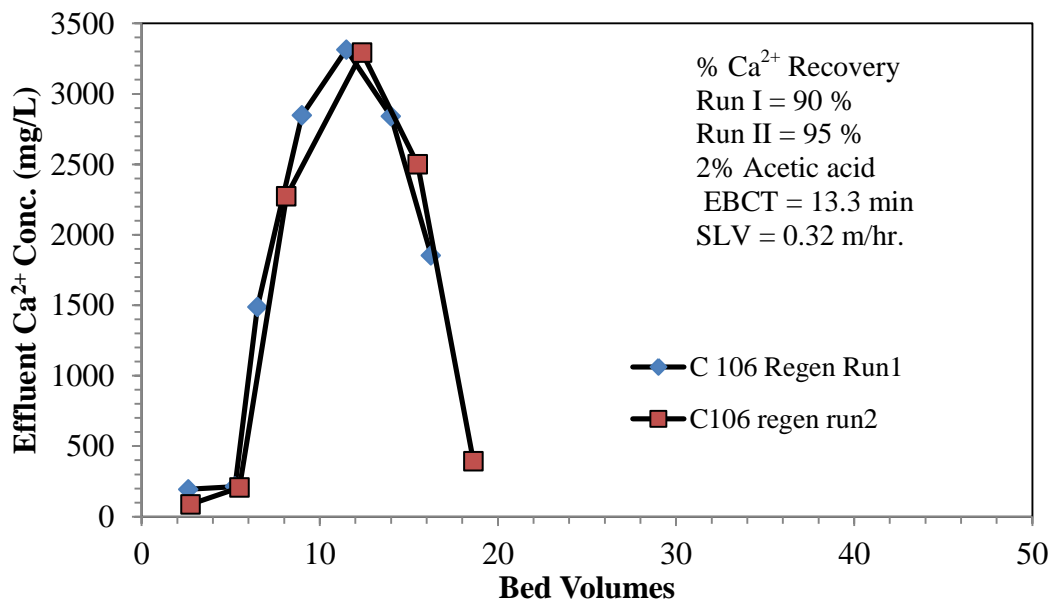


**Figure 7.8** Diluted acetic acid regeneration (2% acetic acid) of traditional weak acid cation exchanger C106

### **7.2.5 Hardness Removal at Ca<sup>2+</sup> 70 mg/L and 2% Acetic Acid**

After gaining experience for hardness removal and regeneration, high calcium recovery from both ion exchangers can be achieved with less than 10 bed volumes. For this experiment, the influent calcium concentration was lowered to the 70 mg/L or 175 mg/L as CaCO<sub>3</sub>, which is categorized as hard water usually found in natural water. Both Purolite C106 and SST104 resins can remove calcium very well with calcium breakthrough around 450 bed volumes as shown in figures 7.9 and 7.11. Upon exhaustion, the resins were regenerated by using 2% acetic acid as previously used in section 7.2.4. The high calcium recovery (89-98 %) can be obtained with only 10 bed volumes. From the previous regeneration in figures 7.6 and 7.8, high calcium recovery can be obtained but we need up to 20 bed volumes of regeneration solution. High regeneration efficiency and waste minimization can be possible.

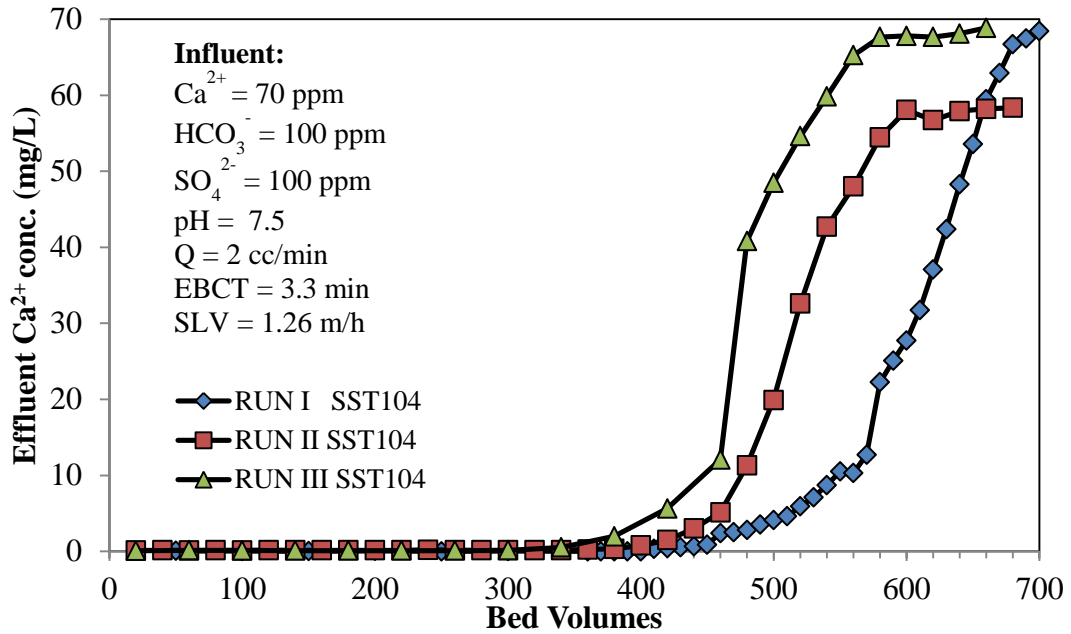


**Figure 7.9** The results of  $\text{Ca}^{2+}$  removal on fixed bed column runs using WAC resins SST104 at influent  $\text{Ca}^{2+}$  70 mg/L

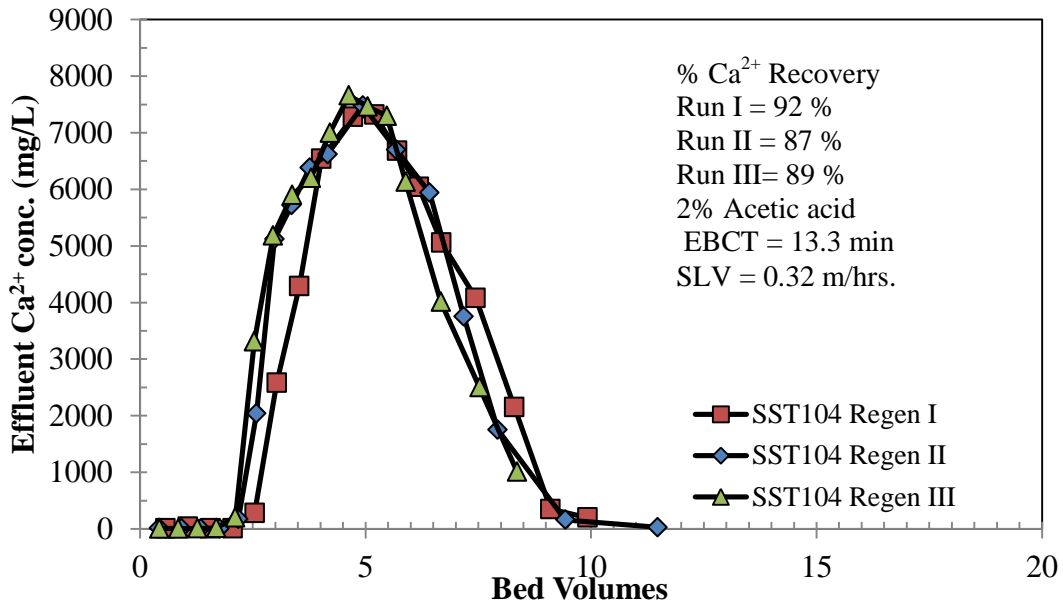


**Figure 7.10** Diluted acetic acid regeneration (2% acetic acid) of shallow shell technology WAC resin (SST 104)



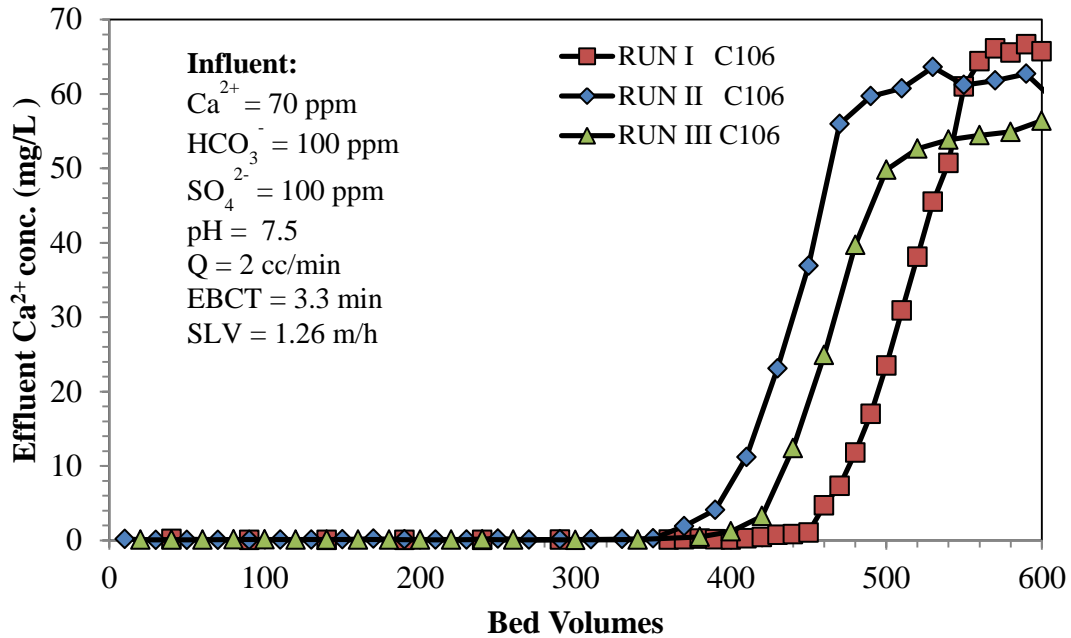


**Figure 7.11** The results of  $\text{Ca}^{2+}$  removal on fixed bed column runs using WAC resins (C106) at influent  $\text{Ca}^{2+}$  70 mg/L

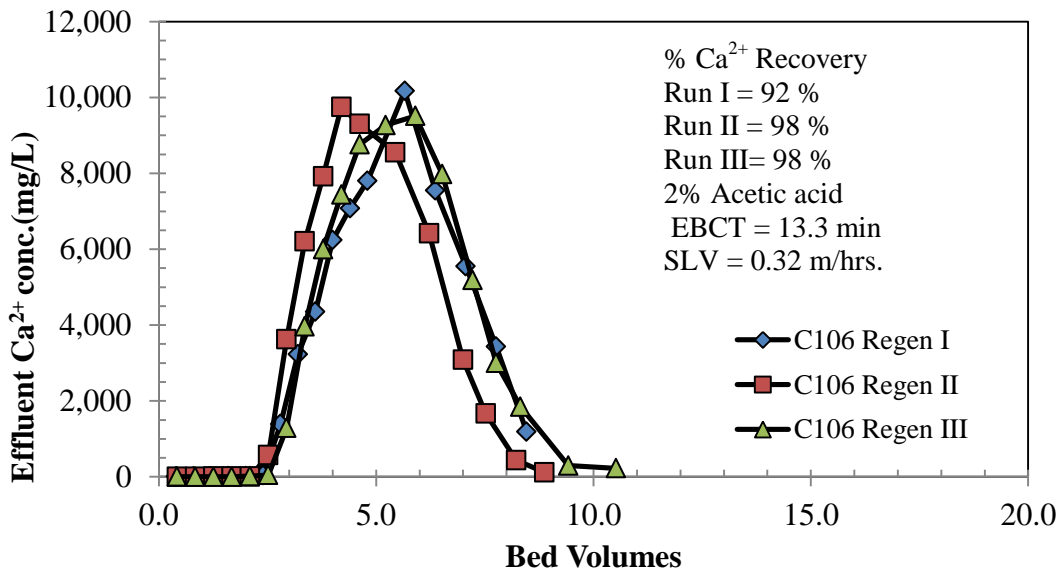


**Figure 7.12** Diluted acetic acid regeneration (2% acetic acid) of traditional weak acid cation exchanger C106

## 7.3 Water Softening Using Strong Acid Cation Exchanger in Al<sup>3+</sup> form

### 7.3.1 Hardness Removal at Initial Ca<sup>2+</sup> 100 and 50 mg/L

Figures 7.13-7.14 provide calcium effluent histories with two different feed calcium concentrations (100 mg/L and 50 mg/L) using Purolite C-145 after being converted from sodium into the aluminum form. The feed water also contained: 5 mg/L fluoride; 250 and 125 mg/L bicarbonate, respectively; 20 mg/L silica oxide (SiO<sub>2</sub>); and pH 7.9 and 9.0 (no pH adjustment), respectively. The calcium from both column runs was removed effectively.

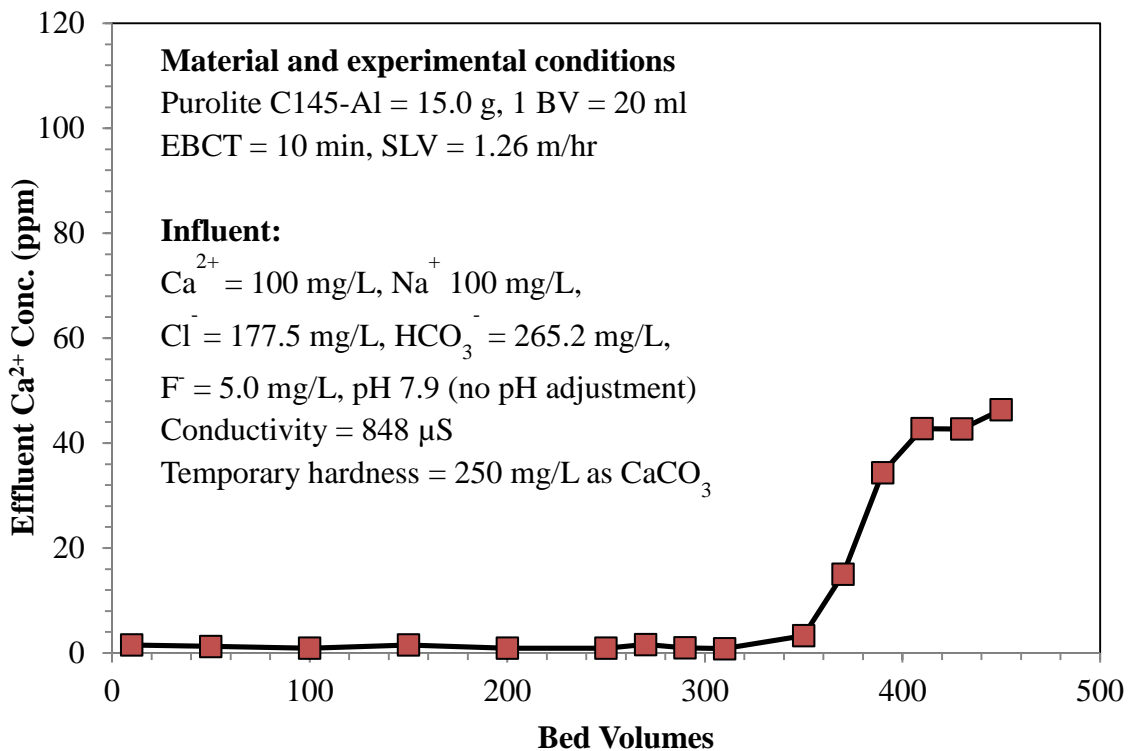


**Figure 7.13** Effluent calcium history for hardness removal with high calcium in feed (100 mg/L) during column runs using macroporous strong acid cation exchanger in Al<sup>3+</sup> form.

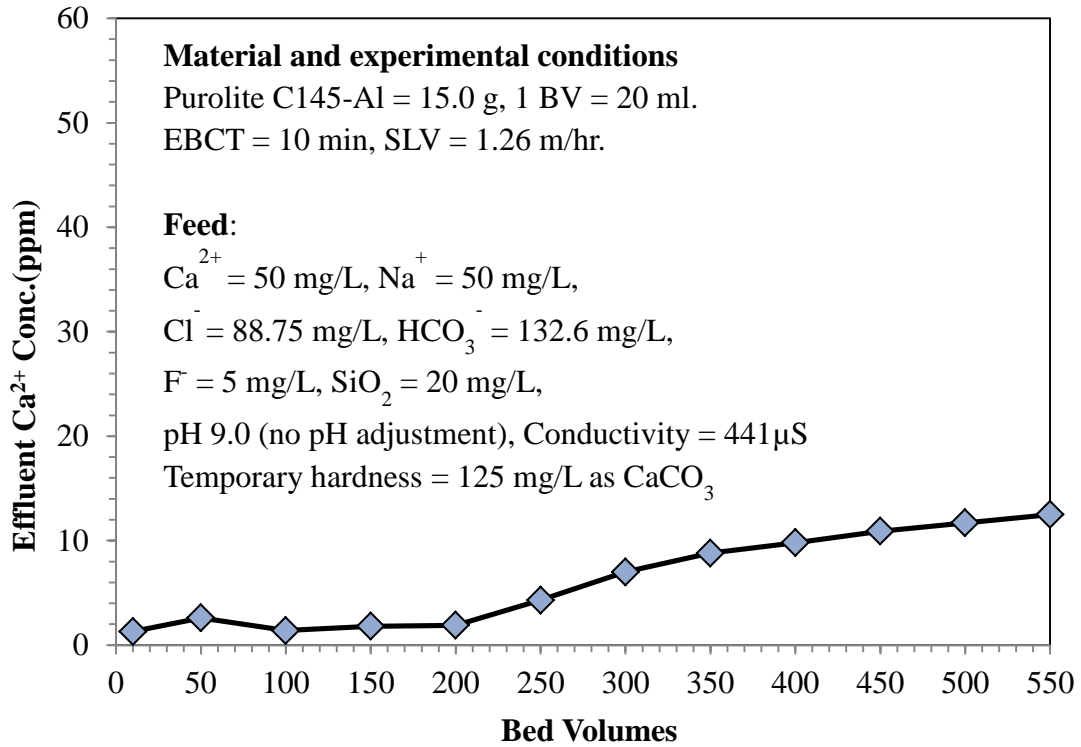


**Figure 7.14** Effluent history for hardness removal with low calcium in the feed (50 mg/L) during column runs using macroporous strong acid cation exchanger in  $\text{Al}^{3+}$  form.

During the calcium removal, aluminum was replaced by calcium and then precipitated as aluminum oxide particles in the matrix of the cation exchange resin. To validate this phenomenon, the level of aluminum ion was monitored in treated water and is plotted in figure 7.15. The aluminum concentration is very low and all of the samples tested exhibit aluminum concentrations less than the United States Environmental Protection Agency (USEPA) secondary maximum contaminant level (MCL): 0.2 mg/L.

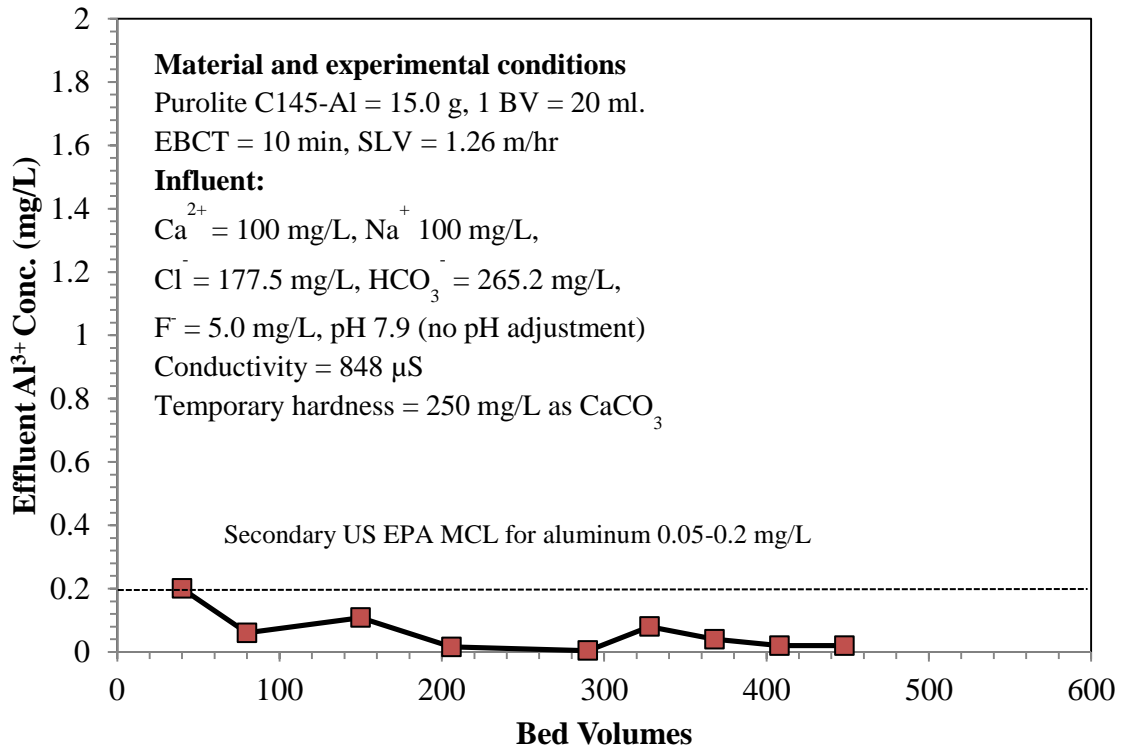


**Figure 7.15** Concentration profiles of aluminum in treated water during column runs using macroporous strong acid cation exchanger in  $\text{Al}^{3+}$  form.

The feed water contained many constituents but is predominantly calcium, sodium and bicarbonate. The salt-free water softening process can also help to reduce total dissolved solid (TDS) levels, as shown in figure 7.16. The main TDS removal mechanism is from acid-base neutralization between alkalinity and protons generated from the aluminum (hydr)oxide formation, as mentioned in eq. 7-10. From figure 7.16, the conductivity was low until 300 bed volumes and then increased to nearly the conductivity of feed. The hydrogen ions ( $\text{H}^+$ ) which are generated from the reaction of

aluminium hydroxide precipitation (eq. 7-9) react with the alkalinity in the water (eq. 7-10) resulting in decreasing of alkalinity. This reaction occurred at the beginning of the run until reaching 300 bed volumes. Then, when all of the aluminum in the ion exchanger was exchanged with the hardness (i.e.,  $\text{Ca}^{2+}$ ), there are no more protons generated from the aluminium hydroxide precipitation to react with the alkalinity in the water, resulting in increasing of conductivity after 300 bed volumes. The hardness removal ended at around 300 bed volumes as shown in figure 7.13. The hardness breakthrough can also be simply monitored by increasing in the conductivity of the effluent as shown in figure 7.16.

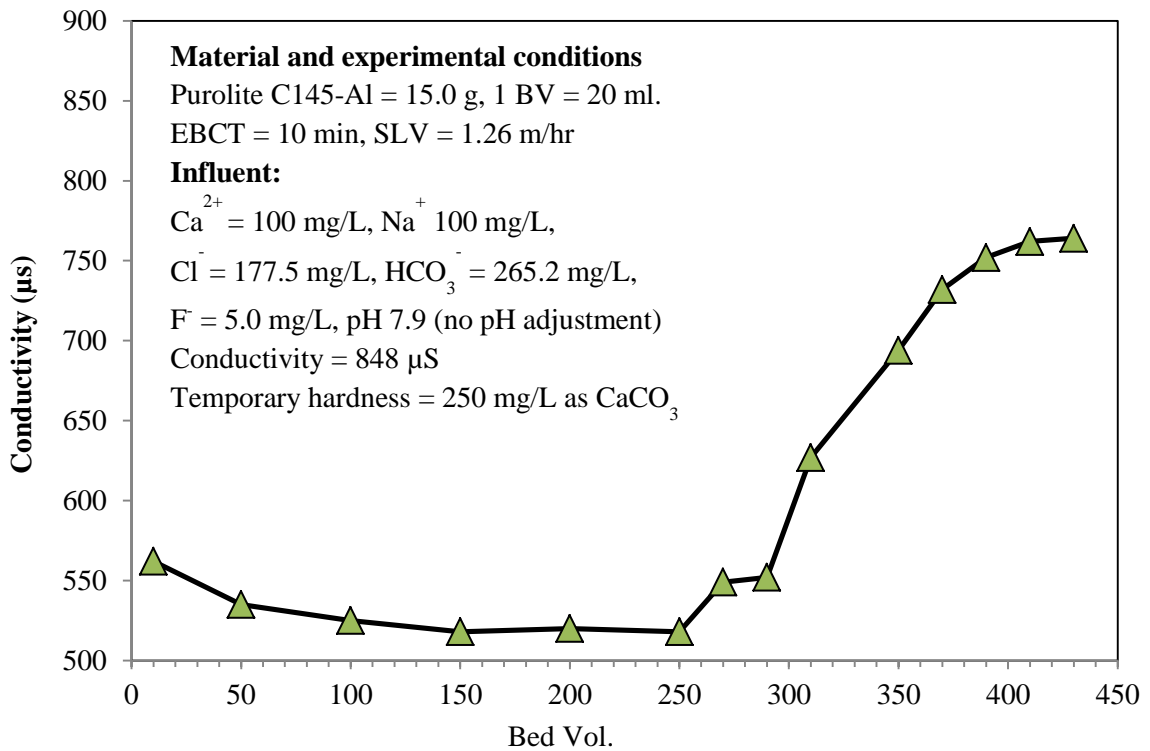


**Figure 7.16** Breakthrough profile of treated water conductivity during column runs using macroporous strong acid cation exchanger in  $\text{Al}^{3+}$  form.

### 7.3.2 Fluoride Removal

It is well-established that polyvalent metal oxides, namely Al(III), Fe(III) and Zr(IV), exhibit amphoteric sorption behaviors, i.e., they can selectively bind both Lewis acids or transition-metal cations (e.g.,  $Zn^{2+}$ ,  $Pb^{2+}$ ,  $Cu^{2+}$ , etc.) and Lewis bases or anionic ligands (e.g., arsenate, phosphate, fluoride, etc.) through the formation of inner-sphere complexes.(15, 29, 37) From the salt-free hardness removal process by using a macroporous cation exchanger in aluminum or other polyvalent cation forms, hydrated polyvalent metal oxide particles, namely Al(III) oxide and Fe(III) oxide are generated and deposited in the matrix of the resin without disturbing the ion exchange sites according to eq.(7-9).

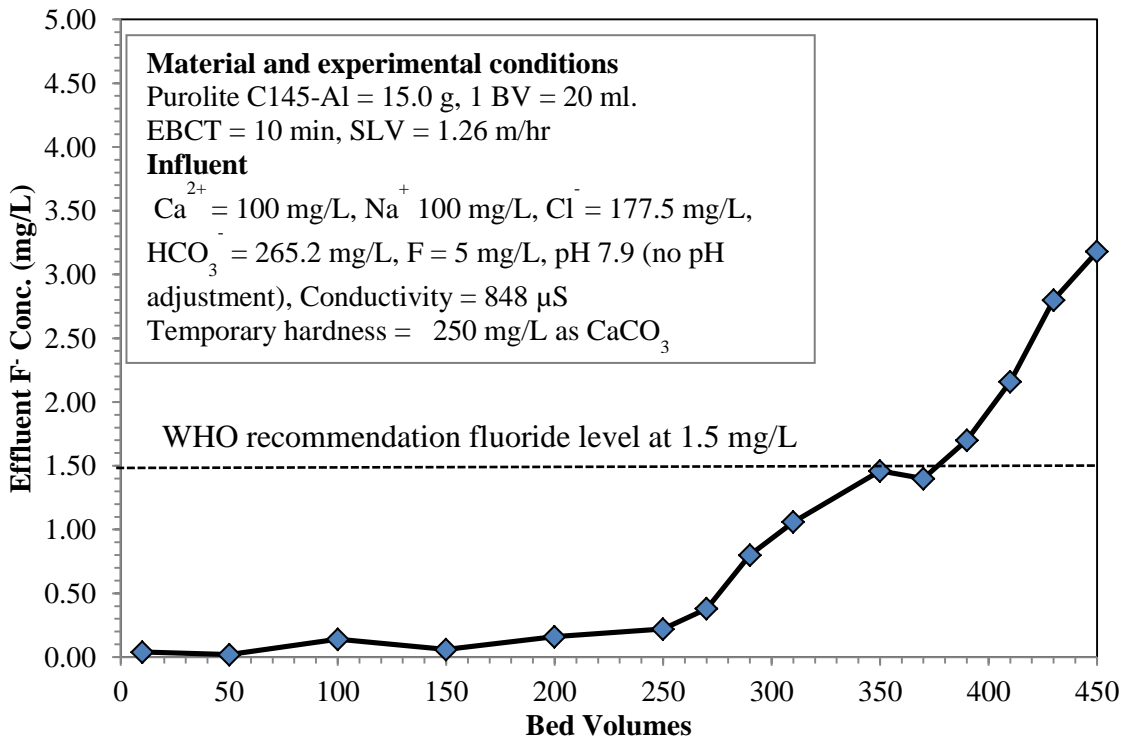


**Figure 7.17** Effluent history for fluoride removal during column runs using macroporous strong acid cation exchanger that started in  $Al^{3+}$  form

To validate trace anionic ligand removal, figure 7.17 shows the effluent history of fluoride removal simultaneously with calcium removal. Fluoride effluent increased above WHO recommendation levels (1.5 mg F/L) after nearly 400 bed volumes. The evidence of aluminum loading including fluoride adsorption in the cation exchanger (C145) is shown in figure 7.18. After hardness removal, the exhausted resin (Purolite C145) was used for elemental analysis using the combination of SEM and EDX techniques to see the distribution of aluminum and fluoride distribution inside the beads.

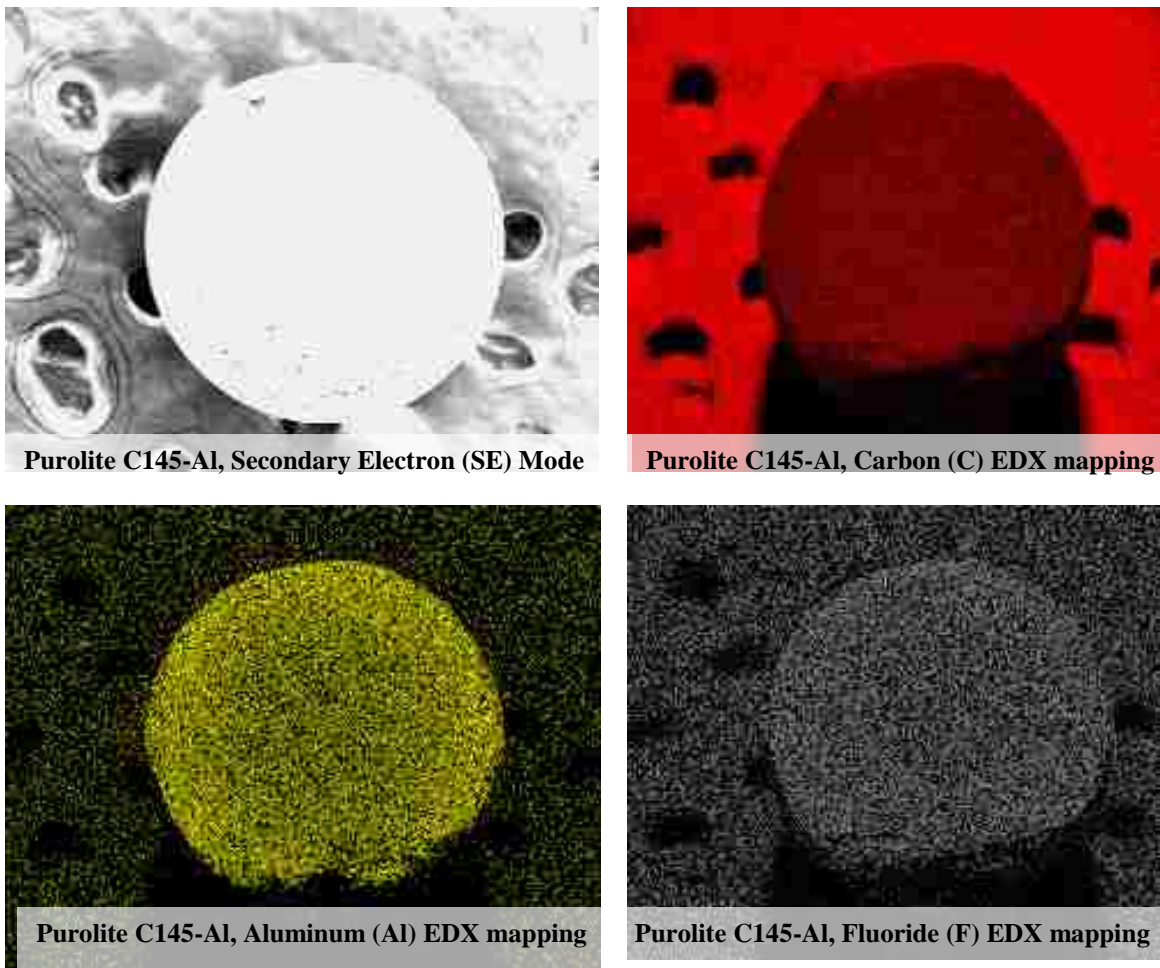


**Figure 7.18** SEM-EDX elemental mapping of Purolite C145 at the end of  $\text{Ca}^{2+}$  removal

## CHAPTER 8

### CONCLUSIONS

In this study, two different hybrid polymeric/inorganic nanosorbents were developed primarily for: first, selective removal of trace heavy metals and anionic ligands (i.e., arsenic and fluoride); and second, removal of hardness from water (water softening) without using salt (NaCl or KCl) in the regeneration process. The goals of development for the two different processes are geared toward efficiency and sustainability. Zirconium oxides were chosen over the previous iron oxides because zirconium oxide exhibits higher chemical stability over wide ranges of pH and redox conditions than the iron oxides. For water softening, new heterogeneous cation exchangers with novel regeneration schemes were introduced to validate the hardness removal efficiency in terms of both sorption and regeneration. Since water softening processes have been applied worldwide, the reduction of salt discharge into natural waters can make a significant impact. The summary findings of two main studies are summarized in the following sections.

#### **8.1 The hybrid polymeric ion exchangers supported hydrated zirconium oxide (HZO) nanoparticles**

##### **8.1.1 Synthesis and Characterization of Hybrid Sorbents**

- The amorphous HZO nanoparticles were uniformly distributed throughout the polymeric ion exchanger phases at an approximately 12% (w/w) with sizes well below 50 nm as confirmed by SEM/EDX, HR-TEM, XRD, and acid double digestion methods.



- Inexpensive industrial grade zirconium oxide can be used as startup materials for preparation of HAIX-Zr. The hybrid sorbents synthesized from industrial grade zirconium oxide exhibit high sorption capacity as good as the materials prepared from reagent grade zirconium salt purchased from Sigma Aldrich. Zirconium is also an abundant and inexpensive material similar to iron based sorbents developed earlier.
- In general, due to the abundance of zirconium in many countries such as China and India and commercial availability of parent anion exchange resins worldwide, the HAIX-Zr can be produced locally with a simple preparation method that can reduce the cost of shipping and promotes the local economy.
- From the operational view point, due to their high mechanical strength, the HAIX-Zr can be used in fixed-bed column configurations without degrading into small particles that create a head loss in the column. Note that commercially available granulated type metal oxide sorbents such as granulated ferric oxide/hydroxide (GFO/GFH), activated alumina, titanium oxide, zirconium oxide and etc. tend to degrade into fine particles in the fixed-bed columns, and they are also inefficient to regenerate.
- The submicron size HZO nanoparticles are easy to prepare and innocuous and have been used in many applications. However, according to the information in the open literature, preparation and development of highly selective hybrid sorbent, HAIX-Zr, using HZO based on the Donnan membrane principle has not been reported to date.
- Due to high chemical stability of HZO nanoparticles, the HAIX-Zr can be disposed of safely in a landfill without risk of toxic leaching. Note that, the iron based sorbent can leach the toxic contaminants because of their instability under reducing conditions such as in a landfill.

- The polymeric anion exchange resins are the most suitable support HAIX-Zr synthesis because they allow enhanced transport of anions into the polymer phase due to their high concentration of fixed positive charges such as quaternary ammonium functional groups ( $R_4N^+$ ) in the strong base anion exchangers. The Donnan membrane effect caused by the support polymeric anion exchangers plays an important role to remove target contaminants and enable tailoring of sorbents for intended applications.

- With the same principle, preparation of HAIX-Zr by loading HZO particles into an anion exchanger is scientifically challenging due to the repulsion between zirconium ions and quaternary ammonium ( $R_4N^+$ ) functional groups of anion exchangers. Previous techniques used anion exchangers in permanganate forms ( $MnO_4^-$ ) followed by passing ferrous sulfate solution into the resin bed. The  $MnO_4^-$  is replaced by sulfate,  $MnO_4^{2-}$  is reduced to  $MnO_2$  (s), the  $Fe^{2+}$  is oxidized to  $Fe^{3+}$ , and finally, the  $Fe(OH)_3$ (s) is precipitated within the anion exchange beads.

- In this study, all of the steps are simplified by loading metal (zirconium) solution directly into the resin simply by using zirconium solution dissolved in methanol followed by in-situ precipitation by alkali solution. Methanol solution can lower the dielectric constant. Therefore, less ionized zirconium ions can transport into the parent anion exchanger without being subjected to an electrical repulsion between zirconium ions and quaternary ammonium ( $R_4N^+$ ) functional groups of the anion exchangers.

- Two main preparation methods were developed in this study. The batch method is simple and can be prepared even in remote locations. However, this method takes longer preparation time, consumes more chemical, and generates more waste sludge than the column method. The column method usually takes only 1 cycle and uses only 3-5 hours

for preparation. Moreover, the chemical requirements and waste generation are much lower than the batch method. Depending on the situation, the batch method is suitable for using onsite preparation because of its simplicity. However, for manufacturing, the column method is more efficient and is a cleaner process.

### **8.1.2 Development of Hybrid Anion Exchanger Supported HZO Nanoparticles (HAIX-Zr) for Removal of Trace Anionic Ligands (i.e., arsenic and fluoride)**

- From the equilibrium batch isothermal test, the arsenic and fluoride sorption behaviors follow the Langmuir isotherm with the maximum sorption capacity of 20 mg As(V)/g at pH 7.5 and 35 mg F/g at pH 5.5, respectively. The sorption capacity of the HAIX-Zr for both arsenic and fluoride is three times higher than the most commonly used activated alumina (AA).

- For fluoride removal, HAIX-Zr can remove fluoride selectively. Activated alumina (AA) can remove fluoride, but the removal capacity was significantly lower than the HAIX-Zr. In contrast, iron based nanosorbents have very low affinity toward fluoride ions resulting in nearly immediate breakthrough.

- According to the hard and soft acid and base (HSAB) principal, hard acids such as zirconium and aluminum are likely to bind with hard bases such as fluoride. Iron is categorized as a transition metal (borderline), thus it has less affinity toward fluoride ions.

- After two runs of fluoride sorption/desorption, some of the activated alumina (AA) was degraded into very fine particles and blocked the water flow through the column.

- From the column run studies using NSF Challenge Water Standards 53, the HAIX-Zr selectively removed arsenic with high concentrations of competing ions. HAIX-Zr can remove As(V) effectively for nearly 6,000 bed volumes before reaching the maximum contamination level (MCL) of arsenic at 10 ppb. As(III) was also effectively removed by HAIX-Zr until around 4,000 bed volumes before the effluent exceeded the MCL (10 ppb)
- Due to the Donnan membrane effect, the cation exchanger supported zirconium oxide or HCIX-Zr exhibits low arsenic and fluoride removal capacity.
- HAIX-Zr is amenable to efficient regeneration using 3% NaOH/ NaCl solution 15 bed volumes without significant loss in capacity. More than 90% of arsenic and fluoride were recovered from the regeneration processes.
- The spherical HAIX-Zr beads are robust and durable. There are no signs of particle breakdown into powder. XRD diffractograms confirm that the HZO particles are still amorphous after being used for many cycles of sorption/desorption. The regenerable nature of HAIX-Zr reduces the volume of disposable arsenic-laden waste 100-fold versus single-used granular metal oxide adsorbents (67).
- Silica and phosphate at concentrations greater than 30 mg/L as SiO<sub>2</sub> and 200 µg P/L result in reduction of arsenic sorption capacity. Sulfate ions have a minor effect toward arsenic sorption onto HZO nanoparticles especially in the dilute ranges.
- A kinetic study on arsenate and fluoride adsorption onto the HAIX-Zr confirmed that intraparticle diffusion was the rate limiting step and the effective intraparticle diffusivity of arsenic and fluoride are  $2.3 \times 10^{-11}$  and  $8 \times 10^{-11}$  cm<sup>2</sup>/sec, respectively.

- For fluoride removal technology, activated alumina (AA) has been widely used. However, due to the amphoteric properties of aluminum, significant aluminum ions leach out during regeneration with alkaline solution and during material conditioning with acid solution. For HAIX-Zr under identical conditions, insignificant amount of zirconium ions are found in the solution.

### **8.1.3 Development of Hybrid Cation Exchange Fibers Supported HZO Nanoparticles (HCIXF-Zr) for Removal of Heavy Metals (i.e. Zinc)**

- Hybrid strong acid cation exchange resin beads and fibers loaded with hydrated zirconium oxide (HZO) nanoparticles were prepared and used for selective removal of toxic heavy metals such as zinc. Both hybrid cation exchange beads and fibers exhibit high selectivity toward transition metals (i.e. zinc) for more than 5,000 bed volumes in the presence of high concentration of competing cations such as calcium and sodium at neutral to alkaline pH.

- Hydrated Zr(IV) oxide (HZO) nanoparticles can be dispersed in both cation and anion exchangers. The HZO particles can bind with both trace toxic heavy metals and anionic ligands such as arsenic and fluoride. Due to the Donnan membrane effect, the toxic heavy metals removal capacity can be greatly improved by dispersing HZO onto the cation exchangers because the high concentration of sulfonic ( $\text{SO}_3^-$ ) acid functional groups enhance transportation of heavy metals into the material and then bind with the HZO particles.

- Unlike the hybrid cation exchange resin counterparts, the hybrid cation exchange fibers or HCIXF-Zr was able to regenerate with only solid  $\text{CO}_2$  (dry ice) sparged in 1%

calcium solution with high percentage of toxic metal recoveries (i.e., 98% of zinc) within 75 bed volumes.

- Ion exchange fiber based hybrid nanosorbents offer the unique capability to use and consume CO<sub>2</sub> during the efficient regeneration, whereas commercial ion exchange resins impregnated with the same zirconium oxide nanoparticles are not amenable to regeneration with CO<sub>2</sub>.

- A much shorter intraparticle diffusion path length in cylindrical ion exchange fibers (diameter 50µm) as compared to resin beads (diameter 500 µm) is the underlying reason for a highly efficient regeneration of the fibers.

- The HZO surface binding sites are amphoteric; at an acidic pH, the binding sites are protonated and become positive charged. Consequently, positively charge Zn<sup>2+</sup> gets rejected due to the Donnan co-ion exclusion effect and thus desorption is thermodynamically favorable.

## **8.2 Salt-free water softening processes**

Water softening processes using ion exchange technologies are widely used in both household and industrial scales. The traditional strong acid cation (SAC) exchanger in the sodium form is mostly used for softening of hard water. Due to the unfavorable equilibrium, high concentration of brine solution (10-12% NaCl) is required to regenerate the exhausted SAC resin to bring the resin into the sodium form again. At high concentration of salt is discharged into a natural body of water resulting in high total dissolved solid (TDS) especially in arid areas. The ecosystem is affected by the salt

discharge from the softener. Moreover, during the softening process, the sodium ions from the SAC exchanger are being exchanged stoichiometrically with the hardness (i.e.,  $\text{Ca}^{2+}$ ,  $\text{Mg}^{2+}$ , etc.) and released into treated water. High concentrations of sodium ions have an effect on people who have cardiovascular diseases such as hypertension.

In this study, salt free water softening processes were developed using two different cation exchange resins. The processes are not using salts (NaCl and KCl) so that no waste NaCl is generated from the process. Moreover, the treated water does not containing sodium ions. The summary findings of the two main processes are summarized in the following sections:

- By using weak acid cation (WAC) exchange resins in the hydrogen form, we found that diluted 2% acetic acid can regenerate hardness (i.e.,  $\text{Ca}^{2+}$ ) in the resins effectively with more than 95% of calcium recovery at only 10 bed volumes while solid  $\text{CO}_2$  (dry ice) sparged in water at high pressure (150 psi) was not effective with only 20% calcium recovery. Compared with the conventional WAC resin that use aggressive mineral acid (e.g., 5% HCl), diluted acetic acid can be considered to be a good option because it is non-aggressive, inexpensive, requires low volumes and is biodegradable.

- Wide ranges of hardness (i.e.,  $\text{Ca}^{2+}$ ) were tested in these experiments (400, 200, 150, 70 mg/L as  $\text{Ca}^{2+}$ ) by using two different types of weak acid cation exchangers in the hydrogen form, shallow shell technology (Purolite SST104) and traditional spherical resin (Purolite C106). From the column run results, both resins can remove hardness effectively. The chemical composition and properties of two resins are virtually identical.

The SST104 contains an inert core (functional groups of the resin reside on the outer layer), while the C106 resin is homogeneous beads.

- After both resins were exhausted with the calcium ions, 2% acetic acid can successfully regenerate both resins and the calcium ions were recovered at nearly 90% for every run.

- The salt-free water softening by a strong acid cation (SAC) exchanger in the aluminum form can simultaneously remove hardness (i.e.  $\text{Ca}^{2+}$ ) and anionic ligands (i.e. fluoride). This process requires only stoichiometric amounts of regeneration salt. There is no excess regeneration salt except from the hardness being discharged into the regenerant solution. Moreover, since the resin did not start in the sodium form, there are no sodium ions to appear in the treated water.

- Fluoride ions can be co-removed with hardness due to the generation of aluminum hydroxide particles precipitated inside the resin.



## APPENDIX

### Community Based Fluoride Treatment Plant for 1,000 People

#### 1. Design parameters

- Fluoride in the influent = 5.0 mg/L
- Volume of water = 5,000 L/d (assume 1,000 people and 5 L/person/day)
- Regeneration frequency = 1 time/month
- Sorbent = HAIX-Zr (density 1.84 L/Kg)

#### 2. Data from bench-scale column runs

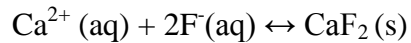
- Fluoride breakthrough at level of 1.5 mg F/L = 1.5 L water/g sorbent (as shown in figure A1 (page 190) and also shown in chapter 5, figures 5.3-5.4)
- Regeneration solution (3% NaOH and 3% NaCl) required = 10 bed volumes including rinse water

#### 3. Design Calculations

- Volume of water to be treated = (5,000 L/d) x (30 d/month) = 150,000 L/month
- Amount of required sorbent = (150,000 L)/(1.5 L/g sorbent) = 100,000 g = 100 Kg
- Volume of sorbent (HAIX-Zr) = (100 Kg) x (1.84 L/Kg) = 184 L
- Design sorbent volume = 200 L
- Assume all of the fluoride is removed from the water and is eluted from the HAIX-Zr during regeneration within 10 bed volumes
  - Mass of fluoride removed from the water each month  
= (5 mgF/L) x (g/1,000 mg) x (150,000 L/month) = 750 g

#### 4. Waste management

For each regeneration cycle (every month), fluoride in the waste regenerant will be removed by precipitation with  $\text{CaCl}_2$  solution as  $\text{CaF}_2$  ( $K_{sp} = 3.45 \times 10^{-11}$ ) (4). One mole of calcium is required to precipitate two moles of fluoride and the reaction as follows:



- Mass of fluoride in regeneration solution =  $750 \text{ g F} \times (\text{mol}/19 \text{ g}) = 39.5 \text{ mol fluoride}$
- Amount of  $\text{CaCl}_2$  required =  $39.5/2 = 19.75 \text{ mol}$  or  $2.2 \text{ Kg}$  of  $\text{CaCl}_2$  (MW  $\text{CaCl}_2 = 111 \text{ g/mol}$ ). Note that, in reality, 50% of more  $\text{CaCl}_2$  will be added to achieve complete precipitation.
- Amount of solid waste ( $\text{CaF}_2$ ) generated each month =  $19.75 \text{ mol} \times 78 \text{ g/mol} = 1540.5 \text{ g/month}$
- After precipitation, the pH of wastewater is adjusted and pumped back to the precipitation tank therefore there is no waste solution discharged from the process. The flow scheme of fluoride treatment plant is illustrated in figure A2.

#### 5. Summary

- The system can serve up to 1,000 people (assume 5 L/person/day)
- The system can treat fluoride contaminated water around 150,000 L/month
- Sorbent (HAIX-Zr) required 200 L (one time)
- Regeneration solution (3% NaCl and NaOH) required  $2 \text{ m}^3/\text{month}$  or (1.2% of treated water)
- Solid waste generated as  $\text{CaF}_2 (\text{s})$  approximately  $1.54 \text{ kg/month}$  or each person generate waste only  $1.54 \text{ g/person/month}$

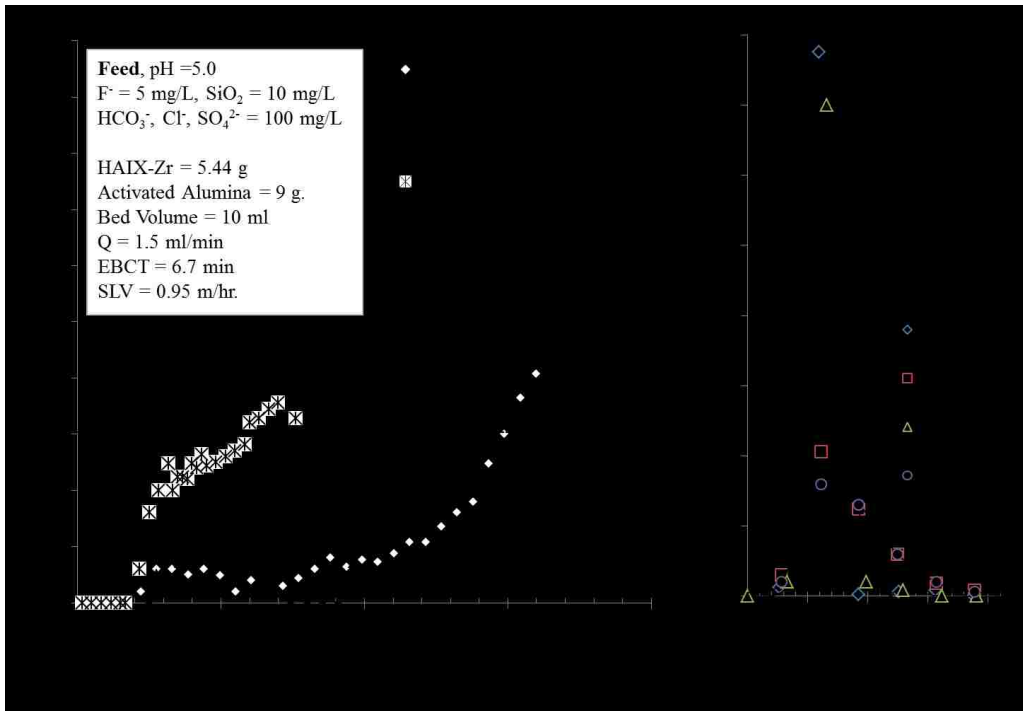


**Figure A1.** Fluoride effluent histories and regeneration profiles using HAIX-Zr and AA

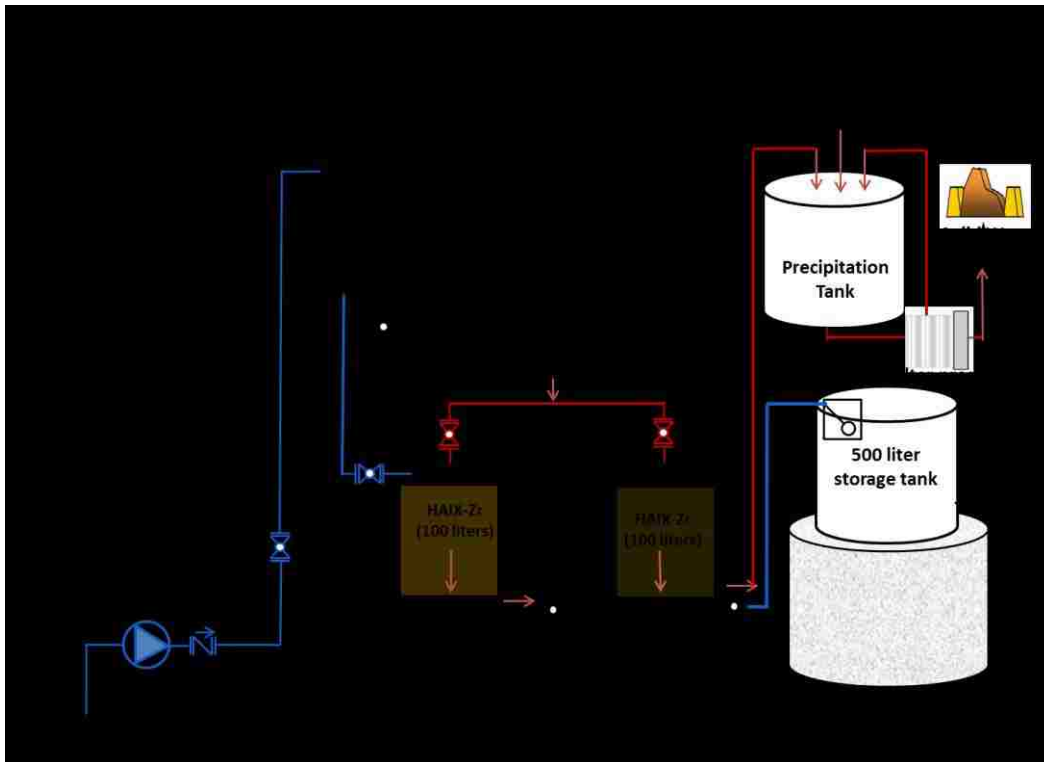


**Figure A2.** Flow scheme for fluoride treatment plant and on-site regeneration facility

## REFERENCES

- (1) Kunin, R. *Ion Exchange Resins*, 2nd ed.; Wiley: New York, 1958.
- (2) Clifford, D.A. Ion Exchange and Inorganic Adsorption. In *Water Quality and Treatment: A Handbook of Community Water Supplies*, 5th ed.; AWWA, Ed.; McGraw-Hill Professional, New York, 1999;pp 1-87.
- (3) Alexandratos, S.D. Ion-Exchange Resins: A Retrospective from Industrial and Engineering Chemistry Research. *Ind. Eng. Chem. Res.* **2008**, 48(1), 388-398.
- (4) Crittenden, J.C.; Trussell, R.R.; Hand, D.W.; Howe, K.J.; Tchobanoglous, G. *MWH's Water Treatment Principles and Design*, 3rd ed.; Wiley: New Jersey, 2012.
- (5) Helfferich, F.G. *Ion Exchange*; Dover Publication Inc.: New York, 1995.
- (6) McGarvey, F.X. *Introduction to Industrial Ion Exchange*.
- (7) SenGupta, A.K., Ed. *Ion Exchange Technology: Advances in Pollution Control*; Technomic Publishing: Lancaster, PA, 1995.
- (8) SenGupta, S.; SenGupta, A.K. Trace Heavy Metal Separation by Chelating Ion Exchangers. In *Environmental Separation of Heavy Metals: Engineering Processes*, 1st ed.; A.K. SenGupta, Ed.; Lewis Publishers, Boca Raton, 2002;pp 45-92.
- (9) Smedley, P.L.; Kinniburgh, D.G. A review of the source, behaviour and distribution of arsenic in natural waters. *Appl. Geochem.* **2002**, 17 517-568.
- (10) Bhatnagar, A.; Kumar, E.; Sillanpää, M. Fluoride removal from water by adsorption—A review. *Chem. Eng. J.* **2011**, 171(3), 811-840.

- (11) Berg, M.; Tran, H.C.; Nguyen, T.C.; Pham, H.V.; Schertenleib, R.; Giger, W. Arsenic Contamination of Groundwater and Drinking Water in Vietnam: A Human Health Threat. *Environ. Sci. Technol.* **2001**, 35(13), 2621-2626.
- (12) Berg, M.; Stengel, C.; Trang, P.T.K.; Hung Viet, P.; Sampson, M.L.; Leng, M.; Samreth, S.; Fredericks, D. Magnitude of arsenic pollution in the Mekong and Red River Deltas -- Cambodia and Vietnam. *Sci. Total Environ.* **2007**, 372(2-3), 413-425.
- (13) Amini, M.; Abbaspour, K.C.; Berg, M.; Winkel, L.; Hug, S.J.; Hoehn, E.; Yang, H.; Johnson, C.A. Statistical Modeling of Global Geogenic Arsenic Contamination in Groundwater. *Environ. Sci. Technol.* **2008**, 42(10), 3669-3675.
- (14) Amini, M.; Mueller, K.; Abbaspour, K.C.; Rosenberg, T.; Afyuni, M.; Møller, K.N.; Sarr, M.; Johnson, C.A. Statistical modeling of global geogenic fluoride contamination in groundwaters. *Environ. Sci. Technol.* **2008**, 42(10), 3662-3668.
- (15) DeMarco, M.J.; SenGupta, A.K.; Greenleaf, J.E. Arsenic removal using a polymeric/inorganic hybrid sorbent. *Water Res.* **2003**, 37(1), 164-176.
- (16) SenGupta, A.K.; Greenleaf, J.E. Arsenic in Subsurface Water: Its Chemistry and Removal by Engineered Processes. In *Environmental Separation of Heavy Metals: Engineering Processes* 1st ed.; A.K. SenGupta, Ed.; Lewis Publishers:, Boca Raton, FL, 2002;pp 265-303.
- (17) Gerelick, H.; Jones, H., *Mitigating Arsenic Pollution: Bridging the Gap Between Knowledge and Practice*, in *Chemistry International*. 2008.

- (18) WHO, *Guidelines for Drinking-Water Quality*, in 3rd ed., Vol 1. Geneva: WHO Press. 2004.
- (19) Tang, Y.L.; Guan, X.H.; Su, T.Z.; Gao, N.Y.; Wang, J.M. Fluoride adsorption onto activated alumina: Modeling the effects of pH and some competing ions. *Colloids Surf., A* **2009**, 337(1-3), 33-38.
- (20) *Fluorosis worldwide*, in *Unicef WATERfront*. 1999. p. 12.
- (21) Puttamraju, P.; SenGupta, A.K. Evidence of tunable on-off sorption behaviors of metal oxide nanoparticles:role of ion exchanger support. *Ind. Eng. Chem. Res.* **2006**, 45(22), 7737-7742.
- (22) Suzuki, T.M.; Chida, C.; Kanamoto, M.; Yokoyama, T. Removal of fluoride-ion by a porous spherical resin loaded with hydrous zirconium-oxide. *Chem. Lett.* **1989**,(7), 1155-1158.
- (23) Suzuki, T.M.; Bomani, J.O.; Matsunaga, H.; Yokoyama, T. Preparation of porous resin loaded with crystalline hydrous zirconium oxide and its application to the removal of arsenic. *React. Funct. Polym.* **2000**, 43(1-2), 165-172.
- (24) Suzuki, T.M.; Bomani, J.O.; Matsunaga, H.; Yokoyama, T. Removal of As(III) and As(V) by a porous spherical resin loaded with monoclinic hydrous zirconium oxide. *Chem. Lett.* **1997**,(11), 1119-1120.
- (25) Piriälä, M.; Martikainen, M.; Ainassaari, K.; Kuokkanen, T.; Keiski, R.L. Removal of aqueous As(III) and As(V) by hydrous titanium dioxide. *J. Colloid and Interface Sci.* **2011**, 353(1), 257-262.

- (26) Pena, M.E.; Korfiatis, G.P.; Patel, M.; Lippincott, L.; Meng, X. Adsorption of As(V) and As(III) by nanocrystalline titanium dioxide. *Water Res.* **2005**, 39(11), 2327-2337.
- (27) Balaji, T.; Matsunaga, H. Adsorption characteristics of As(III) and As(V) with titanium dioxide loaded amberlite XAD-7 resin. *Anal. Sci.* **2002**, 18(12), 1345-1349.
- (28) Blaney, L.M.; Cinar, S.; SenGupta, A.K. Hybrid anion exchanger for trace phosphate removal from water and wastewater. *Water Res.* **2007**, 41(7), 1603-1613.
- (29) Cumbal, L.; SenGupta, A.K. Arsenic removal using polymer-supported hydrated iron(III) oxide nanoparticles: role of donnan membrane effect. *Environ. Sci. Technol.* **2005**, 39(17), 6508-6515.
- (30) Liu, R.P.; Gong, W.X.; Lan, H.C.; Gao, Y.P.; Liu, H.J.; Qu, J.H. Defluoridation by freshly prepared aluminum hydroxides. *Chem. Eng. J.* **2011**, 175 144-149.
- (31) Hristovski, K.D.; Westerhoff, P.K.; Crittenden, J.C.; Olson, L.W. Arsenate removal by nanostructured ZrO<sub>2</sub> spheres. *Environ. Sci. Technol.* **2008**, 42(10), 3786-3790.
- (32) Driehaus, W.; Jekel, M.; Hildebrandt, U. Granular ferric hydroxide - a new adsorbent for the removal of arsenic from natural water. *J. Water Serv. Res. Technol.-Aqua.* **1998**, 47(1), 30-35.
- (33) Suzuki, T.M.; Tanaka, D.A.P.; Tanco, M.A.L.; Kanesato, M.; Yokoyama, T. Adsorption and removal of oxo-anions of arsenic and selenium on the

- zirconium(IV) loaded polymer resin functionalized with diethylenetriamine-N,N,N',N'-polyacetic acid. *J. Environ. Monit.* **2000**, 2(6), 550-555.
- (34) DeLemos, J.L.; Bostick, B.C.; Renshaw, C.E.; Stürup, S.; Feng, X. Landfill-stimulated iron reduction and arsenic release at the Coakley Superfund Site (NH). *Environ. Sci. Technol.* **2005**, 40(1), 67-73.
- (35) Blaney, L.M.; SenGupta, A.K. Comment on Landfill-Stimulated Iron Reduction and Arsenic Release at the Coakley Superfund Site (NH). *Environ. Sci. Technol.* **2006**, 40(12), 4037-4038.
- (36) Stumm, W.; Morgan, J.J. *Aquatic chemistry: chemical equilibria and rates in natural waters*; Wiley-Interscience: New York, 1996.
- (37) Cumbal, L.; Greenleaf, J.; Leun, D.; SenGupta, A.K. Polymer supported inorganic nanoparticles: characterization and environmental applications. *React. Funct. Polym.* **2003**, 54(1-3), 167-180.
- (38) Ramana, A.; Sengupta, A.K. Removing selenium(IV) and arsenic (V) oxyanions with tailored chelating polymers. *J. Environ. Eng. Div. (Am. Soc. Civ. Eng.)*. **1992**, 118(5), 755-775.
- (39) Sengupta, A.K.; Zhu, Y.; Hauze, D. Metal(II) ion binding onto chelating exchangers with nitrogen donor atoms: some new observations and related implications. *Environ. Sci. Technol.* **1991**, 25(3), 481-488.
- (40) Pourbaix, M. Atlas of electrochemical equilibria in aqueous solutions. 2nd English ed. 1974, Houston, Texas.: National Association of Corrosion Engineers. **1974**.



- (41) Brown, G.E., Henrich, V.E., Casey, W.H., Clark, D.L., Eggleston, C., Felmy, A., Goodman, D.W., Grätzel, M., Maciel, G., McCarthy, M.I., Nealon, K.H., Sverjensky, D.A., Toney, M.F., and Zachara, J.M. Metal oxide surfaces and their interactions with aqueous solutions and microbial organisms. *Chem. Rev.* **1998**, 99(1), 77-174.
- (42) Alkaline Water News Webpage. <http://alkalinewaterplus.info/blog/tag/hard-water/> (accessed January 5, 2013).
- (43) The USGS Water Science School Webpage. <http://ga.water.usgs.gov/edu/characteristics.html> (accessed January , 2013).
- (44) Greenleaf, J.E.; Lin, J.C.; Sengupta, A.K. Two novel applications of ion exchange fibers: Arsenic removal and chemical-free softening of hard water. *Environ. Prog.* **2006**, 25(4), 300-311.
- (45) Greenleaf, J.E.; Sengupta, A.K. Environmentally benign hardness removal using ion-exchange fibers and snowmelt. *Environ. Sci Technol.* **2006**, 40(1), 370-376.
- (46) Padungthon, S.; Greenleaf, J.E.; Sengupta, A.K. Carbon dioxide sequestration through novel use of ion exchange fibers (IX-fibers). *Chem. Eng. Res. Des.* **2011**, 89(9), 1891-1900.
- (47) Clark, J.R. Electrothermal atomisation atomic absorption conditions and matrix modifications for determining antimony, arsenic, bismuth, cadmium, gallium, gold, indium, lead, molybdenum, palladium, platinum, selenium, silver, tellurium, thallium and tin following back-extraction of organic aminohalide extracts. *J. Anal. At. Spectrom.* **1986**, 1(4), 301-308.

- (48) Ficklin, W.H. Separation of arsenic(III) and arsenic(V) in ground waters by ion-exchange. *Talanta*. **1983**, 30(5), 371-373.
- (49) APHA, *Standard methods for the examination of water and wastewater, 15th Ed*, in American Public Health Association, America Water Works Association and Water Pollution Control Federation. Washington D.C. 1985.
- (50) Zhao, D.; Sengupta, A.K. Ultimate removal of phosphate from wastewater using a new class of polymeric ion exchangers. *Water Res.* **1998**, 32(5), 1613-1625.
- (51) Kressman, T.R.E.; Kitchener, J.A. Cation exchange with a synthetic phenolsulphonate resin. Part V. Kinetics. *Disc. Faraday Soc.* **1949**, 7(0), 90-104.
- (52) Cumbal, L. Polymer-Supported Hydrated Fe Oxide (HFO) Nanoparticles: Characterization, and Environmental Applications. Ph.D. Dissertation, Lehigh University, Bethlehem, PA, June, 2004.
- (53) Lin, J.C.; SenGupta, A.K. Hybrid anion exchange fibers with dual binding sites: Simultaneous and reversible sorption of perchlorate and arsenate. *Environ. Eng. Sci.* **2009**, 26(11), 1673-1683.
- (54) SenGupta, A.K. Hybrid Anion Exchanger for Selective Removal of Contaminating Ligands from Fluids and Method of Manufacture Thereof. U.S. Patent 7291578 B2, 2007.
- (55) Sengupta, A.K.; Lim, L. Modelling chromate ion-exchange processes. *AIChE J.* **1988**, 34(12), 2019-2029.
- (56) Kosmulski, M. The significance of the points of zero charge of zirconium (hydr)oxide reported in the literature. *J. Dispersion Sci. Technol.* **2002**, 23(4), 529-538.

- (57) Li, P.; SenGupta, A.K. Intraparticle diffusion during selective sorption of trace contaminants: The effect of gel versus macroporous morphology. *Environ. Sci. Technol.* **2000**, 34(24), 5193-5200.
- (58) Tanaka, D.A.P.; Kerketta, S.; Tanco, M.A.L.; Yokoyama, T.; Suzuki, T.M. Adsorption of fluoride ion on the zirconium(IV) complexes of the chelating resins functionalized with amine-N-acetate ligands. *Sep. Sci. Technol.* **2002**, 37(4), 877-894.
- (59) Yuchi, A.; Matsuo, K. Adsorption of anions to zirconium(IV) and titanium(IV) chemically immobilized on gel-phase. *J. Chromatogr., A.* **2005**, 1082(2), 208-213.
- (60) Yuchi, A.; Ogiso, A.; Muranaka, S.; Niwa, T. Preconcentration of phosphate and arsenate at sub-ng ml<sup>-1</sup> level with a chelating polymer-gel loaded with zirconium(IV). *Anal. Chim. Acta.* **2003**, 494(1-2), 81-86.
- (61) Liao, X.P.; Tang, W.; Zhou, R.Q.; Shi, B. Adsorption of metal anions of vanadium(V) and chromium(VI) on Zr(IV)-impregnated collagen fiber. *Adsorption.* **2008**, 14(1), 55-64.
- (62) Liao, X.P.; Ding, Y.; Wang, B.; Shi, B. Adsorption behavior of phosphate on metal-ions-loaded collagen fiber. *Ind. Eng. Chem. Res.* **2006**, 45(11), 3896-3901.
- (63) Peräniemi, S.; Ahlgrén, M. Optimized arsenic, selenium and mercury determinations in aqueous solutions by energy dispersive x-ray fluorescence after preconcentration onto zirconium-loaded activated charcoal. *Anal. Chim. Acta.* **1995**, 302(1), 89-95.

- (64) Viswanathan, N.; Meenakshi, S. Synthesis of Zr(IV) entrapped chitosan polymeric matrix for selective fluoride sorption. *Colloids Surf., B.* **2009**, 72(1), 88-93.
- (65) Sundaram, C.S.; Meenakshi, S. Fluoride sorption using organic-inorganic hybrid type ion exchangers. *J. Colloid and Interface Sci.* **2009**, 333(1), 58-62.
- (66) Samatya, S.; Mizuki, H.; Ito, Y.; Kawakita, H.; Uezu, K. The effect of polystyrene as a porogen on the fluoride ion adsorption of Zr(IV) surface-immobilized resin. *React. Funct. Polym.* **2010**, 70(1), 63-68.
- (67) Sarkar, S.; Gupta, A.; Biswas, R.K.; Deb, A.K.; Greenleaf, J.E.; SenGupta, A.K. Well-head arsenic removal units in remote villages of Indian subcontinent: Field results and performance evaluation. *Water Res.* **2005**, 39(10), 2196-2206.
- (68) Davis, C.C.; Chen, H.-W.; Edwards, M. Modeling Silica Sorption to Iron Hydroxide. *Environ. Sci. Technol.* **2001**, 36(4), 582-587.
- (69) Swedlund, P.J.; Webster, J.G. Adsorption and polymerisation of silicic acid on ferrihydrite, and its effect on arsenic adsorption. *Water Res.* **1999**, 33(16), 3413-3422.
- (70) Li, P.; SenGupta, A.K. Intraparticle diffusion during selective ion exchange with a macroporous exchanger. *React. Funct. Polym.* **2000**, 44(3), 273-287.
- (71) Crank, J. *The Mathematics of Diffusion*, 2nd ed.; Oxford Science Publications: Oxford, UK, 1975.
- (72) Pearson, R.G. Hard and soft acids and bases, HSAB, part II: Underlying theories. *J. Chem. Educ.* **1968**, 45(10), 643.

- (73) Pearson, R.G. Hard and soft acids and bases, HSAB, part 1: Fundamental principles. *J.Chem. Educ.* **1968**, 45(9), 581-587.
- (74) Blackwell, J.A.; Carr, P.W. Study of the fluoride adsorption characteristics of porous microparticulate zirconium-oxide. *J. Chromatogr.* **1991**, 549(1-2), 43-57.
- (75) Viswanathan, N.; Meenakshi, S. Effect of metal ion loaded in a resin towards fluoride retention. *J. Fluorine Chem.* **2008**, 129(7), 645-653.
- (76) Sasaki, T.; Kobayashi, T.; Takagi, I.; Moriyama, H. Solubility measurement of zirconium(IV) hydrous oxide. *Radiochim. Acta.* **2006**, 94(9-11), 489-494.
- (77) Dzombak, D.A.; Morel, F.M.M. *Surface Complexation Modeling: Hydrous Ferric Oxides*; Wiley-Interscience: New York, 1990.
- (78) Helfferich, F. Ion exchange kinetics. V: Ion exchange accompanied by chemical reactions. *J. Phys. Chem.* **1965**, 69 1178-1187.
- (79) Chen, L.Q.; Yang, G.L.; Zhang, J. A study on the exchange kinetics of ion-exchange fiber. *React. Funct. Polym.* **1996**, 29(3), 139-144.
- (80) Dominguez, L.; Benak, K.R.; Economy, J. Design of high efficiency polymeric cation exchange fibers. *Polym. Adv. Technol.* **2001**, 12(3-4), 197-205.
- (81) Hoell, W. Optical verification of ion exchange mechanisms in weak electrolyte resins. *React. Polym.* **1981**, 2 93-101.
- (82) Greenleaf, J.E.; SenGupta, A.K. Flue gas carbon dioxide sequestration during water softening with ion-exchange fibers. *Environ. Eng. Div., ASCE.* **2009**, 135(6), 386-396.
- (83) Tossell, J.A. H<sub>2</sub>CO<sub>3</sub>(s): A new candidate for CO<sub>2</sub> capture and sequestration. *Environ. Sci. Technol.* **2009**, 43(7), 2575-2580.

## VITA

Surapol Padungthon was born in 1981 in Phra Nakhon Si Ayuttaya, Thailand. He earned the BS in Environmental Health Science (First honor) from Burapha University, Thailand in 2002 and an MS in Environmental Technology from Mahidol University, Thailand in 2004. He started his career as an environmental engineer at KYTBW, Thailand which is responsible for the construction and management of the integrated waste management plant in Chonburi, Thailand. In 2006, Surapol was awarded the Royal Thai Scholarship to take further advanced studies at Lehigh University. As a Royal Thai Government Scholar, he came to Lehigh in 2007 to study Environmental Engineering and completed his MS in 2008. He continued to pursue his PhD. After completing his doctoral studies he will return to Khon Kean University, Thailand to start his high academic profession in the department of Environmental Engineering. At Lehigh, Surapol worked as a Research Assistant for the experimental work and served as Teaching Assistant for Hand on Engineering (ENGR 98 ) for 2 years and for Environmental Water Chemistry (CEE 381), Reaction Kinetics in Environmental Engineer (CEE 470), and Environmental Separation and Control (CEE 473). During the graduate study, his research work has earned the following publications, conferences presentations, patents, and awards.

## Publications and Conferences

1. Padungthon, S.; J.E. Greenleaf; A.K. SenGupta. Carbon dioxide sequestration through novel use of ion exchange fibers (IX-fibers). *Chem. Eng. Res. Des.* **2011**, 89,(9), 1891-1900.
2. Padungthon, S; A.K. SenGupta. Development and characterization of ion exchanger supported zirconium oxide nanoparticles as a durable fluoride-selective sorbent (In submission process)
3. Padungthon, S: A.K. SenGupta. Comment on “Polymerization of silicate on hematite surfaces and its influence on arsenic sorption; *Environ. Sci. Technol.* 2012, 46, 13235-13243. (In submission process)
4. Paper presentation: Ion exchanger supported zirconium oxide nanoparticles as a robust reusable sorbent. 86<sup>th</sup> ACS Colloid & Surface Science Symposium, June 10-13, 2012 Johns Hopkins University, MD, USA
5. Poster presentation: Carbon dioxide sequestration through novel use of ion exchange fibers, 2011 EES Student Symposium, Lehigh University, PA, USA.
6. Poster presentation: Ion exchanger-supported zirconium oxide nanoparticles as a robust reusable sorbents, 2012 EES Student Symposium, Lehigh University, PA, USA.

## **Patents**

1. Hybrid Anion Exchanger Impregnated with Hydrated Zirconium Oxide for Selective Removal of Contaminating Ligand and Method of Manufacture Thereof (U.S. Provisional patent, application number 61/623,138, filing date April 12, 2012)
2. Ion Exchange Process for Hardness Removal (Softening) without Requiring Salt or Mineral Acid as a Regenerant (U.S. Provisional patent, application number 61709761, filing date Oct 04, 2012)

## **Awards**

1. Daimler Chrysler and UNESCO Mondialogo Engineering Silver Award Winner, Iron oxide adsorbents for arsenic removal: low cost treatment for rural areas and mobile applications, November 2009, Stuttgart Germany.
2. EPA P<sup>3</sup> Honorable mention awards, Development of community operated HAIX-Zr for arsenic removal in Cambodia, Washington DC, USA, May 2011.
3. Eureka! Venture Competition Series: Social Venture Creation Competition, Second place winner, Baker Institute, Lehigh University, 2012